Retrograde protein trafficking of Emp47p in the early secretory pathway of *S. cerevisiae*: A novel mutant-screen uncovers the influence of oxidative stress on protein trafficking.

Inaugural-Dissertation

zur Erlangung des akademischen Grades eines

Doktors der Naturwissenschaften

im Fachbereich 19 Biologie/Chemie

der Universität Gesamthochschule Kassel

vorgelegt von

Alexei Matiach

aus Wolgograd / Rußland

Kassel, März, 2001

Erster Gutachter:	Prof. Dr. M. Maniak
Zweiter Gutachter:	Prof. Dr. W. Nellen
Tag der mündlichen Prüfung:	

Contents I

Zusammenfassung V

1. Introduction 1
1.1. Structural organisation and the dynamics of the early secretory pathway of protein transport in eukaryotic cells 1
1.1.1. COP II vesicle formation 3
1.1.2. COP I coat-mediated transport 6
1.1.3. COP I-dependent mechanisms of protein retention within the early secretory compartments 8
1.1.4. Transport properties of the yeast di-lysine protein Emp47p resemble that of its mammalian homologue ERGIC-53 9
1.2. Cysteine and glutathione biosynthetic pathways in *Saccharomyces cerevisiae*: viewed from compositional and regulatory aspects 12
1.2.1. Essential role of glutathione and thioredoxins in yeast *S. cerevisiae* 17
1.3. The aims of the research work 20
1. A novel genetic screen for the mutants affected in retrograde transport 20
2. Characterization of the subcellular localization of Ylr080wp and its function in the secretion 21

2. Materials 22
2.1. Yeast and bacteria strains 22
2.2. Plasmids 23
2.3. Oligonucleotides 25
2.4. Antibodies 27
2.5. Enzymes and Kits 27
2.6. Media components 28
2.6.1. Growth media for *E. coli* 28
2.6.2. Growth media for *S. cerevisiae* 28
2.7. Chemicals 29
2.8. Radiochemicals 29
2.9. Laboratory hardware equipment 29
2.10. Diverse materials 30
2.11. Frequently used solutions and buffers 30

3. Methods 32
3.1. Cell cultures 32
3.1.1. *E. coli* cultures 32
3.1.2. *S. cerevisiae* cultures 32
3.1.3. Preparation of *E. coli* and *S. cerevisiae* permanent cultures 32
3.2. DNA isolation techniques 33
3.2.1. Transformation of *E. coli* by electroporation 33
3.2.2. Transformation of *S. cerevisiae* cells 33
3.2.3. Analytical plasmid isolation from *E. coli* 34
3.2.4. Preparative plasmid isolation from *E. coli* 35
3.2.5. Analytical plasmid isolation from yeast cells 35
3.2.6. Rapid isolation of yeast chromosomal DNA 35
3.3. Enzymatic modifications of DNA 35
3.3.1. Digestion of double-stranded DNA by restriction endonucleases 35
3.3.2. Treatment of linearized plasmid DNA with alkaline phosphatase 36

3.3.3. Fill-in of 5'-overhangs 36
3.3.4. Creating blunt ends with T4 DNA polymerase 36
3.3.5. Ligation of double-stranded DNA fragments 37
3.3.6. Polymerase chain reaction 37
3.3.7. QuickChange™ site-directed mutagenesis 38
3.3.8. Electrophoretic DNA separation 39
3.3.9. Isolation of DNA fragments from preparative gels 40
3.4. Methods of yeast genetics 40
3.4.1. Crossing of yeast strains 40
3.4.2. Sporulation of yeast cells 41
3.4.3. Analysis of yeast tetrads 41
3.4.4. Reversion of *cys3-2* to *CYS3* by homologous recombination 41
3.4.5. PCR-targeted gene disruption using the kanMX module 41
3.4.6. EMS-mutagenesis of yeast cells 42
3.4.7. Colony-blot assay 42
3.5. Protein analysis techniques 43
3.5.1. TCA-precipitation of yeast proteins 43
3.5.2. Measurement of protein concentration 43
3.5.2.1. Bradford assay 43
3.5.2.2. Spectrophotometric determination of protein concentration 43
3.5.3. Separation of proteins by denaturing gel electrophoresis (SDS-PAGE) 44
3.5.4. Transfer of proteins on nitrocellulose filter (Western blot) 45
3.5.5. Ponceau-staining of nitrocellulose filter-bound proteins 45
3.5.6. Immunological detection of proteins on the nitrocellulose membrane 45
3.5.7. Removal of antibodies from nitrocellulose filter 46
3.5.8. Evaluation of the levels of different Golgi proteins in the yeast cell lysates 46
3.5.9. ^{35}S-pulse-chase experiments to follow protein transport 47
3.5.10. Invertase secretion assay 48
3.5.11. Protein molecular size determination by gel-filtration chromatography on Sephacryl S-6 column 50
3.6. Subcellular fractionation 50
3.6.1. Preparation of frozen step-gradient tubes 50
3.6.2. Subcellular fractionation by velocity sedimentation on sucrose gradient 50
3.7. Determination of the levels of low molecular weight sulfhydryl groups in the cell lysates 51
3.8. Yeast cell morphology investigation techniques 52
3.8.1. Morphological investigation of yeast cell vacuoles 52
3.8.1.1. Quinacrin vacuolar staining assay 52
3.8.2. Indirect immunofluorescence 52
3.9. Lipid analysis techniques 53
3.9.1. Metabolic labeling of the yeast lipids 53
3.9.2. Extraction and TLC-analysis of yeast lipids 53
3.9.3. Isolation of the heat-inducible phospholipid ("PLX") 54
3.9.4. Phospholipase A_2 treatment of extracted [^{32}P]-labeled lipids 54
3.9.5. Base treatment of extracted lipids 54

4. Results 55
4.1 Isolation of a mutant mislocalizing the Golgi-protein Emp47p to the vacuole 55
4.1.1. The genetic screen 55
4.1.2. Proteinase A-deficient strains were prepared out of selected mutants 57

4.1.3. Emp47p is mislocalized to the vacuole in the #937 mutant 58
4.1.3.1. Indirect immunofluorescence analysis visualizes Emp47p in the vacuole 58
4.1.3.2. Western-blot analysis indicates *PEP4*-dependent degradation of Emp47p in the vacuole 59
4.2 Identification of a novel *cys3*-allele 60
4.2.1. The temperature-sensitivity and cysteine auxotrophy of the #937 mutant is rescued by 2µ-*CYS3* plasmid 60
4.2.2. Transition point-mutation in *CYS3* disables cystathionine-γ-lyase due to conserved serine to phenylalanine exchange 60
4.3. Identification of the mutated alleles responsible for the reduced levels of Emp47p 62
4.4. The physiological effects of the malfunction in cysteine biosynthesis 64
4.4.1. In contrast to *cys3*-2 mutant, *gsh1Δ* cells are not temperature-sensitive for growth on rich YPUAD medium 64
4.4.2. *gsh1Δ* cells are less sensitive to the presence of oxidizing agent in rich incubation medium than *cys3-2* 64
4.4.3. Cysteine production, but not glutathione is required for normal Emp47p biosynthesis and trafficking 65
4.4.4. Cytosolic and organellar proteins are affected differentially in *cys3-2* mutant cells 67
4.4.5. *cys3*-2 and *gsh1Δ* mutants are distinguished by differential response of Golgi protein-markers to the presence of the oxidizing agent in the medium 68
4.4.6. The secretory pathways to the Golgi, vacuole, plasma membrane and extracellular periplasmatic space are not adversely affected by oxidative stress in *cys3-2* mutant at 37°C 70
4.4.7. *cys3-2* and *gsh1Δ* mutants are characterized by low intracellular levels of reduced low molecular weight sulfhydryl groups (LMWS) 71
4.4.8. Supplementation of cysteine and/or glutathione rescues the temperature sensitivity and the mislocalization of Emp47p in *cys3-2* mutants 74
4.4.9. Response of phospholipid metabolism to elevated temperature is impaired in both *cys3-2* and *gsh1Δ* mutant cells 77
4.5. Characterization of Ylr080wp, a close homologue of Emp47p 81
4.5.1. Deletion analysis 83
4.5.2. Invertase glycosylation and secretion are affected neither in the mutant deleted for *YLR080W* alone nor in the *YLR080W / EMP47* double deletion mutant 85
4.5.3. Construction of c-myc-epitope tagged Yrl080wp 86
4.5.4. Expression of c-myc-Ylr080wp is growth phase dependent 89
4.5.5. Localisation of c-myc-Ylr080wp is growth phase dependent 89
4.5.6. Ylr080wp recycles between the Golgi and the ER compartments 94
4.5.7. The ER-Golgi distribution of Ylr080wp depends on di-lysine signal and intact components of COP I Golgi-to-ER retrieval machinery 97
4.5.7.1. Construction of c-myc-Yrl080wp „tail"-mutants 97
4.5.7.2. The ER-Golgi localization of Ylr080wp requires functional di-lysine motif 97
4.5.7.3. The Golgi-to-ER retrieval pathway of Ylr080wp is a coatomer-mediated process 102
4.5.8. Molecular size determination by gel-filtration analysis reveals Ylr080wp (48 kDa) migrating as a high molecular weight protein associate of 120-140 kDa 106

5. Discussion 107
5.1. Oxidative stress induced by *CYS3* inactivation changes protein localisation and turnover, and causes impaired CDP-DAG metabolism at high temperatures 107
5.1.1. Characterization of *cys3-2* mutant cells 107
5.1.2. Depletion of cysteine due to Cys3p-dysfunction leads to more profound heat-mediated oxidative stress than shortage of GSH 110
5.1.3. The role of redox potential in the secretory pathway 112
5.1.4. Cys3p- and Gsh1p-deficient cells are both defective in adaptation of lipid-synthesis in response to high temperature 115
5.1.5. In addition to mutation in *CYS3*, the level of Emp47p is adversely influenced by mutations in *CYS4*, *YEF3* and *HTL1* genes 117
5.2. Intracellular trafficking and distribution of the di-lysine protein Ylr080wp 119
5.2.1. Ylr080wp is confined to the ER-Golgi part of the yeast *S. cerevisiae* early secretory pathway and is required for efficient recovery from stationary phase at lower temperature 119
5.2.2. The ER-Golgi subcellular distribution of Ylr080wp requires the di-lysine motif and is dynamically maintained by the functions of conventional antero- and retrograde transport machineries 122
5.2.2.1. Ylr080wp undergoes retrieval to the ER from the Golgi compartments 122
5.2.2.2. Role of COP I in the recycling of Ylr080wp 124
5.2.2.3. Ylr080wp depends on its di-lysine motif for the retention in the Golgi-ER space of the yeast secretory pathway 125
5.2.3. Indications of Ylr080wp form a homo-oligomer *in vivo* 125

6. Summary 127

7. References 129

Acknowledgements 142

Zusammenfassung

Der retrograde membranvermittelte Transport vom Golgi-Komplex zurück zum Endoplasmatischen Reticulum (ER) wird durch COP I Transportvesikel bewirkt. Die Hülle dieser Vesikel besteht aus coatomer, einem Komplex aus sieben Untereinheiten, und der kleinen GTPase Arf1/2p. Zusätzliche, in der Hefe *S. cerevisiae* für den retrograden Transport benötigte Faktoren sind die SNARE-Proteine Ufe1p und Sec22p sowie der ER Proteinkomplex bestehend aus Sec20 p und Tip20p. Allerdings ist die Liste dieser Faktoren angesichts der Vielzahl unterschiedlicher Fracht und der Notwendigkeit diesen Transport zu regulieren und zu koordinieren höchstwahrscheinlich sehr unvollständig. Daher habe ich in einem genetischen Ansatz nach neuen Faktoren gesucht, die an der Lokalisierung des nicht essentiellen TypI Golgi-Transmembranproteins Emp47p beteiligt sind. Emp47p enthält ein di-Lysin Signal an seinem zum Zytosol gerichteten C-Terminus und wird kontinuirlich zwischen dem Golgi-Komplex und dem ER rezykliert in abhängigkeit von der oben beschriebenen Transportmaschinerie. Mutationen in der COP I Maschinerie führen zu einer Fehllokalisierung von Emp47p zur Vakuole, wo das protein rasch durch vakuoläre Proteasen abgebaut wird. In meiner Arbeit benutzte ich chemische Mutagenese, um Zufallsmutanten zu erzeugen, unter denen ich nach solchen suchte, die auf Temperatur-sensitive Weise eine verminderte Menge von Emp47p aufwiesen. Zumindest in einigen dieser Mutanten war zu erwarten, dass dieser Phänotyp von einer Beeinträchtigung der Sortierfunktion des frühen sekretorischen Weges herrühren würde. Eine Mutante, die Emp47p zur Vakuole fehlleitete wies einen Defekt in *CYS3* auf. Diese Gen kodiert für Cystathionine-γ-Lyase (Cys3p), dem terminalen Enzym im metabolischen Weg, der zur de-novo Synthese von Cystein führt. Ich fand Hinweise für den Schluss, dass die Störung der Lokalisation von Emp47p tatsächlich auf der Unfähigkeit der Mutante beruht, Cystein zu produzieren, das als Bestandteil des Tripeptids Glutathion (GSH) und der aktiven Zentren von Mono- und Dithiolproteinen entscheidend für die Reduktionskraft des Zytosols verantwortlich ist.

Der biosynthetische Transport der Carboxypeptidase Y zur Vakuole und des GPI-verankerten Plasmamembranproteins Gas1p vom ER zum Golgi war hingegen ebenso normal wie die Sekretion von Invertase in den periplasmatischen Raum. Ich fand zudem Hinweise, die die allgemeine Wichtigkeit von Glutathion beim Schutz vor Hitze und oxidativem Stress weiter stützen. Insbesondere identifizierte ich ein Phospholipid, CDP-Diacylglcerol, als ein GSH-abhängiges Substrat im Adaptationsprozess bei Hitze-Stress, der in cys3-2 –Zellen defekt ist.

In der vorliegenden Arbeit wurde auch die intrazelluläre Lokalisation und das Recycling-Verhalten des bislang nicht charakterisierten Produktes des Leserahmens *YLR080W* untersucht, eines nicht essentiellen TypI-Transmembranproteins, das 45% Identität mit der Primärsequenz von Emp47 aufweist. Beide, Ylr080wp und Emp47p können aufgrund von Sequenzähnlichkeiten der Klasse von intrazellulären Lektinen zugeordnet werden, deren Prototypen aus Säugerzellen ERGIC-53 und VIP36 sind. Hinweise für eine Rolle von ERGIC-53 im intrazellulären Transport von Glykoproteinen wurden erhalten, aber die genaue Funktion der dieser Proteine im Allgemeinen und Emp47p im Besonderen ist nicht geklärt. Zellbiologische Untersuchung von Ylr080wp und die Aufdeckung des Deletions-Phänotyps war deshalb wichtig. Es konnte von mir gezeigt werden, dass der ein Di-Lysin-Motiv enthaltende C-Terminus des Ylr080w-Protein dessen Lokalisation auf den Bereich ER/Golgi begrenzt. In Zellen aus der frühen logarithmischen Wachstumsphase ist die Lokalisation von Ylr80wp nicht von der von Emp47p zu unterscheiden. Zur stationären Phase hin jedoch wird – völlig im Unterschied zu Emp47p – die Produktion von Ylr080wp um einen Faktor von mindestens 50 erhöht. Gleichzeitig wird das Protein vom Golgi zum ER umverteilt. Die massive Akkumulation von Ylr080wp deutet auf eine wichtige Funktion in der stationären Wachstumsphase hin. Tatsächlich ist das Vorhandensein von Ylr080wp - unabhängig von Emp47p - wichtig dafür, dass die Zellen bei 15°C wieder von der stationären Phase erholen können. Die beiden homologen Proteine haben sich also im Laufe der Evolution spezialisiert. Darüber hinaus sind *YLR080W*- und *EMP47*-Doppeldeletions-Mutanten vollständig lebensfähig und zeigen keinen deutlichen sekretorischen Defekt.

Ähnlich wie bei Emp47p ist die Lokalisation von Ylr080wp abhängig vom di-Lysin-Signal und „Coatomer“. Mutationen im di-Lysin-Motiv und in Genen, die für „Coatomer“-Untereinheiten kodieren, führen beide zur Fehllokalisation von Ylr080wp zur Vakuole. Interessanterweise stellt die Anwesenheit des Wildtyp-Ylr080wp die korrekte Lokalisation des mutierten Ylr080wp ohne eigenes di-Lysin-Motiv wieder her. Dies kann auf Homooligomerisation beruhen, wofür in dieser Arbeit Hinweise mit Hilfe von Gelfiltrations-Experimenten gefunden wurden.

Die Blockierung des Proteinstransports aus dem ER heraus mit Hilfe von konditionalen COP II-Mutanten wie zum Beispiel *sec23-1* und gleichzeitiger Hemmung der Proteinbiosynthese führte zu einer Umverteilung von Ylr080wp zum ER. Dies gilt als Beweis dafür, dass ein Protein zwischen Golgi und ER zirkuliert. Die Golgi-ER-Verteilung von Ylr080wp wird demnach in einer Wachstumsphasen-abhängigen dynamischen Weise durch Zurückführen des Proteins aus einem dem ER nachgeschalteten Kompartiment ins ER aufrecht erhalten, die von einem C-terminalen di-Lysin-Motiv und „Coatomer“ abhängt.

1. Introduction

1.1. Structural organisation and the dynamics of the early secretory pathway of protein transport in eukaryotic cells

Gradual increase in the cell size that accompanied the evolutionary development of eukaryotic cells lead to the proportional decrease in the ratio between the cell surface and volume. The dramatically increased cell volume made the development of internal membraneous systems favourable, in that the cell interior could be partitioned into smaller compartments that overtake the function of oxidative energy production and also expedite and coordinate the delivery of both internally synthesized biomolecules and those imported from outside to the specific subcellular locations according to the metabolic demands.

At the end of 19th century, Camillo Golgi impregnated Purkinje cells with silver salts to reveal a network of interconnected structures: the internal reticular apparatus (Golgi, 1898). Thus the Golgi complex was discovered. The precise number of the Golgi-compartments are still debated, but most investigators currently recognize four: *cis* (biochemically and functionally closest to the ER part of the Golgi membranes), *medial*, *trans* and *trans*-Golgi network (TGN). Each of these compartments has protein-markers used for distinction, but the boundaries between these compartments are rather fluent. In 1984, Saraste and Kuismanen reported the existence of a novel pre-Golgi compartment located between the transitional ER and *cis*-Golgi. Recognition of the distinct morphological and biochemical features of this compartment, now commonly referred to as ERGIC (endoplasmic reticulum-Golgi intermediate compartment) or VTC (vesicular-tubular clusters) was strengthened by the discovery of the marker for this compartment in human cells, p53 (Schweizer et al., 1996), and its rat homologue, p58 (Saraste et al., 1987; Lahtinen et al., 1996), now called ERGIC-53/58. At present, the existence of this pre-Golgi intermediate compartment is accepted in higher eukaryotes, but its boundaries, origin and functions are still debated. To date, the ER-Golgi intermediate compartment was not, however, found in yeast cells, and it is assumed that transport from the ER to the earliest Golgi compartment in yeast, characterized by the α-1,6-oligosaccharyltransferase Och1p, occurs in one step.

The work of Pallade on the exocrine pancreas (Palade, 1975) established that secretory proteins move vectorially through the cell from transitional ER elements through the Golgi and are finally packaged into secretory granules for exocytosis. The work of Palade established that protein transport from the ER to Golgi is energy-dependent and operates through vesicles. The major question about the vesicle transport between the ER and the

Golgi since early 70th was whether that transport is selective or occurs more or less indescriminately by bulk flow.

Newly synthesized proteins enter the biosynthetic pathway by co- or posttranslational transport from the cytosol into the lumen of the ER. Subsequent transport is mediated by vesicles, which carry proteins from the ER to the Golgi complex. Those vesicles are formed by the coat protein complex COP II. Transport across the Golgi stack may also occur by vesicles, a concept supported by reconstituting intra-Golgi transport in a cell-free system (Rothman, 1994), which appear to utilize COP I coated vesicles. These considerations led to the establishment of the stable compartments model for the Golgi (Dunphy and Rothman, 1985; Farquhar, 1985). However this model has been challenged on several grounds. Firstly, it was shown that resident Golgi proteins are not strictly localized to specific compartments, as initially believed (Mellman and Simons, 1992; Rabouille and Nilsson, 1995; Roth, 1997). Secondly, experiments with algae demonstrated that particles far too large to be transported in vesicles moved through the secretory apparatus in a vectorial fashion (Melkonian et al., 1991). Thirdly, in the yeast system it has been clearly demonstrated that COP I vesicles are responsible for retrograde transport within the secretory pathway (Letourneur et al., 1994; Cosson and Letourneur, 1997; Pelham, 1995). A cisternal maturation model has developed (Bonfanti et al., 1998), that holds that new cisternae form at the *cis*-side of the Golgi stack by coalescence of ER-derived membranes, and then move progressively across the stack from *cis*- to *trans*-face, while the cisternae of TGN are fragmented into secretory vesicles. Bonfanti et al. (1998) reported the best evidence to date for cisternal progression, showing that an oligomeric complex of procollagen moves across the Golgi stacks without ever leaving the lumen of the Golgi cisternae. On the basis of such evidence, Glick and Malhotra (1998) have presented a hypothetically unified model that incorporates both cisternal progression and vesicular transport. The secretory cargo is carried forward by cisternal progression, while the role of the COP I vesicles, originally proposed to be responsible for anterograde intra Golgi transport, is now believed to recycle resident Golgi proteins in a retrograde fashion. This unified model can explain the polarity of the Golgi stack as follows. If Golgi proteins compete with each other for incorporation into COP I vesicles, the strongest competitors are recycled efficiently from the *cis*-cisternae, whereas weaker competitors are only recycled efficiently from *medial*- or *trans*-cisternae; as a result, each Golgi protein is concentrated in the part of the stack at which retrograde vesicular trafficking of this protein balances forward cisternal progression (Glick et al., 1997). The final stage of ER-Golgi system is TGN. This compartment serves as a sorting station where the cargo molecules are packaged into either secretory vesicles or vesicles destined to endosomal/lysosomal system (Mellman and Simons,

1992). Transport to endosomes and lysosomes involves the budding of clathrin- and adapter-containing vesicles from the TGN.

Essentially, the two models differ in that vesicular transport model relies on stationary and stable compartments, each with its own composition of processing enzymes, whereas the cisternal maturation model relies on the continuous remodelling of inherently dynamic compartments. In the vesicular transport model, anterograde input of the anterograde proteins is balanced by an equal anterograde output to downstream compartments. On occasion, some resident enzymes might escape. These are then returned by a process termed recycling. The cisternal maturation model, by contrast, requires that all components that make up the cisternal bulk flow recycle to balance the anterograde movement of the bulk carrier and to maintain an assymetric distribution of processing enzymes. Although two models differ greatly in the extent of recycling, both rely on recycling for their function. It seems, therefore, that recycling is a key event in the functioning of the secretory pathway.

1.1.1 COP II vesicle formation

The intracellular transport of secretory proteins from the endoplasmic reticulum to the Golgi complex is essentially mediated by vesicles that collect and potentially concentrate cargo from the donor compartment and deliver it to the subsequent compartment. Each step of vesicle budding, targeting and fusion implies that resident proteins from the donor compartment should be excluded from the forming vesicle, whereas cargo is to be selected and concentrated into it (Rothman and Orci, 1992; Schekman and Orci, 1996; Schekman et al., 1995). The isolation of several yeast mutants impaired in ER-to-Golgi transport led to the identification and finally the purification of a set of five cytosolic proteins sufficient to reconstitute the process of ER vesicle formation *in vitro* (Kaiser and Schekman, 1990; Barlowe et al., 1994). This COP II coat complex consists of Sar1p, Sec23-Sec24p, and Sec13-Sec31p complexes (Pryer et al., 1992; Salama et al., 1993). To date, quite a number of protein factors (more than 30 individual proteins) have been identified in yeast *S.cerevisiae* participating at different steps of the COP II-vesicles mediated ER-to-Golgi transport. Fig.1 collectively represents the protein complexes known to be directly influencing the ER-to-Golgi secretory routes in yeast. Apart from COP II coat components, additional proteins are required in both uni- and multicellular eukaryotes to participate in the regulation of the process of cargo selection and concentration at the sites of exit from the ER. A special subset of proteins is needed to enter the board of a travelling anterograde vesicle, to ensure its proper targeting to an acceptor membrane. Specialized proteins localized to the destination compartment are also necessary to orchestrate a vesicle fusion with an acceptor membrane.

Proteins of the core secretory machinery are well conserved throughout evolution, as homologous COP II proteins from the yeast to man were identified. The *in vitro* reconstitution of mammalian ER vesicle formation was documented recently and found to correspond to that in yeast (Aridor et al., 1998). During vesicle formation, cargo proteins are concentrated into the budding vesicle, and ER resident proteins are selectively excluded (Balch et al., 1994; Mizuno and Singer, 1993). Two models can account for this process of cargo selection and concentration into the nascent vesicle. The first model proposes the existence of molecular sieves that allow only secretory molecules to selectively enter the vesicle. The yeast protein Shr3p could be such a sieve for a particular set of yeast proteins, the amino acid permeases (Kuehn et al., 1996). The second model postulates that vesicle coat components interact with putative cargo receptors to sort and concentrate cargo molecules. By interacting either directly with determinants found on secretory membrane proteins or indirectly with putative "cargo-receptors", the COP II coat would thus participate in both cargo-selection and bud formation (Kuehn and Schekman, 1997). The latter model recently received support from work carried out in yeast where it was shown that purified COP II components interact with vesicle integral membrane proteins and soluble cargo (Kuehn et al., 1998). Moreover, in mammalian cells the transmembrane VSV-G protein was selectively recruited into the forming vesicle by the pre-budding complex composed of Sar1p and Sec23-24p complex, but no direct interaction between the cytosolic portion of VSV-G with the Sec23-24p complex could be demonstrated (Aridor et al., 1998). Potential cargo receptors have been identified recently. One is the p24 family of transmembrane proteins found both in yeast and mammals. These proteins, located mainly between the ER and the Golgi apparatus, recycle between these organelles and are incorporated into both COP I and COP II vesicles (Belden and Barlowe, 1996; Fiedler et al., 1996; Dominguez et al., 1998). However, their role is still unclear, as p23 in particular appeared to be restricted to a structural role rather than in sorting (Rojo et al., 1997). In yeast, however, the deletion of members of this family delays the secretion of a subset of secretory protein (Belden and Barlowe, 1996; Schimmöller et al., 1995; Elrod-Erickson and Kaiser, 1996). But a deletion of all eight members of the family has no stronger phenotype than single mutations (Springer et al., 2000). The cytoplasmic tail of mammalian p24 proteins interacts with coatomer (COP I) (Fiedler et al., 1996), but it also binds specifically to the mammalian COP II component Sec23Ap via a di-aromatic motif (Dominguez et al., 1998). Putative anterograde signals include the di-phenylalanine (FF) motif (Fiedler et al., 1996), the carboxyl-terminal LV motif of the yeast Emp24p (Nakamura et al., 1998) and the DXE motif (Nishimura and Balch 1997), although the latter appears to mediate concentration rather than sorting per se (Nishimura et al., 1999). The members of the p24 family of integral membrane

proteins are the most abundant of the di-lysine- and di-phenylalanine-containing proteins of the early secretory pathway (Fiedler et al., 1996; Rojo et al., 1997; Dominguez et al., 1998), but it is still a debate whether the cytoplasmic tail of p24-related proteins represents the major binding site for COP I complex on donor membranes (Pavel et al., 1998; Bremser et al., 1999; Rojo et al., 2000).

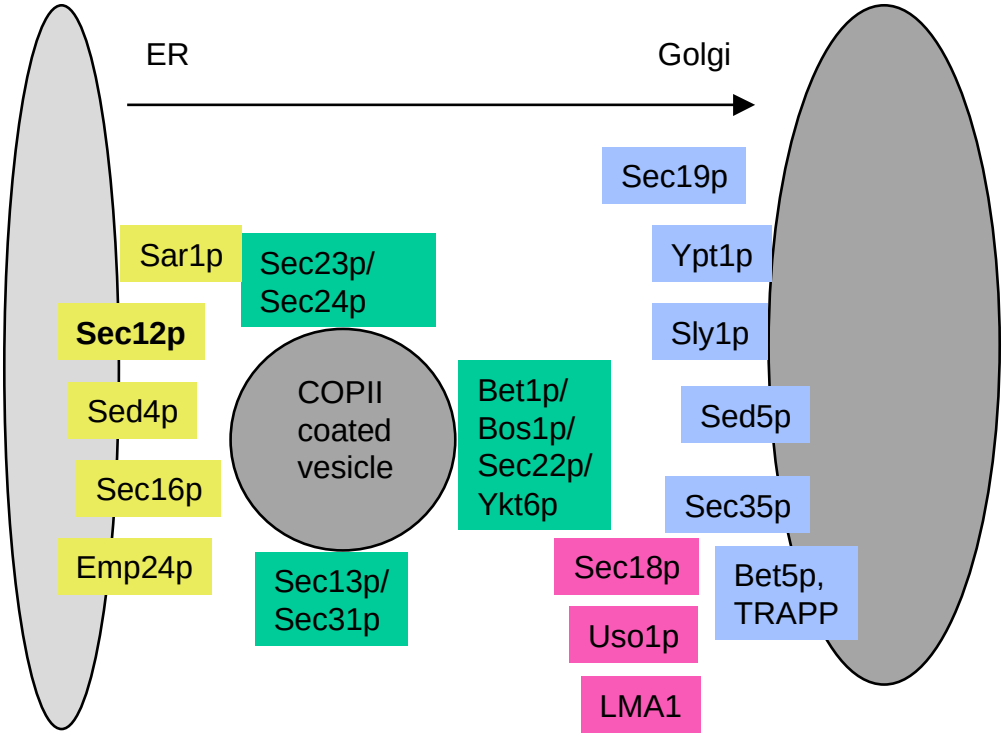


Fig. 1: Proteins involved in ER to Golgi transport
The membrane of the donor compartment in the ER-to-Golgi transport is loaded with proteins that function as cargo receptors (Emp24p) or drive the COP II vesicle formation (guanine nucleotide exchange factor Sec12p, small GTPase Sar1p). Additional factors participating in COP II vesicle budding are physically interacting proteins Sec16p and Sed4p (Gimeno et al., 1995). Membrane bound and activated Sar1p recruits the Sec23p/Sec24p complex and, finally, Sec13p/Sec31p complex binds to the membrane and forms a vesicle. Four of the yeast membrane proteins (Bet1p, Bos1p, Ykt6p and Sec22p) exhibit the basic properties of v-SNAREs by forming NSF (Sec18p) sensitive complexes with the Golgi-localized protein from t-SNARE family Sed5p. Bet1p, Bos1p and Ykt6p were shown to be v-SNAREs essential for the vesicle delivery from the ER to the Golgi (Newman et al., 1990; Shim et al., 1991; Dascher et al., 1991; McNew et al., 1997). Uso1p mediates the COP II vesicle docking whereas Sec18p and LMA1 are not required for the docking phase, but are required for efficient fusion of ER-derived vesicles with the Golgi complex (Barlowe, 1997). Together Sec18p, Uso1p and LMA1 (low molecular activity 1 protein complex composed of thiredoxin dimerized with IB2 (Xu and Wickner, 1996; Xu et al., 1997)) were shown to fully substitute for a crude yeast cytosol in catalizing ER-derived vesicle fusion with Golgi membranes in a cell-free assay (Barlowe, 1997). The genetic and biochemical results (VanRheenen et al., 1998) suggest that Sec35p acts with Uso1p to dock ER-derived vesicles to the Golgi complex. Sly1p, an essential member of the Sec1 protein family, together with Ypt1p, a member of Rab GTPase protein family, are implicated in the regulation of SNARE complex assembly. TRAPP (transport protein particle), a multiprotein complex containing ten subunits, was recently shown to play a key role in the targeting and/or fusion of ER-to-Golgi transport vesicles with their acceptor compartment in the yeast *Saccharomyces cerevisiae* (Sacher et al., 1998; Sacher et al., 2000). Sec19p is a GDP dissociation inhibitor that plays an essential function in the ER-to-Golgi membrane traffic and the recycling of proteins of the Sec4/Ypt/rab family from their target membranes back to their vesicular pools (Garrett et al., 1994).

Recently it has been demonstrated by Lavoie et al. (1999) that the p24 family member, α_2p24, and its cytosolic coat ligand, COP I coatomer, play a role in the de novo formation of VTCs and the generation of ER cargo exit sites in mammalian cell-free assay that reconstituted the generation of a nascent secretory apparatus from ER-derived low density microsomes (LDMs). Another potential candidate as cargo receptor is the mannose-specific lectin transmembrane molecule ERGIC-53. This protein cycles between the ER and the Golgi and is implicated in the forward transport of glycosylated proteins out of the ER (Itin et al., 1995; Vollenweider et al., 1998; Appenzeller et al., 1999). Its short cytosolic tail contains a KKFF retrieval motif (see below), which mediates its interaction with both the COP I complex (Schindler et al., 1993), and the mammalian Sec23-24p complex, via its di-phenylalanine motif (Kappeler et al., 1997).

1.1.2. COP I coat-mediated transport

As outlined before, vesicular retrograde transport has to occur to balance anterograde transport. It is clear that COP I coated vesicles are mediators of retrograde transport from the Golgi to the ER (Cosson and Letourneur, 1997). However, additional involvement of COP I in anterograde and/or retrograde transport at various transport steps has been suggested (Cosson and Letourneur, 1997) including (a) intra-Golgi anterograde transport, (b) intra-Golgi retrograde transport, (c) ER to Golgi anterograde transport, (d) Golgi to ER retrograde transport, (e) maintenance of Golgi function and structural integrity, and (f) endosome function and structure (COP I functions are classified according to Gaynor et al., 1998). Although the general mechanism of COP I-coated vesicle formation is quite well described (Schekman and Orci, 1996; Rothman and Wieland, 1996; Spang and Schekman 1998; Bremser et al., 1999), the specific roles of the individual COP I subunits in this process are not yet clear. COP I consists of coatomer, a complex composed of seven subunits (α-, β-, β'-, γ-, δ-, ε-, and ζ-COP (Waters et al., 1991; Stenbeck et al., 1992) and the small GTP-binding protein ARF, which may also be considered as a component of the coat (Serafini et al., 1991; Ktistakis et al., 1996; Stamnes et al., 1995) (Table 1.1).

Table 1.1: The seven yeast coatomer subunits

Molecular wieght, kDa	Subunit	Gene	Identified by
170	α	*RET1*	screen for retention mutants (Waters et al., 1991)
109	β	*SEC26*	Microsequencing (Duden et al., 1994)
99	β'	*SEC27*	genetical interaction with *SEC26* (Duden et al., 1994)
105	γ	*SEC21*	screen for secretion mutants (Hosobuchi et

			al., 1992)
61	δ	*RET2*	screen for retention mutants (Cosson et al., 1996)
34	ε	*SEC28*	high copy suppressor of *ret1-3* (Duden et al., 1998)
21	ζ	*RET3*	screen for retention mutants (Cosson et al., 1996)

Interestingly, COP I and the coat component of clathrin coated vesicles, can be viewed as equivalent. β-, γ-, δ-, and ζ-COPs correspond more closely to the AP subunits since they share sequence similarities, whereas α- and ε–COPs resemble clathrin heavy and light chains, respectively (Duden et al., 1991; Cosson et al., 1996). Additionally, both α- and β'-COPs contain N-terminal WD-40 motifs (Letourneur et al., 1994; Harrison-Lavoie et al., 1993), which may potentially mediate both protein-protein and protein-membrane interactions.

COP I-coated vesicles have been assembled stepwise from isolated Golgi membranes and the cytosolic components ADP-ribosylation factor 1 (ARF1) and coatomer (Ostermann et al., 1993) (Table 1.1). The initial step in COP I coated vesicles assembly involves recruitment of the small GTPase ARF1 in GTP-bound form. Activation of ARF by exchange of GDP for GTP is catalyzed by guanine exchange factors (GEF). Recruitment of ARF1 precedes the recruitment of the remaining coat subunits to the membrane. COP I coat bud formation is initiated by recruitment of preassembled coatomer (coat promoter) (Orci et al., 1993). This involves a direct interaction with membrane-bound ARF1-GTP and coatomer via its β-COP and γ-COP subunit (Zhao et al., 1997; Zhao et al., 1999) and results in clustering of ARF1-GTP and deformation of the membrane into a coated bud and subsequent scission. Fusion of the vesicles with their target membrane requires prior dissociation of the coat. This is achieved by GTPase activating proteins (GAP) that increase the rate of hydrolysis of GTP bound to ARF1 and leads to dissociation of ARF from vesicles thus destabilizing the coat. In the COP II system, Sec23p acts as GAP for Sar1p (Yoshihisa et al., 1993), whereas in the COP I system an ARF specific GAP is recruited to the membrane from the cytosol (Cukierman et al., 1995). In particular, two yeast ARF-GAPs, Gcs1p and Glo3p provide an essential overlapping function in retrograde Golgi-to-ER transport (Dogic et al., 1999; Poon et al., 1999). Efficient GTP hydrolysis by ARF/GAP was also found to depend on coatomer (Goldberg, 1999). Upon dissociation of the coat, vesicles can fuse with the target membrane.

1.1.3. COP I-dependent mechanisms of protein retention within the early secretory compartments

It has been proposed that different parts of COP I bind to distinct cytosolic signals to mediate sorting in different directions, such as α/β'/ε binding to di-lysine motifs for retrograde transport (Cosson and Letourneur, 1994; Fiedler et al., 1996; Lowe and Kreis, 1995) and β/γ/ζ binding to FF motifs for anterograde transport in the secretory pathway (Fiedler et al., 1996). However, other studies have shown that γ-COP can be crosslinked to KKXX motifs (Harter et al., 1996), and indirect evidence suggests that coatomer has at least two di-lysine binding sites (Hudson and Draper, 1997).

It has been proposed that the COP I coat mediates sorting and incorporation of cargo molecules into nascent vesicles through direct interactions with sorting determinants in the cytoplasmic tails of cargo proteins or indirectly through receptor proteins (Rothman and Wieland, 1996). Several sorting signals have been identified in the early biosynthetic pathway between the Golgi complex and the ER, including (a) the KKXX and KXKXX, or di-lysine, retrieval motifs for integral membrane proteins, (b) K/HDEL for soluble lumenal proteins of the ER (reviewed in Ref. Teasdale and Jackson, 1996), (c) unknown signal in the transmembrane domain of type-II membrane protein Sec12p (Boehm et al., 1994; Sato et al., 1996), and d) di-arginine motif in type II membrane proteins (Teasdale and Jackson, 1996). A direct interaction has been demonstrated for KKXX-containing proteins with COP I *in vitro* (Cosson and Letourneur, 1994), and COP I mutants in yeast are defective in the retrieval of KKXX- and KDEL-bearing proteins from the Golgi (Letourneur et al., 1994; Schröder et al., 1995; Lewis and Pelham 1996). However, according to recently obtained evidence (Andersson et al., 1999), certain variations of C-terminal KKXX sequences (for instance, KKAA motif) might mediate a direct nonsaturable retention of some mammalian di-lysine proteins in the ER-membranes in addition to indirect retention by saturable COP I coat-dependent retrieval from the post ER-compartments. The retention mechanism mediated by such di-lysine signals is currently unknown. The yeast protein Erd2p (and its mammalian homologue) was identified as a specific receptor for K/HDEL-signal containing proteins. As mammalian homologue of Erd2p was found enriched in COP I vesicles (Orci et al., 1997) and Golgi-to-ER retrieval of Erd2p was blocked in at least one COP I mutant (Lewis and Pelham, 1996), the receptor itself together with its K/HDEL-containing substrates was suggested to recycle in COP I vesicles. A Golgi-localized protein Rer1p was identified (Nishikawa and Nakano, 1993; Boehm et al., 1994) as a factor mediating the retention/retrieval of Sec12p (a guanine nucleotide exchange factor for Sar1p (Barlowe and Schekman, 1993)) via proposed interaction with the transmembrane domain of Sec12p (Sato et al., 1995). A specific mutant

allele of α-COP I subunit was isolated that exhibits specific defects in retrieval of both Rer1p and Sec12p but not di-lysine-containing proteins from the Golgi to the ER (Boehm et al., 1997). From the data presented above it is evident that the COP I complex drives the retrieval of at least three different classes of proteins along the Golgi-ER pathway.

The COP I coat was thought to be the only operational molecular system responsible for the cargo transport in the backward Golgi-to-ER direction until recent work of Girod et al. (1999), in which the existence of COP I-independent, but, instead, Rab6p-dependent pathway of Golgi-to-ER recycling for the Shiga toxin/Shiga-like toxin-1 and the Golgi-resident glycosylation enzymes was suggested (see also Storrie et al., 2000).

I will focus our attention, however, on di-lysine signal containing proteins as they provide a model for studying the COP I-mediated Golgi-to-ER retrograde transport.

1.1.4. Transport properties of the yeast di-lysine protein Emp47p resemble that of its mammalian homologue ERGIC-53

The two yeast di-lysine proteins Emp47p (characterized by Schröder et al., 1995) and Ylr080wp (an Emp47p homologue characterized in this study) share sequence homology to the mammalian protein ERGIC-53 (see review by Hauri et al., 2000), and to VIP36, which belong to a class of animal lectins structurally reminiscent of leguminous lectins of plants. The lectin ERGIC-53, a type-I transmembrane protein that cycles between the ER and the ERGIC (Klumperman et al., 1998), may operate as a cargo receptor (Fiedler and Simons, 1994; Itin et al., 1996). It was originally identified as a marker protein for the ERGIC (Schweizer et al., 1990) which is composed of a multitude of tubulovesicular clusters in the vicinity of the Golgi. Sequence analysis (Schindler et al., 1993) revealed that ERGIC-53 is identical to the mannose-specific membrane lectin MR60 (Arar et al., 1995). Although it was subsequently shown that ERGIC-53 binds mannose in a calcium-dependent manner due to a carbohydrate receptor domain (CRD) on its lumenal side (Itin et al., 1996), not a single precise ligand for ERGIC-53 has been determined for a long time. However, the results of the chemical crosslinking experiments carried out in hamster cells (Santamaria et al., 1998; Appenzeller et al., 1999) point to cathepsin-Z-related glycoprotein (catZr) as being a direct ligand for ERGIC-53. Notably, the crosslinking occurred in a carbohydrate- and Ca^{2+}-dependent manner.

ERGIC-53 contains determinants of a di-lysine ER-retrieval signal in its cytoplasmic domain (Schindler et al., 1993**)** and two phenylalanine residues at the C-terminus serve as an ER-exit determinant where the COPII coat component Sec23p might bind (Kappeler et al., 1997). Thus, ERGIC-53 continues recycling between the ER, ERGIC, and cis-Golgi

(Schindler et al., 1993; Kappeler et al., 1997). The recycling of ERGIC-53 seems to be required for efficient intracellular transport, because the mistargeting of ERGIC-53 to the ER impairs the secretion of a limited set of glycoproteins, for example, procathepsin C, but not of the majority of glycoproteins (Vollenweider et al., 1998). Moreover, Nichols et al. (1998) demonstrated that combined deficiency of factors V and VIII, which is an autosomal recessive bleeding disorder, results from mutations in the ERGIC-53 gene. The precise role of ERGIC-53 is still unknown, but these findings suggest that ERGIC-53 may function as a molecular chaperone for the transport of a specific subset of glycoproteins from the ER to the Golgi by recognizing not only oligomannosyl structure but also a specific common sequence within catZr, procathepsin C, factors V and VIII. According to Hauri et al. (2000) the following model for ERGIC-53 function was suggested. After synthesis, ERGIC-53 oligomerizes in the ER to form disulphide-linked homodimers and homohexamers or even higher-order assemblies (Vollenweider et al., 1998). Cysteine residues at positions 466 and 475 (counting from the N-terminus of the protein) were shown to drive the homoligomerisation of ERGIC-53 (Lahtinen et al., 1999; Appenzeller et al., 1999). Assembled ERGIC-53 then binds via its luminal CRD domain to some soluble glycoproteins in the ER-lumen in Ca^{2+}- dependent manner. The cargo-receptor complex is then actively recruited into COP II vesicles via direct interaction of cytosolic di-phenylalanine motif of ERGIC-53 with COP II coat proteins. In the ERGIC compartment, after cargo dissociation possibly due to a drop in Ca^{2+}-concentration, the di-lysine motif of ERGIC-53 is recognized by COP I coats that enables retrieval of ERGIC-53 to the ER for a next round of transport.

The nonessential type-I transmembrane protein Emp47p appears to be the yeast homologue of ERGIC-53 (Schröder et al., 1995). According to the YPD data-base, there is another, hitherto uncharacterized yeast homologue, the di-lysine protein Ylr080wp (45% of amino acid sequence identity with Emp47p). However, the putative CRD of Emp47p and Ylr080wp lack some residues known to be important for sugar binding properties of the ERGIC-53 class of animal lectins (Schröder et al., 1995; this study). This fact raises some doubts as to whether Emp47p and Ylr080wp have a lectin function. However, similar to ERGIC-53, Emp47p recycles through the early secretory pathway in *S.cerevisiae* (Schröder et al., 1995). Additionally, both di-lysine proteins ERGIC-53 and Emp47p were shown to localize to post-ER compartments at steady state as opposed to the ER-localisation of the majority of di-lysine proteins in yeast and mammals. In particular, it was demonstrated that the Golgi-localization of Emp47p at steady state is dynamically maintained by means of the protein's continuous recycling between the Golgi and the ER with the help of COP I retrieval machinery (Schröder et al., 1995). COP I might physically interact with the di-lysine motif of Emp47p *in vivo* as is

suggested by *in vitro* binding studies (Schröder-Köhne et al., 1998). A mutation in the structure and the position of di-lysine motif leads to mislocalization of Emp47p to the vacuole by the proposed default pathway for membrane proteins. Interestingly, the chimeric protein composed of the α-pheromone receptor Ste2p tagged at its C-terminus with the Emp47p di-lysine motif was found to be localized to the ER. Therefore, the di-lysine motif alone does not apparently possess all the information needed for the proper targeting of Emp47p. Additional features in the lumenal, transmembrane or cytoplasmic domains might possess localization determinants to account for the difference in the behaviour of native Emp47p with respect to Ste2-Emp47p-tail chimera. The Emp47p mislocalization to the vacuole is also achieved by mutations in any of the coatomer subunits, except α-COP (Schröder et al., 1995; Schröder-Köhne et al., 1998). Additional factors required for the proper localization and retrograde transport of Emp47p were the ER protein complex Sec20p/Tip20p (Cosson et al., 1997) and the ER t-SNARE Ufe1p, mutation in which prevents both the K/HDEL receptor and Emp47p from recycling to the endoplasmic reticulum (Lewis and Pelham, 1996). All the currently known molecular components pertaining to the Golgi-to-ER transport of the transmembrane protein Emp47p are summarized in the Fig. 2. Thus, compared to a multitude of factors known to ensure an orderly flow of the ER-to-Golgi forward transport (Fig. 1), the number of identified factors that orchestrate the retrograde Golgi-to-ER trafficking of cargo proteins appears to be relatively low.

One of the proposed functions for Emp47p in yeast (Schröder et al., 1995) is that of a receptor for the retrieval of certain glycoproteins, similar to the role of ERGIC-53. Although the *in vivo* and *in vitro* interacting partner for the lumenal part of Emp47p as well as the sugar-binding properties of its putative CRD remain unknown, the proposed model of Emp47p functioning as a transport receptor is highly compatible with the steady state and dynamic localization of the protein reported by Schröder et al. (1995). However, Emp47p is not essential for yeast growth and no influence of *EMP47* deletion on the secretory pathway and processing of some yeast glycoproteins was detected (Schröder et al., 1995). The effect of Emp47p could, however, be restricted to a subset of glycoproteins, which remained beyond the scope of previous studies (Schröder et al., 1995), or involve nonprotein molecules. Another possible function of Emp47p could be an assisstance in the operation of the ER-Golgi-localized quality control mechanism. The putative CRD of Emp47p could be tuned to sense incorrectly modified glycoprotein substrates in the cis-Golgi part of the secretory pathway and help to retrieve them to the ER for quality control examination by the calnexin/calreticulin system.

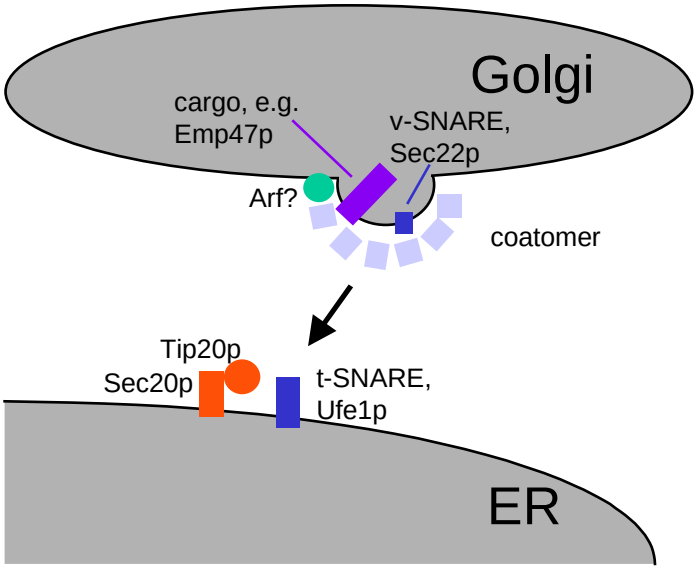


Fig.2: Known factors involved in retrograde transport
The Golgi-to-ER retrograde cargo proteins flow is mediated by the heptameric COP I coatomer complex that drives the retrograde vesicle formation on the Golgi membranes. At the initial step of COP I vesicle assembly, the GDP-to-GTP nucleotide exchange occuring on a small ARF GTPase molecule leads to an association of an activated form of ARF-GTP with the donor membranes and subsequent recruitment of cytosolic COP I components to the place of vesicle formation. COP I coat assembly induces the local changes in the donor membrane curvature facilitating the nascent vesicle budding and fission. Proteins of v-SNARE family like Sec22p as well as some putative cargo receptors like di-lysine protein Emp47p are probably selectively sorted by retrograde vesicle and subsequently delivered to the acceptor membranes of the ER. Additonally, the process of cargo-delivery to the ER by retrograde vesicle requires the presence of the t-SNARE protein Ufe1p and also depends on the ER-protein complex Sec20/Tip20.

Regardless of the function of Emp47p and its homologue Ylr080wp in yeast cells, both proteins exemplify good models for studying the factors required for the retrograde transport in yeast *S.cerevisiae*. Emp47p is especially suitable for such a purpose, because it resides in the Golgi, the starting point of the retrograde transport.

1.2. Cysteine and glutathione biosynthetic pathways in *Saccharomyces cerevisiae*: viewed from compositional and regulatory aspects

In yeast, as in other sulphate-reducing microorganism, reduced sulphate is used in the biosynthesis of organic sulphur metabolites such as cysteine, methionine, and S-adenosylmethionine (AdoMet or SAM). The first steps in the assimilation of sulphur atoms from inorganic sulphate sources requires sulphate activation that is achieved by adenylation. Adenylation lowers the electropotential of sulphate so that it can then be reduced by means of NADPH oxidation to sulphite and ultimately to sulphide (Siegel, 1975). Sulphide can be incorporated into carbon chains. This set of reactions composes the sulphate assimilation pathway (see Fig. 3). The last step of the sulphate assimilation pathway is catalyzed by Met25p and consists of the incorporation of sulphide into a carbon chain (Fig. 3).

The biosynthesis of cysteine in *S. cerevisiae* was unravelled by genetic analysis of two cysteine auxotrophs (*str1* and *str4*) that were unable to grow on methionine and homocysteine (Cherest and Surdin-Kerjan, 1992). *str1* and *str4* mutant cells lack cystathionine γ-lyase and cystathionine β-synthetase activity, respectively (Cherest and Surdin-Kerjan, 1992). As the inactivation of both *STR1* and *STR4* genes resulted individually in cysteine auxotrophy it was assumed that conversion of homocysteine into cysteine is the only means of de novo cysteine biosynthesis in yeast (Barton et al., 1993; Cherest et al., 1993). Subsequently *STR1* and *STR4* were shown to be equivalent to *CYS3* and *CYS4*, respectively (Ono et al., 1984; Ono et al., 1988; Ono et al., 1992). A prerequisite for the biosynthesis of homocysteine and subsequently cysteine is the activation of homoserine through esterification. In *S. cerevisiae*, homoserine *O*-acetyltransferase catalyzes a reaction in which one molecule of acetyl coenzyme A is consumed (Fig. 3). In *S. cerevisiae*, homoserine *O*-acetyltransferase is encoded by *MET2* (Cherest et al., 1969). Since *O*-acetylhomoserine is required for the synthesis of cystathionine from cysteine (Fig. 3), *met2* mutant is unable to grow on cysteine. For the same reason, as Met4p is the transcriptional activator of *MET2*, a *met4* mutant is unable to grow on cysteine. Homocysteine is the product of the *O*-acetylhomoserine sulfhydrylase reaction (Fig. 3). The amino acid composition of the purified enzyme corresponds to that of the deduced *MET25*-encoded product (Kerjan et al., 1986; Yamagata, 1976). Met25p has significant sequence similarity to the cystathionine γ-lyase (encoded by *CYS3*) from *S. cerevisiae* and rats. All these enzymes belong to one protein family and have probably evolved from an ancestral pyridoxal phosphate enzyme (Cherest et al., 1973).

The transsulfuration pathway consists of reactions that allow for the interconversion of homocysteine and cysteine via the formation of cystathionine intermediate (Fig. 3). In contrast to the transsulfuration pathways of enteric bacteria and mammals, in *S. cerevisiae* transsulfuration operates in both directions and involves two different sets of enzymes (Fig. 3). The synthesis of cysteine from homocysteine requires two successive steps, β addition (catalyzed by cystathionine β-synthetase (Cys4p)) and γ elimination (requires cystathionine γ-lyase (Cys3p)) (Fig. 3). In yeast *S. cerevisiae*, cystathionine γ-lyase is encoded by *CYS3*, whose mutation leads to a nutritional requirement for cysteine or glutathione (Cherest and Surdin-Kerjan, 1992; Cherest et al., 1993; this study).

The transsulfuration pathway in the reverse direction produces homocysteine out of cysteine and involves cystathionine γ-synthase and cystathionine β-lyase respectively catalyzing two successive steps (Fig. 3). To date, the enzymes of this pathway are unknown. Two genes that presumably encode cystathionine γ-synthase and cystathionine β-lyase were,

however, recently identified by genetic disruption (ORFs YJR130c and YGL184c), yielding yeast strains unable to convert cysteine into homocysteine (Hansen and Johannesen, 2000). De novo synthesis of methionine from homocysteine uses a methyl group, which originates from single-carbon metabolism involving the derivatives of tetrahydrofolate (THF) (Jones and Fink, 1982). Homocysteine methyltransferase catalyzes the transfer of activated methyl group to homocysteine thus giving yield to methionine (Fig. 3). This enzyme is encoded by *MET6* (Csaikl and Csaikl, 1986; Mountain et al., 1991).

In addition to methionine and cysteine synthesis, the sulfur pathway is responsible for the AdoMet biosynthesis (Fig. 3). AdoMet is second only to ATP in cellular metabolism for the variety and number of reactions, in which it participates as a cofactor (Cantoni, 1977).

Cystathionine γ-lyase (Cys3p) generates cysteine, a precursor of glutathione (GSH). The tripeptide glutathione (γ-glutamylcysteineglycine) is an abundant and ubiquitous low-molecular-mass thiol with a presumed role in many cellular processes, including protection of cells against carcinogens, xenobiotics, radiation and reactive oxygen species (ROS) (reviewed in Pennickx and Elskens, 1993; Sies, 1993; Carmel-Harel and Storz, 2000). GSH is synthesized in two ATP-dependent steps, catalyzed by γ-glutamylcysteine synthetase (Gsh1p) and glutathione synthetase (Gsh2p) respectively (Fig. 3). In the first rate-limiting step, Gsh1p catalyzes the formation of γ-glutamylcysteine from glutamic acid and cysteine (Kistler et al., 1990; Ohtake and Yabuuchi, 1991); and in the second step, Gsh2p catalyzes the ligation of glycine with the dipeptide (Grant et al., 1997). This mechanism of synthesis has two consequences: firstly, it is mRNA-independent, and secondly, the glutamic acid residue is joined in unusual peptide linkage of the γ-C-atom to the cysteine residue which is thought to protect GSH from proteolytic cleavage (Meister, 1988). In contrast to bacterial cells (Greenberg and Demple, 1986), in eukaryotes GSH is an essential tripeptide (Wu and Moye-Rowley, 1994; Grant et al., 1997). Recent findings of Spector et al. (2000) indicate that the gain-of-function mutations in the proline pathway are the only suppressors of the lethal phenotype of *gsh1Δ* strain. This suppression was shown to involve the biosynthesis of a small amount of GSH through a modified proline biosynthesis pathway.

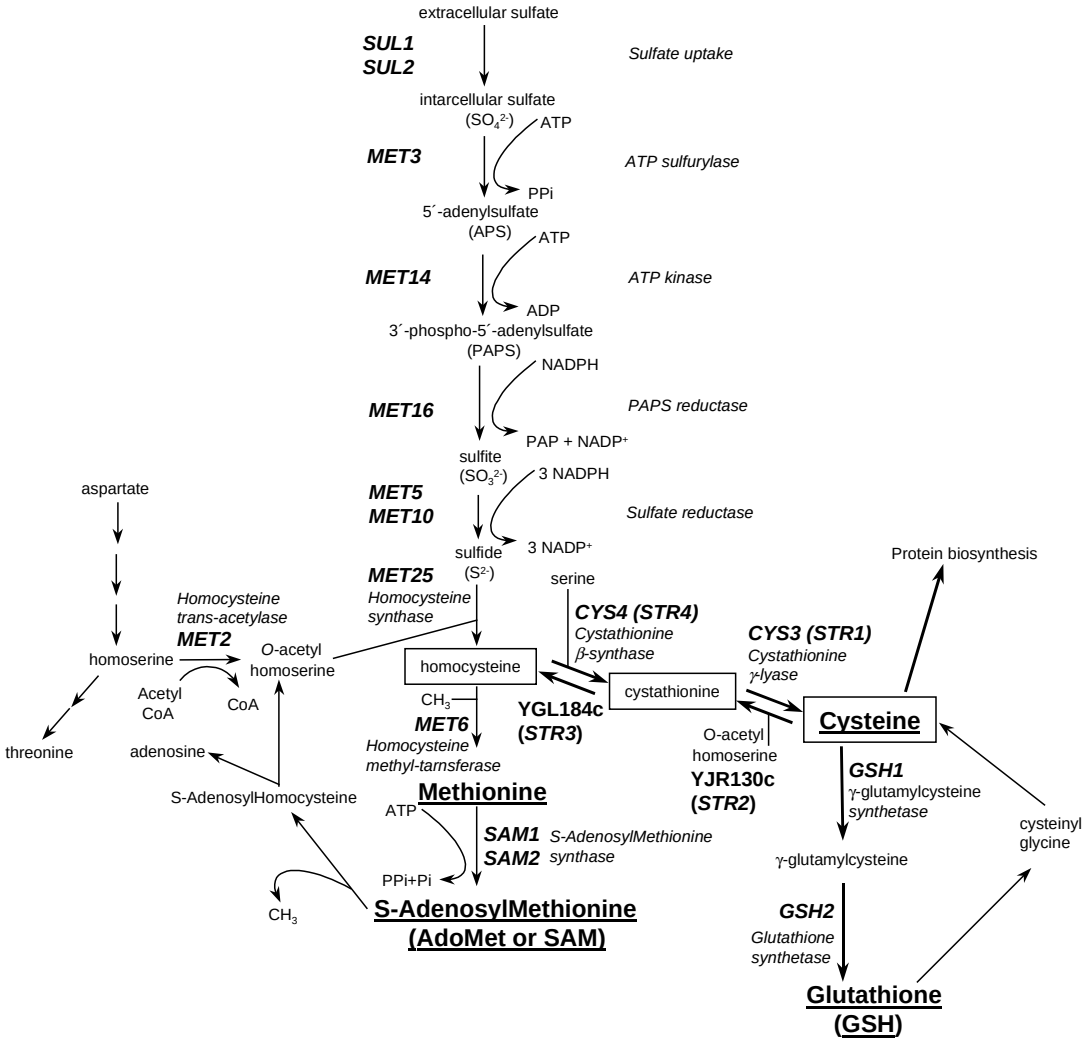


Fig. 3: Sulfur amino acid and glutathione biosynthesis in *S. cerevisiae*
The biosynthetic pathways of sulfur-containing organic compounds are represented according to review of Thomas and Surdin-Kerjan (1997) with an addition of the biosynthetic branch leading to glutathione and an indication of the enzymes involved in the reverse transulfuration pathway yielding homocysteine from cysteine (according to Hansen and Johannesen, 2000). Metabolic intermediates of the transsulfuration pathway are shown in black boxes. Physiologically most important terminal products of the sulfur-pathways are shown in bold and underlined.

The requirement of *S. cerevisiae* for sulfur may be fulfilled through uptake of sulfur-containing amino acids or through assimilation of inorganic sulfur into organic sulfur compounds such as methionine, cysteine or SAM (Fig. 3). The levels of required *MET* genes activities are regulated in response to intracellular concentrations of organic sulfur. In particular, it has been demonstrated in yeast that *MET2, 3, 5, 6, 10, 14, 16, 25, SAM1 and SAM2* are differentially repressed in their transcriptional activities by millimolar concentrations of methionine or SAM present in the growth medium (Cherest et al., 1985; Sangsoda et al., 1985; Baroni et al., 1986; Langin et al., 1986; Thomas et al., 1990; Korch et al., 1991; Mountain et al., 1991; Thomas and Surdi-Kerjan, 1991; Hansen et al., 1997). Although methionine and SAM were able to repress the activities of *MET* genes, it has been found recently that it is actually cysteine that is crucial for methionine- and SAM-mediated

repression to take place. Firstly, it was demonstrated that in strains deficient for Cys4p, *O*-acetylhomoserine sulfhydrolase activity was not repressed by addition of exogenous methionine (Paszewski and Ono, 1992; Ono et al., 1996). Moreover it was shown that cysteine, but not methionine, represses Cys3p in a *cys4* mutant (Ono et al., 1991). Secondly, it was shown that repression of *MET14* cannot be accomplished by SAM or methionine, if demethylated SAM cannot be converted into homocysteine (Hansen and Johannesen, 2000). Thirdly, the ability of methionine and cysteine to repress *MET14* and *MET25* transcription in yeast strains deficient for production of cysteine from homocysteine (*cys3Δ* and *cys4Δ*) as well as for biosynthesis of γ-glutamylcysteine (*gsh1Δ*) was investigated. The outcome of these studies (Hansen and Johannesen, 2000) was that, if cysteine formation is abrogated, cysteine but not methionine is repressive, whereas γ-glutamylcysteine formation is not important for methionine repression. Moreover, as repression of *MET* genes by cysteine was possible in yeast mutants incapacitated in the production of homocysteine from cysteine (*str2Δ* and *str3Δ* mutant conditions), cysteine alone (or some unknown derivative thereof), rather than SAM or methionine, was proposed to be the sole pathway-specific effector of *MET* genes repression (Hansen and Johannesen, 2000). Therefore according to Hansen and Johannesen (2000), the repressive effect of methionine or SAM on transcription of *MET* genes relies on the conversion of the latter through S-adenosylhomocysteine, to homocysteine, and further, via cystathionine, to cysteine (Fig. 3).

A key component in the transcriptional regulation of *MET* genes is the transcriptional activator Met4p and its associated cofactors Cbf1p, Met28p, Met31p and Met32p (reviewed in Thomas and Surdin-Kerjan, 1997). As has been shown by Patton et al. (1998) and Rouillon et al. (2000), the repression of Met4p-dependent transcription occurs in response to increased intracellular levels of SAM and is mediated by the SCF^{Met30} complex, an E3 ubiquitin ligase. Taken into account the above-discussed role of cysteine in the *MET* genes repression, it is important to note here that, although it is SAM that is always referred to as an intracellular effector of *MET* genes regulation (Patton et al., 1998; Patton et al., 2000; Rouillon et al., 2000), it is appropriate to assume that regulatory function of SAM or methionine is actually mediated by cysteine. When intracellular concentration of SAM is low (cysteine concentration is probably low too), Met4p-containing transcription activating complexes promote expression of the *MET* gene network, including *MET30*. Once expressed, Met30p targets Met4p for degradation via SCF^{Met30} and thereby limits *MET* gene expression in response to high intracellular SAM and methionine (Rouillon et al., 2000). Most striking and unexpected was the observation that misregulation of the genes under control of Met4p inhibits passage of yeast cell through cell cycle commitment point (Start) by preventing

accumulation of important G_1 phase transcripts coding for some G_1 cyclins (Patton et al., 2000). In particular, it was demonstrated that unregulated activity of Met4p under conditions of *MET30* deletion was sufficient to cause an enlargement of the cell size and G_1 growth arrest (Patton et al., 2000). Although the exact mechanism of the cell cycle arrest caused by the lack of activity degrading Met4p is not known, the important message of the studies on the *MET* gene regulation is in the disclosing of an existence of a close link between the sulfur amino acid metabolism and yeast cell progression through the cell cycle.

The following model developed out of the one proposed by Hansen and Johannesen (2000) might account for the accomplishment of a cysteine-mediated transcriptional control over the optimal production of cysteine, glutathione and SAM. Sulphate is turned into homocysteine, which is further converted into methionine, SAM and cysteine. As the preferred storage form of cysteine is glutathione (Elskens et al., 1991), the pool of it at some point will become full, resulting in high intracellular levels of cysteine. Cysteine then represses its own biosynthesis (via inhibition of *CYS3*) and further sulfur assimilation (by repressing the *MET* genes via Met30p-initiated targeting Met4p for degradation), thus saving energy and sparing yeast cells from intoxication by high cysteine levels (Ono et al., 1999). The sulfur atoms would be recycled between SAM, SAH, homocysteine and methionine (and possibly cystathionine), and sulfur atoms utilized in the form of amino acids for protein biosynthesis would be replaced through transsulfuration. When glutathione stocks are depleted due to protein biosynthesis and to utilization for other purposes (e.g. detoxification, ROS scavenging activity, resisting heating stress etc.), repression would be alliviated (due to upregulation of Met4p activity), and sulfur assimilation and formation of cysteine from homocysteine would re-initiate.

1.2.1. Essential role of glutathione and thioredoxins in yeast *S. cerevisiae*

The tripeptide glutathione (GSH) and the small protein thioredoxin are reductants in many cellular reactions. GSH is a widely conserved tripeptide with a highly reactive thiol and a very low redox potential of about –240 to –250 mV. GSH is maintained in its reduced state by NADPH-dependent glutathione reductase and reaches the concentration of up to 10 mM inside the cell. Therefore, GSH is considered the major molecule of a cellular redox buffer (reviewed in Meister, 1988). As a redox buffer, GSH plays a major role in maintaining a reducing cytoplasmic thiol disulphide balance. GSH is also important for enzymes, such as ribonucleotide reductase, performing catalytic reduction of their respective substrates (Holmgren, 1976). In these situations, electrons from GSH are generally transduced to their substrates through glutaredoxins (Fig. 4 A). GSH may protect protein sulfhydryls from

irreversible oxidation by glutathionylation (Thomas et al., 1990). GSH also participates in detoxification of peroxides, either directly or indirectly as a cofactor of glutathione peroxidase (Fig. 4 B) (Meister and Anderson, 1983; Jamieson, 1988), and of several chemicals such as cadmium (Li et al., 1997; Vido et al., 2000) and xenobiotics. For instance, if cells are invaded by xenobiotics, glutathione-S-conjugates are formed by glutathione S-transferase and the toxic conjugates are exported from cell cytoplasm to the vacuole by ATP-binding cassette transporter (Szczypka et al., 1996). Similarly, thioredoxin proteins act as disulphide oxidoreductases (Fig. 4 A) and as electron donors for thioredoxin peroxidases (Fig. 4 B) in both prokaryotic and eukaryotic cells. Glutathione disulphide (GSSG), which is formed upon oxidation, is reduced by glutathione reductase at the expense of NADPH (Fig. 4 A). Oxidized thioredoxin is reduced by thioredoxin reductase at the expense of NADPH too (Fig. 4 A). In both cases, NADPH is regenerated by glucose-6-phosphate dehydrogenase.

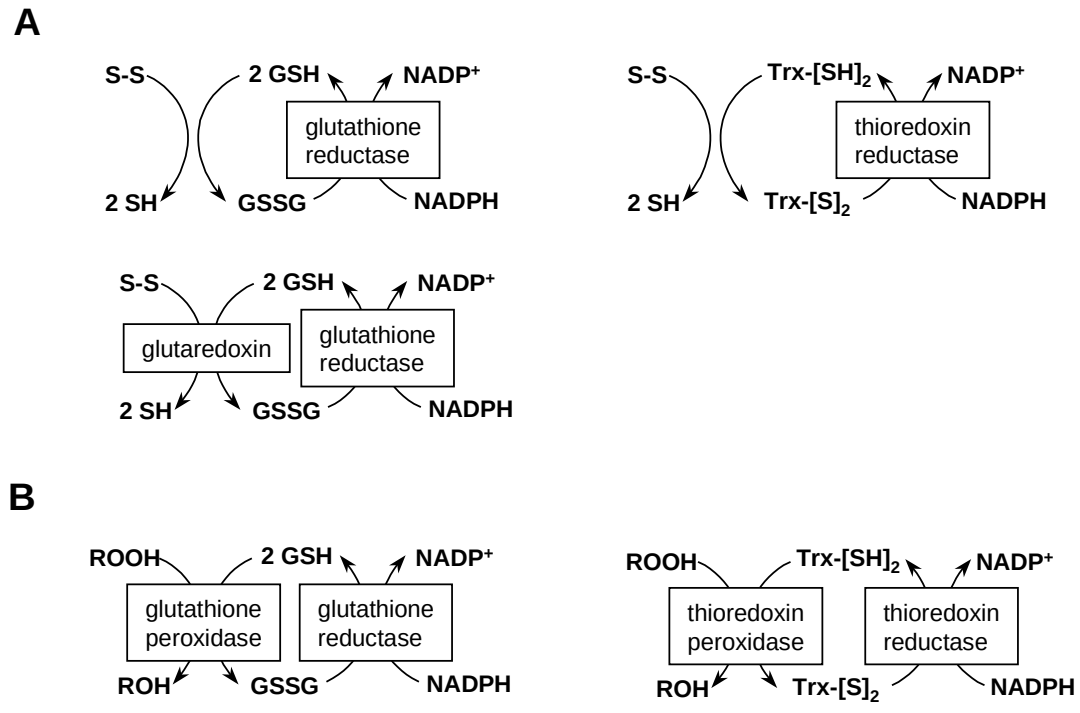


Fig. 4: Roles of glutathione (GSH)- and thiredoxin (Trx)-dependent reduction systems in Saccharomyces cerevisiae
A. Reduction of disulphide bond by GSH, by GSH together with glutaredoxin, and by Trx.
B. Peroxide elimination by GSH- or Trx-dependent peroxidases.

Given the GSH and thioredoxin requirements for disulphide bond reduction and for peroxidase activities, as well as the fact that GSH is the major cellular thiol, the GSH and thioredoxin-based systems have been proposed to protect cells against oxidative stress (Anderson and Meister, 1983; Spector et al., 1988). Oxidative stress occurs when cells are exposed to elevated levels of reactive oxygen species (ROS) such as superoxide (O_2^-),

hydrogen peroxide (H_2O_2), and alkyl hydroperoxides (ROOH). Oxidative stress can lead to DNA damage and mutations, lipid peroxidation, the disassembly of iron-sulfur clusters, disulphide bond formation, and other types of protein oxidation (reviewed by Jamieson, 1998). In eukaryotes, the electron-transport chain (respiratory chain) exists in mitochondria; therefore this organelle is a major source of ROS. The oxygen respiration rate of the yeast *S. cerevisiae* could be increased by heat-shock stress, which results in increased intracellular oxidation levels (Sugiyama et al., 2000). Therefore, heat-shock stress may result in oxidative stress. In addition to so-called *HSP* (heat shock protein) genes, several genes involved in antioxidant systems were found to be induced by heat shock in *S. cerevisiae*, such as *CTT1* (Wieser et al., 1991), encoding cytosolic catalase (Hartig and Ruis, 1986) and *TSA1* (Lee and Park, 1998), coding for thioredoxin peroxidase (Netto et al., 1996). Sugiyama et al. (2000) reported also that expression of *GSH1* and *GSH2* in *S. cerevisiae* was induced by heat shock and consequently intracellular GSH content was increased. It has also been demonstrated that one of the important physiological roles of induction of GSH synthesis by heat shock in yeast is to protect the mitochondrial DNA from oxidative damage and that GSH can partially suppress cell death induced by heat shock (Sugiyama et al., 2000).

As has been described in the previous chapter, glutathione biosynthesis requires *GSH1* and *GSH2* gene products. *gsh1* mutants are hypersensitive to hydrogen peroxide, whereas *gsh2* are insensitive to this and other oxidative agents (Grant et al., 1997). These phenotypes indicate that γ-glutamylcysteine can be a substitute antioxidant for glutathione. In compliance with its main role in oxidative stress response, only *GSH1* is induced by oxidants (Stephen et al., 1995). The transcriptional factor Yap1p mediates both basal and hydrogen peroxide-induction of *GSH1* (Stephen et al., 1995). In addition, *gsh1* mutants are unable to grow on non-fermentable carbon sources, suggesting an essential role for glutathione in protecting mitochondria from ROS produced by respiration (Moradas-Ferreira et al., 1996). Moreover, null mutations in *GSH1* result in GSH auxotrophy, demonstrating that GSH is essential in yeast (Wu and Moye-Rowley, 1994; Grant et al., 1996). However, GSH is not essential in bacterial cells (Miranda-Vizuette et al., 1996). The reason for the absolute requirement of GSH in eukaryotes is not known. However, it is likely that this essential function is not related to ribonucleotide reduction since *gsh1Δ* arrests in G_1 with predominantly unbudded cells, but not in S-phase (Spector et al., 2000). The GSH auxotrophy of *gsh1Δ* is also not due to a defect in sulphate assimilation since methionine and cysteine cannot rescue growth defect of *gsh1Δ* (Spector et al., 2000). What could then be the essential function of GSH in yeast? This essential function is clearly dependent on the redox properties of GSH since it can be replaced by a thiol, such as DTT (Grant et al., 1996), but not by a GSH analog with a methyl

group instead of thiol. Since GSH is reductant for glutaredoxins, and glutaredoxins are also essential (Rodriguez-Manzaneque et al., 1999), their essential functions might be the same. Therefore a search for the cellular targets of glutaredoxins might help in understanding the essential requirement for GSH in yeast.

Most glutaredoxins (Grx) and all thioredoxins (Trx) and thioredoxin-reductase (Trr) contain a conserved motif of two cysteines separated by two amino acids (CXXC) at their active sites. Besides GSH, thioredoxin is also a major redox buffer in the yeast cells. In general, thioredoxins are better disulphide bond reductants than glutaredoxins. In a reduced state, the dithiol group of the active site of thioredoxin is able to catalyze the reduction of disulphides in a number of proteins. The thioredoxin system is composed by thioredoxin, thioredoxin reductase and NADPH and in yeast there are two such systems, one in the cytoplasm with two thioredoxins (Trx1p and Trx2p) and one thioredoxin reductase (Trr1p) and a second in the mitochondria with one thioredoxin (Trx3p) and one thioredoxin reductase (Trr2p) (Pedrajas et al., 1999). Besides defects in cell cycle and methionine/cysteine metabolism (Muller, 1991), deletion of *TRX1* and *TRX2* causes sensitivity to various peroxides (Mouaheb et al., 1998; Lee et al., 1999) and also results in an elevated level of GSSG (Muller, 1996), indicating a link between the thioredoxin system and the redox status of GSH in the cell. Both *TRX2* and *TRR1* are induced by oxidative stress in a Yap1p- and Skn7p-dependent manner (Morgan et al., 1997).

1.3. The aims of the research work

1. A novel genetic screen for the mutants affected in retrograde transport.

The majority of the constituents of the retrograde trafficking in yeast were identified in a screen for the mutants mislocalizing α-factor receptor with an engineered di-lysine motif to the plasma membrane (Letourneur et al., 1994). Thus, mutants were uncovered affected in components of COP I coatomer. Additionally, the ER-protein complex Sec20p/Tip20p (Cosson et al., 1997), t-SNARE Ufe1p (Lewis and Pelham, 1996), small GTPase ARF and a pair of recently identified ARF-GAPs (Dogic et al., 1999; Poon et al., 1999) complete the list of known so far factors involved in the backward Golgi-to-ER transport. That situation characterized by low number of factors (a bit more than 10) known to mediate the retrograde pathway stands in clear contrast to the abundance of the proteins (around 30 factors) driving the forward ER-to-Golgi transport. Therefore, a novel genetic screen was initiated for the identification and characterization of the new mutants influencing the retrograde transport of the di-lysine signal-containing reporter protein Emp47p. The following considerations served

as the conceptual basis of the screen. A mutation in the di-lysine signal of Emp47p abolishes its recycling and leads to the mislocalization of the protein to the vacuole (possibly via the postulated „default"-transport for the membrane proteins to the vacuole (Roberts et al., 1992)). The escaped protein is rapidly degraded in the vacuole ($t_{1/2,\ 30^oC}$ =0.8 hr). The half-life time-value of wild-type Emp47p is approximately six-times higher than that of the „tail"-mutant ($t_{1/2,\ 30^oC}$ =5 hrs) (Schröder et al., 1995). It was expected that some mutations in the machinery recognizing the di-lysine signal of Emp47p would have the same effect on the localization of the reporter protein as mutations in the di-lysine signal, namely disruption of the Emp47p Golgi-localization and transport of the protein to the vacuole for rapid degradation by vacuolar proteases. The aim of my work was to develop a new screen that may uncover additional mutants. The following approach was used. The EMS-mutagenized colonies are transferred to the nitrocellulose filter-membrane (colony-blot assay, Lyons and Nelson, 1984), lysed and the Emp47p content is then probed with the specific antibodies reactive with Emp47p. Among those mutants, characterized by a specifically lowered Emp47p content, some could be affected in the retrograde transport of the di-lysine reporter protein and, thus, be interesting for further studies involving identification of the mutant gene with subsequent analysis of biochemical and molecular biological properties of its product.

2. Characterization of the subcellular localization of Ylr080wp and its function in the secretion

Ylr080wp is 45% identical to Emp47p and posesses the same set of structural features as Emp47p (Fig. 5). It is tempting to suppose therefore, that the two proteins might have an overlapping and partially redundant intracellular function. That assumption would explain why no specific phenotype has so far been found for the Emp47p deficient yeast strains. We approached the problem of elucidating the function of Ylr080wp and Emp47p by constructing the corresponding double deletion mutant and assaying the invertase secretory routes and its Golgi-conferred glycosylation pattern. It was also important to show firstly that the structural homology existing between the pair of di-lysine proteins goes along with similarities in their respective intracellular localizations and ways of recycling. Consequently, I analysed the dynamics of intracellular amounts, localization and transport properties of Ylr080wp in comparison to Emp47p.

2. Materials

2.1. Yeast and bacteria strains

Saccharomyces cerevisiae:

Strain	Genotype	Source
RH448	*MATa, leu2, ura3, lys2, his4, bar1*	H. Riezman, Basel, Switzerland
RH732	same as RH448, but *pep4::URA3*	H. Riezman, Basel, Switzerland
AMY2	*MATa, cys3-2, leu2, ura3, lys2, his4, bar1*	This study, derived from RH448
AMY3	same as AMY2, but *pep4::URA3*	This study, derived from AMY2 and RH732
AMY4	same as AMY2, but *cys3-2::CYS3*	This study
49	same as RH448, but *cys3-3*	This study
651	same as RH448, but *cys3-4*	This study
712	same as RH448, but *cys4*	This study
712-D	same as 712, but *pep4::URA3*	This study
748	same as RH448, but *htl1-1*	This study
748-D	same as 748, but *pep4::URA3*	This study
623	same as RH448, but *htl1-2*	This study
623-D	same as 623, but *pep4::URA3*	This study
81	same as RH448, but *yef3*	This study
81-D	same as 81, but *pep4::URA3*	This study
412	same as RH448, but *sec27*	This study
119	same as RH448, but lesion in chromosome VI, residue 104221 to 110828	This study
119-D	same as 119, but *pep4::URA3*	This study
BY4742	*MATa, his3D1, leu2D0, lys2D0, ura3D0, YJL101c::kanMX4*	Euroscarf yeast strains collection
C181	*MATα, ade2, his3, leu2, trp1, ura3, str1(=cys3)::URA3*	Y. Surdin-Kerjan (Gif sur Yvette, France)
MLY-101	*MATα, ura3, ade2, his, trp1, ufe1::TRP1*, including pUT1	Mike Lewis
359-7D 2688	*MATa, sec27, his4, ura3, leu2, bar1*	S. Schröder-Köhne
1436	*MATa, sec23, his4, leu2, ura3, bar1*	S. Schröder-Köhne
3609	same as 2688 but *pep4::URA3*	S. Schröder-Köhne
239-5C 1469	*MATa, sec21, ura3, his4, leu2, lys2 ,bar1*	Linda Hicke
2047	same as 1469 but *pep4@::URA3*	S. Schröder-Köhne
PC130 3440	*MATa, leu2, ura3, his4, lys2, suc2, ret2-1* (ts; deltaCOP)	Pierre Cosson
3441	same as RH3440 but *pep4::URA3*	S. Schröder-Köhne
FLY89	*MATa, ret3-1 (ts,zeta-COP) ura3*	François Letourneur

3449	*leu2 his3 trp1 suc2@9*	
585-9B 3187	*MATa, ret1-1, ura3, leu2, trp1, his, BAR1*	S. Schröder-Köhne
PC139 10002	*MATa, sec20-1, tip1-5, ura3, leu2, his4 lys2, trp1, suc2Δ*	Pierre Cosson
PC137 10000	*MATa, tip1-5, ura3, leu2, his4, lys2, trp1, suc2Δ*	Pierre Cosson
PC138 10001	*MATa, tip1-8, tip1-5, ura3, leu2, his4, lys2, trp1, suc2Δ*	Pierre Cosson
3045	same as RH448 but *emp47::lys2*	S. Schröder-Köhne
2825	same as RH732 but *emp47::LYS2*	S. Schröder-Köhne
10044	same as 2825 but *ylr080w::kanMX4*	This study
10045	same as RH448 but *ylr080w::kanMX4*	This study
10053	same as RH732 but *ylr080w::kanMX4*	This study
732-M	same as RH732 but *ylr080w::myc-YLR080W*	This study
3605	*MATα, ura3, leu2, mycEMP47::LEU2*	S. Schröder-Köhne

Escherichia coli:

Strain	Genotype	Source
DH5α	*F^-/endA, hsdR17(rk^-m^+), supE44, thi-1, recA1, gyrA1 (Nal^r), relA1 Δ(lacZYA-argF), U169 (m80lacZΔM15)*	Gibco BRL, Eggenstein

2.2. Plasmids

Plasmid	Description	Source
pBS KS(+)	cloning vector	Stratagene, San Diego, USA
pRS315	Centromeric *LEU2* yeast vector	Sikorski and Hieter, 1989
pRS202	2µ, *URA3* yeast vector	R. Sikorski
pRS326	2µ, *URA3* yeast vector	Sikorski and Hieter, 1989
pFA6a-*kanMX4*	amp^r (*E. coli*), contains *kanMX4* module for gene disruption in *S.cerevisiae*	Wach et al., 1994
pUT1	*ufe1-1, LEU2, CEN6, ARSH6*	Mike Lewis
pYIplac128	*amp^r* (*E. coli*), *LEU2* (Yeast)	Gietz and Sugino, 1988
URA3/2µ library	Yeast genomic library (*Sau3A* fragments (6-8 kb) cloned into pRS202 digested with BamH I/Bgl II).	Dieter Gallwitz, Goettingen
2µ-*CYS3*	pRS202-X(937); a yeast genomic library plasmid	This study

	that rescues ts-phenotype and cysteine auxotrophy of the mutants #937, #651, #49. Contains a 2.7 kbp fragment of chromosome I (nucleotide 129954-132702) that encompasses complete sequence of *CYS3*.	
pRS326-*CYS3*	pRS326(Sma I)-*CYS3*(*Nsi I*); genomic fragment (*Nsi I*).	This study
PB-SK(+)-*CYS3*	PB-SK(+)-*CYS3;* 1,3kb PCR-fragment (*Hind III*).	This study
PB-SK(+)-*cys3-2*	PB-SK(+)-*cys3-2;* 1,3kb PCR-fragment (*Hind III*).	This study
pRS202-X(119)	pRS202-X(119); a yeast genomic library plasmid that rescues ts of the mutant #119. Contains a fragment of Chromosome VI (residue 104221 to 110828).	This study
pRS202-X(81)	pRS202-X(81); a yeast genomic library plasmid that rescues ts of the mutant #81. Contains a fragment of Chromosome XII (residue 634246 to 640395)	This study
pRS326-*YLR249w*	pRS326(*Xho I/Sac I*)-*YLR249w*(*Xho I/Sac I*); contains complete ORF (*YLR249w)* for YEF3.	This study
pRS202-X(748)	pRS202-X(748); a yeast genomic library plasmid that rescues ts of the mutant #748. Contains a fragment of Chromosome III (residue 152364 to 158938) that encompasses complete ORF (*YCR020W-B*) for Htl1p.	This study
pRS326-*YCR020W*-B	pRS326(*Cla I/Sma I*)-*YCR020W*-B(*Cla I/EcoR VI*), contains complete ORF (*YCR020W-B*) for Htl1p.	This study
pRS202-X(623)	pRS202-X(623); a yeast genomic library plasmid that rescues ts of the mutant #623. Contains a fragment of Chromosome III (residue 154681 to 161414) that encompasses complete ORF (*YCR020W-B*) for Htl1p.	This study
pRS202-X(712)	pRS202- X(712); a yeast genomic library plasmid that rescues ts and cysteine auxotrophy of the mutant #712. Contains a fragment of Chromosome VII (residue 795786 to 800452) that encompasses complete ORF (*YGR155w*) for Cys4p.	This study
pPLA1	pB-SK(+)(*EcoR V*)-*YLR080W* (*Pvu II/Sca I*); *YLR080W* was PCR-amplified from genome with primers PlaN5´/PlaN3´, digested with *Pvu II/Sca I* and cloned to pB-SK(+)(*EcoR V*).	This study
pPLA2	pB-SK(+)(*EcoR I*-destroyed)-*YLR080W*; derived from the pPLA1 by *EcoR I* digestion, flushing the ends with Klenow fragment of DNA-polymerase I and religation of blunt-ends with T4 DNA-ligase.	This study
pPLA3	pB-SK(+)(*EcoR I*-destroyed)-*YLR080W* (*EcoR I*-introduced;L(F)); derived from the pPLA2 by	This study

	Pfu-polymerase-dependent PCR-amplification (Quick change™ reaction) with oligonucletides STS37/38.	
pPLA4	pB-SK(+)-*mycYLR080W*; myc-epiope was introduced to *YLR080W* by digesting pPLA3 with *EcoR I*, annealing with oligonucletides STS39/40 and ligating. Right orientation of myc-epitope was checked by triple digestion with *EcoR I, Nde I, Nco I*.	This study
pPLA5	pRS315(*Sal I/Not I*)- *mycYLR080W* (*Sal I/Not I*); *mycYLR080W* –fragment (*Sal I/Not I*) was excised from pPLA4 and cloned to pRS315 vector (*Sal I/Not I*).	This study
pPLA6	pYIplac128(*Xba I/Sal I*)- *mycYLR080W* (*Xba I/Sal I*); *mycYLR080W*–fragment (*Xba I/Sal I*) was excised from pPLA5 and cloned to pYIplac128 vector (*Xba I/Sal I*).	This study
pPLA-SS	pB-SK(+)-*mycYLR080W*-SS; two codons for C-terminal serine residues were introduced to *mycYLR080W* sequence by Pfu-polymerase-dependent PCR-amplification (Quick change™ reaction) of pPLA4 with oligonucletides STS45/46.	This study
pRS315-SS	pRS315(*Sal I/Not I*)- *mycYLR080W*-SS (*Sal I/Not I*); *mycYLR080W*-SS–fragment (*Sal I/Not I*) was excised from pPLA-SS and cloned to pRS315 vector (*Sal I/Not I*).	This study
pRS315-QQ	pRS315- *mycYLR080W*-QQ; K(-5)Q and K(-3)Q a.a. substitutions were introduced to myc-Ylr080wp sequence by Pfu-polymerase-dependent PCR-amplification (Quick change™ reaction) of pPLA5 with oligonucletides STS43/44.	This study
pRS315-Q	pRS315- *mycYLR080W*-Q; K(-3)Q a.a. substitution was introduced to myc-Ylr080wp sequence by Pfu-polymerase-dependent PCR-amplification (Quick change™ reaction) of pPLA5 with oligonucletides STS41/42.	This study

2.3. Oligonucleotides

Name	Nucleotide sequence	Purpose
T3	5´-ATT AAC CCT CAC TAA AG-3´	T3 sequencing primer
T7	5´-AAT ACG ACT CAC TAT AG-3´	T7 sequencing primer
K2	5´-CCT AGC AAG ATT TTA AAA GG-3´	Kanamycin gene primer
K3	5´-AAA ATA TTG TTG ATG CGC T-3´	Kanamycin gene primer
AM1	5´-TTT TTT AAG CTT ATA CAT ATA CAC ACA	For PCR-

AM2	AGA CAA AAC C-3´ 5´-CCC CCC AAG CTT AAA AAG GTC CGG TCG AAG GCA GAG ACG-3´	amplification from the genome and for sequencing of both *cys3-2* and *CYS3*
AM3 AM4	5´-CGT TGT CCA CTC CGC TAC AAA GTA CAT CAA CGG-3´ 5´-ATT-AGT GGC CAG GAC ACC GAG CAC AAC GTC TG-3´	For sequencing of both *cys3-2* and *CYS3*
STS32 STS33 STS34 STS35 STS36	5´-TAT TAC AAC ATT AAC AGG-3´ 5´-TTC ACA ATG GAC TTT GGG-3´ 5´-AAT ACC AGG ATT CCA TGG-3´ 5´-AAA AGA TGA ACA AGT TGG-3´ 5´-TAT GGT TGG CAC TGC TG-3´	For sequencing *YLR080W*
STS37 STS38	5´-G AAG GAT GAA TTC AAA TGG AAT AAA GG-3´ 5´-CC TTT ATT CCA TTT GAA TTC ATC CTT C-3´	For creating *EcoR* I restriction site in *YLR080W* sequence by QuickChange™ PCR-reaction
STS39 STS40	5´-AAG GAT GAA TTA GAA CAA AAG TTG ATT TCT GAA GAA GAC TTG AAC GAA TTC AAA-3´ 5´-TTT GAA TTC GTT CAA GTC TTC TTC AGA AAT CAA CTT TTG TTC TAA TTC ATC CTT-3´	For tagging with c-myc-epitope and destroying *EcoR* I restriction site in *YLR080W*
STS41 STS42	5´-ATC AAG AAG GTC CAA CTT CTG TAA GC-3´ 5´-TTA CAG AAG TTG GAC CTT CTT GAT GTC-3´	For introducing K(-3)Q a.a. exchange in di-lysine motif of Ylr080wp by QuickChange™ PCR-reaction
STS43 STS44	5´-ATC AAG CAG GTC CAA CTT CTG TAA GC-3´ 5´-TTA CAG AAG TTG GAC CTG CTT GAT GTC-3´	For introducing K(-5)Q and K(-3)Q a.a. exchange in di-lysine motif of Ylr080wp by QuickChange™ PCR-reaction
STS45 STS46	5´-GTC AAA CTT CTG AGT TCC TAA GCT CTT GTG TC-3´ 5´-GA CAC AAG AGC TTA GGA ACT CAG AAG TTT GAC C-3´	For introducing two serine residues right after di-lysine motif of Ylr080wp by QuickChange™ PCR-reaction
PlaN5´ PlaN3´	5´-CCT TTG CAT CAG CTG AAC TGG-3´ 5´-GTT TGA TGC AAA GTA CTT GCC-3´	For PCR-amplification of *YLR080W* from genome
PLA444-5´ PLA444-	5´-CAT ATT TCA TTG TAG TAT TTC GTC AAA GCG AGT TAG GGG AGG CGT ACG CTG CAG GTC GAC-3´ 5´-TAT CTT GTA CCC ATA TAA CAA AGA CAC	For PCR-amplification of *KanMX4* with subsequent utilization of the

3´	AAG AGC TTA CAG AAG ATC GAT GAA TTC GAG CTC G-3´	resulting PCR-product in short-flanking-homology protokol of EUROFAN aimed at creating a deletion in *YLR080W*
5´check	5´-TAT TAC AAC ATT AAC AGG-3´	For use in analytical PCR in conjunction with K2-primer to verify the substitution of *YLR080W with KanMX4* cassette
3´check	5´-TTA ACA GTT GAT TTT CCC-3´	For use in analytical PCR in conjunction with K3-primer to verify the substitution of *YLR080W* with *KanMX4* cassette

2.4. Antibodies

Monoclonal mouse anti-c-myc-antibodies 9E10 (Cambridge Research Biochemicals Ltd., Cheshire, GB); Peroxidase-conjugated secondary antibodies (sheep-anti-rabbit Ig) (Amersham Buchler, Braunschweig); Peroxidase-conjugated secondary antibodies (donkey-anti-rabbit Ig) (Amersham Buchler, Braunschweig); Peroxidase-conjugated secondary antibodies (sheep-anti-mouse Ig) (Amersham Buchler, Braunschweig); polyclonal secondary anti-mouse-(Cy2) and anti-rabbit-(Cy3) (Dianova, Hamburg); polyclonal rabbit anti-Emp47-antibodies (‘anti-luminal’ serum (Schröder 1995); polyclonal rabbit anti-Rer1p-antibodies (H. D. Schmitt, Göttingen); polyclonal rabbit anti-CPY-, -Yip1p-, -Sed5p-antibodies (D. Gallwitz, Göttingen); polyclonal rabbit anti-Gas1p-antibodies (H. Riezman, Basel, Switzerland); polyclonal rabbit anti-Sso1p/Sso2p-antibodies (E. A. Craig, Madison, WI); polyclonal rabbit anti-δ-COP-,-Hexokinase-antibodies (this study); polyclonal rabbit anti-Kar2p-antibodies (R.Schekman, Berkley, CA).

2.5. Enzymes and Kits

β-glucuronidase/arylsulphatase out of *Helix pomatia* (Boehringer, Mannheim). Zymolase-6000 out of *Arthrobacter luteus* (Seikagaku Kogyo Company, Tokyo). Lyticase (Grade: „partially purified“) from *Arthrobacter luteus* (Sigma, Deisenhofen). Restriction

endonucleases and DNA-modifying enzymes (Boehringer, Mannheim and New Englands Biolabs, Schwalbach), Taq-DNA-polymerase (Perkin Elmar), Vent-DNA-polymerase and Deep-Vent-DNA-polymerase Thermococcus litoralis (New Englands Biolabs, Schwalbach). Ribonuclease A (*Sigma*, Deisenhofen). Phospholipase A_2 from bee venom (Apis mellifera) (Sigma, Steinheim). QuickChange^{TM} site-directed mutagenesis kit (Stratagen, CA) QIAquick Gel Extraction Kit (Quiagen, Düsseldorf). ECL-Western blotting detection reagents (Amersham Life Science, UK).

2.6. Media components

Bacto-Agar, Bacto-Peptone, Bacto-Tryptone, Bacto-Yeast-Extract and Bacto-Yeast Nitrogen Base w/o Amino Acids (Difco, Detroit, MI, USA). Oxoid Agar, Bacteriological Agar No.1 (Oxoid Basingstoke, UK). Adenine-sulphate and Uracil (Merck AG, Darmstadt). Amino acids (L-Histidine-HCl, L-Leucine, L-Lysine, L-Tryptophan, L-Cysteine, L-Methionine) (Serva, Heidelberg). Glutathione in reduced and oxidised (disodium salt) forms (Sigma, Steinheim). Ampicillin (sodium salt) (Appli Chem, Biolith Diagnostica, Göttingen). Cycloheximide (CHX) (Sigma, Steinheim). Geneticin (GibcoBRL Life Technologies) and Kanamycin (Serva, Heidelberg). 5-fluoro-orotic-acid (5-FOA) (WAK Chemie Medical GmbH). 1-chloro-2, 4-dinitro-benzene (Merck AG, Darmstadt).

2.6.1. Growth media for *E. coli*

Full medium (L-Broth-Medium)	5 g/l yeast-extract 10 g/l tryptone 5 g/l NaCl 5 ml/l 1 N NaOH
Selective medium	L-Broth-Medium with 50-100 mg ampicillin

2.6.2. Growth media for *S. cerevisiae*

Full medium (YPUAD)	10 g/l yeast-extract 20 g/l peptone 20 g/l D-glucose
PM-glucose medium	20 g/l peptone 20 g/l D-glucose 6,5 g/l yeast nitrogen base
Minimal medium (SD)	6,5 g/l yeast nitrogen base 20 g/l D-glucose 20 mg/l adenine-sulphate 20 mg/l uracil 20 mg/l L-tryptophan 20 mg/l L-histidine-HCl 30 mg/l L-leucine

	30 mg/l L-lysine-HCl

Corresponding agar plates were prepared by adding 20 g of agar per 1 liter of liquid medium.

2.7. Chemicals

Bovine serum albumin (BSA), 2‘-deoxynucletides (dATP, dTTP, dCTP, dGTP), Ptotease inhibitor cocktail, Pefablock (Boehringer, Mannheim). Protein molecular weight standard marker („high“ and „low“) (Gibco-BRL, Eggenstein). Protein molecular weight standard marker („Rainbow“) and Amplify^{TM} solution (Amersham Buchler, Braunschweig). Protein A sepharose (CL-4B) (Pharmacia, Freiburg). Dimethylsulfoxid (DMSO) and formamide (Fluka, Neu-Ulm).

Ammonium persulphate, Sodium laurylsulphate (SDS), N,N,N‘,N‘-tetramethylendiamin (TEMED), Triton X-100 (Serva, Heidelberg). 5, 5´-dithio-bis-2-nitrobenzoic acid (Ellman reagent), ethylmethane sulfonate (EMS), D-Sorbitol, agarose (type 1 and type 2), bromphenol blue, Coomassie Brilliant Blue G, DL-Dithiotreitol (DTT), ethidium bromide, ethylendiamintetra acetate (EDTA), phenylmethylsulfonyl chloride (PMSF), triethanolamin, Ponceau Red, lithium acetate, Ovalbumin Grade V, polyethylenglycol (PEG) 4000, PEG 8000, poly-L-lysine (Sigma, Deisenhofen). Sucrose (ultra-pure) (Gibco BRL Life Technologies). Paraformaldehyde (Electron Microscopy Sciences, Fort Washington, USA). Chloroform p.a., 2-propanol p.a., ethyl acetate p.a., methanol p.a. (Merck AG, Darmstadt).

2.8. Radiochemicals

Tran[^{35}S]-label^{TM} (10^3 Ci/mmol; ICN Biomedicals, Meckenheim). Myo-[2-^{3}H]-inositol (10-20 mCi/mmol), [methyl-^{3}H]-choline cloride (60-85 mCi/), L-[U-^{14}C]Serine (151 mCi/mmol), [U-^{14}C]Glycerol (160 mCi/mmol), [1-^{14}C]Palmitic acid (57 mCi/mmol), [2-^{14}C]Cytidine (55 mCi/mmol) and [^{32}P]-orthophosphate (10 mCi/ml) (Amersham, Braunschweig).

2.9. Laboratory hardware equipment

General-purpose glassware (Schütt, Göttingen). Autoclave “Sanoclav” (Wolf, Geislingen). Eppendorf thermomixer and Eppendorf desktop-centrifuge (Schütt, Göttingen). Electroporator Gene Pulser (BioRad, Richmond, USA). Incubation shaker “Gyratory Shaker” and “Controlled Environment Incubator shaker” (New Brunswick, Edison, USA). Micromanipulator (Singer Instruments, Watchet, England). Microscope “Laborlux D” and “Orthoplan” (Wolf, Geislingen).

Microscope “Axiophot” (Zeiss, Oberkochen). Transilluminator (302 nm and 366 nm wavelength) (Bachofer, Reutlingen). Scintillation counter “Tri-Carb, Liquid Scintillation Analyzer” (Packard, Frankfurt). Vortex™ Genie (Bender und Holbein, Zürich, CH). PCR-device Hybaid Omn-E (MWG-Biotech, Ebersberg). Photometer Uvicon 860 (Kontron Instruments, Eching). Centrifuges Sorvall RC-5B, RC-3B and corresponding rotors (DuPont Instruments, Bad Homburg). Ultracentrifuges L7 and L8-M and corresponding rotors (45 Ti and 70 Ti) (Beckman, München). Lumi-Imager™ (Boehringer, Mannheim). PhosphorImager™ and phosphoimager cassettes (Molecular Dynamics, CA). Speedvac (Bachofer, Germany).

2.10. Diverse materials

Silicagel 60 chromatography plate (Merck, Darmstadt). Nitrocellulose membranes BA 45, Protran BA-85 round membrane filters and nylon membrane filters Nytran-N (Schleicher & Schuell, Dassel). X-ray film X-Omat AR (Eastman Kodak, rochester, USA). Hyperfilm-ECL™ (Amersham-Buchler, Braunschweig). Cronex Intensifying Screens Quantall (DuPont, Dreieich-Sprendlingen). HiLoad Superdex200 (16/60) gel-filtration column (Pharmacia LKB, Freiburg). Whatman 3MM paper (Whatman, Maidstone, GB). Cuevettes for electroporation (Invitrogen, Leek, NL).

2.11. Frequently used solutions and buffers

30% acrylamide-solution:	29,2 % (w/v) acrylamide 0,8 % (w/v) bis-acrylamide
Ammonium persulphate-solution:	10 % (w/v) ammonium persulphate
Potassium acetate-solution:	5M potassium acetate buffered to pH 4,8 with acetic acid
PBS-buffer:	137 mM NaCl 3 mM KCl 8 mM Na_2HPO_4 1,5 mM KH_2PO_4
TE-buffer:	10 mM Tris/HCl, pH 7,5 1 mM EDTA
Laemmli sample buffer (2 x):	0,1 M Tris/HCl, pH 6,9 2 % (w/v) SDS 2 % (v/v) β-mercaptoethanol 20 % (v/v) glycerin 0,002 % (w/v) Bromphenol Blue stain
Phenol:	Phenol saturated with TE-buffer, pH 8,0 0,1 % (w/v) hydroxychinolin
TAE-buffer (50 x):	2 M Tris-acetate 1 M sodium acetate 50 mM EDTA, pH 8,0

P1-solution:	50 mM Tris/HCl, pH 8,0 10 mM EDTA, pH 8,0 100 µg/ml RNase
P2-solution:	1% (w/v) SDS 0,2 M NaOH
P3-solution:	3 M potassium acetate, pH 5,5
TLC solvent system:	chloroform: 2-propanol: ethyl acetate: methanol: 0.25% aqueous KCl (25/25/25/10/9, v/v/v/v/v)
Lipid extraction solution:	Chloroform: methanol (3/1, v/v)

3. Methods

3.1. Cell cultures

3.1.1. *E. coli* cultures

Different *E. coli* strains were transferred into a liquid medium from permanent cultures or from freshly prepared plates. Transformants were placed in the media containing an antibiotic (e.g. ampicillin). Liquid cultures were incubated at 37°C on shakers (200 rpm). Selection of a particular cellular clone originating from a single colony was done on antibiotic-containing agar plates at 37°C.

3.1.2. *S. cerevisiae* cultures

Yeast cultures originated from permanent culture stock or from a single colony were placed onto agar plates and then transferred into a liquid medium or new plate. Glucose, galactose or glycerol/ethanol mixture was used as a source of carbohydrates. For cells lacking any temperature-sensitive mutations incubation temperature was 30°C. Shaking of liquid cultures was done at 200 rpm. Minimal media were used for the selection of particular transformants. For the induction of sporulation, diploid yeast cells from logarithmically growing culture were transferred onto potassium acetate agar plates without nitrogen source and then incubated for 3-5 days at 25°C or 30°C.

3.1.3. Preparation of *E. coli* and *S. cerevisiae* permanent cultures

Bacterial and yeast cultures can be stored alive for several weeks on selective plates at 4°C. A long-term storage of such cultures was achieved via preparation of permanent culture stocks. 500 µl of fresh saturated liquid culture was mixed with 500 µl of sterile glycerol. Eppendorf tubes with the mixture were quickly frozen in liquid nitrogen and then stored at -80 °C. Reanimation of *E. coli* strains was done by inoculation on a selective agar plate, streaking for single colonies. Yeast strains were streaked on agar plates for single colonies first.

3.2. DNA isolation techniques

3.2.1. Transformation of *E. coli* cells by electroporation

Electroporation with high voltage is currently the most efficient method for transforming *E. coli* with plasmid DNA. With freshly grown cells, it routinely gives more than 10^9 bacterial transformands per microgram of input plasmid DNA.

For preparing cells competent for electroporation the bacteria culture was grown to OD_{600nm} of 0,4-0,6 in 500 ml LB medium in a 2-liter flask at constant shaking at 37°C. Cells were then chilled for 10-15 min in an ice-water bath and centrifuged 15 min at 4500 rpm in Beckman J-6M at 2°C. The cell pellet was subsequently washed 3 times with ice-cold sterile double distilled water. It was important to keep cells at 2°C at all steps. If frozen cells were to be used for electroporation, 40 ml ice-cold 10% glycerol was commonly added to the bacterial pellet after the washing step and mixed thoroughly. Cells were then centrifuged at 4000 rpm for 5 min at 2°C and dissolved in the volume of ice-cold 10% glycerol roughly equal to the one of cell pellet. Aliquots of 50-100 µl of cells were then transfered into prechilled Eppendorf tubes and frozen in liquid nitrogen. The cells could be stored at –80°C for many months without losing their high competence for transformation. Immediately before electroporation 50 µl of cells was thawed on ice and mixed with a volume of plasmid DNA not exceeding 2,5-3 µl, which usually contained from several nanogramms to 1 µg of DNA. The mixture of cells and DNA were placed subsequently into prechilled cuvette for electroporation and subjected to a pulse of a strong electric field in the electroporation apparatus (Gene Pulser, Bio-Rad, USA) set to 2,5 kV, 25 µF and 200-400 ohms. Right after the electrical shock, cells were placed on agar plates with LB media containing appropriate antibiotics for the selection of transformands.

3.2.2. Transformation of *S. cerevisiae* cells

Lithium acetate solution:	0, 2 M lithium acetate in TE buffer
PEG solution:	40% (w/v) PEG 3500 0,2 M lithium acetate in TE buffer (filter-sterilized or autoclaved solutions)

The yeast transformation used in this work was described by Ito et al., 1983. Incubation of yeast cells with alkali metal cations such like lithium ions leads to permeabilization of the cell wall so that yeast cells can take up plasmid DNA. Cells can also be transformed with linear DNA fragments, which then can be integrated into the yeast genome by homologues recombination. For selection of transformed cells in the minimal medium the DNA sequences

contained special markers (e.g. *URA3, LEU2* or *HIS3* gene). Yeast cells were grown to 0.5-2.0 OD_{600nm}. 50 ml of this culture was centrifuged at 3000 g and washed with TE buffer. Then cells were resuspended in 500 µl TE-Puffer and 500 µl lithium acetate and incubated 1-2 hours at 30°C (alternatively 25°C for temperature sensitive strains). 5 to 15 µg DNA per 100 to 150 µl of competent cells were taken for transformation. A sample without DNA was used as a control. After 30-60 min of incubation at 30°C (25°C for temperature sensitive strains) 0.7-1 ml PEG-3500 solution was added and incubation continued for 1-2 more hours at the same temperature. Finally either 10 min-long temperature shock at 42°C or 5 min-long one at 37°C (in case of ts-mutants) was applied. Then cells were collected by centrifugation at 2000 g for 3 min. PEG solution was removed as completely as possible. Cells were resuspended in 100 µl of TE buffer or full medium and applied onto selective agar plates. After 2-3 days of incubation at 30°C or 25°C single colonies can be transferred onto new plates and subsequently analyzed.

3.2.3. Analytical plasmid isolation from *E. coli*

The following procedure of analytical isolation of plasmid DNA from bacterial cells based on protocol described by Birnboim and Doly (1979) and can be easily modified. It was used for qualitative analysis of a large number of separate clones obtained after transformation with a modified plasmid.

Recombinant colonies were grown in 0,8 ml L-Broth-ampicillin medium in 1,5 ml- or 2 ml-Eppendorf tubes over night at 37°C with shaking. In parallel, the same colonies were grown on L-Broth-ampicillin agar plates over night at 37°C and then stored at 4°C. Bacteria from liquid culture were centrifuged for 30 seconds in a table centrifuge at 16.000 x *g*. Cell pellet was resuspended in 100 µl of P1-buffer and incubated for 10 min at room temperature. 200 µl of freshly prepared alkali-SDS solution (P2-solution) was added and cells were incubated 10 more minutes on ice. 150 µl of chilled 5M-potassium acetate (P3-solution) was added to lysate for neutralization and in order to precipitate the SDS-protein complexes by K^+. After 10 minutes of incubation on ice, the cell-lysate was centrifuged for 15 minutes at 16.000 x *g* and 4°C. The supernatant was centrifuged one more time. Plasmid DNA was precipitated from the cleared supernatant with 1 ml of 100% ethanol centrifuged 2 minutes at 16.000 x *g* and the pellet was washed twice with 70% ethanol. The pellet was dried in a vacuum rotor and resuspended in 20 µl of TE-buffer or double-distilled water. 5 or 10 µl of this DNA solution was used for restriction analysis. Alternatively, the isolation of analytical amounts of plasmid DNA can be done with a help of Qiaprep-spin Plasmid Isolation Kit

(Quiagen, Düsseldorf) using ion-exchange columns with described buffers and supplied columns.

3.2.4. Preparative plasmid isolation from *E. coli*

Using the preparative plasmid isolation kit from Quiagen (Düsseldorf) 100-200 µg of plasmid DNA could be isolated routinely from 200-500 ml of bacterial culture.

3.2.5. Analytical plasmid isolation from yeast cells

Yeast cells were grown in appropriate medium overnight to stationary phase at suitable temperature in a shaking incubator. 1,5 ml of the overnight culture was transferred to a microcentrifuge tube and spun 15 seconds at high speed. The cell pellet was then disrupted by vortexing for 4 min with glass beads in 300 µl of breaking buffer (phenol/chloroform/isoamyl alcohol, 25/24/1 (v/v/v)). The mixture was then centrifuged at the highest speed in an Eppendorf centrifuge for 5 min at room temperature. 2-3 µl of the aqueous layer was then used for direct transformation of competent *E. coli* to amplify the amount of plasmid extracted from the yeast cells.

3.2.6. Rapid isolation of yeast chromosomal DNA

The procedure for rapid plasmid isolation could easily be scaled up to prepare chromosomal DNA for use in PCR amplification or restriction enzyme digest. For that purpose the aqueous solution with chromosomal DNA recovered after phenol-extraction generally required further purification by ethanol precipitation. A volume of the TE buffer equal to the volume of the aqueous DNA solution was added, vortexed briefly, spun in a microcentrifuge and the clear aqueous layer was then transferred to a new microcentrifuge tube. The genomic DNA was subsequently precipitated with ethanol, the pellet was dried and dissolved in TE buffer. The procedure typically gave a yield of chromosomal DNA in a range of several hundred nanogramms from 1 OD_{600nm} of yeast cells.

3.3. Enzymatic modifications of DNA

3.3.1. Digestion of double-stranded DNA by restriction endonucleases

Restriction endonucleases can be used for cloning of a DNA fragment into a vector and for identification of restriction site positions on plasmid DNA (restriction analysis). Type II restriction enzymes obtained from different bacterial strains recognize a specific palindromic motif of DNA sequence and split the double strand at that position. Upon restriction DNA

ends can be blunt or sticky with 3'- or 5'-overhanges. The 3'-hydroxyl end is always free, whereas 5'-end carries a phosphate group (Roberts, 1983).

The restriction enzymes vary in temperature, pH and salt optima and are supplied along with optimised buffers. 1 unit of enzyme was used for the digestion of 1 µg of DNA in 10 µl of restriction buffer. The incubation can last from 1 hour to over night at assigned temperature.

3.3.2. Treatment of linearized plasmid DNA with alkaline phosphatase

10x phosphatase buffer:	100 mM Tris-HCl, pH 8,0 10 mM $ZnCl_2$ 10 mM $MgCl_2$

Alkaline phosphatase catalyses the removal of the 5'-phosphate group on DNA fragments. The enzyme is used in cloning procedures to prevent ligation of the vector with itself, thus favoring ligation of the vector with insert.

5 pmol of DNA is added to 90 µl of water, 10 µl of 10x phosphatase buffer and 0,5-1 unit of alkaline phosphatase. The mixture was incubated 15 min at 37°C. Alkaline phosphatase can then be removed by preparative agarose gel electrophoresis or via phenol/chloroform/isoamyl alcohol extraction.

3.3.3. Fill-in of 5'-overhangs

Desoxynucleotide mixture:	1 mM dATP, 1 mM dCTP, 1 mM dGTP, 1 mM dTTP
10x Klenow buffer:	0,5 M Tris-HCl, pH 7,2 0,1 M $MgCl_2$ 1 mM DTT

Klenow-fragment is obtained by proteolytic processing of the DNA-polymerase I (Klenow and Hennigsen, 1970). It is used when overhangs of the fragments that have to be ligated do not fit one to another. The enzyme fills in 5´-overhangs by 3´-5´polymerisation so that blunt ends are formed.

3-5 µg of linerized DNA were mixed with 31 µl H_2O, 4 µl of 10x Klenow buffer and 1 µl of 4 deoxynucleotide solutions. Upon adding of 5 units of Klenow enzyme the mixture was incubated for 30 min at 37°C. Then DNA was concentrated by ethanol precipitation or purified by preparative agarose gel electrophoresis.

3.3.4. Creating blunt ends with T4 DNA polymerase

1x T4 DNA polymerase reaction buffer	100 µM of each four dNTPs; 50 mM Tris.HCl, pH 8,0; 5 mM Mg_2Cl
Reaction conditions for creating blunt ends	10 units of T4 DNA polymerase per 2 µg of DNA; incubate 20 minutes at 11°C

T4 DNA polymerase, the product of gene 43 of bacteriophage T4, is a single polypeptide of molecular weight 112 kDa. In addition to its DNA-dependent DNA polymerase activity, it has a very active single-stranded and double-stranded 3´-5´exonuclease. It lacks 5´-3´exonuclease activity. T4 DNA polymerase is an enzyme of choice for converting the ends of any duplex DNA fragment to blunt-ended structures suitable for blunt-end ligation for cloning. In the presence of high concentrations of all four dNTPs, the degradation of 3´-protruding termini in 3´-5´ direction will stop when T4 DNA polymerase reaches the duplex region. Similar to Klenow fragment, if the DNA-termini have 5´-protruding region, the enzyme will extend the 3´-termini until the end is blunt.

3.3.5. Ligation of double-stranded DNA fragments

5x ligase buffer:	250 mM Tris-HCl, pH 7,8 50 mM $MgCl_2$ 5 mM DTT 5 mM ATP 25% (w/v) PEG 8000

Linearized DNA molecules can be joined (ligated) by forming phosphodiester bonds between 3'-hydroxyl group and 5'-phosphate group. T4-DNA-ligase catalyses this reaction in ATP-dependent manner. DNA fragments with complementary sticky ends are ligated more efficiently than those with blunt ends. The molar ratio between the vector and the fragment was 1:10. An improvement of ligation for blunt-end fragments can be achieved by further increasing this ratio. That may lead, however, to insertion of concatemers. 6 µl 5x ligase-mix and 2 units of T4-DNA-ligase were used for 30 µl of total volume of reaction mix. It was incubated 15 minutes at 37°C, 1 hour at room temperature and from 10 to 20 hours at 16°C.

3.3.6. Polymerase chain reaction

Polymerase chain reaction (PCR) is a process of DNA amplification. Oligonucleotides corresponding to flanking regions of the (+) and (-) strands of DNA fragment that needs to be amplified are synthesized and used as primers. In every round the number of DNA molecules is theoretically doubled. At the first step of each round a double-stranded DNA molecule is denatured by heating up to 95^oC. Then the temperature of reaction mix drops down to 40-

60°C depending on the length and composition of the primers (not too low to avoid non-specific annealing, not too high to allow for efficient specific annealing) so that oligonucleotides can anneal with complementary sequences on the template DNA. Then both oligonucleotides are elongated by the heat-resistant *Taq* DNA polymerase (from *Thermos thermophilus*) at 72°C. Each new cycle begins with denaturation of the DNA fragments.

PCR mix (example):	1 ng of DNA (plasmid or chromosomal) in 10 µl 2 µl of oligonucleotide 1 (10 pMol/µl) 2 µl of oligonucleotide 2 (10 pMol/µl) 10 µl of 10-fold *Taq* reaction buffer (*Promega*) 10 µl of deoxynucleotide mix (2,5 mM of each) 1-4 µl of $MgCl_2$ (25 mM) 1 µl of *Taq*-DNA-polymerase (5 units) 14-11 µl of water 100 µl
Conditions (example):	Denaturation: 95 °C for 1 min Hybridization (annealing of primers with template DNA): 55 °C for 1 min Polymerization: 72 °C for 1 min (per each 1000 base pares)

These cycles are repeated about 31-33 times. During the last cycle the polymerization step can be prolonged up to 10 min to efficiently fill in possible overhangs. As *Taq*-DNA-polymerase amplified fragments contain single nucleotide 3´-overhangs, the PCR reaction mix is treated then, if necessary, with T4 DNA-polymerase to make the ends blunt and therefore suitable for ligation. To increase the fidelity of DNA-fragment amplification by PCR, the proofreading capable *Vent* or *Pfu*Turbo™ DNA-polymerases were often used together with *Taq*-enzyme.

3.3.7. QuickChange™ site-directed mutagenesis

The QuickChange™ site-directed mutagenesis kit (Stratagen, CA) is used to make point mutations, and thus to switch, delete or insert single or multiple amino acids in the encoded protein. The method is performed using *Pfu*Turbo™ DNA polymerase (it has 6-fold higher fidelity in DNA synthesis than *Taq* DNA polymerase due to 3´-5´ exonuclease activity displayed on occasions of spontaneous mispairing) and a thermal temperature cycler. The procedure utilizes a supercoiled double-stranded DNA (dsDNA) vector with an insert of interest and two synthetic oligonucleotide primers containing the desired mutation. The oligonucletide primers, each complementary to opposite strands of the vector, are extended during temperature cycle by using PfuTurbo™ DNA polymerase. Incorporation of the oligonucleotide primers generates a mutated plasmid containing staggered nicks. Following temperature cycle, the product is treated with Dpn I. Dpn I endonuclease is specific for

methylated and hemimethylated DNA and used to digest the parental DNA strands and to select for mutation-containing synthesized DNA. DNA isolated from almost all *E. coli* strains is dam methylated and therefore susceptible to Dpn I digestion. The nicked vector DNA incorporating the desired mutations is then transformed into *E. coli* competent cells. The small amount of starting DNA template required to perform this method, the high fodelity of the PfuTurbo™ DNA polymerase, and the low number of PCR cycles all contribute to high mutation efficiency and decreased potential for random mutations during the reaction.

QuickChange™ reaction mix (recommendation of Startagen, CA)	5 µl of 10x reaction buffer 5-50 ng of dsDNA template 125 ng of oligonucletide primer #1 125 ng of oligonucletide primer #2 1 µl of dNTPs mix ddH_2O to a final volume of 50 µl Then add 1 µl of PfuTurbo™ DNA polymerase (2,5 U/µl)

Cycling parameters for the QuickChange™ site-directed mutagenesis method

Segment	Cycles	Temperature	Time
1	1	95°C	30 seconds
2	12-18	95°C	30 seconds
	55°C		1 minute
	68°C		2 minutes/1 kb of plasmid length

3.3.8. Electrophoretic DNA separation

TAE buffer:	40 mM Tris-acetate, pH 7,2 20 mM sodium acetate 1 mM EDTA
Loading buffer:	0,25% (w/v) bromphenolblue 0,25% (w/v) xylencyanol 25% (w/v) ficoll (Type 400) in H_2O
Ethidium bromide solution:	1 µg/ml ethidium bromide in H_2O

Agarose gel electrophoresis is used for separation, purification and identification of plasmid DNA and DNA fragments. Because of the negative charge of their phosphate groups, the DNA molecules move towards plus-pole in the electric field. Under constant voltage the migration speed of linear, double-stranded DNA in agarose gel is proportional to the logarithm of its molecular weight. The size of a DNA fragment can be determined by comparison with standard DNA fragments of identified size (DNA-marker). Rough estimation of the DNA-concentration can be done by comparison of band intensity of the sample and marker DNA upon staining with ethidium bromide.

Agarose horizontal gels were used for analytical and preparative separation of DNA fragments. Depending on the size of the DNA molecules the agarose concentration was chosen between 0.7% and 2.0% (w/v). The agarose was molten by heating and, after addition of DNA-intercolating stain ethidium bromide, poured into electrophoresis chamber. Then a comb was inserted to create the wells for DNA loading. DNA-samples were mixed with one-third volume of loading buffer and applied into the wells.

In parallel a marker (e.g. 1 μg *EcoRI*/*HindIII*-cut double-stranded DNA of phage lambda) was loaded. TAE buffer was used for agarose solution and as electrophoretic buffer. The electrophoretic separation was done at 3 to 5 volts/cm. Separated fragments were visualized by UV-light (λ = 302 nm). Preparative gels were exposed to UV-light (λ = 366 nm) as shortly as possible to avoid photocrosslinking of DNA molecules.

3.3.9. Isolation of DNA fragments from preparative gels

Glassmax^{TM}-DNA isolation kit (*GibcoBRL*, Eggenstein) was commonly used for the purpose of isolation of DNA fragments from preparative gels as described by the supplier.

3.4. Methods of yeast genetics

3.4.1. Crossing of yeast strains

S. cerevisiae cells can grow as diploids or haploids. As soon as diploid cells are grown without nitrogen source, they step into the meiotic cycle. As a result, an ascus with 4 haploid spores is formed which is named “tetrad”. It is possible to separate these 4 spores with the help of a micromanipulator and to grow them as haploid strains. These haploid cells originating from spores have different mating types – two of spores are of type **a** (*MAT*a) whereas two others of type α (*MAT*α). Natural mating of haploid yeast cells occurs between cells of opposite mating type. Mating of the haploid cells leads to formation of a diploid zygote. Most laboratory yeast strains are heterothallic – they preserve their mating type. In contrast, homothallic strains change their mating type via gene-regulated mating type switching. For convenient selection of newly produced diploid strains used for crossing should differ in two auxotrophic markers. Yeast strains of different mating type were grown in liquid medium. Concentrated cell suspensions of both cultures were mixed on full-medium agar plate with a loop. Then the plates were incubated about 12 hours at 25°C or 30°C to allow for mating. Cells were then transferred by streaking onto SD-minimal medium plates for diploid selection. If there was no suitable phenotype for the selection of diploid cells, two

different mating type haploid cells with desired sets of genes were pulled together on the agar plate with the help of micromanipulator. Only when a zygote was distinctly visible under the light microscope, the cultivation of diploid cells could be continued.

3.4.2. Sporulation of yeast cells

For sporulation diploid yeast cells were grown to logarithmic phase in full medium. Cells were collected at 3.000 rpm and resuspended in the medium remaining in the tube. This concentrated suspension was then applied as droplets onto potassium acetate plates. After 3-5 days of incubation at 30°C or 25°C, the formation of asci was usually observed.

3.4.3. Analysis of yeast tetrads

Sporulating yeast cells were added to 10 µl β-glucuronidase/arylsulfatase solution and 500 µl of sterile water. During 10 min of incubation at room temperature the wall of ascus was partly destroyed. For tetrad analysis four spores from one ascus were separated with glass-pin of micromanipulator and applied onto full medium plates. It is important to separate only spores belonging to one and the same tetrad. Therefore, it is recommended to choose tetrads with still recognizable ascus wall. The four spores were deposited at defined positions on agar plate surface. Plates were incubated for several days at 25°C to let the spores grow. As soon as spores have grown up into colonies, the phenotypes of the four derivatives of one particular meiosis can be idenfined.

3.4.4. Reversion of *cys3-2* to *CYS3* by homologous recombination

Cys3-2 cells were transformed with a *Nsi I/Nsi I* fragment comprising the wild type *CYS3* gene. As a result of a homologous recombination event between genomic *cys3-2*-locus and *Nsi I/Nsi I-CYS3*-fragment, some cells reverted to *CYS3*. They were selected by growth at 37°C and confirmed by their ability to grow without cysteine (AMY4).

3.4.5. PCR-targeted gene disruption using the kanMX module (Wach et al., 1994)

The plasmid pFA6a-*kanMX4* contained the *kanMX4* module consisting of the E.coli *kan*^{r} coding sequence under the transcriptional and translational control sequences of the *A. gossypii TEF* gene. We have used the *kanMX4* module in a transformation with a PCR-generated DNA fragment designed to replace most of *YLR080W,* an open reading frame coding for protein of unknown function with 45% identity to Emp47p. The disruption fragment generated by PCR (obtained with primers PLA444-5´ and PLA444-3´, see chapter 2.3) contained the *kanMX4* module flanked by 43 bp homologous to the region directly

upstream of the start codon of *YLR080W* or 44 bp overlapping and downstream of the stop codon of *YLR080W*. G418 (kanamycin)-resistant clones were obtained by transformation of two haploid yeast strains RH732 and RH448 (see chapter 2.1). Analysis of these clones was performed by analytical PCR using two sets of primers K2/5´-check and K3/3´-check (see chapter 2.3). If *YLR080W* is correctly deleted by the *kanMX4* module, K2/5´-check and K3/3´-check sets of primers should both yield 480 bp long fragments of the *YLR080W::kanMX4* allele.

3.4.6. EMS-mutagenesis of yeast cells

Ethylmethane sulfonate (EMS) (Sigma) (caution: EMS is a strong volatile mutagen, use gloves and work under hood!) was used to generate randomly mutagenized cells from strain RH448. In essence mutagenesis was performed as described (Lawrence 1991). In short, various mutagenesis-reactions were performed by incubating 2-5x10^8 cells for 30-60 min in 10 ml KP_I-Buffer, pH 7.0, at room temperature in the presence of 2-5% EMS. Such reactions were used for mutant-screens, in which 20-50% cell death had occurred as determined by plating serial dilutions.

3.4.7. Colony-blot assay

Our assay was based on a protocol developed by Lyons and Nelson (Lyons and Nelson, 1984). EMS-mutagenised cells were plated on YPUAD medium solidified with 1% agarose in quantities of 400-600 cells per plate. Plates were incubated for 3 days at 24°C. Yeast colonies were then replica-plated to nitrocellulose filters (Schleicher & Schuell, Germany) which were in turn accommodated on top of several sheets of Whatman #1 filter paper (Whatman, Clifton, NJ) soaked with liquid YPUAD medium containing 20 µg/ml cycloheximide (CHX). The setup was then shifted to 37°C for 3 hrs. CHX was included to stop protein-biosynthesis and thus more efficiently deplete Emp47p in mutants that would mislocalize Emp47p to the vacuole. Colonies attached to the filters were then lysed with lysis buffer (0.2 M NaOH, 0.1% SDS, 35 mM DTT) for 30 min at room temperature. Cell debris was thoroughly removed from the filters under a stream of water. Filters were then incubated in 0.1 M acetic acid for 30 min followed by treatment with PBS/1% SDS/100 mM β-mercaptoethanol for 30 min at 50-70°C. After the last treatment nitrocellulose filters were washed for at least 1 hr with several changes of PBS/ 0.1% Triton-X100. Finally immunodetection of Emp47p was carried out with the antiluminal-serum directed against Emp47p (Schröder et al., 1995) and an HRP-coupled secondary antibody followed by detection of chemiluminescence (ECL, Amersham) in a Lumi-Imager™ (Boehringer, Mannheim).

3.5. Protein analysis techniques

3.5.1. TCA-precipitation of yeast proteins

Lysis-buffer:	2 M NaOH, 5% (v/v) β-mercaptoethanol
TCA solution:	100% (w/v) trichloracetic acid in water

An equivalent of 1 OD_{600nm} of logarithmically growing cells was resuspended in 100 µl of alkaline lysis-buffer. After 10 min of incubation on ice proteins were precipitated by adding 100% TCA to final concentration of 7% and incubated again 10 min on ice. The denatured proteins were then collected by centrifugation in a table-top centrifuge and treated with 300 µl of 1 M Tris-HCl (pH 8,0) for neutralization. After short centrifugation the supernatant was removed and the pellet was resuspended in 30 µl of Laemmli loading-buffer. Before loading onto a SDS polyacrylamide gel, samples were boiled for 5 - 10 min at 95°C.

3.5.2. Measurement of protein concentration

3.5.2.1. Bradford assay

The Bradford assay (1976) relies on the binding of Coomassie-dye to proteins. The dye has an absorption maximum at wavelengths 465 nm (in the absence of protein) and 595 nm in protein-bound form. The quantitative analysis of protein concentration was performed with the help of a staining solution according to protocol from *BioRad* (Richmond, USA). The protein concentration was determined by plotting the absorbance value (measured at wavelength of 595 nm) of a sample with unknown protein concentration on the calibration curve obtained for standard solutions of bovine serum albumin (BSA) with concentrations ranging from 1000 to 150 µg/ml.

3.5.2.2. Spectrophotometric determination of protein concentration

Determination of protein concentration by measuring absorbance at 280 nm (OD_{280nm}) is based on the absorbance of UV light by aromatic amino acids in protein solutions-due primarily to tryptophan and tyrosine residues and to lesser extent phenylalanine residues. The measured absorbance was used to calculate the concentration by comparison with a calibration curve prepared from measurements with standard protein solutions. This assay was applied to solutions with protein concentrations of 20 to 3000 µg/ml

3.5.3. Separation of proteins by denaturing gel electrophoresis (SDS-PAGE)

Laemmli loading-buffer (2x):	0,1 M Tris-HCl, pH 8,0 2% (w/v) β-mercaptoethanol 20% (w/v) glycerol 0,002% (w/v) bromphenol blue
SDS-gel buffer (4x):	0,5 M Tris-HCl, pH 8,0 0,4% (w/v) SDS
Electrophoresis buffer (10x):	1,9 M glycine 0,25 M Tris-Base 1% (w/v) SDS
6% stacking gel (60 ml):	10 ml 30% acrylamide/bis-acrylamide stock solution 12,5 ml SDS gel buffer (4x) 60 µl of TEMED stock solution 600 µl of 10% ammonium persulphate solution 27 ml of water
10% separating gel (100 ml):	33,3 ml 30% acrylamide/bis-acrylamide stock solution 25 ml SDS gel buffer (4x) 100 µl of TEMED stock solution 1 ml of 10% ammonium persulphate solution 40 ml of water
Staining solution:	50% (v/v) methanol 10% (v/v) acetic acid 0,1% (w/v) Serva Blue R250
Destaining solution:	45% (v/v) methanol 10% (v/v) acetic acid

The electrophoretic mobility of a native polypeptide in an poly-acrylamide gel depends on its size, spatial structure and isoelectric point of the molecule. The anionic detergent sodium dodecylsulphate binds to proteins in large molar excess and together with β-mecraptoethanol fully denatures the proteins. The charge of the sulphate group of the bound SDS brings such a strong negative total charge to the SDS-protein complex that the endogenous charge of a protein can be disregarded. Thus the migration speed of proteins in the SDS-PAGE depends mainly on the sieve effect of the gel matrix and correlates with molecular weight of the proteins. The SDS-PAGE was performed as discontinuous gel-electrophoresis with stacking and separating gels. The SDS-PAGE was generally used in form of flat gels (70x100x0,75 mm (mini-gel) or 170 x 180 x 1,5 mm (maxi-gel)) at acrylamide concentration of 8, 10, 12,5 and 15% for the separating gel. Upon addition of ammonium persulphate solution and TEMED, the separating gel was poured in a slot between two glass plates (separated by 2 spacers) with 1,5 cm interval between gel surface and upper rim of a plate. The separating gel was covered by isobutanol (water-saturated) mainly to enforce a smooth surface of the gel.

After polymerization the isobutanol was removed completely. Stacking gel-solution was loaded after addition of ammonium persulphate and TEMED on top of the separating-gel. To create wells, a 0,75 mm-thick comb was inserted. The comb was removed after polymerization had occured. Then the gel was set in the electrophoresis chamber so that its upper and lower parts were in contact with buffer. Protein samples were diluted with an equal volume of Laemmli buffer (2x) and boiled for 5 min. The electrophoresis was done at the permanent current of 30 to 50 mA and finished as soon as the bromphenol blue of the loading buffer reached lower border of the gel. Then glass plates were removed and the gel was stained with Coomassie-dye or used in Western-blot procedure. If the gel was stained with Coomassie blue dye it was then de-stained by incubation with acetic acid/methanol solution.

3.5.4. Transfer of proteins on nitrocellulose filter (Western blot)

Transfer buffer (1x):	20 mM Tris-base 150 mM glycine 20% (w/v) methanol

Electrophoretic transfer of proteins was used in order to detect particular proteins with the help of antibodies. Electrophoretic transfer of proteins from poly-acrylamide gels onto nitrocellulose filters was described by Burnette (1981). After SDS-PAGE the unstained gel was covered by nitrocellulose membrane soaked in the transfer-buffer. Protein transfer was performed for 1 to 3 hours at 400 mA in special Western blot-chamber filled with the transfer-buffer.

3.5.5. Ponceau-staining of nitrocellulose filter-bound proteins

Ponceau-red solution (Ponceau S):	40% methanol (v/v) 15% acetic acid (v/v) 2,5 g per liter Ponceau-red

To check the efficiency and homogeneity of the protein transfer onto the nitrocellulose filter, it was stained with Pounceau-red dye. The filter was held 10 seconds in Ponceau-red solution and after short destaining with water protein bands became visible.

3.5.6. Immunological detection of proteins on the nitrocellulose membrane

PBS-Triton buffer:	1x PBS buffer 0,1% Triton X-100
quenching buffer:	PBS-Triton buffer 2% milk powder (w/v)

After the electrophoretic transfer, the nitrocellulose membrane was washed several times in PBS-Triton buffer at room temperature. After that the filter was incubated in quenching buffer for 15 minutes. The filter was then transferred to the quenching buffer supplied with antibody diluted to an appropriate extent and incubated for at least 90 minutes at room temperature. Milk powder and detergent (Triton X-100) in the quenching buffer was required to saturate the binding capacity of the nitrocellulose filter and to diminish the unspecific reactivity of the antibody with different antigens. The filter was then washed repeatedly with PBS-Triton buffer. Secondary HRP-conjugated antibody (dilution rate was 1/5000 typically) was applied and filter was incubated for 90 minutes. Filter was then washed with several changes of PBS-Triton buffer and the last times with 1x PBS buffer alone to remove Triton X-100.

Visualization of proteins was done via application of chemo-luminescent system ECL™ from Amersham. Luminol, which is contained in the reaction mix, is oxidized by hydrogen peroxide with help of horseradish peroxidase coupled to secondary antibody. In this reaction luminol is turned in an excitation state. The energy released from the return of the luminol to its ground-state is partly emitted as visible light that can be detected by X-ray film or by the Lumi-Imager™ system (Boeringer). The precise reaction time and conditions are described by ECL™ manufacturer (Amersham).

3.5.7. Removal of antibodies from nitrocellulose filter

Glycine stripping solution:	0,2 M glycine, pH 2,5
SDS/ β-ME-stripping solution: (Amersham)	1% SDS 80 mM Tris-HCl, pH 7,0 100 mM β-mercaptoethanol

If the nitrocellulose filter was to be incubated consecutively with two different primary antibodies, it was stripped off the first antibodies by incubation either with glycine solution for 30-60 min at room temperature or SDS/ β-ME-stripping solution for 30 min at 50-70°C. In either case the antibodies were efficiently removed and after extensive washing with large volumes of PBS-Triton buffer and subsequent incubation in quenching buffer the blot was ready to be treated with the next primary antibody.

3.5.8. Evaluation of the levels of different Golgi proteins in the yeast cell lysates

10^8 yeast cells of every strain grown up in the liquid YPUAD medium were harvested and lysed by vortexing for 10 min in the presence of glass-beads in lysis buffer (1% SDS, 35 mM β-mercaptoethanol, 50 mM Tris-HCl, pH 7.3, protease inhibitor tablet (Boehringer Mannheim)). The lysate was cleared by centrifugation for 10 min at 10000x g. The efficiency

of cell lysis was assessed by measuring the optical density of the cleared lysate at 280 nm. Calibrating amounts of extract from wild-type cells encompassing the amount of mutant-extract were separated together on the same SDS-polyacrylamide gel. Proteins were transferred to nitrocellulose and visualized by Ponceau S staining. The integrated staining-intensities for each lane were determined with the help of a Lumi-Imager™ in top-illumination mode (Boehringer Mannheim). Subsequently the blot was treated with polyclonal sera directed against one of various marker-proteins followed by incubation with HRP-coupled secondary antibodies. The intensities of the enhanced chemiluminescence reactions (ECL, Amersham) were measured using a Lumi-Imager™. A calibration curve for each antigen was constructed from the Ponceau-S-staining-intensities and the chemiluminescence signals. These curves served for the determination of the relative levels of the marker proteins in the mutant strains compared to wild-type.

3.5.9. ^{35}S-pulse-chase experiments to follow protein transport

To trace the transport and enzymatic processing of a protein in a cell, pulse-chase experiments are commonly resorted to. Yeast cells, grown on medium free of methionine and cysteine, are labeled with radioactive [^{35}S]-methionine and cysteine („pulse**“**) for a certain time. Then non-radioactive amino acids and inorganic sulphate are added („chase**“**). After cell lysis, the labeled protein is then specifically isolated by immunoprecipitation.

Cells were grown to mid-log phase at 25°C in YPUAD. 15 ml were harvested from each culture and washed twice with 10 ml SD medium at room temperature. Cells were resuspended in 10 ml SD and shifted to 37°C for 30 min. All subsequent steps were also performed at 37°C. Cells were harvested again and resuspended in 1 ml labeling mix consisting of SD medium supplemented with 50 µl Tran[^{35}S]-label™ (10^3 Ci/mmol; ICN Biomedicals, Meckenheim, Germany). After a pulse time of 5 min prewarmed chase-medium was added (YPUAD supplemented with 1 mM $(NH_4)_2SO_4$ and 0.003% methionine). Aliquots of the cell suspension were taken at 0, 15, 30 and 60 min and transferred into tubes prefilled with 1 M NaF/NaN_3 stock-solution (end-concentration 10 mM each) to stop energy production. Cells were then harvested and resuspended in 1 ml reducing HEPES-Buffer (10 mM HEPES, pH 7.0, 1 M sorbitol, 100 mM β-mercaptoethanol and 10 mM each NaF/NaN_3). After 10 min cells were spun down and resuspended in 300 µl HEPES-buffer without reducing agent but containing 3 u lyticase (Sigma). Cells were converted to spheroplasts for 30 min at 30°C. Lysis was achieved by heating the spheroplasts to 95°C for 5 min in the presence of 1% SDS.

Immunoprecipitation of solubilized proteins was then essentially performed as described (Schröder-Köhne et al., 1998). The cell debris was removed by two washes with 450 □l of IP-buffer. After this washing step, the preserved supernatant was mixed with 7 □l of the protein-specific antibody and 50 µl of protein A-Sepharose (Sigma). Antibody binding was done over night at 4°C or 2-4 hours at room temperature on the rotating wheel. After a short centrifugation, supernatant was discarded and the pellet was consequently washed with 1 ml of the following buffers:

IP-buffer:	1% Triton X-100 0.2% SDS 150 mM NaCl 5 mM EDTA 50 mM Tris-HCl, pH 7,4
IP-urea-buffer:	IP with 2 M urea
IP-high-salt-buffer:	IP with 500 mM NaCl
IP-wash-buffer:	IP without SDS and without Triton X-100

Finally the pellet was resuspended in 50 µl of Laemmli loading-buffer and aliquots were applied onto a polyacrylamide gel. The gel was then tested for the efficiency of immunoprecipitation by staining with Coomassie-Blue (approx. 15 min). Then the gel was destained (approx. 45 min) and incubated 30 min with „Amplifier"-solution (*Amersham*). Upon desiccation in a vacuum-dryer, the gel was exposed to X-ray film at -70°C. In an alternative procedure, after destaining step the gel was dried and the image was obtained in phosphoimager cassette and subsequently developed by PhosphoImager^{TM}.

3.5.10. Invertase secretion assay

Lyticase-buffer	1,4 M sorbitol 50 mM K-Pi-buffer, pH 7,5 10 mM NaN_3 80 mM β-mercaptoethanol
Lysis-buffer	50 mM K-Pi-buffer, pH 7,5 10 mM NaN_3 0,1 % (v/v) Triton X-100
Polyacrylamide-gel (7 %)	5 ml 0,6 M Tris-HCl, pH 8,4 8,7 ml 30 % acrylamide solution 30 ml H_2O 17 µl TEMED 333 µl 10 % APS-solution
Electrophoretic buffer	5,2 g Tris-base in 1000 ml of H_2O brought to pH 9,05 with glycin
Sucrose-buffer	0,1 M Sucrose 0,1 M Potassium acetate, pH 4,8
Staining solution	300 mg 2,3,5-triphenyltetrazolium chloride

	4g NaOH 150 ml H_2O
Stop/fixation solution	45% (v/v) methanol 10% (v/v) acetic acid

Invertase is one of the marker-enzyme of the protein secretion. It catalyses the hydrolysis of sucrose to glucose and fructose. As invertase moves along the secretory pathway from the ER to the periplasmatic space it undergoes glycosylation in several steps. Three classes of invertase protein are seen: (1) a cytoplasmic form (60 kDa), (2) an ER form (80-86 kDa), and (3) a secreted form (100-150 kDa). The secreted form of the protein is heterogeneous in size, resulting from varying elongation of core oligosaccharide chains in the Golgi apparatus. Electrophoresis in 7 % acrylamide gel helps to distinguish between the differently glycosylated forms of secreted invertase. The activity of the invertase could be detected in the native polyacrylamide gel after electrophoretic separation via a stain-producing reaction of invertase with 2,3,5-triphenyltetrazolium chloride (Grossmann and Zimmerman, 1979). For the analysis of invertase in the periplasmatic space yeast cells are transformed to spheroplasts and then separated in extracellular and intracellular fractions (Schauer et al., 1985). The derepression of invertase synthesis is achieved by means of growing yeast cells in the medium with low concentration of glucose (Esmon et al., 1981)

S. cerevisiae cells were grown in the rich YPUAD medium to mid-logarithmic phase (OD_{600nm}=1). For the induction of the invertase biosynthesis approximately 20 $O.D._{600nm}$ of yeast cells were precipitated, washed once, and transferred to the YPUAD medium with glucose concentration of 0,1 % (w/v). At this step the cell culture was divided in two portions for incubations at different temperatures (25°C and 37°C). After 1 hour of incubation the cells were collected by centrifugation (4000 x g, 3 minutes) and washed with 10 mM NaN_3 buffer. The cell pellet was then resuspended in 100 µl of Lyticase-buffer in Eppendorf tube. After that cells were allowed to incubate for 60 min at 30°C in the presence of Lyticase (200 units per a tube). The following steps were performed at 4°C. The spheroplasts were then collected by centrifugation at 3000 x g for 5 minutes and, thus, became separated from the periplasmatic fraction (supernatant). The periplasmatic fraction was kept on ice before electrophoresis. The spheroplasts were washed once with 1 ml of 1 M sorbitol, resuspended in the Lysis-buffer and vortexed for 4 minutes to enhance the efficiency of lysis. The cell lysate was then centrifuged at 14000 rpm to remove insoluble junk. The resulting intracellular fraction was then mixed with 20 µl of 1 M sorbitol to enable loading onto polyacrylamide gel. 15 µl of each fraction was then loaded onto 7 % non-denaturing polyacrylamide gel. The electrophoresis was performed at 4°C for approximately 3 hours at 30 mA. The gel was then

incubated in Sucrose-buffer at 37°C for 30 min and finally washed with water. Monosaccharides accumulated as the result of invertase activity were then detected in the freshly prepared Staining buffer. The development of characteristic red stain was greatly enhanced by incubating the gel over hot water bath set to 98°C. The development of stain was then stopped by washing the gel with water and transferring it to stop/fixation buffer.

3.5.11. Protein molecular size determination by gel-filtration chromatography on Sephacryl S-6 column

Yeast cells (1000 OD_{600nm}) were taken for lysis and protein extraction. The cells were prepared for lysis and subsequently lysed exactly as described in the chapter 3.6.2. The lysis buffer employed for the solubilisation of membrane proteins contained 150mM KOAc, 350mM KCl, 5mM $Mg(OAc)_2$, 20mM HEPES (pH 6,8), 250mM Sorbitol, 1% CHAPS, protease inhibitor tablet (Boehringer Mannheim). The cell lysate was then clarified by centrifugation at 15 000 rpm for 30 minutes. Approximately 5 ml of the supernatant were loaded onto the gel-filtration Sephacryl S-6 column (Pharmacia). The column was eluted at 0,5 ml/min and fractions of 2ml were collected. Proteins of equal aliquots were separated by SDS-PAGE, transferred to nitrocellulose filters and probed with different antibodies. The chemiluminescence signals were acquired by Lumi-Imager™ and quantified with Lumi-Imager™ software.

3.6. Subcellular fractionation

3.6.1. Preparation of frozen step-gradient tubes

11 sucrose solutions were prepared containing, respectively, 18%, 22%, 26%, 30%, 34%, 38%, 42%, 46%, 50%, 54%, 60% (w/v) of sucrose, 1mM $MgCl_2$, 10 mM HEPES pH 7,5. Starting with 60% sucrose solution, 1ml aliquot was loaded onto the bottom of 13 ml Ultra-Clear™ centrifuge tubes (Beckman), the tube was put into liquid nitrogen until the solution was frozen then 1 ml of the next solution was added, the freezing procedure was repeated for all the solutions. The gradients were stored at –80°C. 4-5 hours prior to use, the gradients were put at 4°C for thawing slowly.

3.6.2. Subcellular fractionation by velocity sedimentation on sucrose gradient

From 200ml to 500ml of cells grown to mid-log phase were harvested, washed 2 times with 500 ml of distilled water and resuspended in 3 ml of the buffer (250 mM sorbitol, 150 mM KOAc, 5 mM MgOAc, 1 mM DTT, 20 mM HEPES pH 6,8; protease inhibitor tablet

(Boehringer Mannheim)). Immediately afterwards, the cell suspension was rapidly frozen by transferring to porcelain mortar containing liquid nitrogen. Frozen cells were then mechanically destroyed by continuous grinding for 15 min in the presence of liquid nitrogen. The frozen powder was then thawed slowly at 4°C. After that the suspension of broken cells was repetitiously centrifuged at 2000 rpm for 5 min to remove completely the unbroken cells. The protein content of every lysate was estimated spectrophotometrically by measuring optical density at the wavelength of 280 nm. About 2 ml of the cleared cell lysate (still very opaque) were then loaded on top of 11 ml of sucrose-gradient prepared in Ultra-Clear™ centrifuge tubes (Beckman) and centrifuged for 2 hrs at 37000 rpm at 4°C in an ultracentrifuge using a SW40 rotor. 15 fractions of 0,9 ml each were carefully collected from the top. To each fraction 200 µl of 6x Laemmli buffer containing 10 % SDS was added, the fractions were then analysed by SDS-PAGE and by immunoblotting. The chemiluminescence signals were quantified with Lumi-Imager™. Fractions from 1 to 4 contained cytosolic and vacuolar proteins, the Golgi proteins were in fractions 5-11 and ER proteins were in the last four fractions.

3.7. Determination of the levels of low molecular weight sulfhydryl groups in the cell lysates

Yeast cells were grown to early logarithmic phase in YPUAD medium at 30°C overnight. Cells were then shifted to PM-ura-glucose medium for 5 hrs and then split into two aliquots that were incubated for 2 hrs at 30°C and 37°C respectively. Immediately after that cells were poisoned by the addition of NaF/NaN_3 (10 mM each) and collected by centrifugation at 2500 g for 3 min. The cell pellet was washed three times with water containing NaF/NaN_3 (10 mM each). Cells were lysed by vortexing with glass-beads in 100 mM NaP_i buffer (pH 8.0). Lysates of equal protein contents, as assessed spectrophotometrically at 280 nm, were taken for the determination of the levels of low molecular weight sulfhydryl groups with Ellman reagent following an established procedure (Coligan et al., 1995). In short, proteins were precipitated with trichloroacetic acid (final concentration 5%) leaving low molecular weight components of the extracts in the supernatant. NaOH was then added to readjust the pH of supernatants back to pH 8.0. Ellman reagent (5, 5´-dithiobis-(2-nitrobenzoic acid)) (Sigma) was then added to the supernatants to the concentration of 0.8 mg/ml. Stain-development was allowed to proceed for 15 min at room temperature. The concentrations of low molecular weight thiols in the different extracts were then determined spectrophotometrically at 412 nm and compared to a linear calibration curve obtained with cysteine.

3.8. Yeast cell morphology investigation techniques

3.8.1. Morphological investigation of yeast cell vacuoles

The yeast cell vacuolar morphology could be assayed by application of different light-microscopic techniques. Differential-Interference-Contrast microscopy (DIC or "Nomarski-Optic") technique, for example, is based on the detection of the differences in the optical densities between cellular organelles and cytoplasm. Another technique to visualize vacuoles relies on the possibility to stain vacuoles with vital dyes.

3.8.1.1. Quinacrin vacuolar staining assay

The assay was performed according to Wesman et al. (1987). *S. cerevisiae* cells were grown in YPUAD media to 0.5-0.8 OD_{600nm} at room temperature, shifted to 37°C for 2hrs, pelleted and resuspended to the same density in SD-medium. 1ml of that culture was precipitated at 1000x g for 3 minutes and resuspended in 1ml of SD-medium buffered with 50 mM NaH_2PO_4 to pH 7.6. Quinacrine was applied to the concentration of 200 µM and cells were incubated at 37°C for 10 minutes. Cells were harvested by centrifugation at 1000x g for 3 minutes and washed three times with PBS. After the final precipitation yeast cells were resuspended in 100 µl of PBS and 2 µl aliquots embedded in 1 % low-melting agarose matrix were analyzed by light microscopy.

3.8.2. Indirect immunofluorescence

Indirect immunofluorescence was used to identify a cellular localization of proteins by antibody binding. Immunofluorescence was performed as described by Schröder et al. (1995). Cells expressing the antigen of interest were grown overnight in either rich YPUAD or selective minimal medium. An equivalent of 10 OD_{600nm} of cells was collected and resuspended in 0.3 ml of 3,5% formaldehyde in PBS/10% sorbitol buffer. After 2-3 hours of fixation at room temperature the cells were washed with PBS/10% sorbitol, resuspended in 1 ml of this buffer and treated with 60 units of zymolase (Boehringer) in the presence of 1,4 µl/ml β-mercaptoethanol for one hour to partially digest cell walls. Cells were collected by centrifugation, washed two times in PBS/10% sorbitol and resuspended in 100µl of PBS/10% sorbitol. 30 µl of this suspension was applied per slide well, treated with a 0,1% of poly-(L)-lysine solution (Sigma) in H_2O to enhance cell attachment. After 10 min the suspension was removed and 15 µl of blocking solution (PBS/10% sorbitol, 1% Triton X-100, 1% BSA) was applied for 10 minutes. Incubation with the first antibody was carried out overnight at 4°C at appropriate dilution in blocking solution. Cells were then washed seven times with PBS/10%

sorbitol and secondary antibody was added (Cy3-conjugated Fab fragment of goat anti-rabbit or anti-mouse IgG, FITC-conjugated anti-rabbit or anti-mouse IgG). After 1 hour at 30°C the cells were washed ten times with PBS/10% sorbitol solution. Embedding medium (10% p-phenylendiamin in PBS) containing 10 µg/ml of DNA groove-binding dye DAPI (4′, 6-diamidino-2-phenylindole) was applied to the slides, which were then sealed with a cover slip.

3.9. Lipid analysis techniques

3.9.1. Metabolic labeling of the yeast lipids

Yeast cultures were grown to logarithmic phase (OD_{600nm}=0.4-0.7) in YPUAD. 3 ml of each culture was then shifted to PM-ura-glucose medium for 0.5-5 hrs. In some cases cells were preincubated at 37°C for 30 min prior to addition of the label. Radiolabeling was carried out for either 30 min (pulse-labeling conditions) or 5 hrs (steady-state-labeling mode) at 25°C or 37°C in a volume of 0.5 ml PM-ura-glucose and in the presence of 50 µCi [^{32}P]-orthophosphate (10 mCi/ml, Amersham). Incorporation of ^{3}H-inositol, ^{3}H-choline, ^{14}C-serine, ^{14}C-glycerol, ^{14}C-palmitic acid and ^{14}C-cytidine into yeast lipids was performed by pulse-labeling in the presence of 50 µCi of either myo-[2-^{3}H]-inositol (10-20 mCi/mmol, 1 mCi/ml, Amersham) or [methyl-^{3}H]-choline cloride (60-85 mCi/mmol, 1 mCi/ml, Amersham), 5 µCi of L-[U-^{14}C]Serine (151 mCi/mmol, 50 µCi/ml, Amersham), 15 µCi of [U-^{14}C]Glycerol (160 mCi/mmol, 50 µCi/ml, Amersham), 40 µCi of [1-^{14}C]Palmitic acid (57 mCi/mmol, 200 µCi/ml, Amersham) and 30 µCi of [2-^{14}C]Cytidine (55 mCi/mmol, 100 µCi/ml, Amersham). Immediately after the labeling period cells were arrested in growth and metabolism by addition of NaN_3 and NaF to the final concentration of 10 mM each. The cells were pelleted and washed once with 1ml of PBS/1 M sorbitol/10 mM NaN_3/10 mM NaF, pH 6.9. Cells were then resuspended in 0.2 ml of the same buffer and converted to spheroplasts with 3 u of lyticase (Sigma) at 30°C for up to 30 min.

3.9.2. Extraction and TLC-analysis of yeast lipids

Yeast lipids were extracted by three rounds of extraction with 1 ml chloroform:methanol (3:1, v:v) at 50°C for 1 hr with intense shaking. After the final round of extraction the chloroform-methanol solvent was evaporated under vacuum in a speedvac (Bachofer, Germany). The precipitate was resuspended in 30 µl of chloroform:methanol (3:1, v:v) and applied as a dot or thin line to Silicagel 60 chromatography plate (Merck, Darmstadt, Germany). One-dimensional thin layer chromatography (Henderson 1992) was performed employing a

chloroform:2-propanol:ethyl acetate:methanol: 0.25% aqueous KCl (25:25:25:10:9, v:v:v:v:v) mixture as a mobile ascending phase. Images of separated ^{32}P-labeled phospholipids were obtained and quantified with a help of PhosphorImager™ (Molecular Dynamics, CA). Lipids labeled with myo-[2-^{3}H]-inositol or [methyl-^{3}H]-choline were visualized by spraying the TLC plate with Amplify™-solution (Amersham) and exposure to Hyperfilm-ECL™ (Amersham).

3.9.3. Isolation of the heat-inducible phospholipid ("PLX")

PLX was isolated from total [^{32}P]-labeled lipid-extract by a single run on one–dimensional TLC in the organic solvent system described above. The position of PLX migration was determined by exposure of the TLC plate to X-ray film (Kodak). The developed X-ray film was used then as a template with which the TLC plate was overlaid. A thin layer of silicagel was scraped off the chromatography plate at a site matching the location of PLX on the autoradiograph. The silicagel flakes were ground into fine powder and PLX was extracted by three rounds of extraction with 1 ml of the following solvent systems each employed in the succession listed below: chloroform:methanol (3:1, v:v); chloroform:methanol (2:1, v:v); chloroform:methanol (1:1, v:v).

3.9.4. Phospholipase A_2 treatment of extracted [^{32}P]-labeled lipids

Total [^{32}P]-labeled lipid extracts as well as purified PLX were subjected to Phospholipase A_2 (PLA_2, EC 3.1.1.4, Sigma) treatment in 20 µl of water buffered with 10 mM Tris-HCl to pH 8,9 for 1 hr at 25°C (recommendation of Sigma). Approximately 50 units of Phospholipase A_2 were taken per assay. After 1 hr of treatment the water was evaporated in a speedvac and the dry material was dissolved in 30 µl of chloroform:methanol (3:1, v:v) solvent mixture for use in TLC assay.

3.9.5. Base treatment of extracted lipids

In order to determine the potential ceramide nature of radioactively labeled lipids we used the base sensitivity test (Becker and Lester, 1980). 10 µl of ^{32}P-labeled lipid-extracts were diluted with 20 µl of 1:1 chloroform:methanol, 6 µl of 1 M NaOH was added and the mixture was incubated at 30°C for 1 hr with constant shaking. Adding 1 M sodium-acetate to the concentration of 150-200 mM neutralized the samples. They were applied in several aliquots with intermittent drying to the start-line of a TLC plate.

4. Results

4.1. Isolation of a mutant mislocalizing the Golgi-protein Emp47p to the vacuole.

4.1.1. The genetic screen

The non-essential yeast Golgi transmembrane-protein Emp47p contains a di-lysine retrieval signal (Fig. 5) and recycles continuously between the Golgi and the ER in a coatomer-dependent manner (Schröder et al., 1995; Lewis and Pelham,1996; Schröder-Köhne et al., 1998). Mutants in the retrieval machinery (*sec21, sec27, ret2, ret3, tip20, sec20*) mislocalize Emp47p to the vacuole, where it is rapidly degraded, resulting in a reduced steady state level of Emp47p (Lewis and Pelham, 1996; Cosson et al., 1997; Schröder-Köhne et al., 1998).

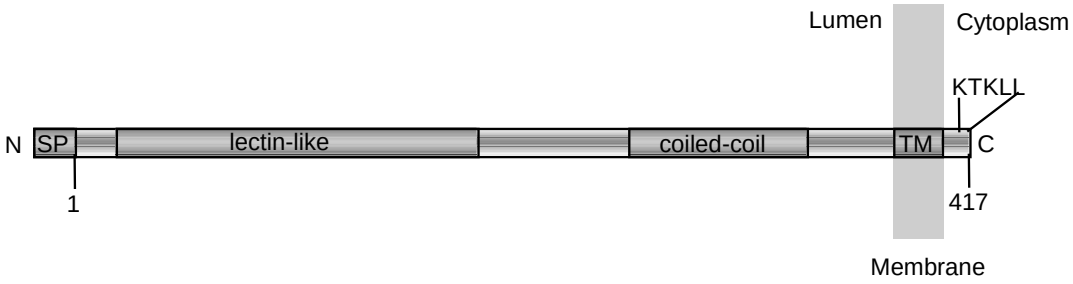


Fig. 5: Primary structure and membrane topology of Emp47p
N= amino-terminus; C= carboxy-terminus; SP= cleavable signal peptide; coiled-coil= potential c.-c. domain; TM= transmembrane domain; numbers indicate the amino-acids positions in the mature protein; KTKLL= di-lysine signal.

Making use of this property of Emp47p we devised a screen for novel mutants affected in the Golgi-localization of di-lysine proteins (Fig. 6). EMS-mutagenised yeast cells (RH448) were plated on YPUAD-plates and screened by a colony-blot assay (Lyons and Nelson, 1984) for colonies with a decreased level of Emp47p, as determined with an antiserum directed against Emp47p (Schröder et al.,1995). I assumed that a reduction of the Emp47p-specific signal would result, at least in some cases, from mislocalization of Emp47p to the vacuole. Mutations in or deletion of *EMP47* have no growth phenotype under laboratory conditions (Schröder et al., 1995). Therefore, in order to exclude any mutations in *EMP47* itself, I restricted my analysis to mutants unable to grow at 37°C. That subset of mutants (209 representatives out of 70000 screened) was crossed back to wild-type yeast cells (RH448). The diploid cells were let to undergo meiosis resulting in formation of packets of four spores enveloped by a single shell (tetrad). By genetic analysis of tetrads I found 21 mutants from 70000 screened in which the decreased level of Emp47p segregated with the inability to grow at 37°C.

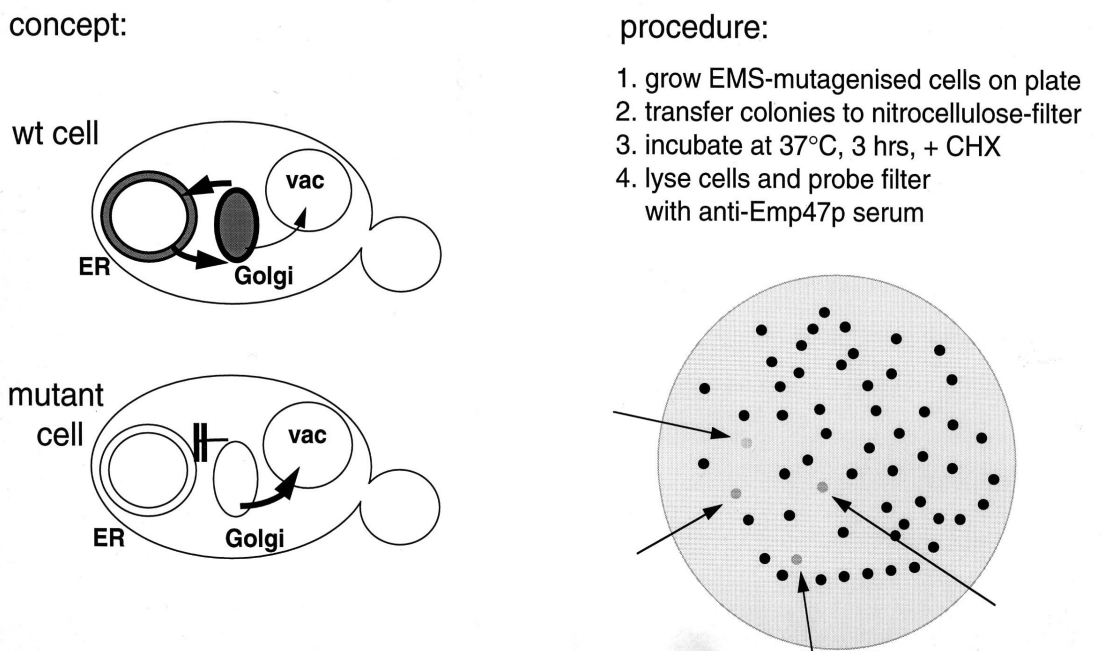


Fig. 6: A new screen for mutants defective in Golgi to ER transport of Emp47p
In wild type cells Emp47p cycles continuously between the Golgi and ER. In mutants, specifically blocked in retrograde transport, the majority of Emp47p leaks to the vacuole and is degraded there by vacuolar peptidases. Specifically reduced levels of Emp47p characterise these mutants.
ER: endoplasmic reticulum; Golgi: Golgi apparatus; vac: vacuole
Light grey colour of some colonies symbolises the reduced amount of Emp47p.

The dissected tetrads for some of the mutants are shown in Fig. 7. Those 21 mutants were subjected to complementation analysis with mutants known to mislocalize Emp47p to the vacuole (*sec21-1*, *sec27-1*, *ret2-1*, *ret3-1*, *tip20-1*, *sec20-1*, and *ufe1-1*) (see chapter 2.1). Two mutants (#297 and #412) not complementing *sec27* were isolated, whereas the other mutants complemented all the tester-strains (data not shown).

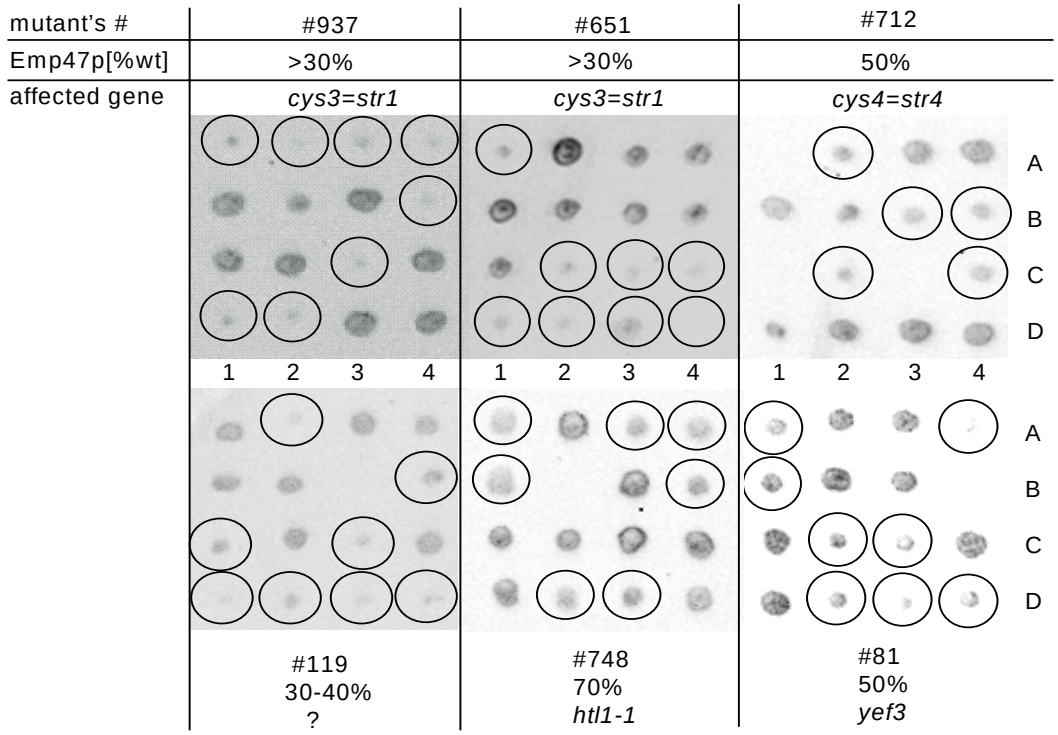


Fig. 7: Cosegregation of temperature-sensitivity with low levels of Emp47p in dissected tetrads as visualised by colony-blot assay.
In short, the diploid yeast cells from crosses between RH448 (wild type) and ts-mutants, preselected by colony-blot assay on the basis of the reduced level of Emp47p, were converted to tetrads (refer to chapter 3.4.2). After tetrad dissection (4 tetrads out of 8 dissected per each diploid strain are represented in the figure), the spores were let to develop into small colonies on solid YPUAD media at 25°C and, subsequently, the colonies were replica-transferred to either nitrocellulose filters for colony-blot assay (see chapter 3.4.7) or to a new YPUAD plate for incubation at 37°C. The nitrocellulose filters containing the replicas of dissected tetrads were probed with anti-Emp47p antibodies and the chemiluminescence signals were then detected and quantified by Lumi-imager™. The developed photo-image was compared with the pattern of the spores' growth abilities obtained at 37°C. Several cases, in which the temperature-sensitivity of the spore segregated flawlessly together with the low level of Emp47p, are represented in the figure. The colonies emerged from the ts-spores are encircled by black rings.

4.1.2. Proteinase A-deficient strains were prepared from selected mutants

Strains deficient for the *PEP4* gene product, proteinase A, are largely deficient in vacuolar protease activity (Jones, 1984). In mutants that mislocalize Emp47p to the vacuole, the protein can be detected there if the strain is *pep4Δ* in addition (Schröder et al., 1995). Therefore, we analyzed the localization of Emp47p by indirect immunofluorescence in *pep4Δ*-variants of the new mutants. *pep4Δ*-variants of the mutants isolated in our screen were produced by crossing with the yeast strain RH732 (*pep4Δ*, but otherwise isogenic with the strain used for mutagenesis) followed by tetrad dissection and selection for the spores distinguished by both temperature-sensitivity and the presence of *pep4::URA3* marker on SD(Ura-)-media. According to colony-blot immunodetection analysis, knocking out *PEP4*-gene brought the level of Emp47p back to wild type situation in nine different mutant strains, including strains #49 and #937 (see below).

4.1.3. Emp47p is mislocalized to the vacuole in the #937 mutant

4.1.3.1. Indirect immunofluorescence analysis visualizes Emp47p in the vacuole

Based on immunofluorescence analysis, Emp47p was mislocalized to the vacuole in only a single novel complementation group exemplified by mutant #937, which later turned out to bear a novel *cys3*-allele (see chapter 4.2 below). Mislocalization of Emp47p was already apparent at 25°C. In addition to some remaining punctate structures indicative of yeast Golgi, a prominent ring-like staining became apparent (Fig. 8). This stain was contiguous with the perimeter of the vacuole, visualized as an indentation in the differential interference contrast (DIC) image. I noted that the vacuoles in those cells were filled with particles that were not visible in the corresponding wild-type cells. The Golgi protein Rer1p colocalizes with Emp47p to about 80% in wild-type cells (Schröder-Köhne et al.,1998). In contrast to Emp47p, it retained a wild-type like punctate Golgi-pattern in the mutant cells (Fig. 8). Therefore, Golgi-structures are not merely reduced in number or absent from the *cys3-2* cells. Indirect immunofluorescence of *cys3-2* mutant with antiserum directed against the ER-resident protein Kar2p also revealed that the ER morphology appeared to be undisturbed in those cells (Fig. 9). Furthermore, EM analysis revealed that no gross morphological changes in internal membranous structures were visible (data not shown).

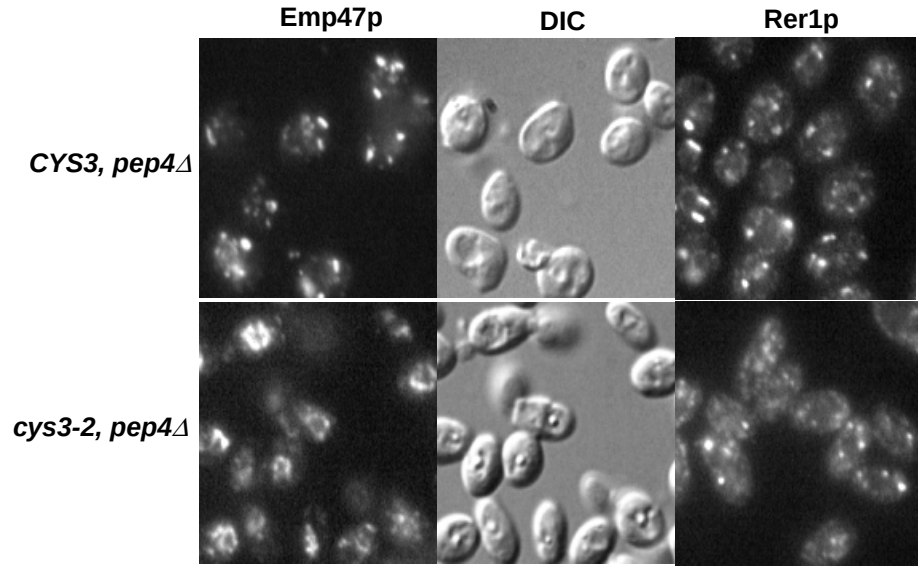


Fig. 8: Emp47p is mislocalized to the vacuole in *cys3-2* mutant cells
RH732 (*CYS3, pep4Δ*) and AMY3 (*cys3-2, pep4Δ*) were grown to log phase in rich YPUAD medium and subjected to immunofluorescence analysis with antiserum against Emp47p and Rer1p. DIC, differential interference contrast. Vacuoles appear as indentations in the DIC-images. Note particles within the vacuoles of AMY3.

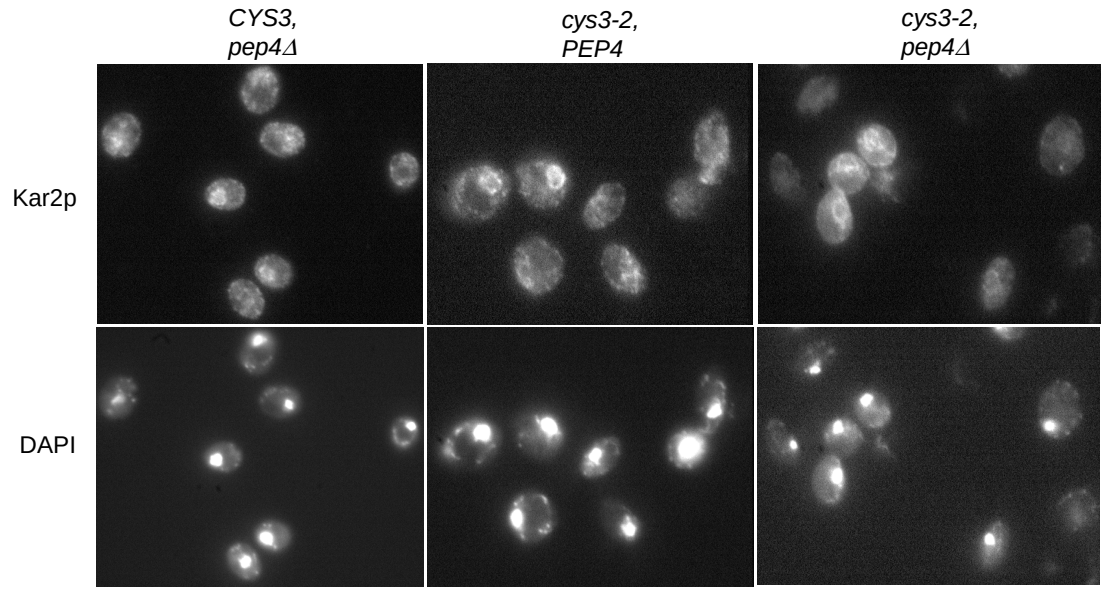


Fig. 9: ER retains wild type morphology in *cys3-2* mutant cells.
RH732 (*CYS3, pep4Δ*), AMY3 (*cys3-2, pep4Δ*) and AMY2 (*cys3-2, PEP4)* were grown to log phase in rich medium (YPUAD) at 25°C then shifted to 37°C for 90 minutes followed by immunofluorescence analysis with antiserum against Kar2p. DAPI (4,6-Diamidino-2-phenylindole, Sigma): fluorescent groove-binding probe for DNA.

4.1.3.2. Western-blotting analysis indicates *PEP4*-dependent degradation of Emp47p in the vacuole

In order to obtain independent evidence for the vacuolar degradation of Emp47p in the *cys3-2* mutant, I measured the amount of *PEP4*-dependent degradation of Emp47p in a quantitative Western-blotting experiment calibrating Emp47p against total cell protein. After incubation at 37°C for 90 min, Emp47p was reduced to 54% of the wild-type level. This reduction was alleviated in a *pep4Δ*-version of the *cys3-2* cells to 71% of wild-type levels (Fig. 10).

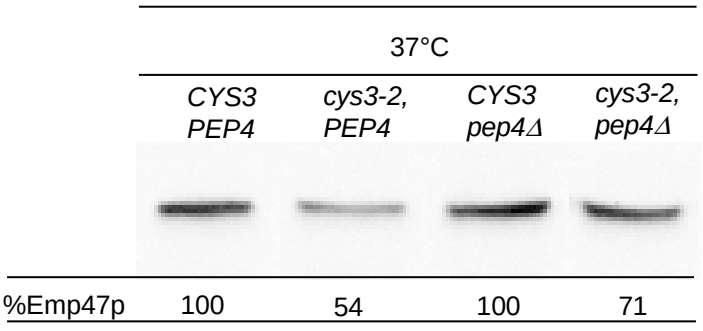


Fig. 10: Dependence of Emp47p turnover on vacuolar proteolysis.
Quantitative immunoblotting (see chapter 3.5.8) for levels of Emp47p in protein extracts prepared from *PEP4* and *pep4Δ* versions of wild-type and *cys3-2* mutant cells respectively, RH448 (*CYS3, PEP4*), RH732 (*CYS3, pep4::URA3*), AMY2 (*cys3-2, PEP4*), and AMY3 (*cys3-2, pep4::URA*) Cells were grown to logarhithmic phase at 25°C in YPUAD medium and then shifted to 37°C for 90 min prior to lysis.

4.2. Identification of a novel *cys3*-allele

4.2.1. The temperature-sensitivity and cysteine auxotrophy of the #937 mutant is rescued by 2µ-*CYS3* plasmid

Fig. 11A demonstrates that the mutant and a *cys3Δ*-strain grew at 25°C on plates with peptone and yeast extract (YPUAD), although already somewhat more slowly than wild-type cells. At 37°C the mutant cells did not grow, which held true for the *cys3Δ*-strain. A growth curve in YPUAD-medium revealed that the mutant stopped growing about 4 hrs after a temperature shift to 37°C (Fig. 11B). Cells were not killed however, as relieve from a prolonged temperature stress (64 hours at 37°C) allowed mutant cells to resume growth on a solid YPUAD agar-plate at 25°C (Fig. 11C). In order to identify the gene affected in the mutant #937 we transformed it with a 2µ-yeast genomic library and selected for rescue of the temperature sensitivity. A complementing plasmid (2µ-*CYS3*, chapter 2.2.) was found to carry a 2.7 kbp fragment of chromosome I (nucleotide 129954-132702). The insert contains a single complete gene (nucleotide 130798 to 131979), *STR1/CYS3* (Cherest and Surdin Kerjan, 1992; Ono et al., 1992; Barton et al., 1993; Yamagata et al., 1993). *CYS3* codes for the pyridoxal-phosphate dependent cystathionine-γ-lyase (EC 4.4.1.1.). Cys3p is a cytosolic enzyme of the reverse transsulfuration pathway in yeast (Fig. 3), catalyzing the final step in the biosynthesis of cysteine (Cherest et al., 1993). Although it was originally selected for different phenotypes, mutant #937 proved to be strictly dependent on cysteine at any temperature. The latter finding argues that the protein encoded by the mutant allele is not temperature sensitive for function. In the presence of the genomic *CYS3*-clone (2µ-*CYS3*) the cysteine auxotrophy was reversed as expected (Fig. 11D).

4.2.2. Transition point-mutation in *CYS3* disables cystathionine-γ-lyase due to conserved serine to phenylalanine exchange

To unequivocally prove that it was *CYS3* that was affected in mutant #937 we sequenced the PCR-amplified gene from wild-type and two mutant strains both derived from the second back-cross of #937 (AMY2 and AMY3). *CYS3* from wild-type coded for a protein that did not differ in amino acid sequence from the sequence in the database (Genbank AAC04945.1). However, both mutant strains carried a single transition mutation at nucleotide 602 of the *CYS3* coding region. A cytidine present in the wild-type was replaced by thymidine, resulting in a serine to phenylalanine exchange in the polypeptide chain at position 201.

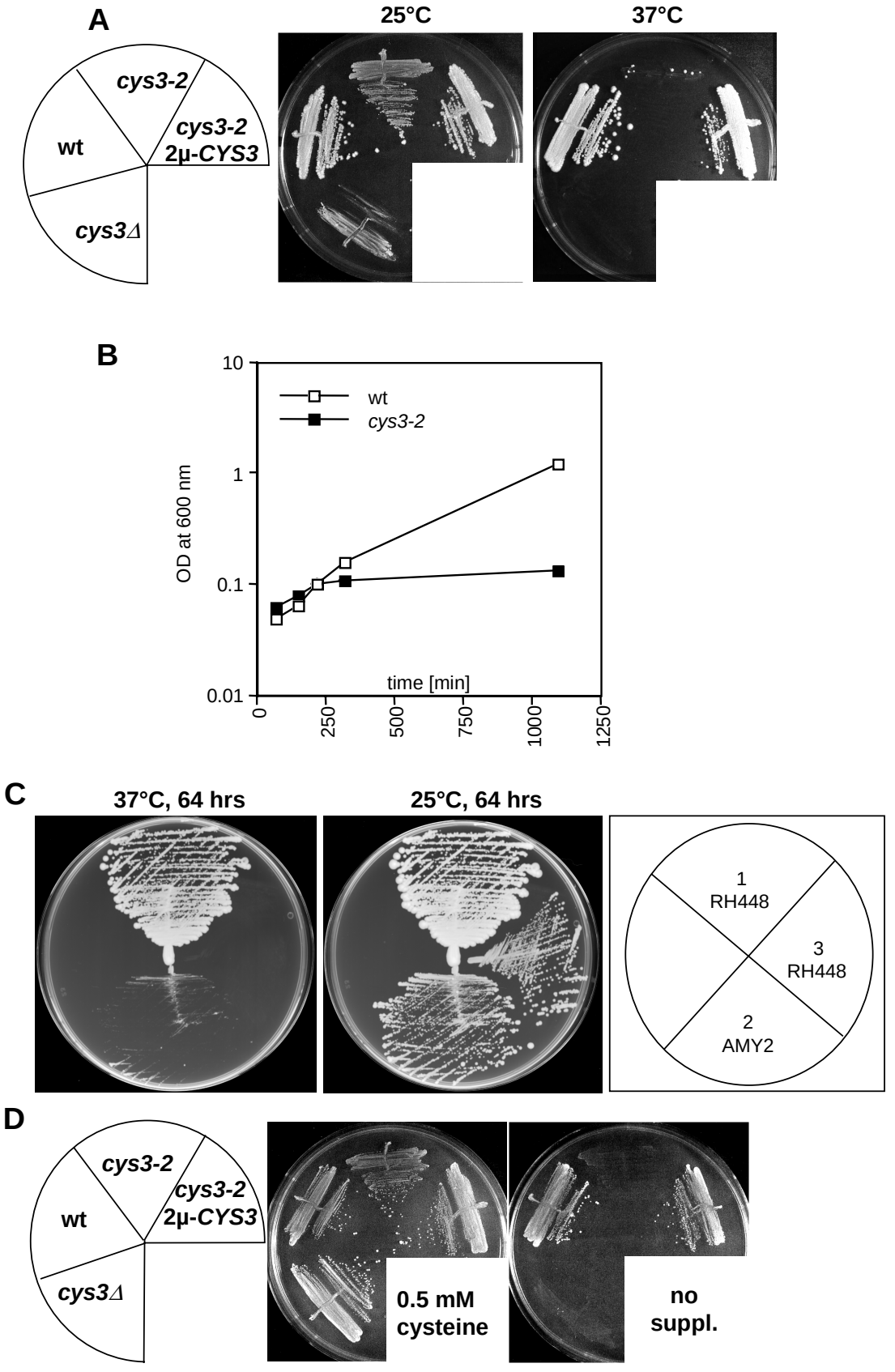


Fig. 11: Growth properties of the *cys3-2* mutant.
A. *cys3*-defective cells are temperature sensitive on YPUAD plates. RH448 (wildtype, "wt"), C181 (*cys3Δ*), AMY2 (*cys3-2*) and AMY2 transformed with the genomic clone comprising *CYS3* (*cys3-2, 2µ-CYS3*) were plated on YPUAD plates and incubated at the indicated temperature.

B. Growth curve of AMY2 (*cys3-2*) in comparison to RH448 (wt) after shift to 37°C. Cells were grown to early log-phase in YPUAD at 25°C. The cultures were then diluted in fresh, prewarmed YPUAD to below 0.1 OD_{600nm} and incubated in a shaking incubator at 37°C for the indicated times.
C. Wild type (RH448, "1") and *cys3-2* mutant cells (AMY2, "2") were plated on YPUAD agar-plate and incubated 64 hrs at 37°C. Then plates were shifted to 25°C for 64 hrs. A fresh streak of RH448 ("3") was administered to the plate immediately following the temperature shift from 37°C to 25°C for comparison.
D. RH448 (wt), C181 (*cys3Δ*), AMY2 (*cys3-2*) *and* AMY2 transformed with the genomic clone comprising *CYS3* (*cys3-2, 2μ-CYS3*) were plated on SD-plates supplemented as indicated and incubated at 25°C.

From the obtained data we infer that mutant #937 bears a *cys3* allele coding for a constitutively inactive Cys3p and that this *cys3-2* allele is responsible both for temperature-sensitivity on rich YPUAD medium and cysteine auxotrophy.

4.3. Identification of the mutated alleles responsible for the reduced levels of Emp47p

As it was mentioned above, the genetic screen yielded a number of mutants which displayed a strict coinheritance of the reduction in the levels of Emp47 with temperature sensitivity (Fig. 7) in tetrad analysis but did not reveal mislocalization of Emp47p to the vacuole when assayed by indirect IF (data not shown). In many instances we succeeded in genetic identification of the particular alleles affected in those mutants (Table 4.1). As in the case with the mutant #937, I transformed all the other mutants represented in the Table 4.1 with a 2μ-yeast genomic library and selected for rescue of the temperature sensitivity. In addition to the mutant #937, I found another two mutants (#49 and #651) that were affected in *CYS3* gene, as they were rescued from both temperature-sensitivity and cysteine auxotrophy with the same 2μ-*CYS3* plasmid that complemented the #937 mutant phenotypes. There was, however, another mutant (#712) displaying cysteine-auxotrophy that was not rescued by 2μ-*CYS3.* The plasmid that restored the cysteine-prototrophy of the mutant #712 as well as its normal growth at 37°C was found to encompass a stretch of the genomic DNA (residue 795786 to 800452 on chromosome VII) containing complete ORF (*YGR155w*) coding for Cys4p. Cys4p (cystathionine-β-synthase) is a cytosolic enzyme of the reverse transsulfuration pathway in yeast (Fig. 3), catalyzing the conversion of homocysteine and serine into cystathionine. This step in the biosynthesis of cysteine precedes immediately the place of Cys3p action (Cherest et al., 1993).

The temperature-sensitivities of the mutants #748 and #623 were found to be rescued by two separate yeast genomic library 2μ–plasmids containing partially overlapping fragments of the chromosome III (residue 152364 to 158938 for #748 and residue 154681 to 161414 for #623). Among other genes, these fragments encompass the complete ORF (*YCR020W-B*) of the gene coding for Htl1p. Indeed, subcloning the *ClaI/EcoR*VI fragment of 700 bp (contains

the only complete ORF *YCR020W-B*) into pRS326(*ClaI/SmaI*) vector fully rescued the ts-phenotype of both #748 and #623 mutants upon transformation (data not shown). According to Proteome and SGD databases, Htl1p is a protein necessary for viability at elevated temperature. In a systematic deletion project (EUROFAN) a null mutant for *HTL1* was found to be viable (Winzeler et al., 1999), but showed temperature-sensitive lethality (SGD database).

Mutant #81 was shown to be complemented by a yeast genomic library 2μ–plasmid that contains a fragment of Chromosome XII (residue 634246 to 640395). Subcloning *XhoI/SacI* fragment (contains the only full length ORF (*YLR249w)* of the gene coding for YEF3) into pRS326(*XhoI/SacI*) vector and introducing the resulting plasmid back to mutant #81, conferred temperature-resistance to the cells growing at 37°C (data not shown). Thus, it appears that a lesion in *YEF3* gene coding for the yeast translation elongation factor EF-3A was responsible both for the temperature-sensitivity and the low level of Emp47p in the mutant #81.

The mutant #119 was found to profit in growth at 37°C from the yeast genomic library plasmid that contained fragment of the yeast chromosome VI (residue 104221 to 110828) (data not shown). That fragment encompassed several ORFs potentially coding for 5 different proteins (refer to Table 4.1 for more details). I did not elucidate, however, supplementation of which particular ORF enables the mutant #119 to resume growth at 37°C. However, according to immunofluorescence analysis, the Golgi-localization of Emp47p was not disturbed in the mutant #119-D deleted for *PEP4* (data not shown).

The evidence on the impairment of *SEC27* allele in the mutants #412 and #297 were obtained purely by a genetic complementation assay, in which the crosses between the ts yeast strain RH3609 (*MATa, sec27*) and either #412 or #297 ts-mutants (MATα, *geneX*) produced diploids non-viable at 37°C (data not shown).

Table 4.1. Identification of the genes affected in the ts-strains of *S. serevisiae* isolated in the genetic screen for mutants with low level of Emp47p

Strain #	Affected gene or chromosomal locus	Protein name
937, 49, 651	*CYS3=STR1*	Cystathionine-γ-lyase (yeast transsulfuration pathway)
712		Cystathionine-β-synthese (yeast transsulfuration pathway)
412		β´-COP subunit of coatomer
748, 623		**High-temperature lethal protein**
81		Translation elongation factor EF-3A, member of

		ATP-binding cassette (ABC) superfamily
119	Chromosome VI, residue 104221 to 110828	5 different complete ORFs (*MDJ1*, *YFL015C*, *HSP12*, *IES1*, *YFL013W-A*) potentially coding for 5 different proteins. Among them 2 ORFs code for proteins of known function: *HSP12*(*GLP1*) and *MDJ1*(heat shock protein-chaperone)

4.4. The physiological effects of the malfunction in cysteine biosynthesis

4.4.1. In contrast to *cys3*-2 mutant, *gsh1Δ* cells are not temperature-sensitive for growth on rich YPUAD medium

It was surprising that the *cys3-2* mutant displayed temperature-sensitivity in rich medium despite the fact that it is a constitutive loss of function allele. I therefore reasoned that the mutant might be arrested in growth due to reasons other then starvation for the amino acid cysteine. Cysteine is part of GSH, an essential antioxidant of the cell (see "Introduction"). In order to assess the oxidative stress as the potential cause for the phenotypes displayed by *cys3-2*, I compared that mutant with a mutant *gsh1Δ* (yeast strain B4742, chapter 2.1), which suffers from the inability to synthesize GSH due to the disruption in *GSH1* gene (GenBank # CAA89396.1) coding for γ-glutamyl-cysteine synthetase (Fig. 3). *GSH1* was shown to be an essential gene in *S. cerevisiae* providing the absence of external supply of glutathione in the medium (Wu and Moye-Rowley, 1994). Accordingly, growth of *gsh1Δ* cells used in our study exhibited strict requirement for the presence of GSH in the incubation medium, as the knock-out grew neither on minimal SD-medium without GSH (data not shown) nor on SD-medium supplemented with cysteine (data not shown). In contrast to the *cys3-2* mutant, the cells knocked out for *GSH1* gene displayed temperature-sensitivity neither in liquid (data not shown) nor on solid rich YPUAD medium (Fig. 12A).

4.4.2. *gsh1Δ* cells are less sensitive to the presence of oxidizing agent in rich incubation medium than *cys3-2*

If, indeed, *cys3-2* mutant cells experience oxidative stress at elevated temperature, than they are likely to reveal hypersensitivity to oxidizing agents supplied to the incubation medium. 1-chloro-2,4-dinitrobenzene (Oluwatosin and Kane, 1997) was added to the solid YPUAD agar-plate to the end-concentration of 50 μg/ml. Cells were administered to the plates as serial dilutions (1:10). Cells were then incubated at 30°C for 64 hours.

The sensitivity of *cys3-2* mutant to the cysteine- and GSH-oxidizing agent 1-chloro-2,4-dinitrobenzene supplemented to the medium was noticeably greater than the sensitivities displayed by both *gsh1Δ* mutant and wild type cells (Fig. 12B).

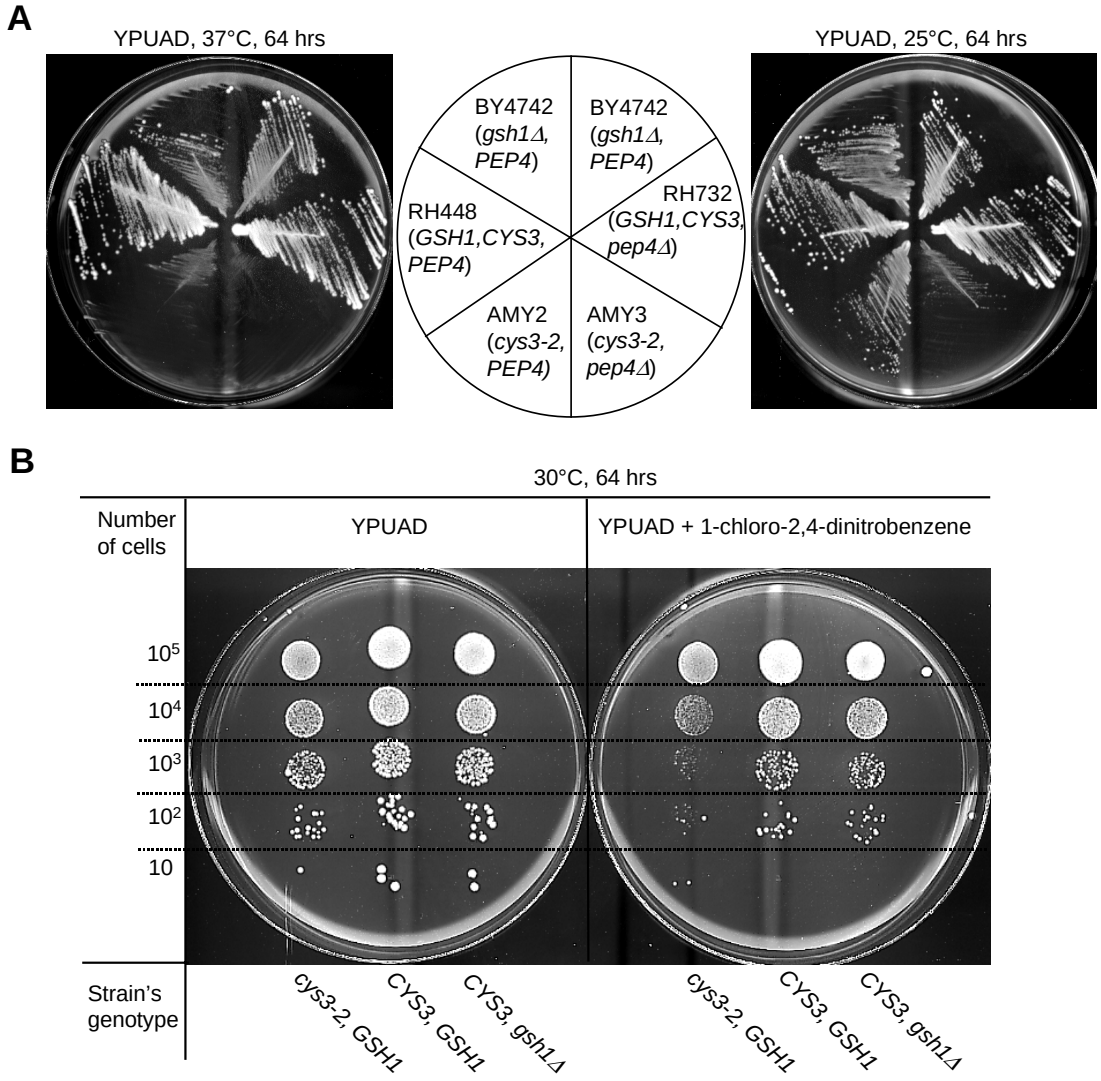


Fig. 12: Growth properties of *gsh1Δ* cells in comparison to *cys3-2* mutant.
A. *gsh1Δ* cells are not restricted for growth on rich YPUAD agar-plates at 37°C. RH448 (wildtype, "wt"), AMY2 (*GSH1, cys3-2, PEP4*), AMY3 (*GSH1, cys3-2, pep4Δ*) and BY4742 (*gsh1Δ, CYS3, PEP4)* were plated on YPUAD plates and incubated at the indicated temperatures.
B. c*ys3-2* mutant displays reduced growth capabilities on a rich medium supplemented with an oxidizing agent at 30°C. RH448 (wild type), AMY2 (*cys3-2, GSH1*) and BY4742 (*CYS3, gsh1Δ*) yeast cell cultures were applied as serial dilutions to the plates containing either solid YPUAD medium alone or YPUAD medium supplemented with an oxidizing agent (1-chloro-2,4-dinitrobezene) in concentration of 50 µM. Note that, in contrast to *cys3-2* mutant cells, the growth of *gsh1Δ* cells is not compromised by these conditions.

4.4.3. Cysteine production, but not glutathione is required for normal Emp47p biosynthesis and trafficking

Next question I addressed was, whether glutathione as such was necessary for the maintenance of the level and proper localization of Emp47p.

Comparative studies of the lysates prepared from the *cys3-2* mutant, *gsh1Δ* and wt cells by subcellular fractionation on sucrose-gradient revealed no major differences in the levels and distributions of Emp47p, Rer1p (data not shown) and Kar2p (data not shown) if cells were grown at 30°C in minimal SD medium supplemented with cysteine (60 µM) (Fig. 13A).

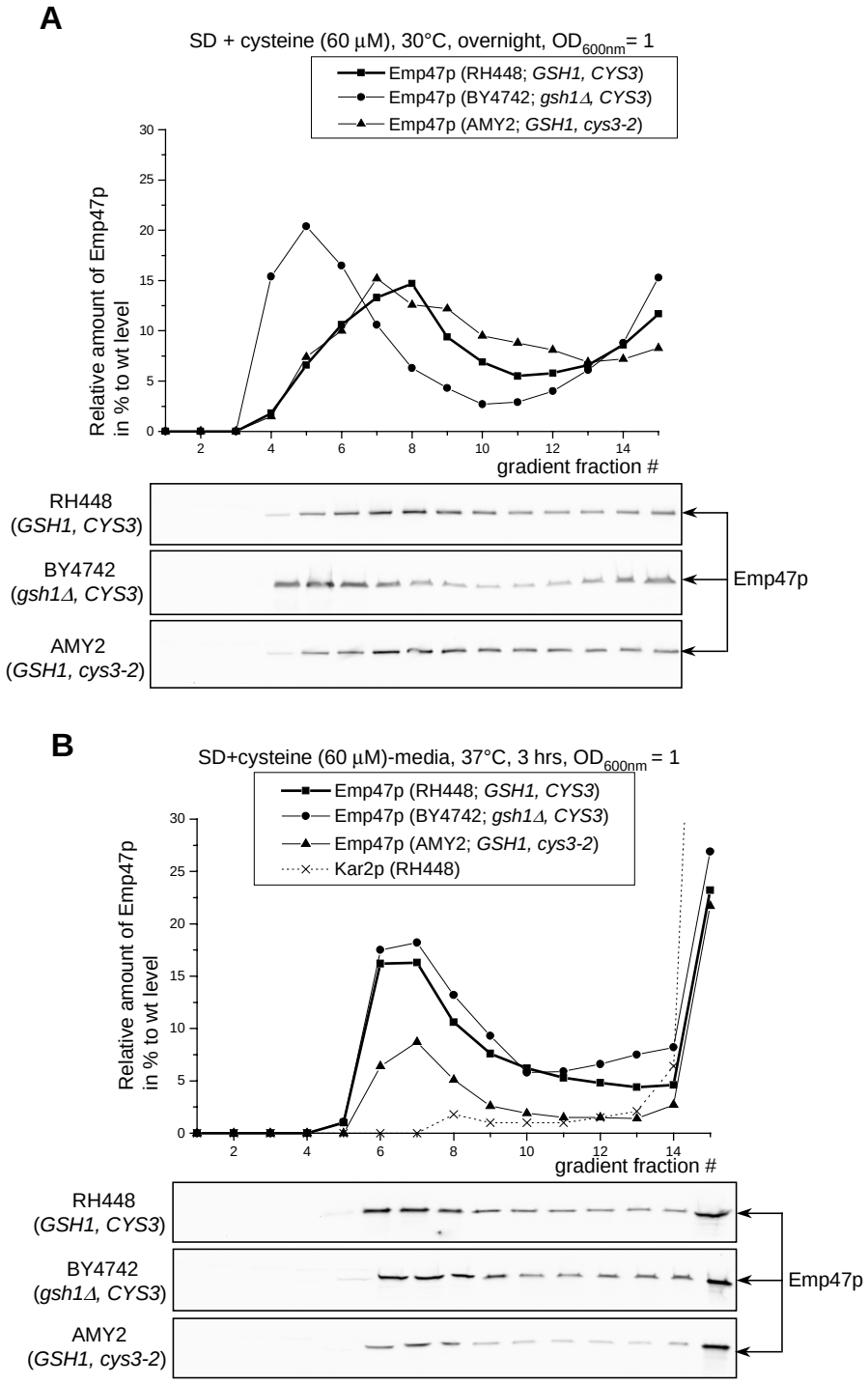


Fig. 13: Level of Emp47p in *cys3-2* mutant is reduced in temperature-dependent manner.

Lysates from different yeast strains (RH448, AMY2 and BY4742) were assayed by velocity sedimentation on sucrose gradient and quantitative immunoblotting for the distribution and the relative amount of the Golgi protein marker Emp47p. The distribution of the Kar2p highlights the location of the sucrose gradient fractions

containing the ER membranes. Before being subjected to the mechanical lysis under liquid nitrogen (3.6.2), the cells were incubated in rich YPUAD medium overnight, shifted then to the minimal SD-medium supplemented with 60 µM of cysteine and incubated at either 30°C ("A") or 37°C ("B"). The total amount of every marker-protein in wild type cells was set to 100%.
A. Neither the distribution nor the amount of Emp47p is severely affected in both *cys3-2* and *gsh1Δ* mutants at 30°C, as compared to wild type cells.
B. The relative amount of Emp47p in *cys3-2* mutant is reduced to around 50% of the wild type level upon shift to 37°C for 3 hrs, whereas the *gsh1Δ* cells do not show reduction in the amounts of Emp47p.

In complience with data obtained by quantitative immunoblotting (Fig. 10), the temperature shift to 37°C for 3 hrs performed in the same medium brought about a drastic (almost 50%) reduction in the levels of Emp47p (Fig. 13B) in *cys3-2* mutant only. The level and distribution of Emp47p assayed by velocity sedimentation on sucrose gradient in *gsh1Δ* mutant and wild-type cells remained unaffected at 37°C (Fig. 13B).

Indirect immunofluorescence analysis of Emp47p distribution performed on *gsh1Δ* cells (strain BY4742) that have been stressed by high temperature for 3 hours in the rich YPUAD medium confirmed the Golgi-localization of the marker-protein (Fig. 14).

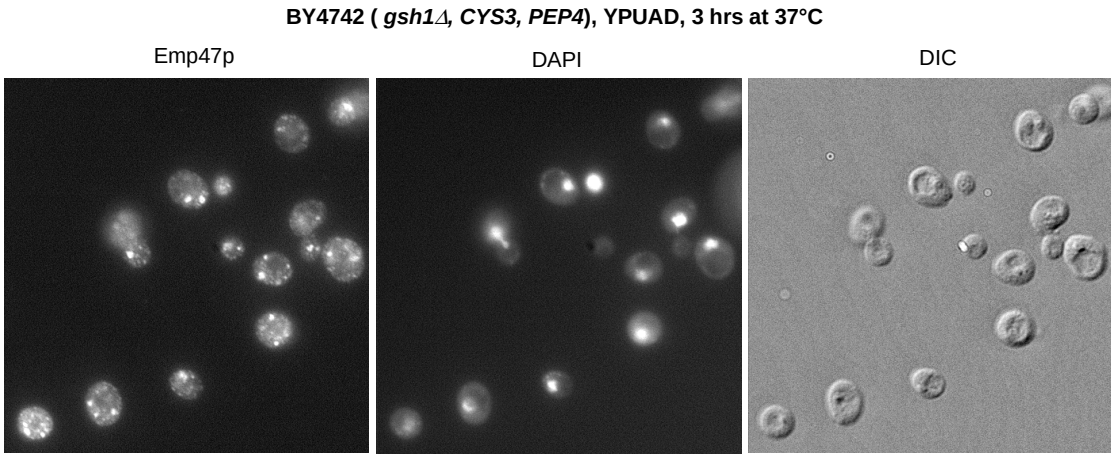


Fig. 14: Indirect immunofluorescence analysis of *gsh1Δ* cells reveals the Golgi localisation of Emp47p.
BY4742 (*gsh1Δ, PEP4*) was grown to log-phase in rich YPUAD medium at 25°C. Cells were then shifted to 37°C for 3 hours and, after that, subjected to immunofluorescence analysis with antiserum against Emp47p. Note the dot-like pattern of immunofluorescence indicative of the Golgi localisation of Emp47p. DIC, differential interference contrast. Vacuoles appear as indentations in the DIC-images.

4.4.4. Cytosolic and organellar proteins are affected differentially in *cys3-2* mutant cells

In order to estimate how specific the *PEP4*-dependent reduction of Emp47p was, we analyzed various other Golgi, vacuolar and cytosolic marker-proteins in the *cys3-2* mutant for *PEP4*-dependent reduction. By immunoblotting we observed three different qualitative types of response to the absence of functional Cys3p (Fig. 15). a) In *PEP4/cys3-2* cells, the Golgi protein Yip1p (Yang et al., 1998), a subunit of the cytosolic protein complex coatomer,

δ-COP (Cosson et al., 1996) and the cytosolic chaperones Ssa1p/Ssa2p (Werner-Washburne et al., 1987) were similarly reduced to 35-67% in comparison to the *PEP4* wild-type. This reduction was largely *PEP4* dependent, because in *pep4Δ/cys3-2* cells, the levels of the respective proteins was restored to 75-126% of the *pep4Δ* version of wild-type cells. b) Rer1p (Boehm et al., 1997), which we had shown to retain a Golgi-like distribution in the *cys3-2* cells (Fig. 8), displayed almost wild-type levels in the *PEP4/cys3-2* cells (82%). However, in *pep4, cys3-2* cells the level was 162% of the corresponding wild-type. Thus, Rer1p also seemed to get increasingly degraded in a *PEP4*-dependent manner, but apparently increased vacuolar turnover was compensated for by increased synthesis. c) The vacuolar carboxypeptidase Y (CPY) was expressed to about twice the levels of wild-type in both *pep4Δ* and *PEP4* derivatives of the *cys3-2* mutant cells.

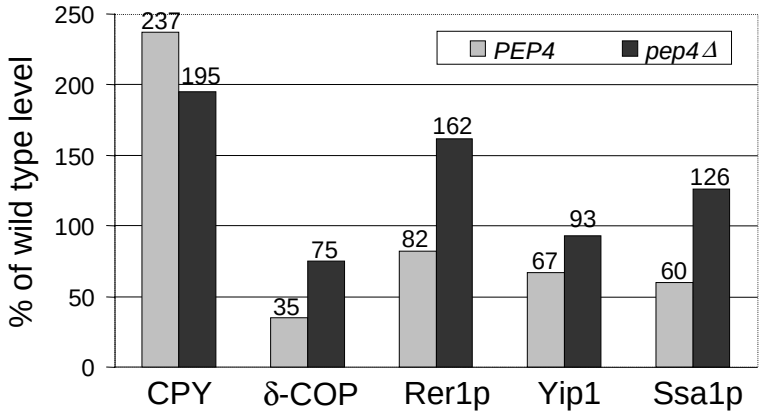


Fig. 15: Marker proteins are differentially affected in *cys3-2* mutant cells.
PEP4 and *pep4Δ* versions of *CYS3* wild-type (RH448, RH732) and *cys3-2* mutant cells (AMY2, AMY3) were grown to log-phase at 25°C in YPUAD medium. They were lysed by vortexing with glass-beads in the presence of protease-inhibitors, SDS and β-mercaptoethanol. Relative amounts of various antigens were determined by quantitative immunoblotting (see chapter 3.5.8). Total yeast protein was resolved by SDS-PAGE. Proteins were then transferred to a nitrocellulose membrane. The blots were analysed by probing with antibodies directed against CPY, δ-COP, Rer1p, Yip1p and Ssa1p. Enhanced chemiluminescent signals from the *PEP4* and *pep4Δ* versions of *cys3-2* mutant extracts were plotted as percent of the signals obtained from the corresponding wild-type extracts.

4.4.5. *cys3*-2 and *gsh1Δ* mutants are distinguished by differential response of Golgi protein-markers to the presence of the oxidizing agent in the medium

I reasoned that, if oxidative stress was the cause of mislocalization of Emp47p, the addition of the strong oxidizer could aggravate the mislocalization and reduce steady-state levels of Emp47p. When the YPUAD incubation medium was supplemented with 100 μM of a strong GSH-oxidizing agent (1-chloro-2,4-dinitrobenzene), the level of Emp47p reduction at that temperature in *cys3-2* mutant cells reached almost 100% as assayed by velocity sedimentation analysis on sucrose gradient (Fig. 16A). The level of Rer1p and Sed5p in *cys3-2* mutant under

this experimental regimen did not differ much from that of wild type cells, constituting around 85% and 120% of the respective wild type levels (Fig.16B and 16D, respectively). Interestingly, although the presence of a strong cysteine- and GSH-oxidizer did not bring the level of Emp47p in *gsh1Δ* cells below that of wild type cell (Fig. 16A), the amount of Rer1p (Fig. 16B) as well as the amount and localization of the Golgi t-SNARE Sed5p (Fig. 16D) were severely disturbed. Fig. 16C shows that the distribution of the soluble ER-chaperone Kar2p was not affected in any of the mutants at any conditions.

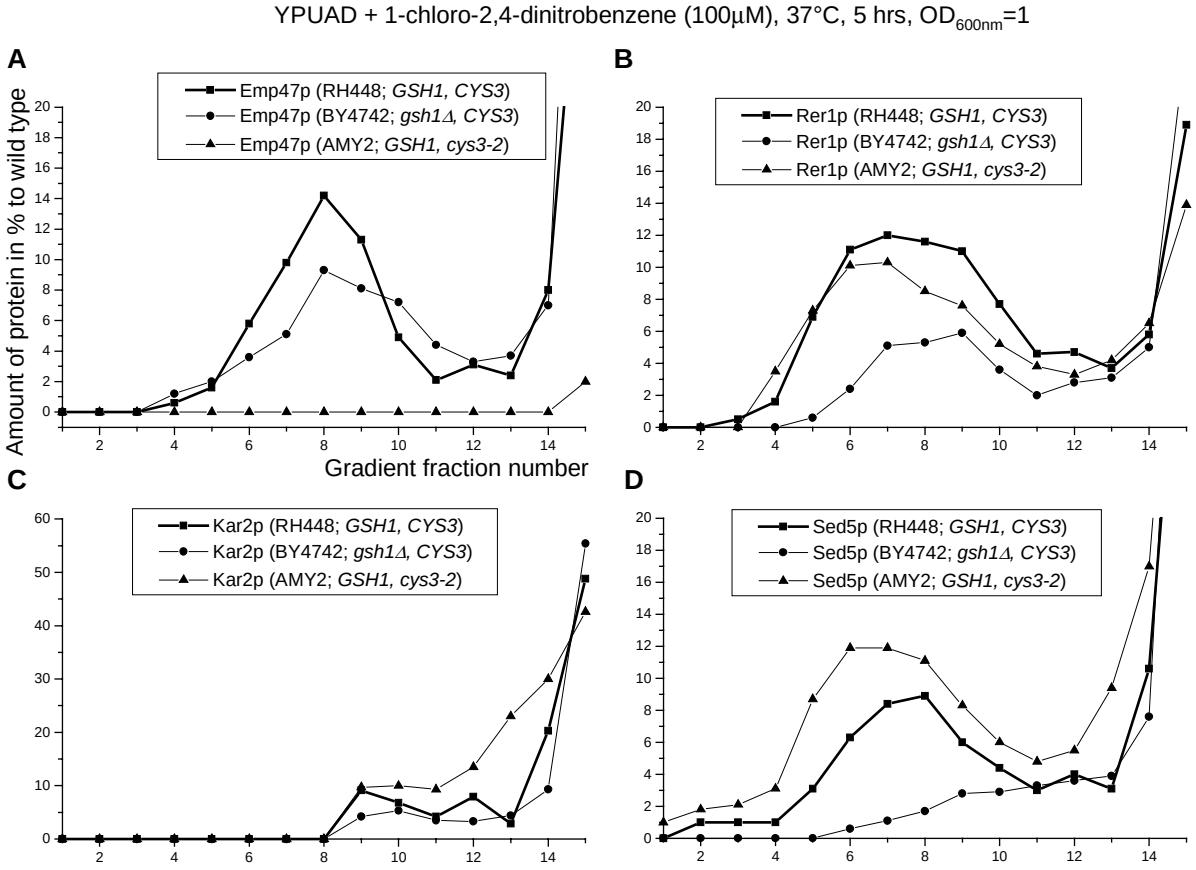


Fig. 16: Levels of various Golgi protein markers in *cys3-2* and *gsh1Δ* mutant are reduced in oxidative stress-dependent manner.

Lysates from different yeast strains (RH448, AMY2 and BY4742) were assayed by velocity sedimentation on sucrose gradient and quantitative immunoblotting for the distribution and the relative amount of such Golgi protein markers as Emp47p (A), Rer1p (B), Sed5p (D) and the ER-marker Kar2p (C) at 37°C in YPUAD media supplemented with 100 µM of 1-chloro-2,4-dinitrobezene. The total amount of every marker-protein in wild type cells was set to 100%.

A. In *cys3-2* mutant cells, the level of Emp47p is severely reduced in the presence of an oxidising agent (1-chloro-2,4-dinitrobezene), as compared to the situation in wild type or *gsh1Δ* cells.

B. The level of Rer1p is reduced to approximately 50% of wt level in the presence of an oxidising agent in *gsh1Δ* cells. Wild type and *cys3-2* mutant cells, however, differ neither in amount nor in the distribution of Rer1p.

C. The level of the ER protein marker Kar2p appears to be unaffected by the presence of the oxidising agent in *cys3-2* mutant and *gsh1Δ* cells, as compared to the situation in the wild type cells.

D. The level of Sed5p in *gsh1Δ* cells goes down to 30% of the corresponding wild-type level, whereas it remains hardly affected in *cys3-2* mutant cells.

4.4.6. The secretory pathways to the Golgi, vacuole, plasma membrane and extracellular periplasmatic space are not adversely affected by oxidative stress in *cys3-2* mutant at 37°C

The general reduction and/or increased turnover of proteins localized to the early secretory pathway begged the question as to whether there was a general deterioration of the biosynthetic transport pathways. We therefore analyzed the secretion of invertase, a marker for the secretory pathway to the yeast periplasmatic space, maturation of CPY, a marker for the biosynthetic pathway to the vacuole (Klionsky et al., 1990), and the GPI-anchored protein Gas1p (Nuoffer et al., 1991), a marker for the plasma membrane (Fig. 17A, B). The transport of CPY and Gas1p can be judged by compartment-specific modifications resulting in characteristic shifts in electrophoretic mobility. A pulse-chase experiment was performed with cells grown at 25°C. After 30 min preincubation at 37°C, cells were pulse labeled with Tran[^{35}S]-label^{TM} at 37°C for 5 min. The chase was carried out for up to 1 hr at 37°C (Fig. 17A). CPY acquired its Golgi specific glycosylation (p1 to p2 transition) and proteolytic maturation in the vacuole (p2 to m transition) equally fast in wild-type and in *cys3-2* mutant cells. The same was true for the maturation of Gas1p into the Golgi-modified 125 kD form.

As invertase moves along the secretory pathway from the ER to the periplasmatic space it undergoes glycosylation in several steps. The normally secreted form of the protein is heterogeneous in size, resulting from the elongation of core oligosaccharide chains in the Golgi apparatus (Schauer et al., 1985). Electrophoresis in the native 7 % acrylamide gel revealed that *cys3-2* mutant was fully proficient in invertase glycosylation and secretion even after being exposed to the restrictive temperature of 37°C for 90 minutes, followed by the period of invertase induction carried out at 37 °C for 1 hour. As fig. 17B demonstrates, the extent of invertase glycosylation in *cys3-2* mutant matches the one in wild type cells.

Thus, even at the restrictive temperature the biosynthetic secretory routes from the ER to the Golgi (Gas1p, CPY and invertase) and on to the vacuole (CPY) and extracellular periplasmatic space (invertase) taken by the three marker-proteins tested appeared to work normally in *cys3-2* mutant cells.

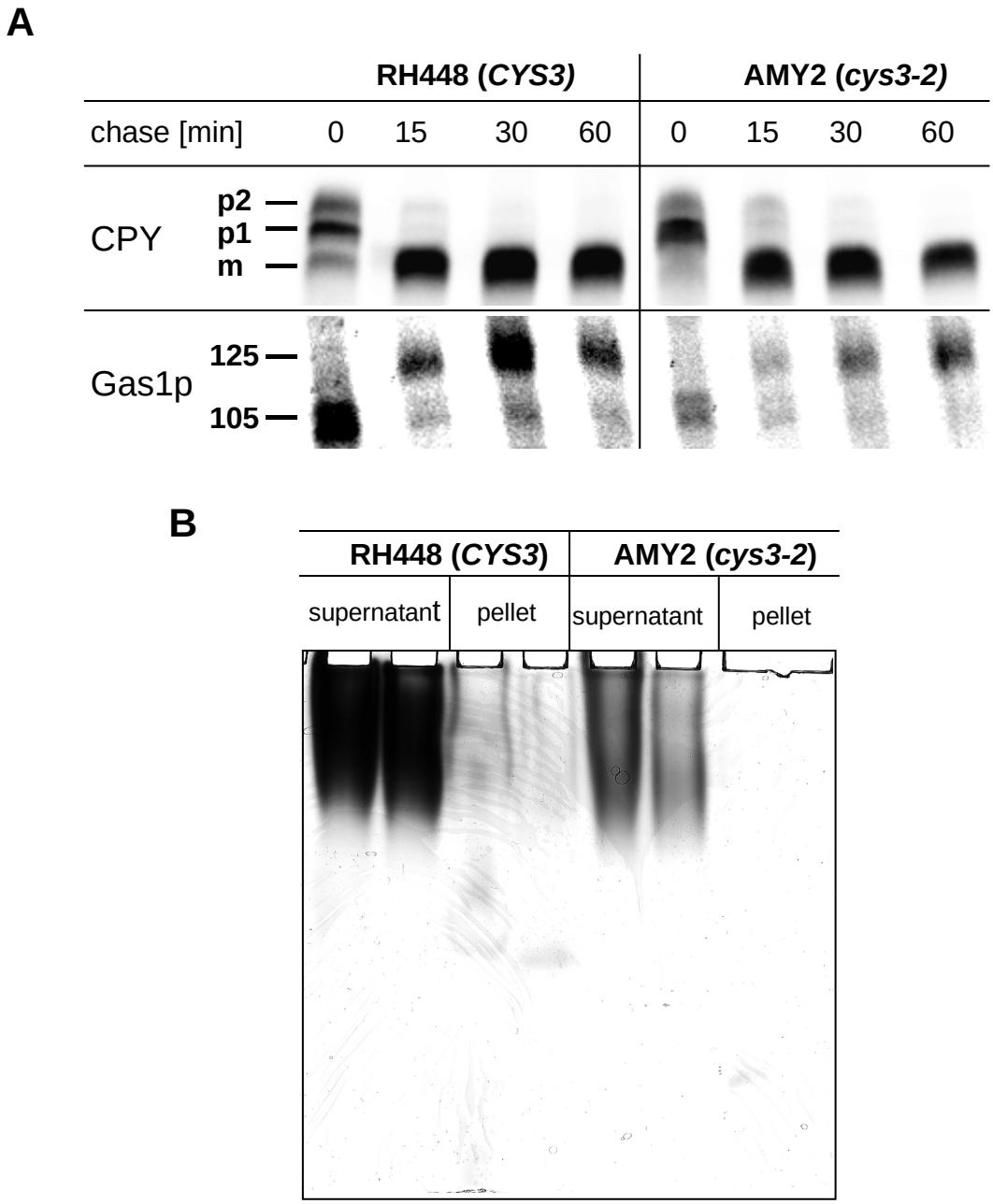


Fig. 17: Biosynthetic transport proceeds with wild-type kinetics in *cys3-2* mutant cells.
A. After 30 min preincubation at 37°C cells from strains RH448 (wt) and AMY2 (*cys3-2*) were pulse labeled with Tran[^{35}S]-label^{TM} for 5 min, followed by a chase for the indicated times. Immunoprecipitated material was analysed by SDS PAGE and autoradiography. CPY was converted from its core-glycosylated ER-form (p1) via the Golgi-glycosylated p2 form to the mature, protease-processed form (m) in the vacuole. Gas1p was made as a 105 kD core-glycosylated ER-form and matured into the Golgi and plasma membrane form of 125 kD.
B. Cells were harvested in amounts of 2x10^8 per assay and incubated for 90 min at 37°C in 10 ml of YPUAD media. After that cells were shifted to YPUAD media exhausted for glucose (0.1%) and incubated for 1hr at 37°C. Patterns of invertase glycosylation were analyzed in the supernatant and pellet fractions of wild type strain (RH448) and *cys3-2* mutant (AMY2). Invertase glycosylation and secretion are not affected by the Cys3p inactivation.

4.4.7. *cys3-2* and *gsh1Δ* mutants are characterized by low intracellular levels of reduced low molecular weight sulfhydryl groups (LMWS)

If, as outlined before, the *cys3-2* mutant may undergo oxidative stress, this may become apparent directly by a drop in the antioxidative tripeptide GSH, of which cysteine is a

constituent. Therefore, I analyzed the correlation of levels of low molecular weight sulfhydryls and temperature sensitivity in *cys3-2*. But in addition to being a precursor for GSH cysteine is also an essential structural component of small dithiol proteins from thioredoxin and glutaredoxin protein families as well as monothiol-dependent glutaredoxin-like proteins. These proteins are shown to execute vital functions in protecting cells against hyperoxidation. Thioredoxin's intracellular activities were shown to partially overlap with the ones of GSH (Sharma et al., 2000). However, reduced GSH makes up to 95% of the low molecular weight sulfhydryls (LMWS) in yeast (Elskens et al., 1991). Therefore, I determined the size of LMWS pool as a measure of the amount of reduced GSH in *cys3-2* mutant and wild-type cells (Fig. 18A). Cells were incubated at 25°C for 5 hrs in synthetic medium containing peptone, but no yeast extract (PM-ura-glucose). One aliquot was kept at 25°C while the other one was shifted to 37°C for 90 min prior to analysis. At 25°C already the mutant contained about 17% less reduced low molecular weight sulfhydryls (LMWS) than the wild-type. LMWS were slightly increased to 109% in the wild-type after exposing cells for 90 min to 37°C, while in the mutant LMWS dropped to 44% of wild-type level at 25°C.

In a similar approach, I also assayed the maximal rate at which *cys3-2*, *gsh1Δ* and wild-type cells exhausted the intracellular level of LMWS. The cell cultures were firstly raised on rich YPUAD medium, shifted then to the minimal SD medium supplemented with 120 μM of cysteine for 4 hrs and transferred finally to the SD-medium devoid of cysteine and GSH for incubation at 37°C and 30°C. It turned out that, at 37°C following the shift, the level of LMWS in *cys3-2* mutant dropped down at a rate of around 10 nmol per 1 hr per 1 OD_{600nm} of cells (Fig. 18B). In comparison to it, the estimations of the same rate values for wild type cells and *gsh1Δ* mutant revealed reduction in LMWS amounts at speeds of 3,7 and 0,4 nmol of LMWS per 1 hr per 1 OD_{600nm} cells, respectively (Fig. 18B). The LMWS levels in both *cys3-2* and *gsh1Δ* mutants constituted around 30% of wt level after 4 hrs of incubation at 37°C in the minimal SD medium without cysteine. As could be inferred from the Fig. 18B, the rates of exhaustion for intracellular LMWS-contents for wt and *cys3-2* mutant cells incubated in the minimal SD medium without cysteine at 30°C were respectively around 40 % and 20 % lower than their corresponding values at 37°C. Note, that the level of LMWS in *gsh1Δ* mutant displayed no dependence on the concentration of cysteine in the minimal SD-medium, reflecting probably the fact that *gsh1Δ* mutant is devoid of means to convert excess cysteine to GSH for storage. The level of LMWS in *gsh1Δ* mutant was influenced, however, by temperature shift from 30°C to 37°C. The fact that *cys3-2* mutant accumulated two times more of cysteine than wt cells when incubated in SD-medium supplemented with 120 μM of

cysteine at 30°C (Fig. 18B) confirms an observation of an incresead exogenous cysteine uptake activity of cysteine-dependent mutants reported earlier by Ono and Kaito (1991).

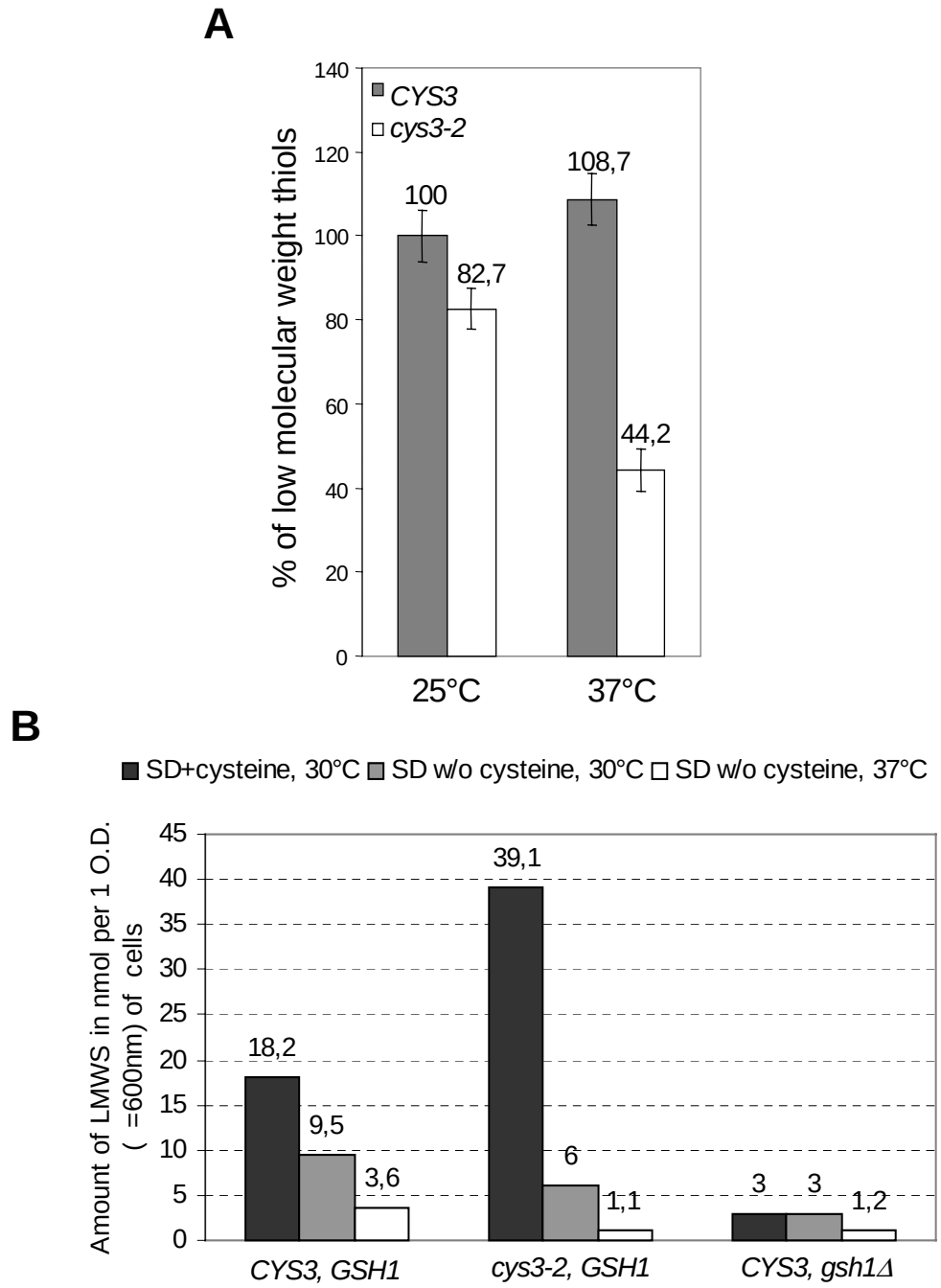


Fig. 18: Intracellular level of low molecular weight thiols (LMWS) is reduced in *cys3-2* and *gsh1Δ* strains at 37°C.

A. Total acid-soluble low-molecular weight sulfhydryl groups from extracts of RH448 (wt) and AMY2 (*cys3-2*) were determined with Ellman reagent (see chapter 3.7.). The signal from extracts of wild-type (RH448) grown at 25°C was set 100%. Values were determined from three independent extracts each. Standard deviations are indicated.

B. As indicated in "A", extracts from RH448 (wild type), AMY2 (*cys3-2, GSH1*) and BY4742 (*CYS3, gsh1Δ*) yeast strains were assayed with Ellman reagent for depletion in the intracellular LMWS-contents under various conditions. After rich YPUAD medium, yeast cultures were incubated for 4 hrs at 30°C in SD-medium supplemented with 120 µM of cysteine and finally shifted to SD-medium without cysteine and grown for 4 hrs at either 30°C or 37°C. LMWS contents for each strain are presented in nanomols of cysteine-equivalents per total amount of cells contained in the liquid yeast cultures of 1,0 OD_{600nm}. Note, that after 4 hrs of incubation at 37°C the levels of LMWS in both *cys3-2* and *gsh1 Δ* mutants constituted around 30% of the wild-type level.

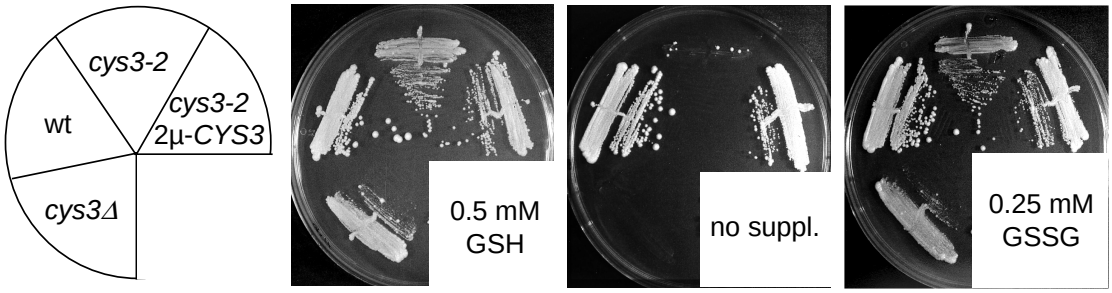
Essentially, the data presented show that the rate of LMWS consumption in the *cys3-2* mutant was almost three times higher compared to the wild type strain at 37°C and that the LMWS utilization in all strains tested increases significantly with the increase in the incubation temperature.

4.4.8. Supplementation of cysteine and/or glutathione rescues the temperature sensitivity and the mislocalization of Emp47p in *cys3-2* mutants.

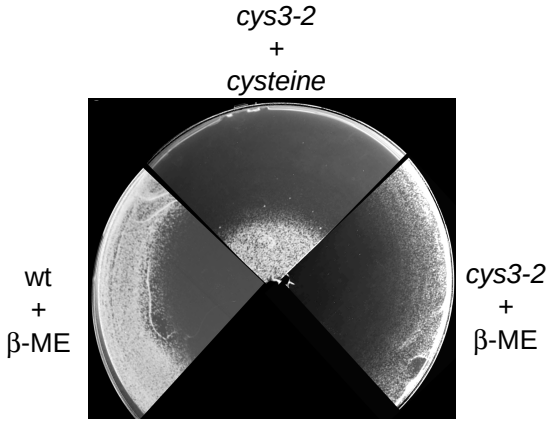
The observation that the depletion of cysteine and reduced GSH in the *cys3-2* mutant cells correlated with temperature sensitivity made it likely that the observed *cys3-2* phenotypes were due to a lack of both. Indeed, similar to the addition of cysteine (Fig. 19A), the addition of 0.5 mM reduced GSH to rich medium fully rescued growth of the *cys3-2* strain and of the *cys3Δ* strain at 37°C. Interestingly, oxidized GSH (GSSG) at 0.25 mM achieved the same effect (Fig. 19A). Thus, only the amount of GSH, but not its oxidation status was important. Replacing the mutant *cys3-2* allele in the strain AMY3 by wild type *CYS3* had the same effect (data not shown). We observed that administration of the membrane-permeable reducing agent β-mercaptoethanol in the center of a plate conferred some degree of temperature-tolerance at 37°C to the mutant at the rim of the plate (Fig. 19B), potentially by relaxing the oxidative stress at elevated temperature in an unspecific way. In a similar plate assay performed at 30°C, *cys3-2* mutant cells also exhibited a slightly better than wild-type resistance to the toxicity of β-mercaptoethanol in high concentrations (data not shown). Another factor that influenced the survival rate of *cys3-2* mutant at 37°C turned out to be the pH value of the incubation medium. Lowering pH of rich YPUAD medium from its usual value of 6,5 to 5,0 by supplementing agar-plate with 40 mM of citric acid contributed to unrestricted growth of *cys3-2* mutant at 37°C (data not shown). The fact that optimal pH of cysteine uptake in *S. cerevisiae* is between 4,5 and 5,0 (Ono and Naito, 1991) may provide an explanation for rescue of *cys3-2* mutant temperature-sensitivity by medium-acidification.

Importantly, GSH was also able to alleviate the mislocalization phenotype of Emp47p, as determined by immunofluorescence analysis. Cells were grown in YPUAD at 25°C either in the presence or absence of 10 mM GSH and were then shifted to 37°C for 90 min. In the presence of GSH, Emp47p was only rarely detected in vacuolar structures (Fig. 19C). Of course, mislocalization of Emp47p to the vacuole after 90 min of incubation at 37°C in the rich YPUAD medium was fully aborted by converting *cys3-2* mutant allele to *CYS3* in AMY4 strain (Fig. 19D). Quantitative immunoblotting confirmed that the addition of GSH made the level of Emp47p independent of vacuolar proteolytic activity (*PEP4* or *pep4Δ*) and elevated it to more than 80% of wild-type in both cases (Fig. 19E).

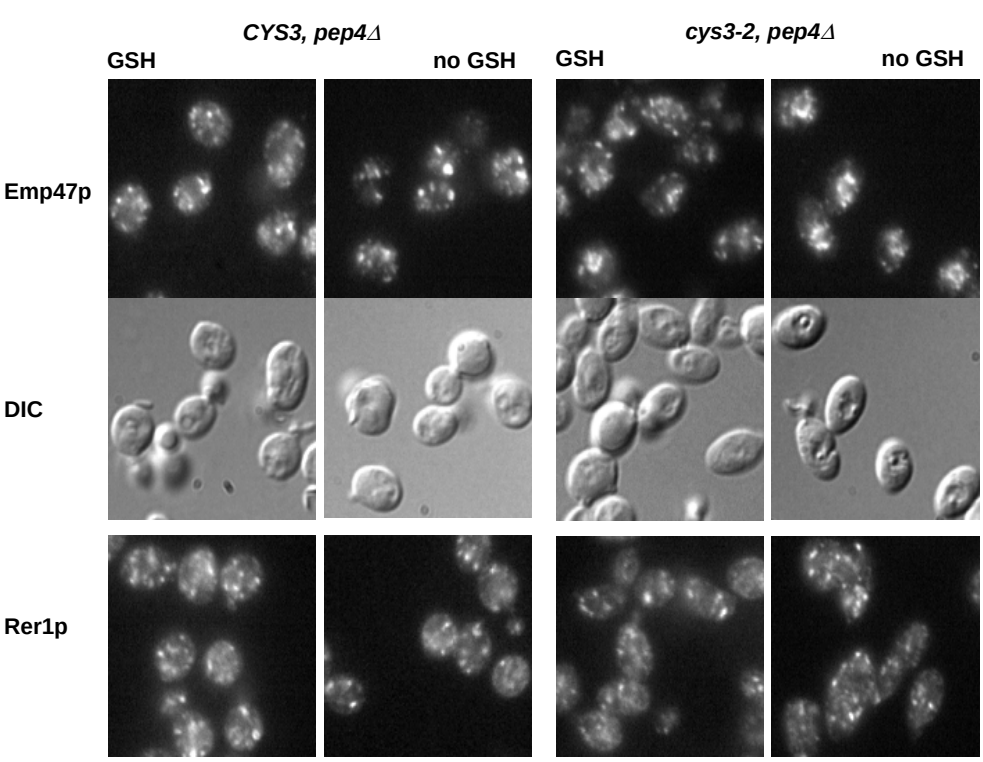
A


cys3-2
wt
cys3-2
2µ-CYS3
cys3Δ
0.5 mM
GSH
no suppl.
0.25 mM
GSSG

B


cys3-2
+
cysteine
wt
+
β-ME
cys3-2
+
β-ME

C


CYS3, pep4Δ
cys3-2, pep4Δ
GSH
no GSH
GSH
no GSH
Emp47p
DIC
Rer1p

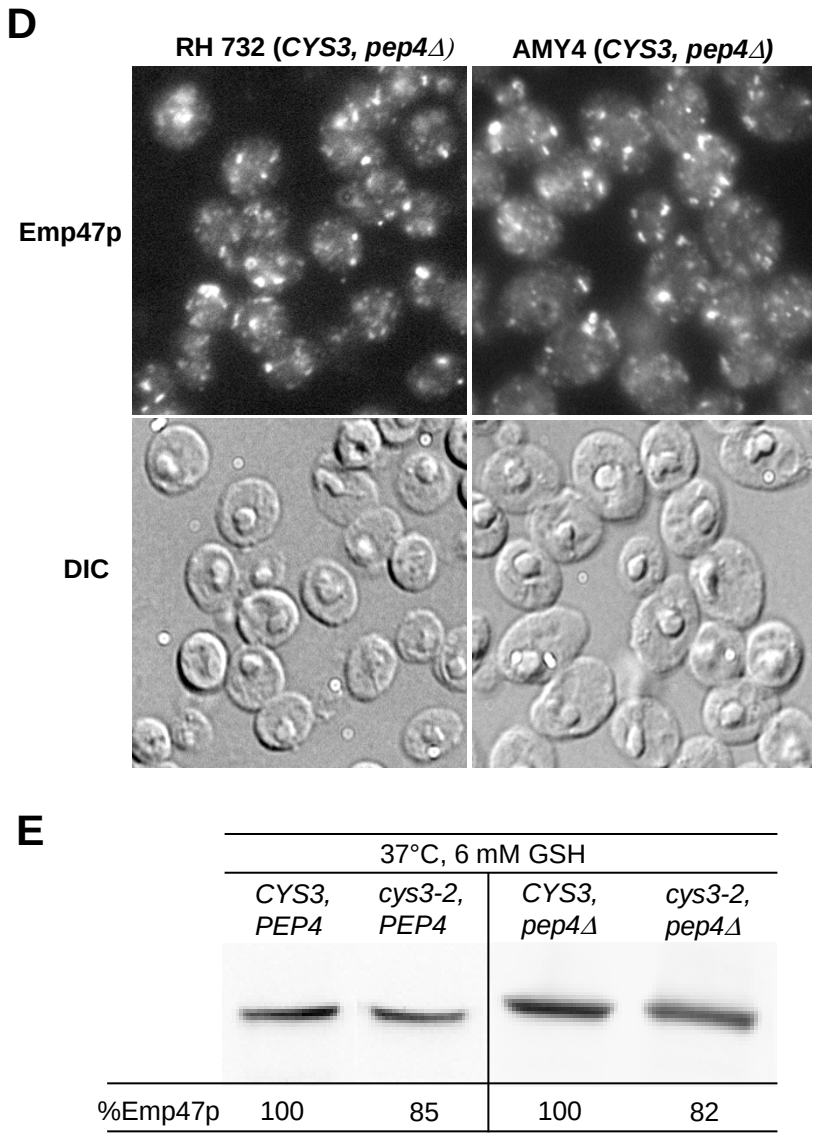


Fig. 19: Alleviating redox-stress rescues *cys3-2* phenotypes.

A. RH448 (wildtype, "wt"), C181 (*cys3Δ*), AMY2 (*cys3-2*) and AMY2 transformed with the genomic clone comprising *CYS3* (*cys3-2, 2µ-CYS3*) were plated on YPUAD agar-plates supplemented as indicated. Incubation was at 37°C.

B. RH448 (wt) and *cys3-2* mutant cells (AMY2) were plated as lawns on separate YPUAD-plates, then either 40 µl of 15 M β-mercaptoethanol (β-ME) or 40 µl of 0.2 M cysteine was applied as indicated to a well in the center of the plates. Images were taken after incubation for 48 hrs at 37°C. Sectors of each plate are shown.

C. Emp47p mislocalisation to the vacuole in *cys3-2* mutant cells is reversed by GSH. Strains RH732 (*CYS3, pep4Δ*) and AMY3 (*cys3-2, pep4Δ*) were grown to log-phase in either rich medium (YPUAD) or YPUAD supplemented with 10 mM reduced GSH at 25°C. Prior to fixation the cultures were shifted to 37°C for 90 min. The localization of Emp47p and Rer1p was determined by indirect immunofluorescence as indicated. DIC, differential interference contrast.

D. Strains RH732 (*CYS3, pep4Δ*) and AMY4 (*cys3-2::CYS3, pep4Δ*) were grown to log-phase in rich YPUAD medium and prepared for immunofluorescence analysis as in "C". Emp47p is localised to the Golgi compartment in both cases.

E. Glutathione reverts increased *PEP4*-dependent turnover of Emp47p in *cys3-2* mutant cells. Strains RH448 (*CYS3, PEP4*), RH732 (*CYS3, pep4::URA3*), AMY2 (*cys3-2, PEP4*), and AMY3 (*cys3-2, pep4::URA3*) were grown to log-phase at 25°C in YPUAD supplemented with 6 mM glutathione and then shifted to 37°C for 90 min prior to lysis. Quantitative immunoblotting was performed (refer to chapter 3.5.8) to determine the amounts of Emp47p in the *cys3-2* mutant cells relative to the corresponding wild-type.

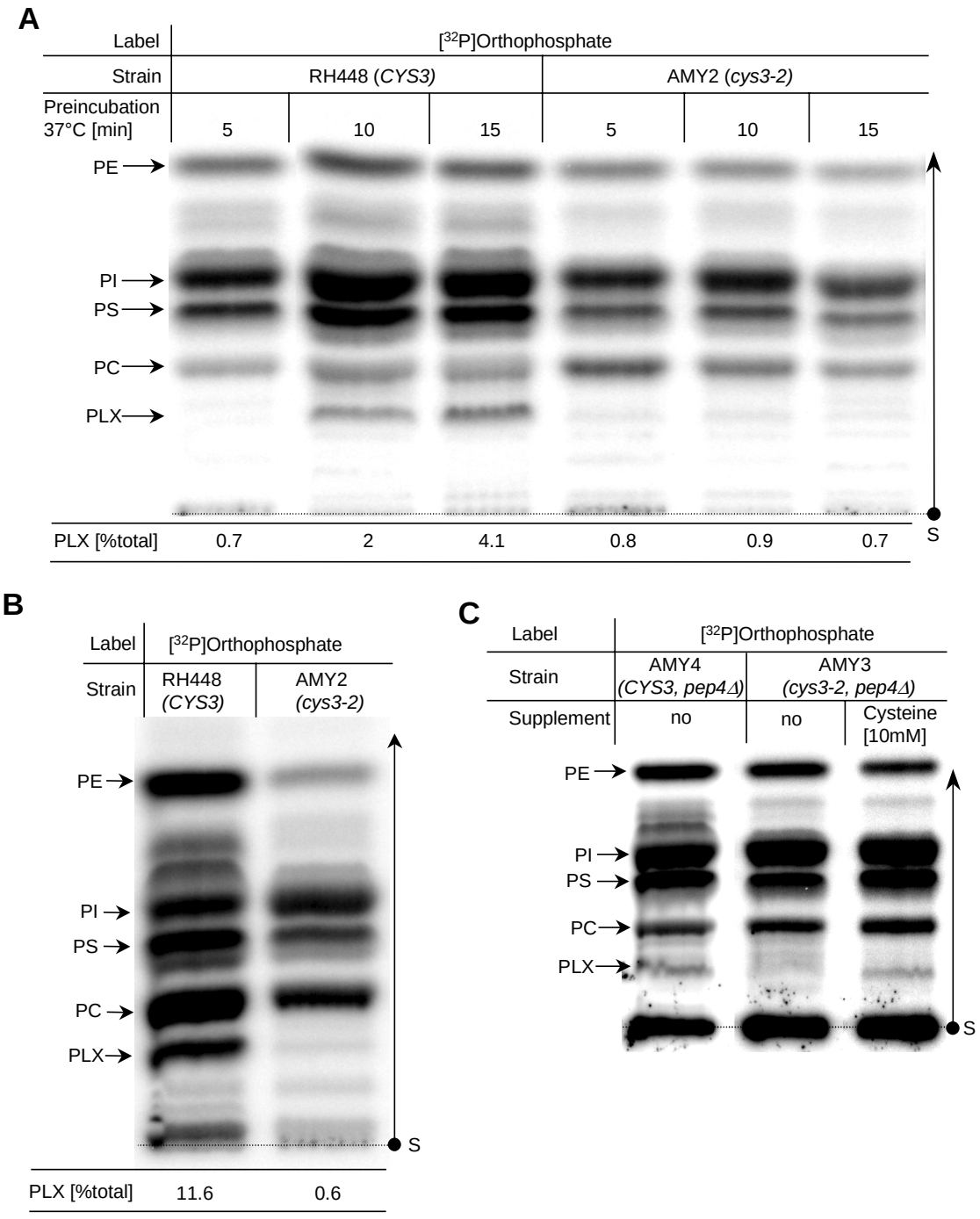
I conclude that excess of extracellular GSH or cysteine as well as unrestricted internal production of cysteine enabled by *cys3-2::CYS3* genetic reversion were able to restore all observed phenotypes of the *cys3-2* cells. The data suggest that *cys3-2* mutant cells experience a shortage of reducing power in the shape of cysteine and GSH as redox-carriers even on rich medium, especially when challenged by high temperature.

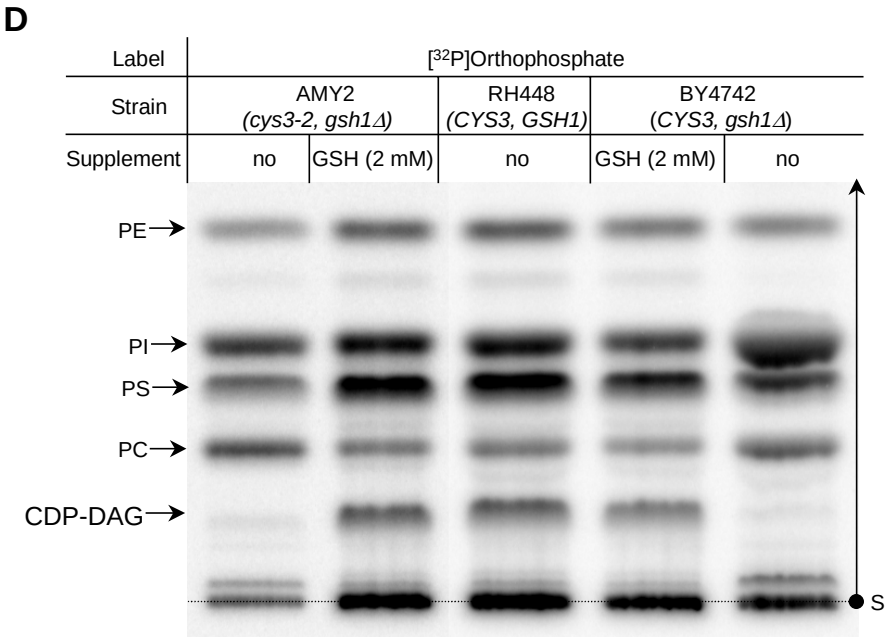
4.4.9. Response of phospholipid metabolism to elevated temperature is impaired in both *cys3-2* and *gsh1Δ* mutant cells.

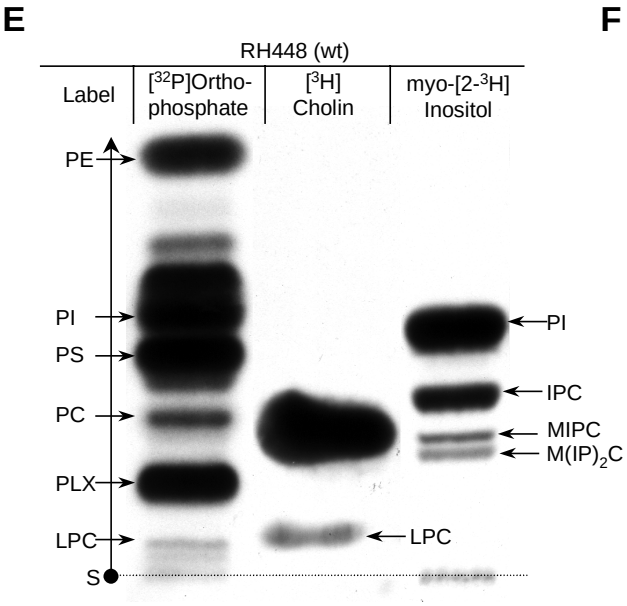
Phospholipids constitute an important structural and regulatory factor in the secretory pathway (Roth, 1999). Thus, lipids are one potential cellular target of the reduced redox-potential that may lead to aberrant membrane trafficking illustrated by the missorting of Emp47p. We performed radioactive ^{32}P-orthophosphate labeling experiments to address that possibility. We could not detect a reproducible difference in the phospholipid patterns between wild-type and *cys3*-mutant cells grown and labeled at 25°C (data not shown). We then shifted cells to 37°C for 5, 15 and 30 min prior to labeling at 37°C for 30 min (Fig. 20A). Note that the incubation at 37°C was within a time-window in which the cells were still growing (compare Fig. 11B). Under this experimental regimen TLC analysis revealed the reproducible induction of a particular phospholipid (denominated "PLX" in Fig. 20) in wild-type cells. That lipid migrated even more slowly than the lowest mobility phospholipid from cells grown at 25°C, which is phosphatidyl choline (PC). Visible induction of PLX required a preshift to 37°C for 15 min with the relative amount of PLX increasing from 0.7% to 4.1% after 30 min preincubation at 37°C (Fig. 20A). The peak-amounts of PLX were somewhat variable between experiments. However, when we labeled wild-type cells for 5 hrs at 37°C, PLX accounted for 11.6% of all labeled phospholipids, indicating a persistent synthesis and/or lack of turnover for at least that period of time (Fig. 20B). PLX completely failed to get induced in the *cys3-2* mutant (Fig. 20A,B,D) as well as in *gsh1Δ* cells (Fig. 20D). Instead, the relative amount remained below 1% throughout.

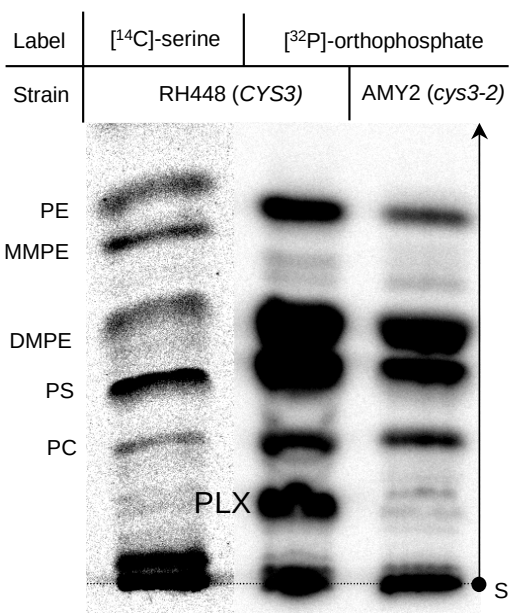
In order to show that the phospholipid phenotype was also a consequence of nonfunctional Cys3p we performed parallel labeling reactions with *cys3-2* mutant cells and cells in which *cys3-2* had been replaced by *CYS3* (strain AMY4, see chapters 2.1 and 3.4.4) or supplemented with 10 mM cysteine. Thin layer chromatography revealed that the genetic reversion of *cys3-2* to *CYS3* and supply of cysteine both restored the induction of PLX (Fig. 20C). Interestingly, in contrast to the partial effect of cysteine (data not shown), supplementation of the labeling media with GSH helped to fully restore the level of PLX in *gsh1Δ* as well as in *cys3-2* cells (Fig 20D) arguing that it is the lack of internally produced GSH that is responsible for the

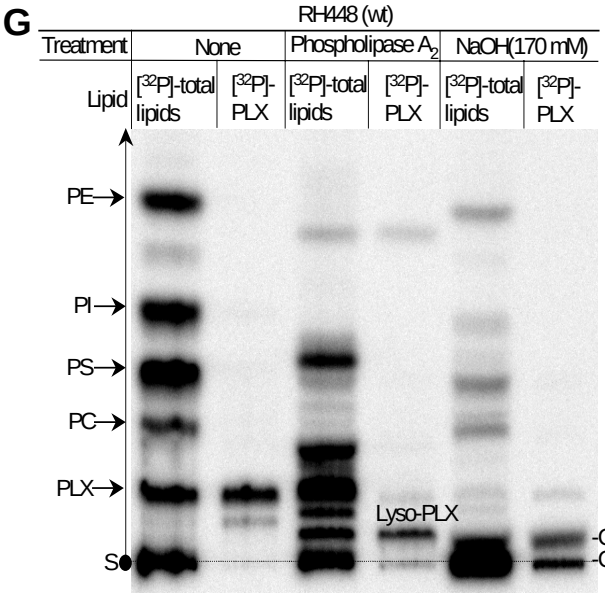
lipid phenotypes of both mutants *gsh1Δ* and *cys3-2*. Thus, the absence of PLX in *cys3-2* mutant cells is most likely a consequence of the lack of sufficient GSH biosynthesis due to limitations in cysteine supply.

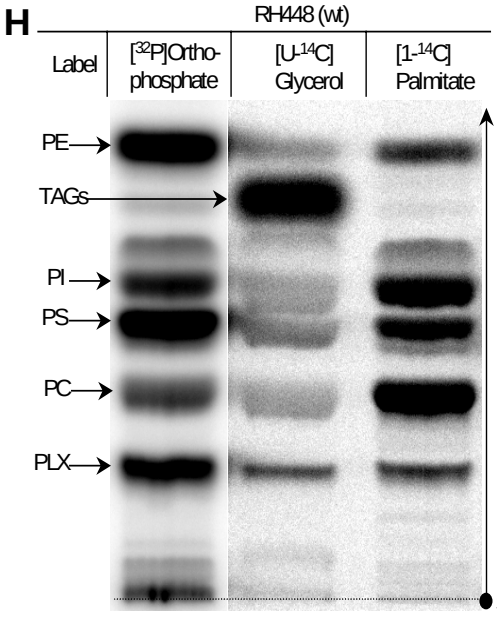



D
Label
[32P]Orthophosphate
Strain
AMY2 (cys3-2, gsh1Δ)
RH448 (CYS3, GSH1)
BY4742 (CYS3, gsh1Δ)
Supplement
no
GSH (2 mM)
no
GSH (2 mM)
no
PE
PI
PS
PC
CDP-DAG
S


E
RH448 (wt)
Label
[32P]Ortho-phosphate
[3H] Cholin
myo-[2-3H] Inositol
PE
PI
PS
PC
PLX
LPC
S
PI
IPC
MIPC
M(IP)2C
LPC


F
Label
[14C]-serine
[32P]-orthophosphate
Strain
RH448 (CYS3)
AMY2 (cys3-2)
PE
MMPE
DMPE
PS
PC
PLX
S


G
RH448 (wt)
Treatment
None
Phospholipase A2
NaOH(170 mM)
Lipid
[32P]-total lipids
[32P]-PLX
[32P]-total lipids
[32P]-PLX
[32P]-total lipids
[32P]-PLX
PE
PI
PS
PC
PLX
S
Lyso-PLX
C1
C2


H
RH448 (wt)
Label
[32P]Ortho-phosphate
[U-14C] Glycerol
[1-14C] Palmitate
PE
TAGs
PI
PS
PC
PLX
S

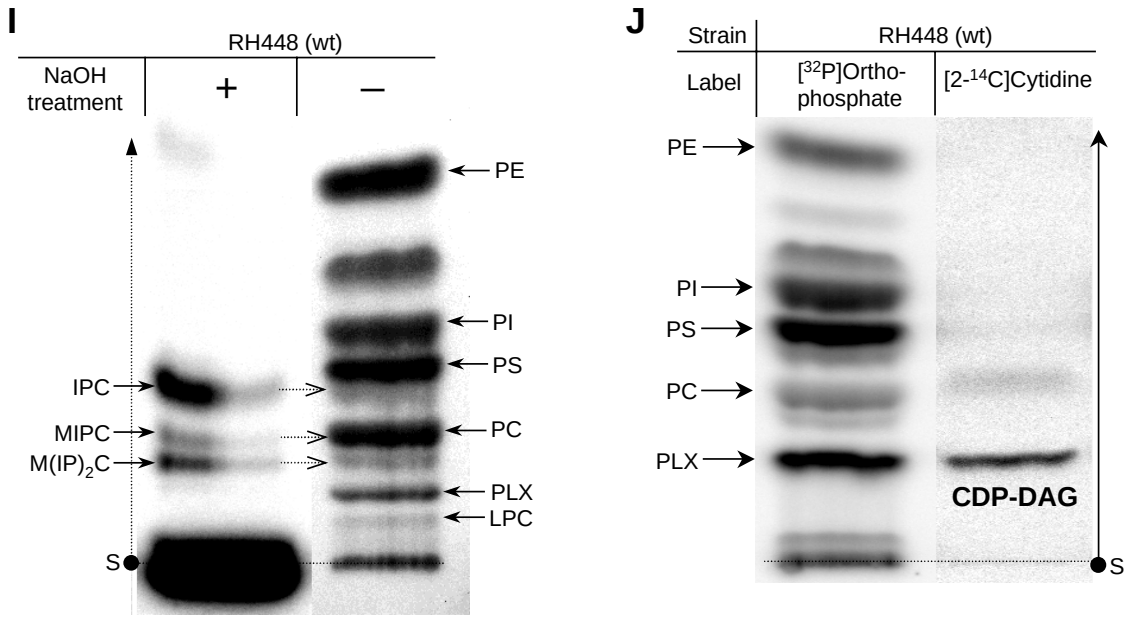


Fig. 20: Temperature-, time-, *CYS3*- and *GSH1*-dependent expression of an inducible phospholipid.

Cells were labelled as indicated, lysed enzymatically and extracted with chloroform-methanol (3:1). Lipid extracts were applied to a thin layer silicagel chromatography plate and resolved in chloroform:ethyl acetate: 2-propanol: methanol: 0.25% aqueous KCl (25:25:25:10:9, v:v:v:v:v). Plates were analysed by exposure to a PhosphorImager™ screen and quantified with a PhosphorImager™ (Molecular Dynamics) unless noted otherwise. When using different isotopes on a single TLC-plate we optimised the presentation of each lane for its dynamic range. PLX: the heat-inducible phospholipid, levels of which are expressed in % of the total integrated signal of each lane; CDP-DAG: cytidinediphosphate-diacylglycerol; PI: phosphatidylinositol; PS: phosphatidylserine; PC: phosphatidylcholine; LPC: lyso-phosphatidylcholine; IPC: inositol phosphoryl-ceramide; MIPC: mannose-inositol-P-ceramide; $M(IP)_2C$: mannose-(inositol-P)$_2$-ceramide; TAGs: triacylglycerides. Phospholipids were identified according to their comigration with bands from [methyl-^{3}H]-choline, myo[2-^{3}H]-inositol, L-[U-C^{14}]-serine, [U-^{14}C]-glycerol, [1-^{14}C]-palmitate and [2-^{14}C]-cytidine labelled extracts, by their relative mobility (Henderson 1992) and base-sensitivity or resistance. S: start line of TLC; arrow indicates direction of solvent-migration.

A. A low-mobility, heat inducible phospholipid fails to be produced in *cy3-2* mutant cells. Strains RH448 (wt) and AMY2 (*cys3-2*) were grown to early log-phase in YPUAD medium overnight at 30°C and were then shifted to PM-ura-glucose for 1 hr. Before addition of radiolabel cells were prewarmed at 37°C for 5, 15 and 30 min respectively. Pulse-labeling was carried out at 37°C for 30 min in the presence of ^{32}P-orthophosphate.

B. The heat-inducible phospholipid remains at high levels for 5 hrs at 37°C. Strains RH448 (wt) and AMY2 (*cys3-2*) were grown to early log-phase in YPUAD medium at 30°C. The cultures were then shifted to PM-ura-glucose for 1 hr. Labeling was carried out for 5 hrs at 37°C in the presence of ^{32}P-orthophosphate.

C. The induction of PLX is restored by supplementation of the growth medium with cysteine or by integrative genetical conversion of *cys3-2* to *CYS3*. Strains were grown to early log-phase in PM-glucose medium (AMY3 (*cys3-2, pep4Δ*) and AMY4 (*CYS3, pep4Δ*)) or in PM-glucose medium supplemented with 10 mM cysteine (AMY3 (*cys3-2, pep4Δ*)). Radiolabeling of the yeast with [^{32}P]-orthophosphate (37°C, 30 min) was preceded by 30 min of incubation of the cells at 37°C.

D. *cys3-2* and *gsh1Δ* mutants are both restricted in CDP-DAG accumulation at 37°C. Deficiencies in CDP-DAG accumulation in both *cys3-2* and *gsh1Δ* mutants at 37°C are circumvented by supplementation of the growth medium with 2 mM GSH. Yeast strains RH448 (wild type), AMY2 (*cys3-2, GSH1*) and BY4742 (*CYS3, gsh1Δ*) were grown to early log-phase in YPUAD medium overnight at 30°C and were then shifted to minimal SD-medium (supplemented with all amino-acids to concentration of 20 µg/ml each) for 6 hours to exhaust for glutathione. Cell cultures were then incubated at 37°C for 30 minutes followed by radiolabelling for 1 hr in the presence of [^{32}P]-orthophosphate.

E. Labelings of the wild-type strain RH448 with [methyl-^{3}H]-choline and myo[2-^{3}H]-inositol were carried out in the presence of 50 µCi of each of the respective radiochemicals for 30 min at 37°C. TLC plates were sprayed with Amplify™-solution (Amersham) and labeled lipids were visualised by exposure to film.

F. Labeling of the wild-type strain RH448 with serine were carried out in the presence of 50 µCi of L-[U-C^{14}]-serine for 30 min at 37°C. Clearly, serine does not enter the structure of PLX.

G. A lyso-form of PLX accumulates as a result of Phospholipase A_2 treatment. C1 and C2 are NaOH-generated cleavage products of PLX. RH448 was grown as described in A, shifted to 37°C for 30 min and labeled with

[^{32}P]-orthophosphate at 37°C for 60 min. PLX was purified in one-dimensional TLC as described in "Material and Methods". [^{32}P]-total lipid extract and [^{32}P]-PLX were treated either with Phospholipase A_2 (Sigma) or NaOH (chapters 3.9.4 and 3.5.9) and subsequently resolved on the same TLC plate together with untreated material for comparison.
H. Glycerol and palmitic acid both constitute structural components of the PLX molecule. RH448 (wt) was grown as described in "A". Incorporations of [U-^{14}C]Glycerol (15µCi/ml) and/or [1-^{14}C]Palmitic acid (40µCi/ml) were carried out for 120 minutes at 37°C.
I. RH448 was grown as described in "A", shifted to 37°C for 30 min and labeled with ^{32}P-orthophosphate at 37°C for 60 min. Lipids were extracted and an aliquot was treated with NaOH (final concentration of 170 mM). Only ceramide-based species (IPC, MIPC, $M(IP)_2C$) remain. Hydrophilic cleavage products of glycerophospholipids accumulated at the startline of the TLC plate.
J. The heat-inducible lipid incorporates cytidine. RH448 (wild type) was grown as described in "A", shifted to 37°C for 30 min and then incubated at 37°C for 1 hr in the presence of [2-^{14}C]Cytidine. Differently labelled lipid extracts were loaded next to each other on a single TLC plate.

Labeling cells with ^{3}H-inositol, ^{3}H-choline (Fig. 20E) or ^{14}C-serine (Fig. 20F) under conditions, in which PLX was induced, revealed that the lipid contained neither of the three lipid headgroups. This confirmed that PLX was neither PC, PS nor phosphatidylinositol (PI), nor any of the inositol phosphoryl-ceramides (IPC, MIPC, $M(IP)_2C$). In addition, PLX was phospholipase A_2 sensitive (Fig. 20G). The presence of fatty acid and glycerol in the molecular structure of PLX was confirmed by labeling with ^{14}C-palmitic acid and ^{14}C-glycerol respectively (Fig. 20H). To further rule out a ceramide-backbone of PLX we treated ^{32}P-orthophosphate labeled extracts of heat-treated cells with mild base. The lipid of interest was clearly base-sensitive (Fig. 20I and 20G). However, we noticed a cleavage product of very low mobility (C1) apart from the fully deacylated material (C2) remaining at the start-line of the chromatogram (Fig. 20G). The presence of a second phosphate containing cleavage product and the very hydrophilic nature of PLX prompted us to test whether PLX could be CDP-DAG. Indeed, direct *in vivo* labeling with [2-^{14}C]-cytidine identified PLX as CDP-diacylglycerol (Fig. 20J).

4.5. Characterization of Ylr080wp, a close homologue of Emp47p

Ylr080wp is a totally uncharacterized homologue of Emp47p (45% of identity according to BLAST alignment) in yeast. It posseses the same set of structural features that distinguishes the primary structure of Emp47p, including the carboxy-terminal di-lysine motif. Both protein are homologous to mammalians ERGIC-53 and VIP36, which in turn share functional homology to leguminous lectins (Fiedler and Simons, 1995; Itin et al., 1996). Fig. 5 schematically represents the structural organisation and membrane topology of Emp47p, which is in essence the same for all homologues. Fig. 22 shows the amino acid sequence of myc-tagged Ylr080wp ("A") and the predicted secondary structure of the native form of Ylr080wp ("C") as well as demonstrates the probability of coiled-coil formation at similar locations in Ylr080wp and Emp47p ("B").

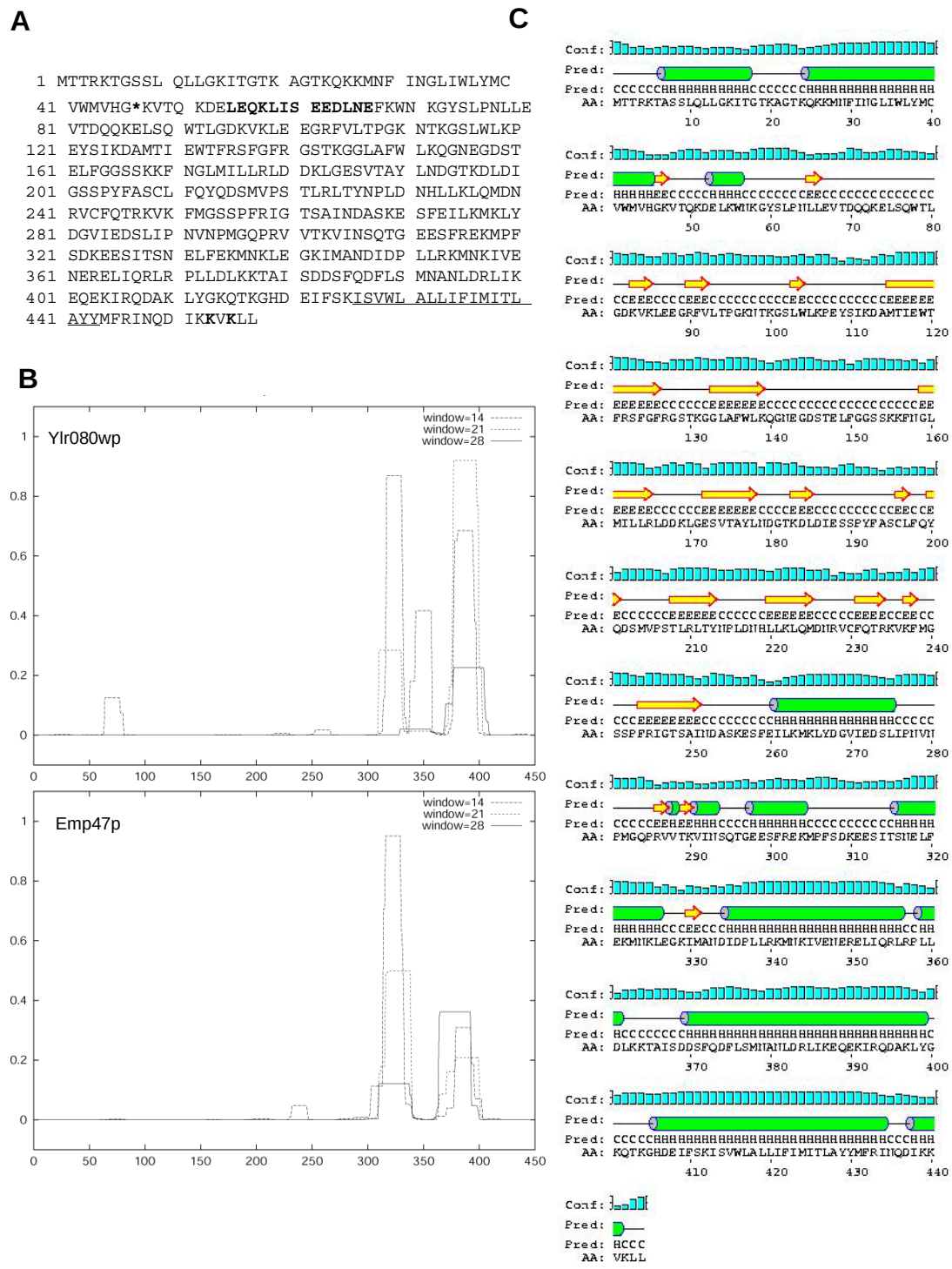


Fig. 22: Structure of Ylr080wp

A. Amino acid sequence of Ylr080wp.
Numbering of amino acids begins at the first amino acid corresponding to the initial codon of *YLR080W* ORF. The putative signal-peptide cleavage site was predicted according to algorithm of Nielsen et al. (1997) and is indicated by asterisk (*****). The location of the putative central transmembrane helix was determined by the latest version of MEMSAT2 (Jones et al., 1998) algorithm developed out of MEMSAT (Jones et al., 1994). The core transmembrane domain together with inside and outside helical loops is underlined. Position of the artificially introduced c-myc-epitope is shown in bold.
B. Coiled-coil probabilities for Ylr080wp (upper panel) and Emp47p (lower panel) according to Lupas et al. (1991).
C. All prominent features of Ylr080wp secondary structure as determined by PSIPRED protein structure prediction server. Conf: confidence of prediction; Pred: predicted secondary structure; AA: target sequence; C: coil; H: helix; E: strand.

It is not known yet whether Emp47p or Ylr080wp are lectins or not. It was found however, that deletion of *EMP47* does not compromise transport pathways in yeast *S. cerevisiae* exemplified by various marker proteins (Schröder et al., 1995). This might be a consequence of the presence of the potentially redundant *YLR080W*, which in itself is also not essential for growth (systematic yeast gene deletion programme, EUROFAN).

In order to learn more about the possibly redundant functions of Emp47p and Ylr080wp and in order to characterize a potentially useful new marker for retrograde transport, I created a double deletion mutant.

4.5.1. Deletion analysis

Firstly, *YLR080W*-deficient yeast strains were prepared by means of homologous recombination, in the process of which *YLR080W* was substituted with a bacterial kanamycin-resistance gene; the latter served to select for the corresponding successful recombination events. In particular, I followed short-flanking-homology protokoll of EUROFAN (Wach et al., 1994) (refer to chapter 3.4.5 for further details) to substitute genomic *YLR080W* with PCR-generated *KanMX4* module (primers PLA444 5´and PLA444 3´(chapter 2.3)) in yeast strains RH732 (*pep4::URA3*) and RH448 (*PEP4*). Successful gene substitution was verified by genomic PCR with two pairs of primers K2/5´-check and K3/3´-check (chapters 3.4.5 and 2.3) that yielded 480 bp long fragments of a predicted size (data not shown). The resulting kanamycin-resistant strain knocked out for *YLR080W* (10053 (*lys2, EMP47, ylr080w::KAN, pep4::URA3)* was crossed with RH2825 (*lys2, emp47::LYS2, YLR080W, pep4::URA3*) to produce progeny knocked out for both *EMP47* and *Ylr080w.* All spores resulting from the tetrad dissection were viable indicating that double knock-out cells were also viable. The corresponding double knock-outs (strain 10044, chapter 2.1) were selected for both the resistance to kanamycin and the lysine-prototrophy.

Although it has been known already from the EROFAN project, in which all the yeast ORFs were systematically deleted, that *YLR080W*-deletion did not lead to growth defect in the strain background used, we nevertheless undertook more thorough investigation of the growth properties of single knock-outs for *YLR080W* (yeast strains 10045 and 10053) and double knock-out for both *YLR080W* and *EMP47* (yeast strain 10044) under various growth conditions. It turned out that neither of the strains displayed a conditional growth defect on rich YPUAD medium at either high (37°C) or low (15°C) temperatures (data not shown). I then assayed the rates of recovery from stationary phase of growth under various environmental conditions. The knock-out strains were grown in liquid rich YPUAD medium reaching stationary phase after 2 days. After 3 more days serial dilutions of the cultures were

plated on rich YPUAD agar plates and let to recover under various growth conditions. It appeared that single and double knock-out strains were not restricted in recovery at 37°C on YPUAD medium alone (Fig. 23A), YPUAD medium supplemented with 0,5 M of sodium chloride (Fig. 23B) or buffered to pH 8,0 by 40 mM of Tris-HCl (Fig. 23C). However, the recovery of the strains deleted for *YLR080W* was significantly delayed when lowering the incubation temperature to 15°C (Fig. 23D). Interestingly, the deletion of *YLR080W* alone was sufficient to contribute full cold-sensitivity for the recovery from stationary phase. We did not observe any aggravation of the recovery phenotype in double-deletion strain. The strain deficient for *EMP47* alone exhibited wild-type rates of recovery under the same experimental regimen (data not shown).

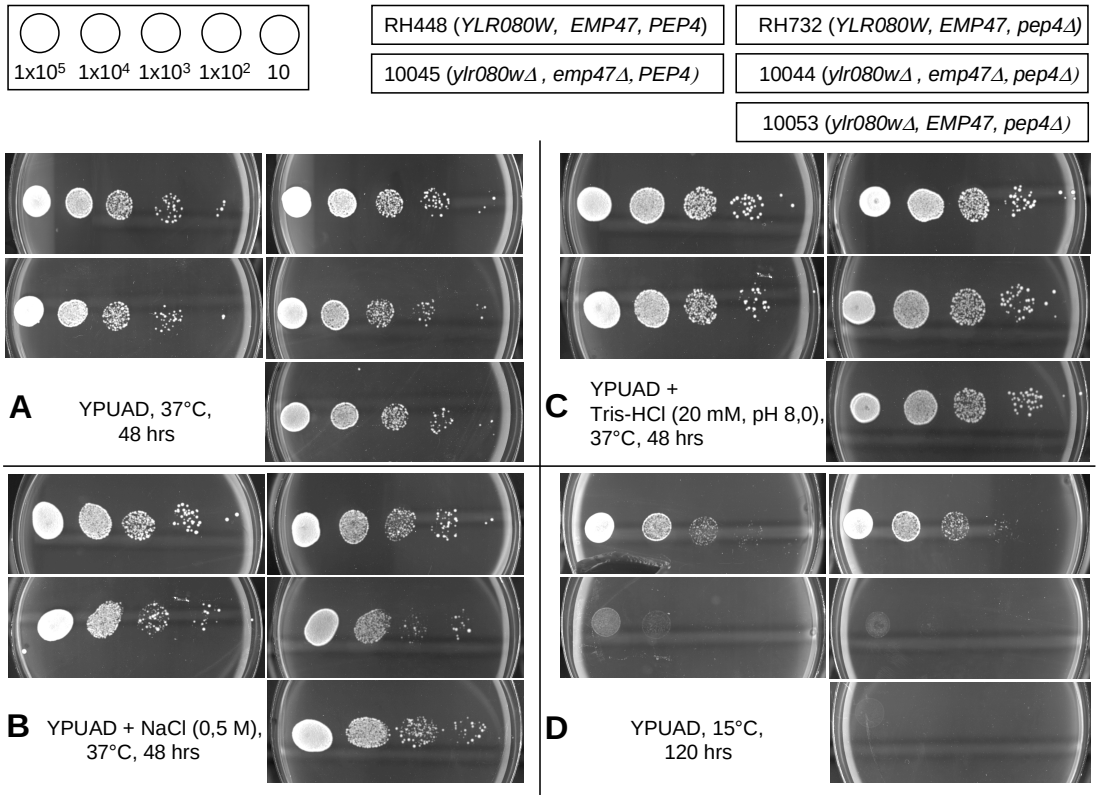


Fig. 23: Growth properties of the strain deficient in *YLR080W* alone or in both *YLR080W* and *EMP47* genes

The knock-out strains 10053 (*ylr080wΔ, EMP47, pep4Δ),* 10044 (*ylr080wΔ , emp47Δ, pep4Δ),* 10045 (*pla444Δ , emp47Δ, PEP4)* as well as wild-type strains RH448 (*YLR080W, EMP47, PEP4*) and RH732 (*YLR080W, EMP47, pep4Δ)* were grown in liquid rich YPUAD medium for 2 days at 30°C reaching stationary phase of growth. The cultures were then let to stay in the same media for 3 more days, reaching OD_{600nm}> 20. Series of cell dilutions for each yeast cell culture were then plated on rich YPUAD agar plates and let to recover under various growth conditions.

A. All yeast strains grow equally well when incubated at 37°C for 48 hrs on rich YPUAD medium.

B. Supplementation of rich YPUAD medium with 500 mM of NaCl does not compromise the yeast cell growth at 37°C.

C. Buffering rich YPUAD medium with 40 mM of Tris-HCl solution to pH= 8,0 does not result in visible growth defect within 48 hours at 37°C.

D. Lowering the incubation temperature to 15 °C results in significant retardation of growth for the strains deleted for *YLR080W.* Note, that at 15°C yeast strains were let to recover from stationary phase for 120 hours.

4.5.2. Invertase glycosylation and secretion are affected neither in the mutant deleted for *YLR080W* alone nor in the *YLR080W / EMP47* double deletion mutant.

One of the reasons for the inability of *ylr080wΔ* to recover from stationary phase at 15°C might stem from a malfunction of the secretory routes. Therefore, I investigated the ability of *ylr080wΔ* mutant cells to glycosylate invertase in a Golgi-specific way and secrete the enzyme to periplasmatic space.

The stationary phase cultures were prepared out of the three yeast strains RH732 (*YLR080W, EMP47, pep4Δ),* 10053 (*ylr080wΔ, EMP47, pep4Δ)* and 10044 (*ylr080wΔ, emp47Δ, pep4Δ)* by incubating the cells for 6 days in rich YPUAD media. For the invertase glycosylation and secretion assay yeast cell cultures were then subjected to incubation overnight at 15°C in the same media. All the following steps of invertase secretion assay (chapter 3.5.10) were also performed at 15°C.

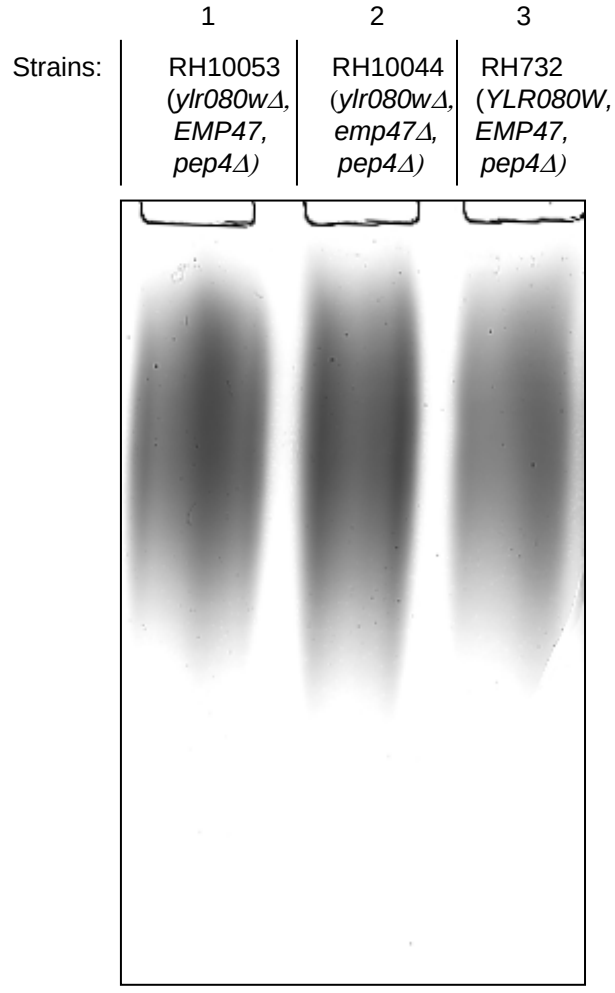


Fig. 24: Invertase glycosylation and secretion are not affected by deletions in *YLR080W* alone or in both *YLR080W* and *EMP47* genes

Invertase acquires its usual Golgi-specific glycosylation and is secreted normally to periplasmatic space in the strains knocked out either for *YLR080W* alone (lane 1) or *YLR080W* together with *EMP47* (lane 2).
Yeast cells were grown to late stationary phase for 6 days in rich YPUAD media at room temperature having reached OD_{600nm} > 20. The cell cultures were then incubated overnight at 15°C in the same media. Following steps of the assay (see chapter 3.5.10) were carried out also at 15°C.

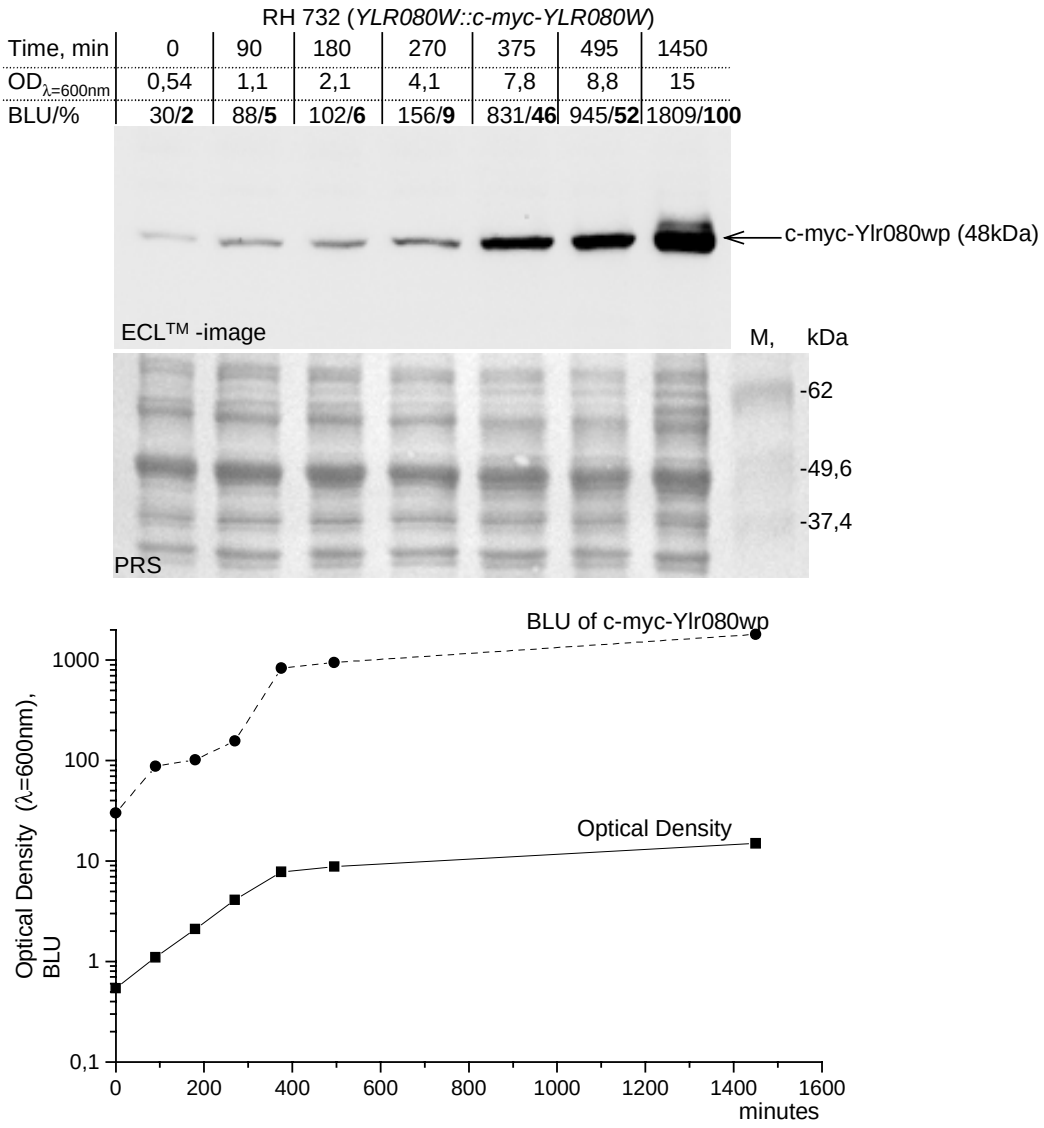
It turned out that under conditions described above the acquisition of Golgi-specific glycosylation and the secretion of invertase are hampered neither in cells knocked-out for *YLR080W* alone nor in *YLR080W / EMP47* double deletion mutant (Fig. 24).

4.5.3. Construction of c-myc-epitope tagged Yrl080wp

YLR080W ORF (residue 287917 to 289251 of yeast chromosome XII, GenBank # CAA97639.1) was amplified from the yeast genomic DNA (derived from yeast strain RH448) with Taq/Pfu polymerase and primers PlaN3´and PlaN5´(chapter 2.3). The resulting 2141 bp PCR-fragment was cut with *PvuII* and *ScaI* restriction endonucleases and ligated into pB-SK(+) vector DNA digested with *EcoRV* resulting in creation of the plasmid pPLA1 (chapter 2.2). The cloned PCR-product was then sequenced with a help of the primers T3, T7, STS32-36 (see chapter 2.3) to compare the identity of the PCR-amplified sequence with the wild-type one. One clone was isolated that contained no mistakes within *YLR080W* except a C(20)G transversion (results in A(7)G exchange in the predicted cleavable leader peptide of Ylr080wp) and A(563)G transition (results in appearance of an additional *BamHI*-site and an E(188)G exchange in the amino acid sequence of Ylr080wp). In order to introduce a c-myc-epitope (13 amino acid residues) into the N-terminal part of Ylr080wp the *EcoRI* site in the non-coding sequence upstream of *YLR080W* was destroyed by cutting, filling in with Klenow enzyme and religation. The resulting plasmid pPLA2 (chapter 2.2) was then subjected to site-directed PCR-mutagenesis (chapter 3.3.6) to introduce a new *EcoRI* site shortly behind the sequence coding for the predicted leader peptide of Ylr080wp. The introduction of the new *EcoRI* site gave rise to the plasmid pPLA3 (chapter 2.2) and resulted in a semi-conservative L(54)F a.a. exchange in Ylr080wp. To introduce a c-myc-epitope the plasmid pPLA3 was cleaved with *EcoRI* and re-ligated with an annealed pair of STS39 and STS40 oligonucleotides coding for c-myc-epitope and containing the sticky ends compatible with the *EcoRI* restriction site (chapter 2.3). The 5´-*EcoRI* restriction site in the resulting plasmid pPLA4 was destroyed as a consequence of integration with c-myc-sequence. Triple digestion of pPLA4 with *EcoR I, Nde I* and *Nco I* restriction endonucleases yielded 617 bp *Nde I/ EcoR I*- and 444 bp *EcoR I/Nco I*-fragments indicating the correct orientation of the integrated sequence coding for c-myc-epitope (antisense-orientation of the c-myc sequence would have yielded 512 bp *Nde I/ EcoR I*- and 549 bp *EcoR I/Nco I*-fragments). The plasmid pPLA4 was used as a starting substrate for cloning of *Sal I/Not I*- and *Xba I/Sal I*-fragments (both encompassing complete *myc-YLR080W* sequence) into the centromeric yeast shuttle vector pRS315 treated with *Sal I* and *NotI* and the yeast integration vector pYIplac128 cleaved with *Xba I/Sal I*, thus, giving rise to the plasmids pPLA5 and pPLA6 correspondingly (chapter

2.2). The centromeric plasmid pPLA5(*LEU2*) was transformed into a variety of *leu2* yeast strains (RH732, RH3609, RH3441, RH1437, 10053, 10044) (chapter 2.1). The integration plasmid pPLA6(*LEU2*) was linearized with *Nco I* cleaving within *YLR080W* and transformed into the yeast strain RH732 (*leu2*), thus integrating *c-myc-YLR080W* and *LEU2* marker-gene into the genome at the *YLR080W*-locus by means of targeted homologues recombination event. All the transformed yeast cells (after selection for leucine-prototrophy) were checked for the expression of c-myc-Ylr080wp hybrid protein by Western-blotting and immunofluorescence analysis with monoclonal anti-c-myc antibodies (9E10) (chapter 2.4).

A



B

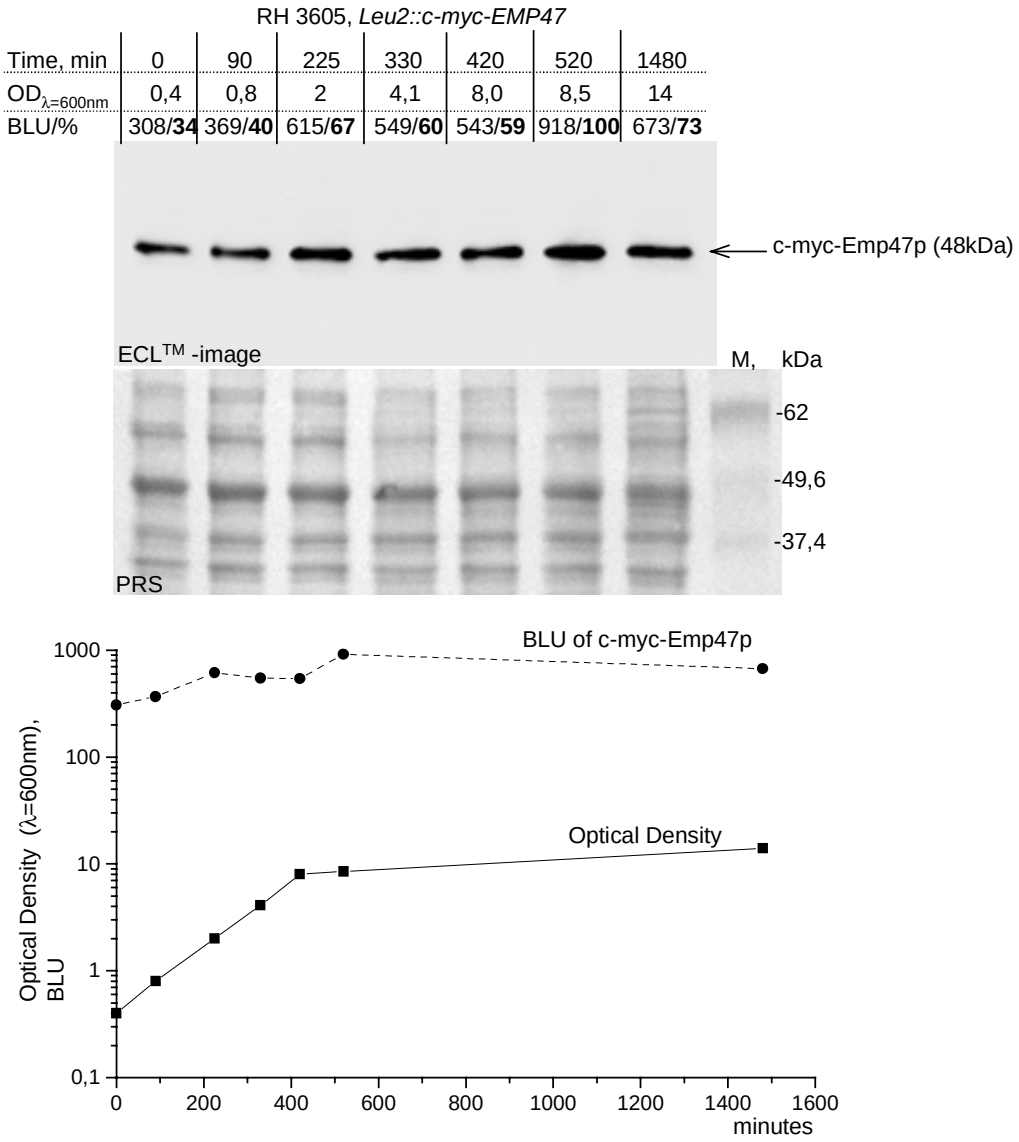


Fig. 25: Growth stage dependence in intracellular accumulation of c-myc-Ylr080wp and c-myc-Emp47p

Yeast strains RH732-M and RH3605 expressing c-myc-Ylr080wp and c-myc-Emp47p respectively were grown in rich YPUAD media from early logarithmic to late stationary phase at 30°C. Small aliquots of yeast cultures containing equal amounts of cells corresponding to different stages of growth were taken at indicated OD_{600nm} and assayed by SDS-PAGE and Western-blot analysis with subsequent immunodetection for the levels of c-myc-Ylr080wp (**A**) and and c-myc-Emp47p (**B**). The signal from c-myc-epitope per each time-point was quantified by Lumi-imager™ (Boehringer) and represented in either original Boehringer Light Units (BLU) or converted to % of c-myc signal to the total signal from c-myc-epitope. OD_{600nm} and BLU values verses the incubation time (measured in minutes) plots were constructed in semi-logarithmic scale for c-myc-Ylr080wp (**A**) and c-myc-Emp47p (**B**). Note, that both yeast cell cultures grew logarithmically up to OD_{600nm} of around 8.
ECL™ –image: an image captured by Lumi-imager™ shows the nitrocellulose membrane probed with anti-c-myc mouse antibodies (9E10) and developed in ECL™ solution. PRS: an image of nitrocellulose membrane stained for proteins with Pounceau-Red stain right after the Western-blotting procedure. PRS images served to verify that equal amounts of total yeast proteins per track were tarnsferred onto nitrocellulose membrane.
A. The intracellular levels of c-myc-Ylr080wp is directly proportional to the age of yeast cell culture.
The intracellular level of c-myc-Ylr080wp increases more than 50-fold in the course of the yeast strain RH732-M transition from the early logarithmic (OD_{600nm}= 0,54) to the stationary phase of growth (OD_{600nm}= 15).
B. The levels of c-myc-Emp47p undergo only slight changes dependent on the growth stage.
c-myc-Emp47p reveals mild variations in its intracellular level in the course of yeast culture maturation. c-myc-Emp47p content reaches its peak value right in the beginning of the stationary phase (OD_{600nm}= 8,5). Note, that at that stage it is only three times bigger than the minimum value for the protein estimated at the early logarithmic phase of growth (OD_{600nm}= 0,4).

4.5.4. Expression of c-myc-Ylr080wp is growth phase dependent

When assaying the expression of Ylr080wp, I realized apparent variations in the expression of the protein depending on the age of the culture. In order to investigate this variation systematically the strain RH732-M (expresses c-myc-Ylr080wp from genome; chapter 2.1) was grown in rich YPUAD medium from early logarithmic to stationary phase for approximately 24 hours at 30°C. Small aliquots of the yeast cell culture were taken at different stages of growth and assayed by quantitative immunoblotting (chapter 3.5.8) for the level of c-myc-Ylr080wp (Fig. 25 A). Yeast cells from the early logarithmicly growing culture expressed the protein very poorly whereas the cells from the aging stationary culture accumulated at least 50 times more of the protein. These data correlates with the about 5-fold increase in the level of Ylr080wp transcription during the diauxic shift of yeast cells from fermentation to respiration (DeRisi et al., 1997). This behaviour of Ylr080wp is in striking contrast to the expression of its close homologue Emp47p. The strain RH3605 (chapter 2.1) expressing the c-myc-version of Emp47p was assayed for the levels of that protein and it appeared that expression was not greatly dependent on culture density. The small peak in expression towards late stationary phase corresponded to a maximum 3-fold increase (Fig. 25B).

4.5.5. Localisation of c-myc-Ylr080wp is growth phase dependent

The interesting expression pattern of Ylr080wp made even more interesting the question where to the protein would be localised. The next logical step of investigation to undertake was to reveal the intracellular localisation of c-myc-Ylr080wp with respect to Emp47p and analyse its dependence on the growth stage of yeast cell culture. I chose to address the question by two techniques - indirect immunoflurescence analysis (chapter 3.8.2) and subcellular fractionation by velocity sedimentation on sucrose gradient (chapter 3.6).

Yeast strain RH732-M was grown essentially as described in chapter 4.5.4 and small aliquots of the yeast cell culture were taken at different time points for assaying the distribution and the level of c-myc-tagged Ylr080wp by indirect immunoflurescence analysis. In logarithmicly growing cells up to 6,8 OD_{600nm} the c-myc-Ylr080wp exhibited a dot-like pattern of distribution indicative of the Golgi localisation of the protein (Fig. 26). At early as well as at advanced stationary phase (OD_{600nm}= 8,4-12) c-myc-Ylr080wp clearly changed its dot-like pattern into a ring-like one. The fact that ring-like stain encompasses the signal from DNA stain DAPI, revealing the locations of the nuclei, points an ER localisation of the protein (Fig. 26). In an agreement with Western-blot analysis data, the immunofluorescent signal from c-myc-Ylr080wp became more and more intense with growing cell density. Thus,

the protein changes its steady-state localisation from the Golgi to the ER with increasing expression level.

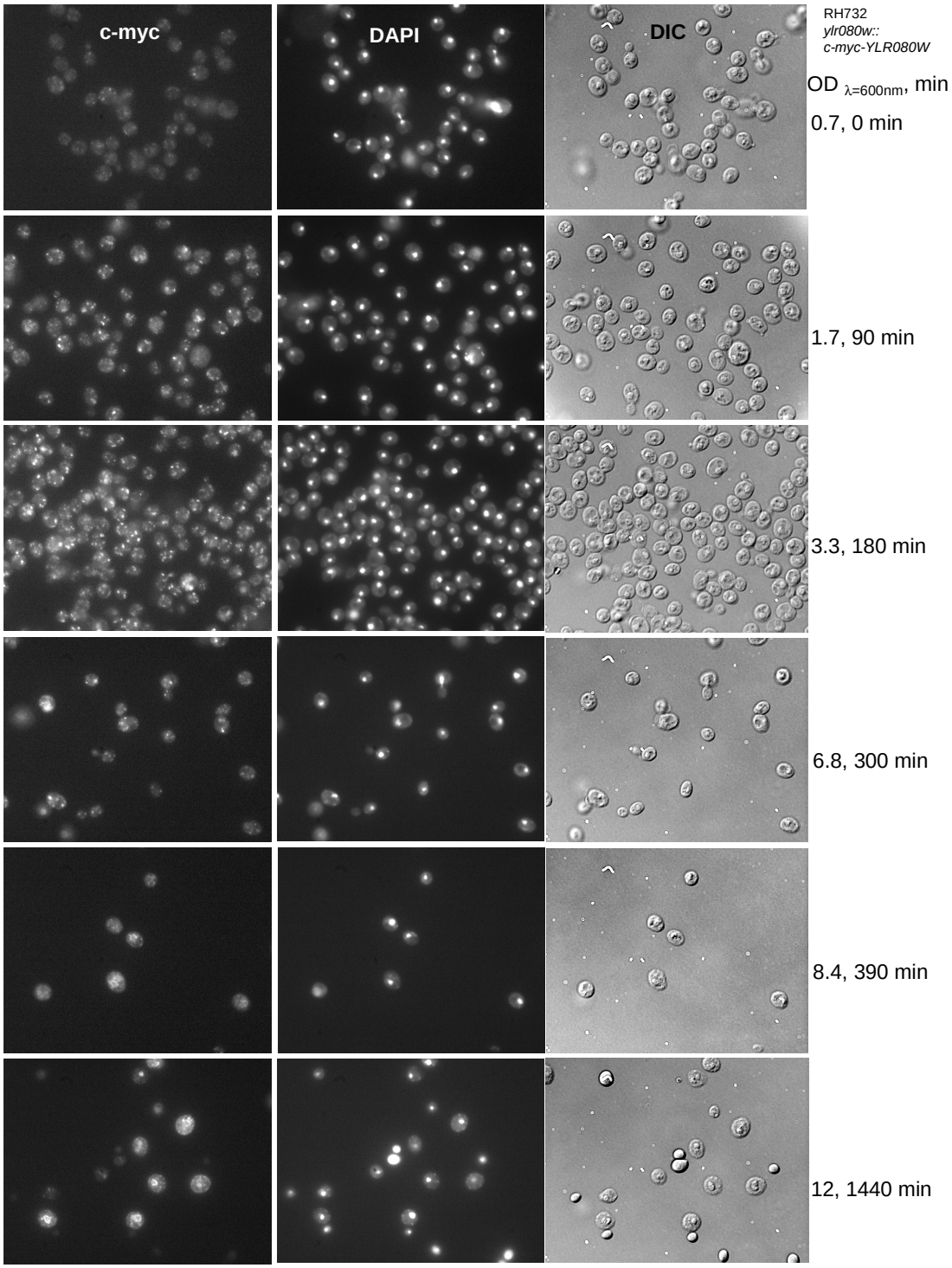
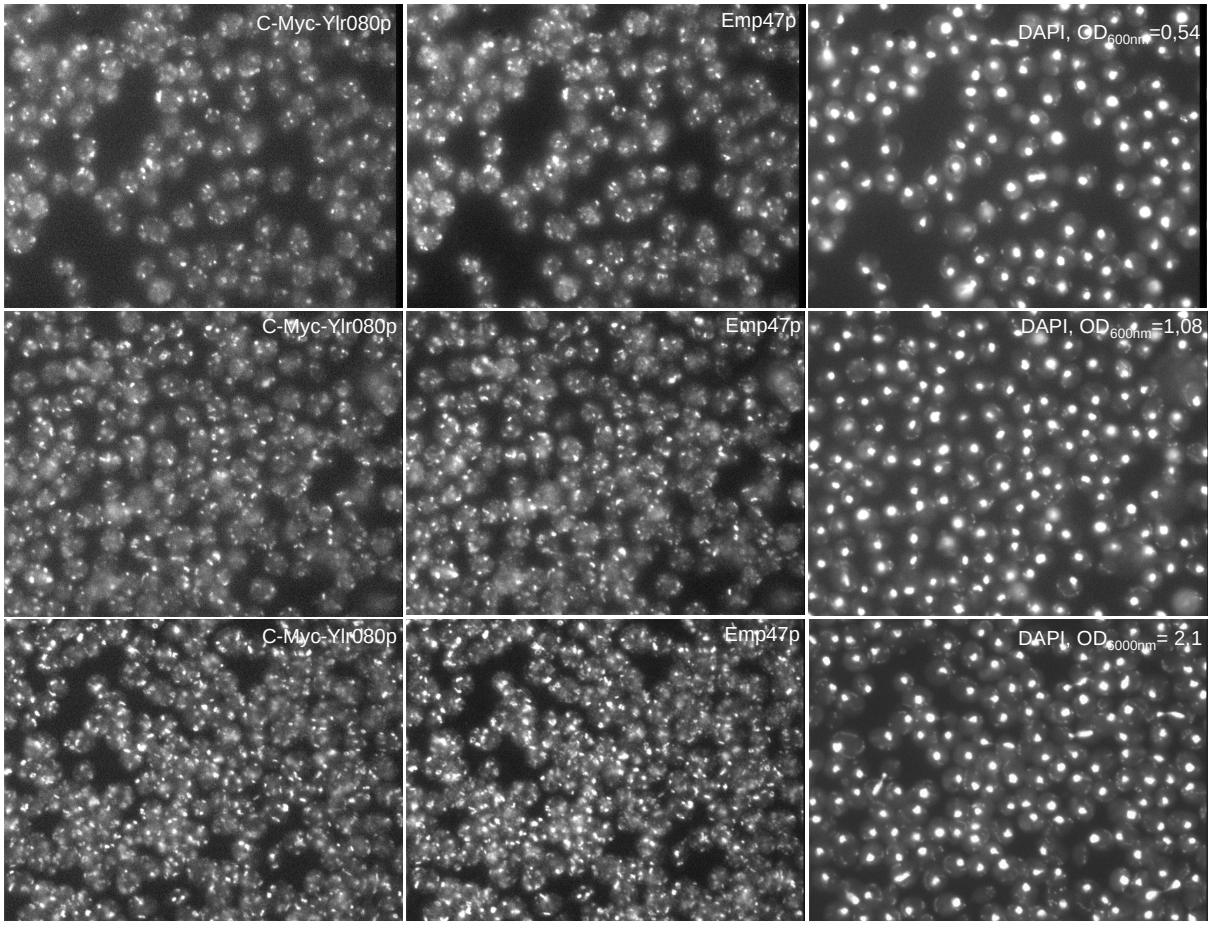


Fig. 26: Immunofluorescence analysis of the subcellular distribution of c-myc-Ylr080wp
RH732-M (*ylr080w::YLR080W, EMP47, pep4Δ*) were grown in rich medium (YPUAD) from the early log phase to the stationary phase. At different time-points small aliquots of yeast cell cultures were subjected to immunofluorescence analysis with antiserum against c-myc and Emp47p. DAPI (4,6-Diamidino-2-phenylindole, Sigma): fluorescent groove-binding probe for DNA. DIC: differential interference contrast. Vacuoles appear as indentations in the DIC-images. The fluorescence pattern of c-myc-Ylr080wp shows the punctate Golgi-staining up to 6,8 OD_{600nm} corresponding to the late log phase (see plots in the Fig. 25A and B). However, starting with early stationary phase (OD_{600nm}= 8,4) the ring-like ER-pattern of c-myc-epitope fluorescence clearly predominates. Note also, that fluorescence intensity builds up as the cells transit gradually from log to stationary phase.

The different expression profile of Emp47p and Ylr080wp prompted us to do colocalisation studies at different points of growth curve. For colocalisation analysis by indirect immunofluorescence we used strain RH732-M that expresses endogenously both c-myc-Ylr080wp and native Emp47p. The cells again were grown as described in chapter 4.5.4 and small aliquots were taken at different time points for the procession in double immunofluorescence analysis (chapter 3.8.2). Fig. 27 demonstrates, that the two different reporter-proteins perfectly colocalize in logarithmicly growing yeast cells with OD_{600nm} ranging from 0,54 to 7,8. At early stationary phase (OD_{600nm}= 8,8), however, the fluorescent signal from c-myc-tagged Ylr080wp changed to the ring-like pattern indicative of ER-localisation. The immunofluorescent image of Emp47p in those cells was generally less crisp than in cells from log-phase, with the signal from Emp47p seen in one case as sparse Golgi-like dots or as fuzzy rings in another (Fig. 27).



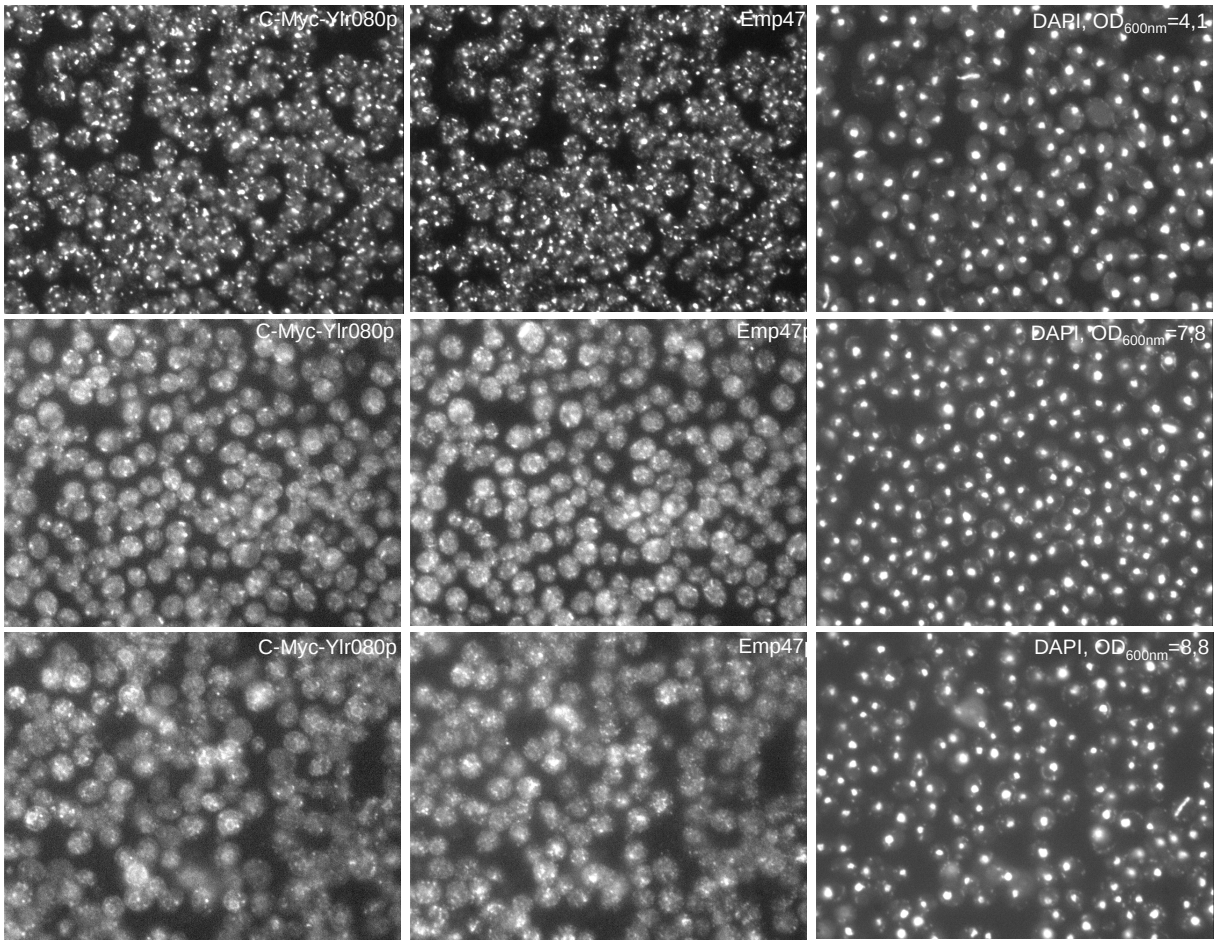


Fig. 27: c-myc-Ylr080wp colocolizes entirely with Emp47p up to the middle logarithmic phase of growth.
The yeast cells were stained simultaneously with both c-myc monoclonal mouse antibodies (9E10) and anti-Emp47p polyclonal rabbit antiserum. Secondary antibodies were anti-mouse antibodies (Cy2) and anti-rabbit antibodies (Cy3). Switching the filters, it was possible to distinguish green fluorescence of Cy2 antibodies from the red one of Cy3. The signals from the two reporter-proteins show perfect colocalisation in the Golgi compartment up to 4,4 OD_{600nm}. In the end of logarithmic and the beginning of stationary phase (OD_{600nm}= 7,8 - 8,8),however, the c-myc fluorescence shifts largely to the ER, whereas the signal from Emp47p degenerates in quality and appears sometimes as an occasional the Golgi-like fuzzy dot or the ER-reminiscent blurred ring.

In order to verify the results obtained by IF, an alternative way was chosen to define the intracellular distribution of c-myc-Ylr080wp. A subcellular fractionation of gently lysed cells on sucrose gradients (chapter 3.6) was applied. The yeast strain RH732-M (*ylr080w::c-myc-YLR080W, EMP47*) was grown under conditions described in the chapter 4.5.4 and approximately 1000 OD_{600nm} of cells each were taken at three different time-points corresponding to three different stages of growth (middle, late logarithmic and early stationary; see Fig. 28A, B for corresponding OD_{600nm} values). The cell lysates were fractionated on sucrose gradients as described in the chapter 3.6.2 and the gradients were disassembled in 15 separate fractions (stepwise from the top of the tube (first cytosol-containing fractions) to the bottom (last the ER-membranes enriched fractions))(chapter 3.6.2). The fractions were then separated by SDS-PAGE and proteins were transferred to

nitrocellulose membranes by Western blotting. The filters were then incubated with either monoclonal antibodies against the c-myc epitope (9E10) or with polyclonal antisera reactive with Emp47p and Kar2p respectively.

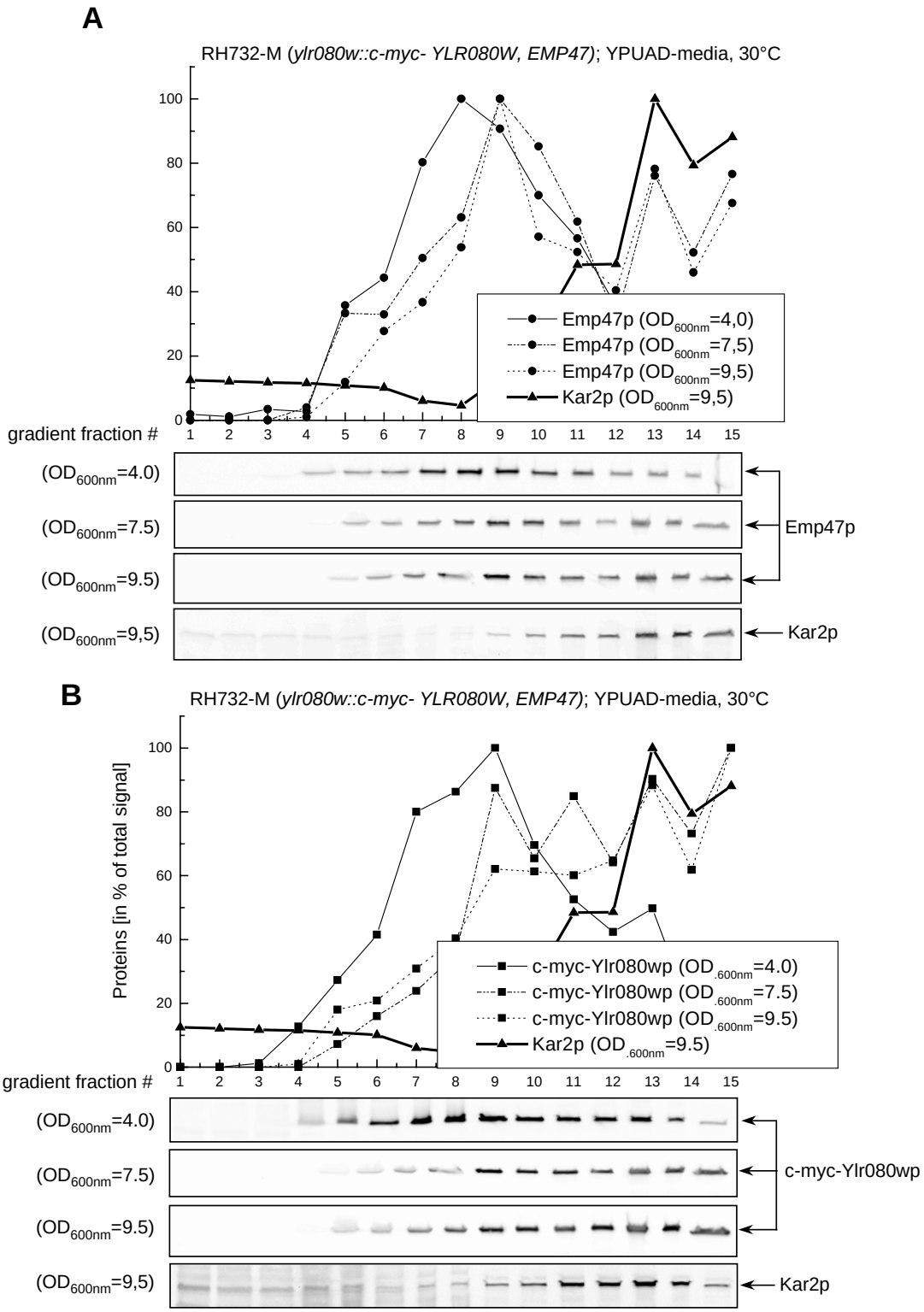


Fig. 28: Distributions of Emp47p and c-myc-Ylr080wp at different growth stages, as determined by subcellular fractionation on sucrose gradients.

Yeast strain RH732-M (*ylr080w::YLR080W, EMP47, pep4Δ*) was grown in rich YPUAD at 30°C from log phase to the stationary one. At three different time points, corresponding to the middle, late and early stationary phases

of growth, aliquots of yeast cells (in quantity of 1000 OD_{600nm} each) were gently lysed and then fractionated on sucrose gradients (see chapter 3.6.2). Following the fractionation step, the gradients were disassembled into 15 fractions that were subsequently resolved by SDS-PAGE, transferred to nitrocellulose membrane filters and probed with antibodies reactive with c-myc-epitope, Emp47p and Kar2p. The intensities of enhanced chemiluminescence per tracks were quantified by Lumi-imager™ software in Boehringer Light Units (BLU). Every BLU value per every track was converted to % of the total signal from corresponding reporter-protein and plotted as such against its respective sucrose gradient fraction number (from 1 to 15).

A. The majority of Emp47p remains in the Golgi following the transition of yeast cells from logarithmic to stationary phase of growth.

The Golgi fractions #7 to #10 clearly dominates in the amount of Emp47p at all growth stages analysed. However, the amount of Emp47p in the last ER-membrane fractions (judging from the distribution of the luminal ER-protein Kar2p) substantially increases towards the stationary phase of growth.

B. As yeast cells enter stationary phase, the majority of c-myc-Ylr080wp shifts form the Golgi compartment to the ER.

c-myc-Ylr080wp distribution in the Golgi fractions is severily reduced upon the entry to stationary phase (OD_{600nm}= 9,5). Note also, that at the intermidiate growth phase with 7,5 OD_{600nm} c-myc-Ylr080wp is equally distributed between the Golgi (fractions #8 to #10) and the ER (fractions #12 to #14).

The Golgi distribution of Emp47p was only slightly changed during transition from the mid-logarithmic phase (OD_{600nm}= 4,0) to the early stationary phase (OD_{600nm}= 9,5). Although the relative amount of Emp47p was steadily increasing in the bottom fractions containing ER-membranes with the progression towards the stationary phase of growth, the peak of Emp47p was only slightly shifted from the gradient fraction 8 (at OD_{600nm}= 4,0) to the fraction 9 (at OD_{600nm}= 9,5) (Fig. 28A).

In contrast to the behaviour of Emp47p, the distribution of Ylr080wp underwent significant changes in growth-stage-dependent manner. In the mid-logarithmic phase of growth (OD_{600nm}= 4,0), the peak of Ylr080wp distribution overlapped exactly with that of Emp47p in fractions 7, 8 and 9 (compare Fig. 28A with 28B). At the end of logarithmic phase (OD_{600nm}= 7,5), Ylr080wp was found almost evenly distributed across the gradient fractions 9 to 15 (Fig. 28B). The transition of Ylr080wp to the ER got even more pronounced with the advent of early stationary phase of growth (OD_{600nm}= 9,5), as the level of the protein peaked in the last three fractions corresponding to the ER-membranes (Fig.28B). Thus, the results of two independent approaches confirm the differential behaviour with regard to steady-state localisation between the two homologous proteins.

4.5.6. Ylr080wp recycles between the Golgi and the ER compartments

The presence of the di-lysine motif as well as an overall high score of structural homology existing between Ylr080wp and Emp47p prompted us to investigate the dependence of Ylr080wp localisation on the function of antero- and retrograde machineries of protein transport in yeast. We addressed the question of Ylr080wp localisation in different COP I- and COP II-mutants at the mid-logarithmic phase of growth (OD_{600nm}= 3,0-4,0) by means of subcellular fractionation of the cellular components on sucrose gradient.

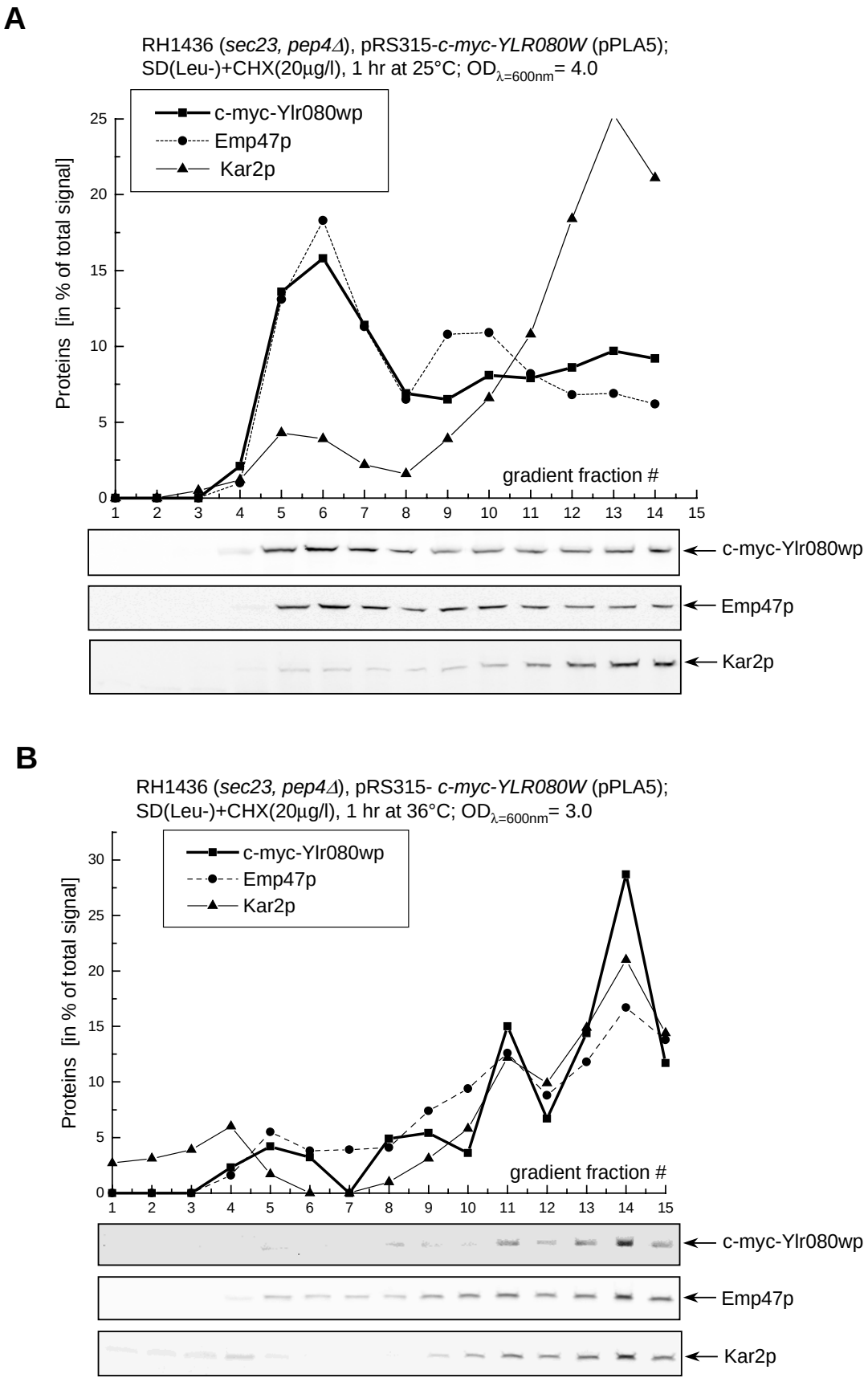


Fig. 29: c-myc-Ylr080wp recycles between the Golgi complex and the ER

Yeast strain RH1436 (*sec23, pep4Δ*) was transformed with a single-copy plasmid pPLA5 expressing c-myc-Ylr080wp. Cells were grown in SD(Leu-)-medium up to 3 OD_{600nm} at 25°C, cycloheximide was then added to end-concentration of 20 µg/ml and the yeast culture was split in 2 parts. One part was left incubating at 25°C the other was shifted to the restrictive for Sec23p function temperature of 36°C. 1 hour after the split, yeast cells

were collected by centrifugation and processed as described in the Fig. 28 for the subcellular fractionation by velocity sedimentation on sucrose gradient. The graphs showing the subcellular distribution of c-myc-Ylr080wp, Emp47p and the ER-marker Kar2p were made as described in the legend to Fig. 28.
A. At permissive temperature c-myc-Ylr080wp localises to the Golgi in *sec23* mutant.
At 25°C c-myc-Ylr080wp as well as Emp47p are found in the same gradient fractions enriched in the Golgi membranes (fractions #5 to #7). Kar2p occupies the last ER-fractions (#12 to #14).
B. At non-permissive temperature c-myc-Ylr080wp is trapped in the ER in *sec23* mutant.
Shift to the restrictive temperature of 36°C for 1 hour brings about a dramatic redistribution of the reporter-proteins from the Golgi fractions to the ER. Thus, the majority of c-myc-Ylr080wp and Emp47p are found to colocalise with the ER-marker Kar2p in the fractions #13 to #15.

The yeast mutant conditionally deficient in an essential COP II-coat protein Sec23p (Hicke and Schekman, 1989) was used to study the role of anterograde transport in the Golgi localisation of Ylr080wp. Yeast strain 1436 (*sec23*, chapter 2.1) was transformed with pPLA5 (chapter 2.2) that expressed c-myc-Ylr080wp. The plasmid was propagated by growing the yeast cell culture overnight at 25°C on a selective minimal SD(Leu$^-$) medium. The culture was then split in two parts, one left to grow in the same medium at 25°C the other shifted to 36°C and incubated for 1 hours in the presence of cycloheximide (20 µg/ml final concentration). The CHX was added to stop protein biosynthesis and, thus, to prevent appearence of newly synthesized proteins in the ER compartment. Under these conditions, the retrieval of c-myc-Ylr080wp from the post-ER compartments back to the ER would be a sole process responsible for the accumulation of the protein in the ER. Both cell cultures were then analysed for the distribution of c-myc-Ylr080wp, Emp47p and Kar2p by subcellular fractionation on sucrose gradient (Fig. 29A, B).

According to our expectations c-myc-Ylr080wp was found to fully colocalise with the Golgi-markers Emp47p (Schröder et al., 1995) and Rer1p (Boehm et al., 1997) providing that the *sec23* mutant was incubated at permissive temperature of 25°C (Fig. 29A). A shift to restrictive temperature of 36°C for 1 hour with simultaneous block in protein biosynthesis by addition of cycloheximide lead to effective return of c-myc-Ylr080wp from the Golgi to the ER (Fig. 29B). The pattern of c-myc-Ylr080wp response to the inhibition of Sec23p-dependent anterograde transport was qualitatively identical to the one displayed by Emp47p. Therefore, similar to Emp47p, c-myc-Ylr080wp undergoes recycling in retrograde way from the Golgi compartment back to the ER.

4.5.7. The ER-Golgi distribution of Ylr080wp depends on di-lysine signal and intact components of COP I Golgi-to-ER retrieval machinery.

4.5.7.1. Construction of c-myc-Yrl080wp „tail"-mutants

Typical di-lysine signals require lysines in positions –3, -4 or –3, -5 from the C-terminus. To address the question of the functionality of the di-lysine signal in the carboxy-terminal part of Yrl080wp several types of structural disturbances were introduced by site-directed PCR mutagenesis into the di-lysine motif region of the myc-tagged version of Yrl080wp.
The plasmid pRS315-SS was constructed from the plasmid pPLA4 (chapter 2.2) by adding two serine-codons to the C-terminus of the coding sequence, displacing the two lysine residues from positions (–3) and (–5) to positions (-5) and (-7) correspondingly. The plasmids pRS315-QQ and pRS315-Q were made as described in chapter 2.2 to incorporate mutations leading to either double (K(-5)Q and K(-3)Q) or single (K(-3)Q) substitutions in the di-lysine motif of c-myc-Yrl080wp. All changes were verified by sequencing with corresponding primers (chapter 2.3).

A number of yeast strains (RH732, 10053, 10044; chapter 2.1) were transformed with each of those three plasmids encoding c-myc-Yrl080wp proteins mutated in their di-lysine signal.

4.5.7.2. The ER-Golgi localization of Ylr080wp requires functional di-lysine motif

By analogy to studies carried out for Emp47p (Schröder et al., 1995), the influence of mutations in di-lysine motif on subcellular distribution of c-myc-Ylr080wp was investigated. We assayed the localisation of the three „tail"-modified versions of c-myc-Ylr080wp (c-myc-Ylr080w-QXQLLp, c-myc-Ylr080w-KXQLLp and c-myc-Ylr080w-KXKLLSSp versions, refer to chapter 4.5.7.1) expressed from single-copy centromeric plasmids pRS315-QQ, pRS315-Q and pRS315-SS (chapters 4.5.7.1and 2.2) either in the strain RH732 *(YLR080W, EMP4, pep4Δ*) or strains 10053 (*ylr080wΔ, EMP47, pep4Δ*) and 10044 (*ylr080wΔ, emp47Δ, pep4Δ*). As reported earlier (Schröder et al., 1995), the disturbances in di-lysine signal of Emp47p resulted in mislocalisation of the protein to the vacuole. Therefore we expected to encounter similar vacuolar missorting of c-myc-Ylr080wp mutated in either the presence or the position of the crucial lysines. If the substantial proportion of the mutated protein takes the default pathway to the vacuole, proteolytic fragments of the protein may be immunodetected in the top-fractions of the sucrose gradient, containing vacuoles and cytosol, after subcellular fractionation of the cell lysate.

Indeed, I only found such fragments of the mutant versions of the protein, but not the intact c-myc-Ylr080wp (Fig. 30A, B, C, D). We observed, however, that the degree of the mutant

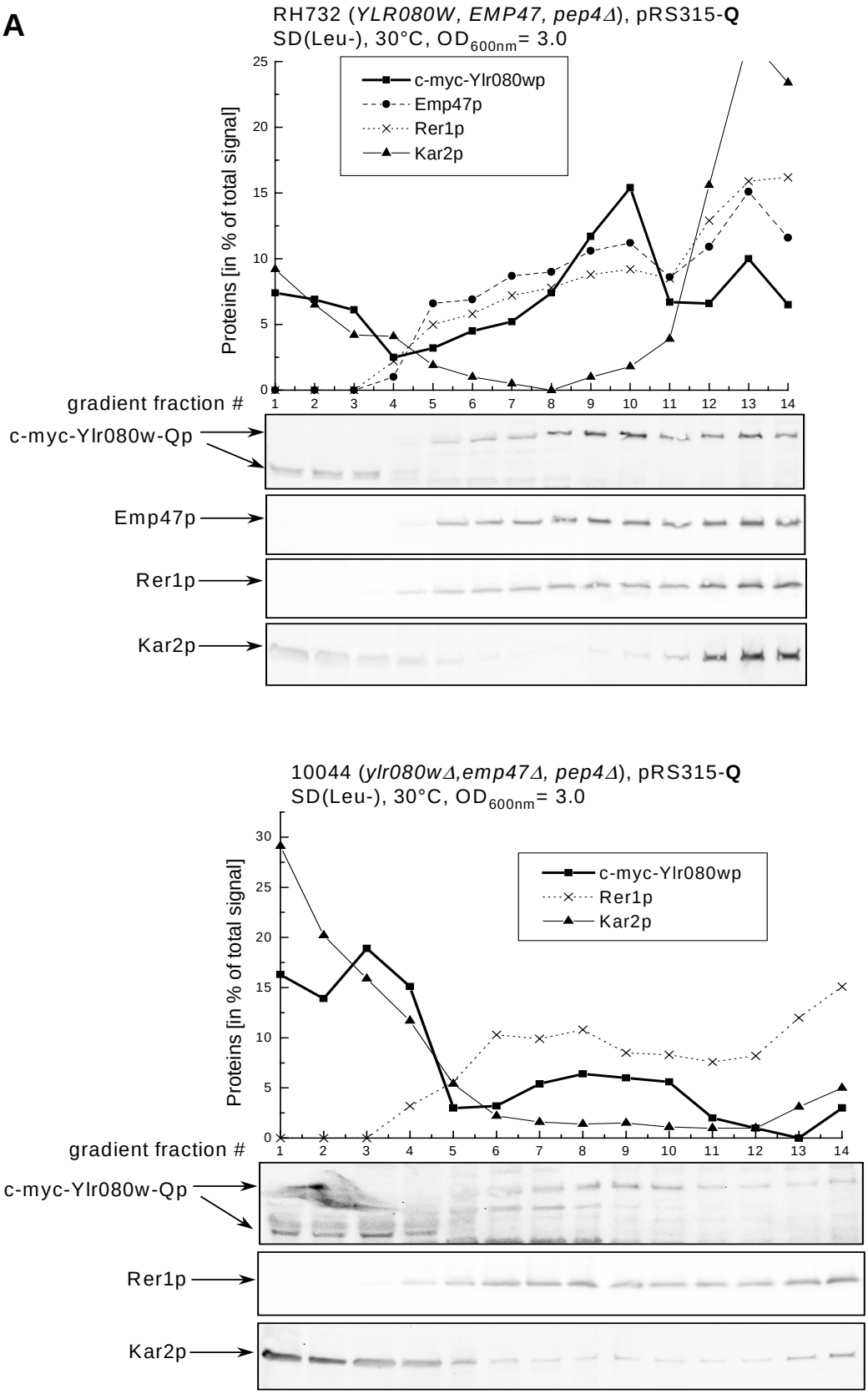
proteins mislocalisation to the vacuole (estimated as a proportion of the signal in the first four fractions to the total amount of immunodetected protein) was more pronounced in the strains deleted for the endogenous copy of *YLR080W* (Fig. 30A, B). However, the majority of the protein with the displaced di-lysine signal retained the Golgi localisation (Fig. 30C) irrespective of whether an endogenous Ylr080wp was present or not. This is in marked contrast to the corresponding mutation in Emp47p, which gives rise to complete loss of Golgi-localisation (Schröder et al., 1995).

Thus, the di-lysine signals of Emp47p and of Ylr080wp are of somewhat different functionality in the context of the respective proteins.

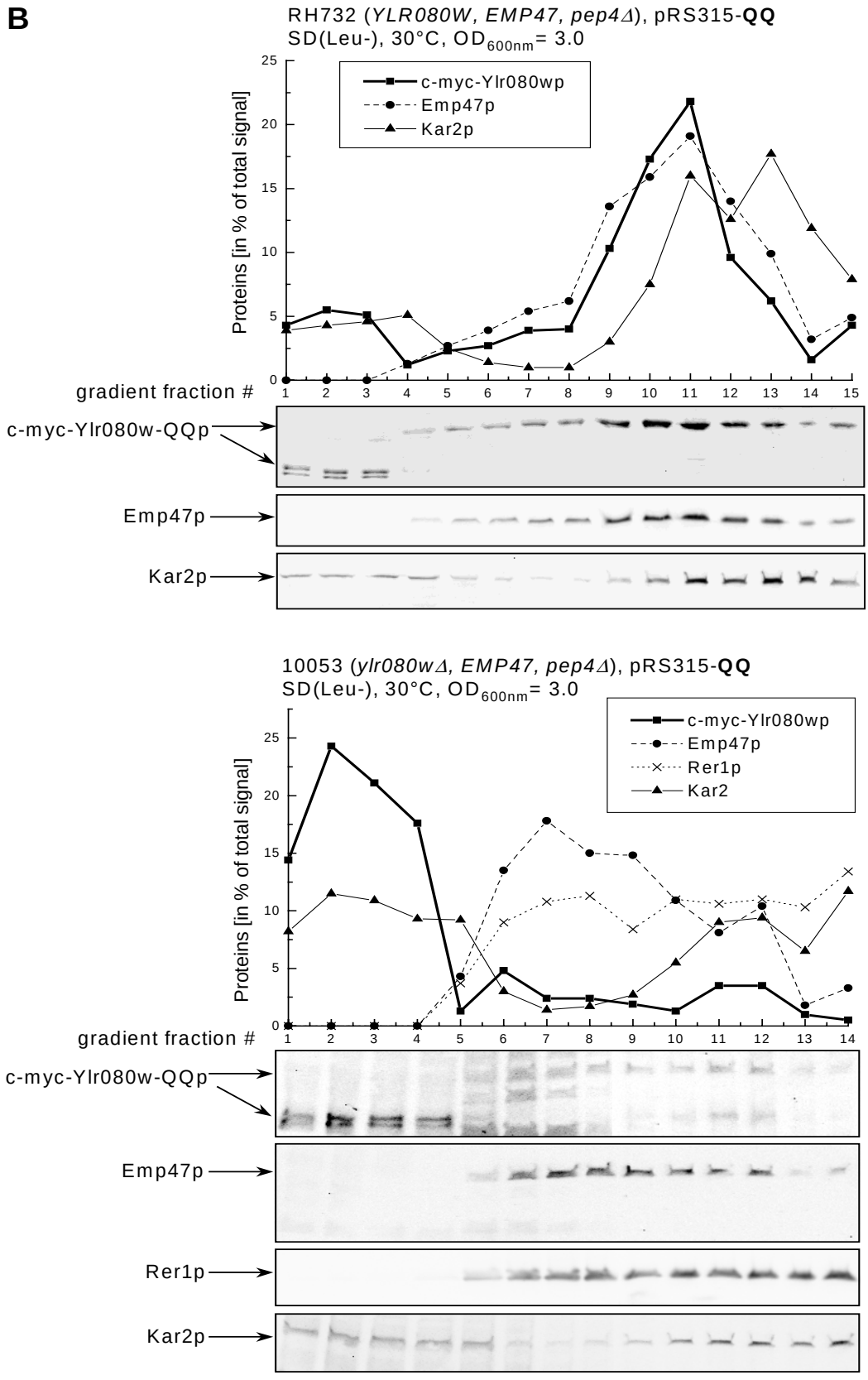
Fig. 30: Mutations in the structure and the position of C-terminal di-lysine signal of c-myc-Ylr080wp result in mislocalisation of the protein to the vacuole.

The strains RH732 *(YLR080W, EMP4, pep4Δ*), 10053 (*ylr080w Δ, EMP47, pep4Δ*) and 10044 (*ylr080w Δ, emp47 Δ, pep4Δ*) were transformed with each of the single-copy centromeric plasmids pRS315-QQ, pRS315-Q and pRS315-SS (see chapters 2.2 and 4.5.7.1). Strain RH732 was also transformed with pPLA5 (see chapter 2.2) to provide a negative control for the rate of vacuolar degradation of c-myc-Ylr080wp with intact di-lysine signal. Transformed yeast cells were then grown in SD(Leu-)-medium up to 3 OD_{600nm} at 30°C. After that, the cell lysates were obtained followed by subcellular fractionation by velocity sedimentation on sucrose gradient. Several antigens were then visualised on nitrocellulose membranes: c-myc-Ylr080wp, Emp47p, Rer1p and Kar2p (the luminal ER-marker). Plots were constructed as described in the legend to the Fig. 28. The appearance of the bands reactive with monoclonal anti-c-myc antibodies in the first four cytosolic and vacuolar fractions (from #1 to #4) reflected an increased probability with which the proteins crippled in their di-lysine motifs reached the vacuolar compartment characterised by a substantially reduced proteolitic activity due to the absence of Pep4p.

Note, that Emp47p (in “B“, “C“ and “D“) and Rer1p reside exclusively in the space occupied by the Golgi and ER membranes (fractions # 6 to the last one) and Kar2p marks the presence of the ER membranes in last three fraction.



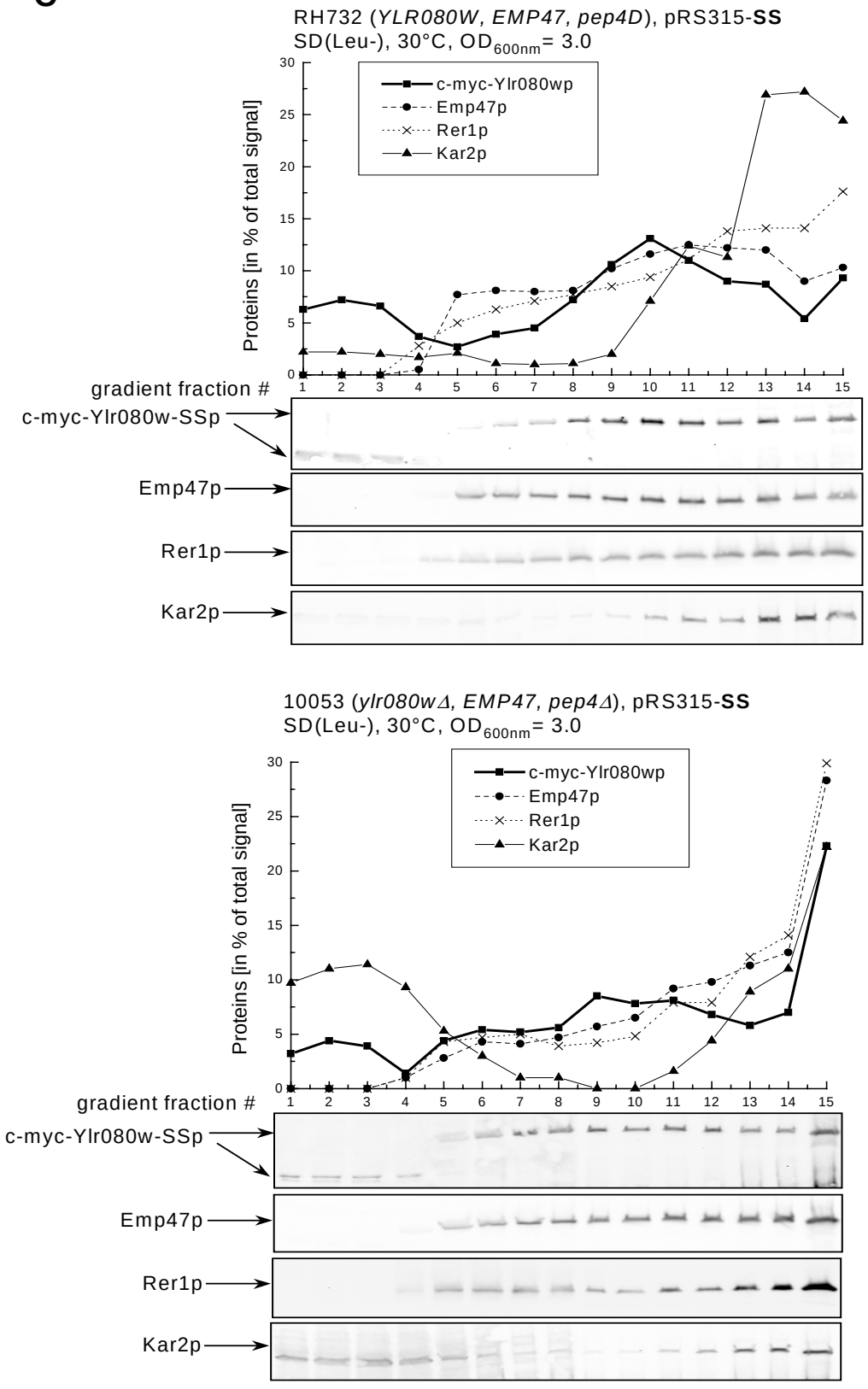
A. K(-3)Q mutation in the structure of di-lysine signal mislocalises the modified protein to the vacuole and disrupts the mutated protein retention in the Golgi in the absence of intact c-myc-Ylr080wp.
The distribution of c-myc-Ylr080w-KXQLLp across the gradient fractions indicates efficient mislocalisation of the mutant protein to the vacuole (note the bands reactive with monoclonal anti-c-myc antibodies in the fractions #1 to #4) as well as abortive retention in the Golgi (valid for the strain 10044 only) providing the absence of intact c-myc-Ylr080wp.



B. K(-5)Q and K(-3)Q double amino-acid substitution mislocalises the mutated protein to the vacuole most efficiently.

Everything observed for c-myc-Ylr080w-KXQLLp in "A" is applicable to c-myc-Ylr080w-QXQLLp mutated protein. Moreover, the phenotypes of mislocalisation to the vacuole as well as of inefficient retention in the Golgi (again valid only for the Ylr080wp deficient strain 10053) are even more pronounced in case of double amino acid substitution. Note that the bands reactive with monoclonal anti-c-myc antibodies (fractions #1 to #4) appear to be more intense in "B" than in "A".

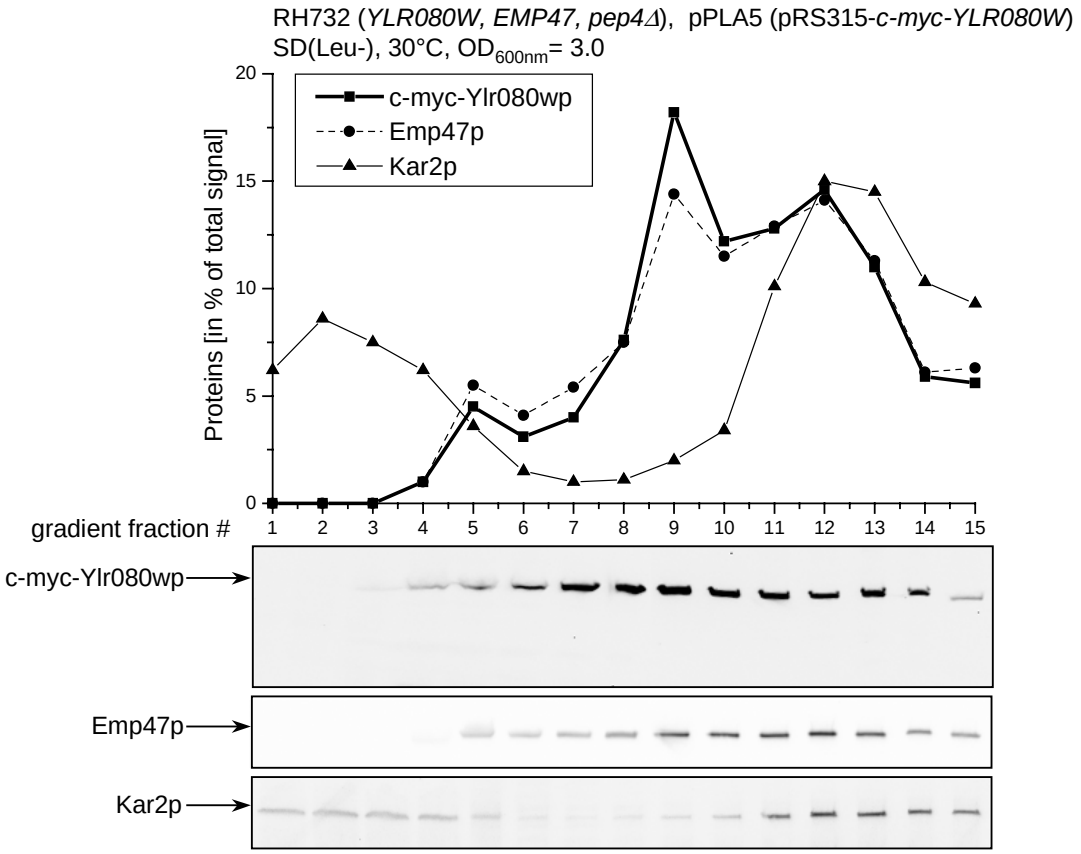
C



C. Displacing di-lysing signal by two amino-acids away from the C-terminal position lead to increase in vacuolar turnover for the mutated protein but is not sufficient to disrupt the retention of the protein in the Golgi.

As an appearance of c-myc-epitope-containing breakdown products of c-myc-Ylr080w-SSp indicates (fractions #1 to #4), a small part of the mutated protein reaches the proteolitic space of the vacuoles in both strains RH732 and 10053. The Golgi distribution of c-myc-Ylr080w-SSp appears to be ,however, not influenced even in the absence of intact c-myc-Ylr080wp (situation in the strain 10053 deleted for *YLR080W*).

D



D. The localisation of c-myc-Ylr080wp expressed from a single-copy centromeric plasmid pPLA5 in the wild-type cells.
In wild-type strain RH732 (*YLR080W, EMP47, pep4Δ*), c-myc-Ylr080wp localises exclusively to the Golgi and ER membranes leaving no trace of its presence in the first four sucrose gradient fractions enriched in vacuolar and cytosolic components.

4.5.7.3. The Golgi-to-ER retrieval pathway of Ylr080wp is a coatomer-mediated process

The fact that the dependence on di-lysine signals seemed to vary between Emp47p and Ylr080wp made for the interesting question if the cell established requirements of COP I components for the recycling of Emp47p would hold true for Ylr080wp.

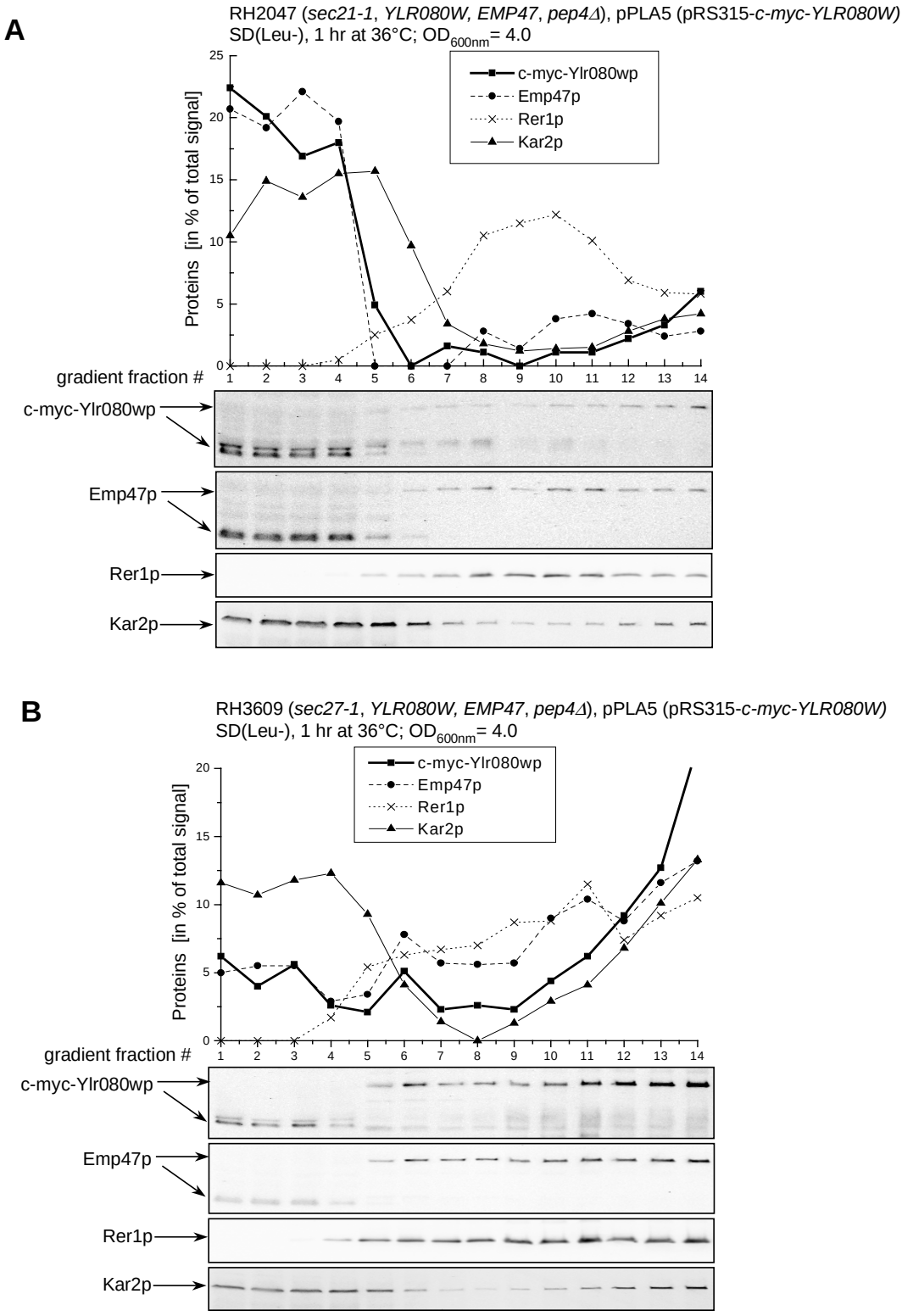
To elucidate the question whether COP I components are involved in the Golgi-to-ER transport of c-myc-Ylr080wp we transformed strains 2047 *(sec21-1*, *pep4Δ*) and 3609 (*sec27-1*, *pep4Δ*) deficient respectively for γ- and β´-COP subunits of coatomer (chapter 2.1) with pPLA5, a single-copy centromeric plasmid expressing c-myc-Ylr080wp (chapter 2.2). The transformed yeast cells were then incubated overnight at 25°C on a selective minimal SD(Leu$^-$) medium. After that the cells were shifted to the restrictive for growth temperature of 36°C and incubated for 1 hour following the analysis of the distribution of c-myc-Ylr080wp, Emp47p, Rer1p and Kar2p by subcellular fractionation on sucrose gradient (Fig. 31A, B).

The wild-type distribution of c-myc-Ylr080wp (Fig. 30D) was lost in strains deficient for the afore-mentioned coatomer subunits (Fig. 31A, B). Although the strain mutated for Sec21p (γ-COP subunit) caused more drastic mislocalisation phenotype for both c-myc-Ylr080wp and Emp47p (Fig. 31A) than the strain deficient in Sec27p (β´-COP subunit) function (Fig. 31B), both mutations lead to visible accumulation of partially digested remnants of c-myc-Ylr080wp and Emp47p in the first four fractions containing vacuoles and cytosol. Note also that, in case of *sec27-1* mutation significant amounts of both c-myc-Ylr080wp and Emp47p appeared to be captured in the ER-membranes (see Fig. 31B, fractions #12 to #14) probably due to some indirect inhibition of anterograde protein export from the ER mediated by *sec27-1* (Schröder et al., 1995). In compliance with some earlier reports (Schröder-Köhne et al., 1998; Boehm et al, 1997), the Golgi-ER-distribution of Rer1p remained unaffected by mutations in COP I subunits (Fig. 31A, B)

I therefore conclude that mutations in at least these two COP I-coat subunits (β´- and γ-COP) result in mistargeting of c-myc-Ylr080wp to the vacuole similar to the effect of mutations in some, but not all, features of the di-lysine signal of Ylr080wp.

Fig. 31: Mutations in coatomer subunits interfere with the Golgi-retention of c-myc-Ylr080wp and missort the protein to the vacuole.

Yeast strains 2047 *(sec21-1, pep4Δ*) and 3609 (*sec27-1, pep4Δ*) deficient respectively for γ- and β´-COP subunits of coatomer were transformed with pPLA5, a single-copy centromeric plasmid expressing c-myc-Ylr080wp (see chapters 2.2). The transformed yeast cells were then incubated overnight at 25°C on a selective minimal SD(Leu$^-$) medium. After that, the cells were shifted to the restrictive for growth temperature of 36°C and incubated for 1 hour followed by the analysis of the distribution of c-myc-Ylr080wp, Emp47p, Rer1p (resides in the Golgi in coatomer-independent manner) and Kar2p (the ER-marker) by subcellular fractionation on sucrose gradient. Plots were made as described in the legend to the Fig. 28. Note, that the distribution pattern of Emp47p is identical to c-myc-Ylr080wp in both mutants *sec21-1* (A) and *sec27-1* (B). As was expected, the majority of Rer1p is confined to the Golgi-ER space (fractions #6 to #14) and Kar2p occupies the last three ER-fractions #12 to #14.



A. Mutation in γ-COP I subunit of coatomer missorts c-myc-Ylr080wp from the Golgi to the vacuole.
Apparently, the majority of c-myc-Ylr080wp is mistargeted to the vacuole (note the bold bands of high intensity in fractions #1 to #4 that are reactive with monoclonal anti-c-myc-antibodies). The Golgi appears to be completely purged of c-myc-Ylr080wp presence (fractions #6 to #10).

B. Mutation in β´-COP I subunit of coatomer also redistributes c-myc-Ylr080wp from the Golgi to the vacuole.
Obviously, the effect of *sec27-1* mitation is the mislocalisation of c-myc-Ylr080wp to the vacuole (fractions #1 to #4). The Golgi level of c-myc-Ylr080wp (fractions #6 to #10) seems to be reduced compared to the wild-type situation (Fig. 30D) but not as drastically as in case of *sec21-1* mutation shown in „B“. Note, that there appear to be a lot of c-myc-Ylr080wp present in the last ER-fractions #12 to #14.

4.5.8. Molecular size determination by gel-filtration analysis reveals Ylr080wp (48 kDa) migrating as a high molecular weight protein associate of 120-140 kDa.

Our finding that the Golgi-localisation phenotype of the "tail"-mutated versions of c-myc-Ylr080wp was not disrupted in the presence of the intact genomic copy of *YLR080W* suggested the possibility of the existence of oligomerization between the mutated versions of c-myc-Ylr080wp and the native genomic Ylr080wp. As we were not successful in the generation of antibodies specific for Ylr080wp that might have made possible the direct identification of potential oligomers, I resorted to molecular size determination by gel-filtration analysis on Sephacryl-6 column (chapter 3.5.11).

Total yeast protein was extracted from the strain RH732-M (*ylr080w::c-myc-YLR080W, YLR080W, EMP47p, pep4Δ*) by means of grinding under liquid nitrogen in the buffer containing 1% of CHAPS and 500 mM of NaCl (chapter 3.6.2). The cell lysate clarified by centrifugation was loaded onto gel-filtration column filled with Sephacryl-6. The resulting eluate fractions #27 to #59 were passed through SDS-PAGE, Western-blotting procedure and finally c-myc-Ylr080wp was immuno-detected by incubating the nitrocellulose membrane with monoclonal anti-c-myc antibodies (9E10).

The intensities of immunological signals from c-myc-Ylr080wp were calculated for each fraction and the profile of the protein distribution in the fractions #27 to #59 was constructed (Fig. 32). Three areas with a strong signal from c-myc-Ylr080wp were revealed in the profile. The first (I) and the second (II) peaks were centred on the ranges of molecular masses of 2 000 kDa and 700 kDa respectively. An incomplete extraction of c-myc-Ylr080wp from the surrounding membranes might possibly account for the appearance of those peaks (I and II) in the profile of the protein distribution across the eluate fractions. As Fig. 32 indicates, there was, however, a third peak (III) in the narrow range of molecular weights of 120-140 kDa. The emergence of the third peak might stem from the di- or trimerization of the c-myc-Ylr080wp with itself or with the native Ylr080wp. Note that the immonological signal from the fraction #56 that corresponds most closely to the molecular weight of monomeric c-myc-Ylr080wp (approximately 48 kDa) was negligibly weak, which is an evidence supportive to the notion that, in the cell environment, Ylr080wp might predominantly exist and function as a homo-oligomer.

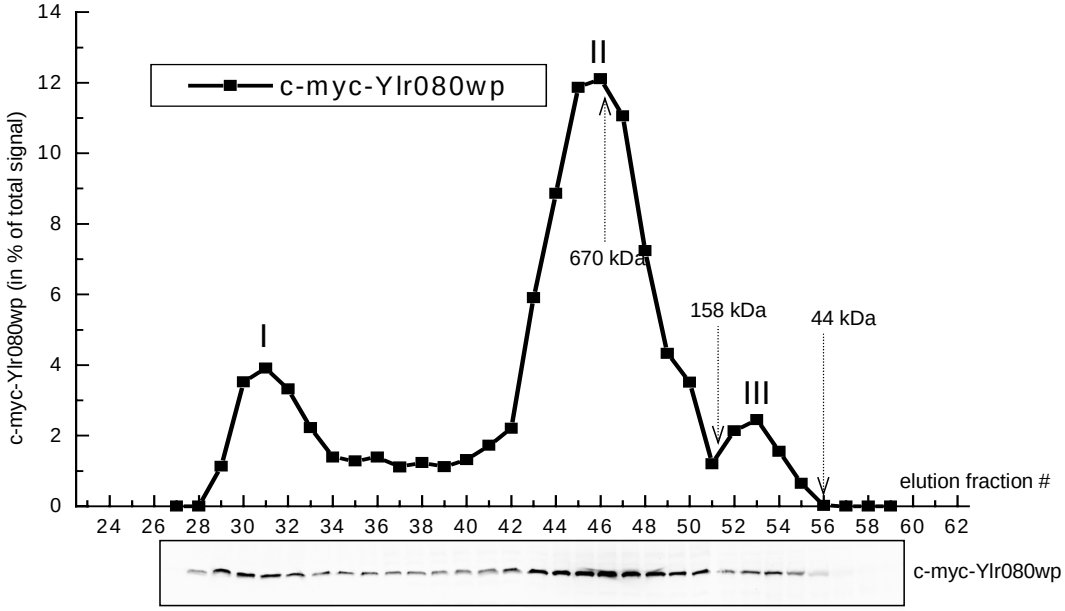


Fig. 32: Molecular size determination by gel-filtration assay reveals that c-myc-Ylr080wp migrates as a protein complex of at least 120-140 kDa.

Yeast strain RH732-M (*ylr080w::c-myc-YLR080W, EMP47, pep4Δ*) was grown to late log phase of 8 OD_{600nm} at 30°C in rich YPUAD medium. The total protein extract was obtained as described in chapter 3.6.2 followed by loading it onto the gel-filtration column filled with Sephacryl S-6 matrix. Subsequently, the eluted fractions were analyzed by SDS-PAGE, Western-blotting procedure and the distribution of c-myc-Ylr080wp in the fractions #27 to #59 was revealed by immunodetection with monoclonal anti-c-myc antibodies (9E10). The chemiluminescence intensities of every fraction were quantified by Lumi-Imager™ and plotted in the graph (represented above) against their respective fraction numbers. The distribution of the standard proteins with known molecular masses (670, 158 and 44 kDa) enabled rough estimation of the molecular weights of the complexes with which c-myc-Ylr080wp was eluted.

There are three peaks (designated as I II and III) in the profile of c-myc-Ylr080wp distribution in the eluted fractions. The peaks II and I correspond to very large macromolecular complexes of over 700 kDa. The peak III, however, centers on a molecular weight of around 120-140 kDa, roughly corresponding to a molecular mass of a putative homodi- or trimeric form of c-myc-Ylr080wp.

5. Discussion

5.1. Oxidative stress induced by *CYS3* inactivation changes protein localisation and turnover, and causes impaired CDP-DAG metabolism at high temperatures.

5.1.1. Characterisation of *cys3-2* mutant cells

In a screen for new complementation groups involved in the protein-targeting of the di-lysine protein Emp47p in the early secretory pathway we have isolated a mutant allele of the gene coding for cystathionine-γ-lyase, *CYS3.* As opposed to the previously described *cys3-1* mutant (Ono et al., 1984, 1988, 1999), the *cys3-2* mutant strain isolated from our screen was completely dependent on cysteine for growth on minimal plates at all temperatures. We conclude that *cys3-2* is a constitutive loss of function allele of *CYS3*. The mutation we have uncovered is a single point mutation, converting S_{201} to F. This serine residue is highly conserved in pyridoxal-phosphate dependent cystathionine γ-lyases and -synthases from bacteria to man. It is located three amino acids N-terminal of the lysine residue to which the cofactor is attached (Barton 1993; Appel 1994). The mutant protein may therefore be inactive because of the inability to bind pyridoxal-phosphate.

The mutant grows on rich medium at 25°C, albeit more slowly than the wild-type. Apparently, rich medium containing yeast-extract and peptone supplies enough cysteine and GSH, which can serve as a source of cysteine (Elskens 1991; Chaudhuri 1997) to support protein biosynthesis and growth at 25°C. Nevertheless the *cys3-2* mutant is unable to grow on rich medium at 37°C. Why? GSH is an important defence agent against oxidative stress caused by chemical oxidants (Penninckx 1993; Jamieson 1998). Under H_2O_2 stress, sulphur metabolism is channelled into the production of cysteine and GSH, while production of methionine and SAM are reduced (Godon 1998). Cys3p was found to be upregulated 3.2 fold under those conditions (Godon 1998), likely representing derepression of transcription due to a deprivation of GSH and its precursor cysteine (Ono 1991). According to Sugiyama et al. (2000), heat-shock conditions are, in some part, equivalent to oxidative stress, because the oxygen respiration rate of the yeast *S. cerevisiae* was found to be increased by heat-shock stress, which resulted in increased intracellular oxidation level. We found that low molecular weight sulfhydryls, which in *S.cerevisiae* reflect the level of reduced GSH (Elskens 1991), were increased in wild-type cells at 37°C by about 10%. In contrast, in the mutant we observed a reduction of low molecular weight sulfhydryls of about 50% within 90 min at

37°C. That level of reduction was likely not the endpoint, as cells were still viable after 2 hrs at 37°C. Our data indicate that GSH plays an essential role in the adaptation to elevated temperatures under aerobic conditions and are fully consistent with a recent report (Sugiyama et. al., 2000) showing the capability of GSH to confer heat-resistance to yeast cells. Our experiments do not distinguish between the essentially irreversible consumption of GSH by conjugation to toxic metabolites as compared to electron-transfer reactions leading to the reversible formation of oxidised GSH (GSSG) (Jamieson 1998). However, GSSG rescued the *cys3-2* mutant as well as GSH, arguing that the cell can supply enough reducing equivalents (NADPH) for the reduction of GSSG to GSH by glutathione reductase. This indicates that it is the amount of GSH independent of its redox-state, which is limiting in the mutant. We conjecture that it is mostly the conjugation of GSH to toxic electrophiles and thus its exit from the redox-cycle that cannot be compensated for by the mutant.

To get further insights into the cause of *cys3-2* mutant growth arrest at elevated temperature on rich YPUAD medium we investigated the rate of exhaustion for LMWS in *cys3-2* and wt cells at different temperatures under conditions of starvation for cysteine. It turned out that the rate of LMWS consumption in *cys3-2* mutant was almost 3 times higher than in wt cells at 37°C. Moreover, as our experiments demonstrate, a shift to 37°C resulted in a 40% increase in the rate of exhaustion for intracellular LMWS contents in wild type cells within 4 hours of incubation at elevated temperature. The same trend of increased LMWS utilisation at 37°C held true for *cys3-2* mutant cells as well. These data lead to conclusion that higher temperature imposes higher demands on the enzymatic systems responsible for the cysteine regeneration through transsulfuration pathway. We may assume therefore, that at 37°C *cys3-2* mutant experiences an unrelented shortage of free cysteine even on rich YPUAD medium probably due to an increased necessity for channelling cysteine supply into biosynthesis of GSH leading, subsequently, to either irreversible exit of the latter from cell metabolism as a result of conjugation with toxic electrophiles or to oxidation to GSSG. The fluctuations in the levels of intracellular cysteine, however, were shown to induce strong repercussions in the whole pathway of sulphur assimilation in yeast *S.cerevisiae* (Ono et al., 1999; Hansen and Johannesen, 2000). Cysteine was proven to be the sole regulatory molecule responsible for changes in the activities of the enzymes of the sulphur assimilation pathway by influencing the level of *MET* genes transcription (Ono et al., 1999; Hansen and Johannesen, 2000). Evidence has accumulated (Thomas and Surdin-Kerjan, 1997; Hansen and Johannesen, 2000; Patton et al., 2000) suggesting that low concentration of cysteine can result in increased transcription of a large set of *MET* genes (*MET25* including) in a *MET4*-dependent manner, whereas cysteine in high concentration appears to repress *CYS3* and *MET*

genes (see chapter 1.2 for details). In wild type cells, once turned on, *MET* genes restore the level of cysteine and GSH. At high concentrations cysteine provides an inhibitory signal repressing further sulphur assimilation by means of *MET30*-dependent targeted degradation of the Met4p transcription activator protein (Patton et al., 2000). Furthermore, it was found (Patton et al., 2000) that unrestricted activation of Met4p-dependent gene transcription (observed in the background of *met30*□ deletion) results in lethality due to cell cycle arrest at the G1 to S transition. According to my observations, the phenotype of *cys3-2* mutant cells indicates that at 37°C they may indeed undergo a growth arrest at the G1 phase as the cells show a significant increase in the cell size compared to wt cells and exist predominantly in the unbudded state. In view of the close link between the cell cycle and sulphur amino acid metabolism, we speculate that the growth arrest of *cys3-2* cells on rich YPUAD medium at 37°C may originate from the inability of those cells to elevate intracellular level of cysteine beyond a certain threshold necessary to trigger the induction of Met30p that would target Met4p for degradation via SCF^{Met30} ubiquitin ligase (Rouillon et al., 2000). According to the outlined scenario *MET* gene regulation in *cys3-2* mutant cells at 37°C approaches the situation of cells knocked-out for Met30p. The questions, however, arises how and why lack of Met4p downregulation would trigger arrest in cell cycle. Some speculations in that direction were provided by Patton et al. (2000). The growth arrest of *cys3-2* cells, however, differs from the one of *met30Δ* in that it proved to be easily reversible. This can be explained by considering that any change in growth conditions leading to an increase of the availability of cysteine would restore the *MET*-genes regulation pathway and thus allow resumption of proliferation.

One of such factors influencing the growth properties of *cys3-2* mutant was found to be the general status of redox potential of the cell. The observation that some intermediate concentrations of β-mercaptoethanol were able to partially rescue the *cys3-2* mutant could be explained by the ability of this membrane permeable reducing agent to counteract the oxidative stress in a non-specific way and thus increase the amount of available cysteine–based intracellular sullfhydryls required to shut off Met4p and allow cell cycle progression.

Another factor defining the level of cysteine requirements was the ambient temperature at which mutant cells were incubated. Although high temperature strictly forbids growth of the *cys3-2* mutant cells, the cells are not dead at elevated temperature but only reversibly arrested in growth. Lowering the temperature from 37°C to 25°C apparently reduces the level of oxidative stress below a restrictive threshold, thus allowing for the continuation of cell growth.

Yet another important factor that directly influences the intracellular level of cysteine is the cell membrane permeability to cysteine and GSH. There is a marked controversy in the

present views on the question of existence of specific cysteine transporters in *S.cerevisiae* (Ono and Naito, 1991; Düring-Olsen et al., 1999). According to the view held by Ono and Naito (1991) there is only one cysteine permease in yeast, which is inhibited only by homocysteine and methionine. The kinetic studies of cysteine uptake revealed saturability and specificity of the cysteine transport system. An alternative view implicates multiple non-specific permeases (Bap2p, Bap3p, Agp1p, Gnp1p, Tat1p, Tat2p and Gap1p) with non-saturable kinetics (Düring-Olsen et al., 1999). Recent studies on glutathione uptake indicate that there is probably a single specific transporter in the plasma membrane of *S. cerevisiae* (Bourbourloux et al., 2000) encoded by *HGT1*. Hgt1p was shown to be a primary glutathione transporter, which was capable also of specific uptake of GSSG and some GSH-conjugates. The optimal pH values for cysteine (Ono and Naito, 1991) as well was for glutathione uptake (Bourbourloux et al., 2000) were found to be in a range of 5,0-5,5, which is consistent with our observation that *cys3-2* mutant was effectively relieved from high temperature–mediated growth arrest when incubated on rich YPUAD medium acidified to pH 5,0 by supplementing agar-plate with citric acid. We assume that greater permeability of the cell membrane to cysteine and GSH at acidic pH-values contributed to an increase in intracellular levels of both, thus switching the *cys3-2* cell metabolism from temperature-imposed dormant state to active proliferation. The finding that cysteine transport system was non-competitively inhibited by methionine (Ono and Naito, 1991) makes it interesting to remark that Met4p-mediated upregulation of *MET* genes activities, speculatively proposed to take place in *cys3-2* mutant at elevated temperatures, bears all the potential to increase the level of methionine thus inhibiting cysteine uptake and thereby further aggravating the deficit of intracellular cysteine in *cys3-2* mutant. We do not, however, have any direct evidence for an increase in the intracellular level of methionine due to Cys3p inactivation.

We may conclude that it seems as though *cys3-2* mutant cells are capable of making fluent transitions between proliferation and dormancy depending on the status of oxidative stress, which is influenced by the intracellular concentration of reducing agents and ambient temperature.

5.1.2. Depletion of cysteine due to Cys3p-dysfunction leads to more profound heat-mediated oxidative stress than shortage of GSH

To distinguish between the effects of GSH-limitations and cysteine-shortages on the observed phenotypic features of *cys3-2* mutant we made use of the yeast strain knocked out for the *GSH1* gene that encodes γ-glutamyl-cysteine synthetase, the first enzyme needed for the GSH biosynthesis. *GSH1* was found to be an essential gene in Saccharomyces cerevisiae as

GS*H1Δ* cells died on a medium devoid of GSH after 6-7 cell-cycles (Sharma 2000; Spector et al., 2000). However, the delay in growth arrest of *gsh1Δ* mutant on a medium devoid of GSH could be effectively prolonged (but never entirely abolished) by overexpressing the *TRX1* gene coding for thioredoxin, a small protein involved in protecting cells against oxidative stress (Sharma 2000). Thioredoxin and GSH/glutaredoxin redox buffers appear to be interconnected and can presumably feed into each other as the loss of two genes (*TRX1* and *TRX2*) coding for cytosolic thioredoxins resulted in elevated levels of GSSG (Muller, 1996). Taken together these facts imply that the pathways of thioredoxins and GSH metabolic reactions are partially overlapping so that thioredoxins are capable to some extent to compensate for the shortage of GSH (Sharma 2000). Moreover, the contribution of TRX and GRX toward the maintenance of the intracellular environments in reduced states was found to be comparable to glutathione (Aslund et al., 1997; Prinz et al., 1997). From that point of view we can explain why the *gsh1Δ* mutant assayed in our study displayed no signs of suffering from oxidative stress in comparison to *cys3-2* mutant at 37°C on rich YPUAD medium under aerobic conditions. Apparently, *gsh1Δ* cells profit from the thioredoxins-dependent protection system even at elevated temperatures especially when incubated in rich YPUAD medium containing small amounts of GSH. The mutation in *CYS3*, however, affects both GSH- and thioredoxins-dependent systems of overcoming the oxidative stress, because both systems include cysteine residues as their most vital structural components. As our experiments show, increase in the ambient temperature imposes higher demands on production of cysteine in order to channel it to the biosynthesis of redox potential "supporters" (presumably GSH, gluta-and thioredoxins). Thus, on the background of inability to produce cysteine internally, the concentration of extracellular cysteine compatible with efficient cell proliferation stands in direct proportion to the ambient temperature. That is not, however, the case with *gsh1Δ* mutant which is limited in GSH only but capable of cysteine production and therefore can rely on the other cysteine-dependent systems in protecting the cell against excessive oxidation. For the reasons discussed above, *cys3-2* mutant also proved to be less proficient than *gsh1Δ* in counteracting the oxidative stress when challenged with a strong oxidising agent 1-chloro-2,4-dinitrobenzene. Therefore I tend to attribute all the signs of *cys3-2* mutant suffering from oxidative stress on rich YPUAD medium (i.e. temperature sensitivity at 37°C on rich medium, the increase of cell size, the ability of β-mercaptoethanol to rescue ts phenotype along with high tolerance to β-mercaptoethanol and increased sensitivity to the GSH-oxidizer 1-chloro-2,4-dinitrobenzene) to the inability of the mutant to provide enough cysteine into the pathways of biosynthesis of cysteine–dependent systems protecting cells from hyperoxidation (i.e GSH-, gluto- and thioredoxins-dependent systems,

monothiol glutoredoxin-like proteins (Draculic 2000)). It appears that, under conditions of limited supply for exogenous cysteine or increased demand in it as a prime source for cellular sulfhydryls, any negative interference with the *CYS3* gene activity must exert a severely detrimental effect on the capacity of the cellular redox-potential regeneration system. There are multiple evidences for cysteine being the limiting amino acid for GSH synthesis especially under oxidative stress conditions (Izawa et al., 1995; Spector et al., 2000). Therefore, even under rich medium conditions, collapse of intracellular redox regeneration system due to *CYS3* dysfunction is very likely to substantially undermine two major redox buffers in *S. cerevisiae* that are GSH and thiredoxins and thereby eventually induce cell growth arrest especially under conditions of temperature-mediated increase in the activity of respiratory metabolism.

Madeo et al. (1999) reported that depletion of GSH induces apoptosis in *S. cerevisiae* that manifests itself via phenotypic features such as chromatin condensation and fragmentation, DNA breakage, exposition of phosphatidylserine on the cell surface, and the formation of minicells approximating apoptotic bodies (Madeo et al., 1997; Ligr et al., 1998). They showed that accumulation of reactive oxygen species (ROS) caused by depletion of GSH in yeast cells triggered the apoptotic pathway in microorganism and the hypoxia or scavenging of the radicals prevented apoptosis. According to our unpresented data, some of the signs of apoptotic events going on in *cys3-2* cells stressed by high temperature were easily observable by staining the mutant's nuclei with DAPI. In particular, the nuclei stained with DAPI appeared to contain strongly condensed chromatin with a ring- or half-ring-like arrangement of fragments or, in addition, we often observed thread-like nuclear fragments randomly dispersed in the cell cytoplasm. I, therefore, propose an additional speculative scenario to account for the growth arrest and ultimately lethality of *cys3-2* mutation under conditions of aerobic growth at elevated temperature. According to it, the heat-shock invoked by incubation of *cys3-2* mutant at 37°C increases the rate of cysteine utilisation needed for backing up the capacities of GSH and thioredoxins redox buffers. If the external cysteine supply is limited and the internal production of cysteine is blocked, the regeneration of the GSH/thioredoxins would be severely diminished, ultimately leading to the shortage of GSH and thereby triggering apoptotic events that could, however, be reversed by mitigating the intensity of oxidative stress.

5.1.3. The role of redox potential in the secretory pathway

As evident from our subcellular fractionation on sucrose gradients and immunofluorescence studies neither the level nor the distribution of Emp47p was disturbed at 25°C in *cys3-2*

mutant cells. Under those conditions the amount of low molecular sulfhydryls was reduced to 83% of the wild-type and the mutant grew more slowly. The trafficking and the level of Emp47p were however affected at 37°C, which positively correlates with a significant drop in the concentration of intracellular thiols. As could be inferred from our LMWS-measurement experiments, when grown on minimal SD-medium, the *gsh1Δ* mutant reached very profound depletion for LMWS that is on par with the one displayed by *cys3-2* mutant. That could be explained by inability of *gsh1Δ* mutant to convert cysteine to its preferred stable storage form GSH. Glutamic acid residue is joined in an unusual peptide linkage of the γ-C-atom to the cysteine which is thought to protect GSH from proteolytic cleavage (Meister, 1988). Despite the very low level of LMWS the *gsh1Δ* mutant did not show any reduction in amounts of Emp47p compared to wild type. The reasons for the differences in Emp47p behaviour in *cys3-2* and *gsh1Δ* mutants remain unidentified. One general explanation, however, could be based on the assumption that misrouting of Emp47p to the vacuole might be triggered not by consequences of depletion in GSH but rather by the synthetic effect of shortages in all thiol-based systems that deal with maintenance of redox potential homeostasis in yeast. As we pointed out above, *gsh1Δ* mutant cells might profit from all other cysteine-dependent systems on a media restricted in cysteine and GSH supply, whereas *cys3-2* mutant cannot. Strangely enough, however, we observed that the level and distribution of the Golgi protein Sed5p, a member of the t-SNARE family, appeared to be markedly affected only in *gsh1Δ* cells under stress-conditions induced by GSH-oxidiser 1-chloro-2,4-dinitrobenzene. Compared to the wild type situation, amounts of Sed5p were found to be drastically reduced and the remaining protein was redistributed from the Golgi to the ER in *gsh1Δ* cells. In that respect, it seems worth noting that one of the putative redox-potential sensitive targets required for the vesicular ER-to-Golgi transport in yeast is represented by LMA1 heterodimeric complex, as it consists of thiredoxin dimerized with IB2 protein (Xu and Wickner, 1996; Xu et al., 1997). Together with Sec18p and Uso1p, the LMA1 complex represents the minimal cytosolic component necessary for the efficient fusion between ER-derived vesicles and the Golgi membranes (Barlowe, 1997). I speculate therefore that the combined effects of shut off in the GSH biosynthesis due to Gsh1p deficiency and lack of GSH supply in the incubation medium may detrimentally affect the function of thiredoxin component of LMA1 complex. That would lead to inefficient cargo delivery via forward ER-to-Golgi secretory routes and may ultimately result in the depletion of the Sed5p pool in the Golgi. However, the proposed scenario, based on the specific impairement of LMA1 complex, is hard to reconcile with the apparently unaffected ER-to-Golgi transport of Emp47p and Rer1p. Moreover, the redox properties of thiredoxin in the LMA1 complex are reportedly not significant for the vesicle

fusion to occur, as the substitution of the two conserved cysteines for two serine residues in the active center of Trx1p does not abrogate the stimulatory effect of LMA1 on the vesicle fusion at least *in vitro* (Xu et al., 1997).

At present we can also not explain the severity and specificity with which the stress conditions induced by 1-chloro-2,4-dinitrobenzene in *cys3-2* mutant at 37°C were able to compromise the level of Emp47p, whereas the distributions and the levels of the other Golgi markers (Rer1p and Sed5p) were not affected. We can not tell at present what the redox potential-dependent targets may be that lead to mislocalization of Emp47p to the vacuole at 37°C and consequently cause drastic reduction in its level. Three possible explanations can be envisaged: 1) indirect, by influencing the machinery that sorts Emp47p; 2) direct, involving the structure and function of Emp47p itself; 3) a combination of both. One such possible indirectly acting target could be the δ-COP-subunit of coatomer, the amount of which was found to be drastically reduced (35 % of wild type level) in *cys3-2* mutant at 37°C. Nevertheless, it is still hard to account for the reason of accelerated degradation or lack of synthesis of that coatomer subunit under conditions of cysteine not being a limiting factor for protein biosynthesis. Alternatively or in addition to it, Emp47p itself contains two cysteine residues placed within the lumen of the Golgi. Using non-reducing gel-electrophoresis we have not been able to find any indication of undue crosslinking of Emp47p with itself or with other proteins, that potentially may have lead to transport to the vacuole for degradation (data not shown). Glutathione, in its oxidised form, was for a long time suspected to be the redox-partner for oxidation of thiols to disulphide bonds during the folding of proteins in the ER (Bader 1999). However, recent work has made it likely that oxidised glutathione is dispensable for disulphide-bond formation. In fact, some amount of reduced GSH may be needed in the oxidising environment of the ER to counteract hyperoxidation of protein thiol-groups. Thus CPY was blocked in the ER in a fully oxidised, unprocessed form in cells that were depleted of reduced glutathione by diamine (Cuozzo 1999). We have, however, not seen any major block or delay in CPY-maturation under our conditions. Thus, the early secretory pathway does not seem to be defective until a more complete depletion of intracellular thiols, which we have not reached in our experiments. The pathway of glycosylated invertase secretion from the ER to the Golgi and further on to the periplasmatic space were also assayed in *cys3-2* mutant to reveal that, within the total of 150 minutes of incubation at 37°C on rich medium, the Golgi apparatus of the mutant stressed by hyperoxidation was, nevertheless, proficient in glycosylating invertase and dispatching it to the periplasmatic space. Here again, we might not reach conditions of more profound depletion of intracellular thiols to influence the pathway of invertase secretion or to compromise the Golgi glycosylating capabilities.

Redox potential is also important for the function of the vacuole. Mutations in *CYS4*, acting upstream of *CYS3*, lead to a defect in vacuolar acidification. A lack of sufficient reducing power (i.e. GSH and thioredoxins) in the mutant caused the formation of inhibitory disulphide bonds within the catalytic subunit of the ATPase (Oluwatosin and Kane, 1997). *In vivo* this could be demonstrated by a lack of quinacrine accumulation in the vacuole. In the case of the *cys3-2* strain we found apparently normal quinacrine staining after incubation in PM-ura-glucose medium for 90 min at 37°C (data not shown). As in the cases of the CPY maturation block and invertase secretion, the level of thiols-depletion reached in our experimental set-up was likely not yet sufficient to affect the vacuolar ATPase function.

Emp47p was however not the only protein undergoing an accelerated *PEP4* dependent proteolysis in *cys3-2* mutant cells at 37°C. In fact, already at 25°C many Golgi and cytosolic markers we have tested were affected to some extent, while CPY, part of the proteolytic machinery of the vacuole, was present at much higher levels. Various stress and starvation conditions, including sulphate starvation, induce autophagy in yeast (Takeshige 1992) and starvation for amino acids leads to autophagy in hepatocytes (Schwörer 1979). We suggest therefore that autophagy may account for the above observations, as many of its hallmarks are present in our mutant. a) Under autophagic conditions cytosolic proteins (Egner 1993) and whole organelles are taken up into the lumen of the vacuole and are digested there (Takeshige 1992), as was the case in *cys3-2* mutant cells. b) In protease deficient cells, autophagic bodies accumulate within the lumen of the vacuole (Takeshige 1992). We observed similar structures in the vacuoles of *pep4Δ/cys3-2* mutant cells, but not in the wild-type cells under the same conditions (compare Figs. 1A, 6C). c) The increased expression of vacuolar proteases, including CPY, under autophagic conditions has been reported (Hansen 1977; Distel 1983). Clearly CPY was induced in *cys3-2* mutant cells. However, Emp47p seems to enter the vacuole primarily via the biosynthetic pathway, as we detected it at the vacuolar membrane rather than within the lumen of the vacuole.

5.1.4. Cys3p- and Gsh1p-deficient cells are both defective in adaptation of lipid-synthesis in response to high temperature

I have shown the induction of a particular phospholipid in wild-type cells upon shift to 37°C. The *cys3-2* as well as *gsh1Δ* mutants failed to induce the biosynthesis of that phospholipid upon temperature-shift. Direct labelling of the heat-inducible lipid with ^{32}P-orthophosphate, ^{14}C-glycerol, ^{14}C-palmitate and ^{14}C-cytidine shows the presence of each of the respective components in the molecular structure of the inducible phospholipid. Phospholipase A_2 sensitivity test performed on the purified PLX helped to identify a glyceride part of the lipid

as a diacylglyceride. Mild base cleavage experiment revealed the presence of phosphate in both of two distinct breakdown components of PLX consistent with the presence of a phosphodiester bond in the lipid. These observations are consistent with PLX representing CDP-DAG, which was confirmed by direct labeling with ^{14}C-cytidine.

CDP-DAG is an important branch point intermediate in glycerophosphate-based phospholipid biosynthesis in both prokaryotic and eukaryotic organisms. In eukaryotic cells, phosphatidic acid (PA) is converted either to CDP-diacylglycerol by the CDP-diacylglycerol synthase or to diacylglycerol by a phosphatase (Shen 1996). In yeast, CDP-DAG is the precursor in the endoplasmic reticulum for the *de novo* synthesis of phosphatidylinositol, phosphatidylserine, phosphatidylethanolamine, and phosphatidylcholine (Shen 1996). CDP-DAG synthase activity in yeast is mainly (if not solely) attributed to the *CDS1* gene product and *CDS1* is an essential gene for cell growth (Shen 1996). A reduction of CDP-DAG synthase activity to 10% of the wild-type level results in an elevation in the rate of PS synthesis relative to PI and leads to inositol excretion phenotype (Shen 1997). We did not however observe any reliable changes in the PI/PS ratio in both *cys3-2* and *gsh1Δ* mutant in relation to wild-type.

The lipids labelling experiments carried out with *gsh1Δ* mutant provide clues for differentiating between the effects of cysteine- and glutathion-shortages on the lipid phenotype. The inability of *gsh1Δ* to synthesise GSH proved to be a sufficient prerequisite for the lack of induction of CDP-DAG biosynthesis at elevated temperatures. Additionally supplementation of the growth media with GSH reversed the lipid phenotype of both *gsh1Δ* and *cys3-2* mutants at 37°C. Therefore we consider the absence of CDP-DAG accumulation in *cys3-2* mutant under conditions of cysteine-limitations to be a consequence of the reduced input to the GSH biosynthesis rather than of insufficient supply of cysteine for the maintenance of any other thiol-dependent system. In other words, lack of cysteine in *cys3-2* mutant exerts its effect on CDP-DAG production via deterioration of GSH biosynthetic pathway.

At least three questions arise from our observations. First, what might be the reasons for the accumulation of CDP-DAG at 37°C, which we have uncovered in our study? Second, why does CDP-DAG not accumulate in the *cys3-2* and *gsh1Δ* mutants? Third, what role does CDP-DAG play in the missorting of Emp47p to the vacuole and other phenotypes of the mutant?

While CDP-DAG has been investigated in great detail as a precursor of various other lipids, nothing is known about its potential alternative roles (Carman 1999). It seems unlikely that the heat-inducible accumulation of CDP-DAG in wild-type cells points to a novel role of

CDP-DAG as a lipidic second messenger. Second messengers are not commonly induced in non-transient fashion and to such high levels. CDP-DAG may serve as an activated lipid storage depot ready to provide building blocks for the biosynthesis of PS, PI, PC, and PE at high temperatures. Alternatively, CDP-DAG may play a structural role in the adaptation of membranes to higher temperatures.

As to the second question, the lack of CDP-DAG accumulation in *cys3-2* and *gsh1Δ* mutant cells at 37°C might be a consequence of a repressed activity of CDP-synthase under conditions of oxidative stress due to GSH-limitations. In an alternative scenario, non-specific phosphatases induced under autophagic conditions in the mutant cells at higher temperatures may prohibit the accumulation of CDP-DAG by preferential conversion of PA to diacylglycerol, thereby leaving CDP-DAG biosynthesis short of substrate. In any event, we think that lack of CDP-DAG production in *cys3-2* mutant cells at 37°C is unlikely to be a direct reason for growth arrest. This is because the *cys3-2* mutant cells grew with kinetics equal to those of wild-type cells for up to 4 hrs at 37°C, while the lack of CDP-DAG accumulation started already after 30 min of temperature shift.

CDP-DAG in wild-type cells was only produced in readily detectable amounts upon shift to 37°C. Despite the fact that, in *cys3-2* cells, Emp47p was misrouted to the vacuole already at 25°C, the protein, however, was drastically reduced in amounts at 37°C only. The latter fact correlates positively with the failure of the mutant to accumulate CDP-DAG at 37°C. However, as *gsh1Δ* mutant reveals normal level and trafficking of Emp47p despite the absence of CDP-DAG induction at 37°C we assume that neither localisation of Emp47p nor its amounts are directly affected by CDP-DAG level.

5.1.5. In addition to mutation in *CYS3*, the level of Emp47p is adversely influenced by mutations in *CYS4*, *YEF3* and *HTL1* genes

Mutation in *CYS3* allele was not represented solely by the mutant #937. We happened to independently isolate from our screen two other mutants (#49 and #651) characterised by lesions in *CYS3*. Supplementing both of those additional mutants with *2μ-CYS3* was able to restore the prototrophy for cysteine and temperature insensitivity, which confirmed that most likely both mutants are affected in the *CYS3* allele. We did not verify, however, the mutations by sequencing the mutated *cys3* alleles nor did we assay the localisation of Emp47p in those two additional mutants. The fact of quite frequent occurrence of *CYS3* gene damage in the population of randomly mutagenised yeast cells (3 mutants out of about 200 ts mutants analysed harboured mutations in *CYS3*) goes in line with the observation of Vedel and Nicolas (1999) that the *CYS3* locus represents a hotspot of meiotic gene conversion in the

genome of yeast *S. cerevisiae.* The high frequency of gene conversion events most likely reflects an active "open" state of chromatin in the region occupied by *CYS3* locus, which makes the gene an easily accessible target for interaction with a chemical mutagen like EMS.

The mutant #712 was found to be impaired in the function of *CYS4 (STR1)* allele coding for cystathionine-β-synthetase. Relying on the data reported by Oluwatosin et al., (1999) and a discussed above, we expected the dysfunction in Cys4p to incapacitate the intracellular redox potential with the severity and consequences similar to the ones displayed by the deficiency in Cys3p, as both enzymes constitute the sole participants of the yeast transsulfuration pathway leading to biosynthesis of cysteine out of homocysteine. Although we did not look into the details of the connections between Emp47p trafficking and Cys4p inactivation, we nevertheless consider the very fact of *CYS4* ability to reduce the level of our reporter-protein as another strong evidence in support of the notion that the activities of the enzymes of cysteine biosynthetic pathway have an effect on the level and subcellular distribution of Emp47p.

Another ts mutant (#81) characterised by low level of Emp47p turned out to be affected in *YEF3* gene coding for the yeast translation elongation factor EF-3A. Emp47p was not found mislocalized to the vacuole under conditions of *yef3* mutation. We believe that the reduction in the levels of Emp47p in the mutant #81 is unspecific and likely stems from the general deterioration of the protein biosynthetic machinery due to the conditional mutation directly affecting protein translation (Sandbaken et al., 1990).

Two ts-mutants (#623 and #748) were isolated from our screen, which were apparently affected in the *HTL1* gene, as the 2μ-plasmid bearing the wild type copy of *HTL1* allele rescued the conditional growth of both. The level of Emp47p was also restored back to normal by supplementing the mutants with *HTL1*. *HTL1* codes for non-essential protein necessary for viability at elevated temperature, but of otherwise unknown function. Despite the decrease in the level of Emp47p in both mutants, the immunofluorescence analysis performed on *pep4Δ* versions of both mutants disclosed an unperturbed Golgi-localisation of Emp47p in both cases.

5.2. Intracellular trafficking and distribution of the di-lysine protein Ylr080wp

5.2.1. Ylr080wp is confined to the ER-Golgi part of the yeast *S. cerevisiae* early secretory pathway and is required for efficient recovery from stationary phase at lower temperature

Ylr080wp is a type I transmembrane protein, closely homologous to Emp47p (66% of similarity according to BLAST alignment (http://www.proteome.com/databases/YPD/blastsw/yeast/yeast/YLR080W.html)). The latter was shown to have remarkable sequence homology to animal lectins ERGIC-53 and to VIP36 (Schröder et al., 1995). The sequence analysis of Ylr080wp revealed that it contains features analogous to those distinguishing the structure of Emp47p. In particular, the structure of Ylr080wp is characterised by a N-terminal domain oriented towards the lumen of the ER with putative CRD followed by a domain with a potential to form α-helical coiled coils (Fig 22, "B" and "C"). A single 18 amino acid long stretch of hydrophobic residues likely represents the membrane-spanning domain followed by a short exoplasmic domain of 14 amino acid harbouring a typical di-lysine signal at positions -3 and –5 (Fig. 22, "A" and "C"). Di-lysine motifs bind to the coatomer complex of COP I coated vesicles in vitro (Cosson and Letourneur, 1994; Schöder-Köhne et al., 1998) and thus mediate COP I-dependent retrograde transport of proteins from the post-ER compartments back to the ER. Apart from the di-lysine signal, the sequences of both proteins (Ylr080wp and Emp47p) are terminated by two leucine residues in their carboxy-termini, which are reminiscent of the ER-export-facilitating LV-motif of Emp24p (Nakamura et al., 1998) or di-phenylalanin signal of ERGIC-53 (Kappeler et al., 1997). Multiple alignment of Ylr080wp, Emp47p, ERGIC-53 and VIP36 sequences revealed that the putative carbohydrate-recognition domains (CRD) of Ylr080wp and Emp47p lack some residues known to be critical for sugar binding (data not shown). Furthermore, no evidence has been obtained for a lectin function of Emp47p up to date, despite several attempts (Stephan Schröder-Köhne, personal communications). So far, the cellular functions of these two yeast lectin-like proteins has not been elucidated at all. However, the biochemical properties and cellular functions of the above-mentioned mammalian homologues of Emp47p and Ylr080wp are comparatively well described. The mannose lectin ERGIC-53 operates as a cargo receptor in transport of glycoproteins from ER to Golgi (Appenzeller et al., 1999) and the homologues lectin VIP36 may operate in quality control of glycosylation in the Golgi by recognising high-mannose glycans (Hara-Kuge et al., 1999). Both mammalian homologues operate at the ER-Golgi interface continuously cycling between

either ERGIC and ER (ERGIC-53) or cis-Golgi and ERGIC (VIP36) (Hauri et al., 2000; Füllenkrug et al., 1999). VIP36 localisation thus only partially overlaps with the one of ERGIC-53, being shifted to a more distal compartment of the mammalian secretory pathway (Füllenkrug et al., 1999). According to the immunofluorescence and subcellular fractionation data, obtained in this study, on the localisations of Ylr080wp and Emp47p in the yeast *S.cerevisiae* secretory pathway, Emp47p appears to be distributed more distally from the ER than Ylr080wp, especially in the late log phase of growth. In that sense the cis-Golgi localisation of Emp47p may correspond more to the one of its distant mammalian homologue VIP36p, whereas the localisation properties of Ylr080wp seem to be closer to the ones of ERGIC-53 as both proteins tend to accumulate in the close proximity to the ER membranes. The question of how far distally from the ER Ylr080wp can penetrate was not addressed in the present study. However, as evident from acquisition of N-linked glycans by VIP36 (Füllenkrug et al., 1999) and a modified version of Emp47p (Schröder et al., 1995), the medial Golgi membranes are easily accessible for at least those two proteins. It has been proposed already by Füllenkrug et al. (1999) that mammalian homologues VIP36 and ERGIC-53 might differ in their lectin specificity and thereby form a molecular team involved in quality control at the level of ERGIC-Golgi interface, similar to calnexin and calreticulin in the ER. The remarkably high score of homology in the structures of the yeast lectin-like proteins Emp47p and Ylr080wp makes it tempting to speculate that, if both proteins actually possess the carbo-hydrate-binding properties, they might utilise them in a team-like fashion by executing similar intracellular functions partially overlapping in time and location but also possibly with specialized functions at different growth stages. Especially the heavy induction of Ylr080wp at stationary phase points to a specialized role of the protein. They might, for instance, represent receptors for some glycoproteinacious cargo molecules or be involved in glycoproteins folding control in a fashion proposed for their distant homologues in mammals. Our data on the increase in the intracellular contents of Ylr080wp in response to the lack of fermentable substances was fully consistent with the observation of 4,8-fold increase in the level of mRNA coding for Ylr080wp during the diauxic shift from fermentation to respiration (DeRisi et al., 1997**)**. The question arises why the increased amounts of Ylr080wp are necessary for a cell switching the energy production from fermentation to mitochondrial-dependent respiration? At present there are only speculations, one of which is that the increased rate of oxidation in mitochondrion results in ROS (reactive oxygen species) generation (Sugiyama et al., 2000), which poses a general threat of hyperoxidation to any vital component of any molecular process. An increase in ROS concentration inflicts oxidative damages to proteins and other cellular components and may lead to improper

protein folding. In its major details, that situation is analogues to the heat-shock stress (Sugiyama et al., 2000). Many molecular shaperons assisting in the proper protein folding, oligomer assembly, traffic between organelles and selective protein degradation are reportedly induced under oxidative stress conditions (Godon et al., 1998). If the function of Ylr080wp is somehow related to the operation of the protein folding quality control system, it is conceivable that an increased level of intracellular oxidation induced by diauxic shift might necessitate the induction of Ylr080wp biosynthesis. Alternatively, oxidative stress triggered by diauxic shift might induce the necessity to repair the damaged cellular components, which would require an increased usage of the early secretory routes where Ylr080wp would be capable of rendering some help by assisting in, for instance, cargo packaging. Alternatively, very high levels of Ylr080wp in the ER-Golgi membranes at stationary phase could serve to preserve the structural integrity of the ER-membranes. This function of Ylr080wp may be essential for yeast in its natural environment outside the laboratory as the rates of recovery from stationary phase for cells knocked out for Ylr080wp were significantly diminished by incubation at 15°C. I did not, however, observe any synthetic effect of the absence of Emp47p on the recovery rates. Also, a knockout strain lacking Emp47p alone revived with wild-type rates (our unpresented observation) again arguing for separate functions at least in stationary phase cells.

Although Emp47p was not essential under any conditions tested in the current and previous studies and Ylr080wp was certainly essential for the efficient recovery from stationary phase at lower temperature, a putative lectin-function of these two homologues in glycoprotein-processing could manifest itself in malfunctions of glycosylation or changes in kinetics of transport of glycoproteins. According to previous studies of Schröder et al. (1995), Emp47p-deleted strains exhibited no defects in maturation of CPY, glycosylphosphatidylinositol-anchored protein Gas1p and invertase. The invertase secretion assay, described in this study, was performed for cells that reached stationary phase and were exposed to lower temperature as these conditions were found to compromise the cells lacking Ylr080wp most severely. Nevertheless, invertase was able to acquire Golgi-specific glycosylation and to reach the periplasmatic space in mutants lacking either Ylr080wp alone or both homologues. Therefore we assume that if, indeed, Ylr080wp and Emp47p share some similar function in the yeast secretory pathway, that function is likely to be backed up by some other protein factors because we failed to observe any defect in any tested secretion process at a variety of growth conditions for the cells lacking either one or both of these two proteins. In addition, the function of Ylr080wp and Emp47p could be restricted to a narrow subset of particular glycoproteins that we did not test in our assay.

5.2.2. The ER-Golgi subcellular distribution of Ylr080wp requires the di-lysine motif and is dynamically maintained by the functions of conventional antero- and retrograde transport machineries

To date it is a well-established fact that di-lysine (K(X)KXX or KKXX) signals confer the ER-Golgi localisation of the type I transmembrane proteins and KDEL signal is needed to maintain the ER-residency of luminal proteins (Teasdale and Jackson, 1996; Pelham, 1995). It has been clearly shown for Emp47p (Schröder et al., 1995) and ERGIC-53 (Schindler et al., 1993) that di-lysine motifs are necessary and sufficient to dictate the recycling of reporter-proteins from the post-ER compartments (the ERGIC or the cis-Golgi) to the ER. In particular, as is suggested by results of *in vivo* and *in vitro* binding studies, both di-lysine proteins exit the ER in COP II coat-mediated process (Schröder et al., 1995; Schindler et al., 1993) and return back to the ER via direct interaction of their di-lysine motifs with subunits of COP I protein complex (Schröder-Köhne et al., 1998; Kappeler et al., 1997). Therefore, in our opinion, Ylr080wp might also represent a useful additional candidate for studying cycling between the two major compartments of the yeast early secretory pathway.

5.2.2.1. Ylr080wp undergoes retrieval to the ER from the Golgi compartments

We succeeded in demonstrating that when the anterograde ER-to-Golgi transport of Ylr080wp is compromised by mutation in *SEC23* coding for the essential for the forward transport COP II coat component (Kaiser and Schekman, 1990) and protein biosynthesis is blocked by CHX, c-myc-Ylr080wp undergoes redistribution in retrograde direction from the post-ER compartments back to the ER. Moreover, the remarkable change in the profiles of subcellular distributions of Ylr080wp and Emp47p was essentially identical for both proteins in *sec23* mutant after 1 hour of incubation at non-permissive temperature. We assume therefore that Ylr080wp returns to the ER from the Golgi with kinetics similar to those of Emp47p at least in logarithmically growing cell culture when the amounts of both homologues were found to be nearly identical.

Anterograde transport involving cargo-selection and concentration with subsequent COP II coat-machinery-driven-vesicle-budding could potentially be a saturable process. Therefore, it is logical to expect that under conditions of overexpression of the specific cargo-molecules, the ER-export of it in a COP II-coated vesicles dependent manner might reach saturation due to exhaustion of the pool of some component determining the bandwidth of the anterograde transport of that cargo. Taking into account these considerations, we speculate that more than 50-fold increase in intracellular level of Ylr080wp under the stationary phase conditions (as compared to the Ylr080wp contents at the early logarithmic phase) might

saturate the transport capabilities of Ylr080wp by COP II coat-mediated pathway. That would lead to Ylr080wp accumulation in the membranes of the ER-compartment, which was determined by indirect immunofluorescence and subcellular fractionation studies, thus providing an explanation for the shift in Ylr080wp localisation from the Golgi more to the ER under conditions of growth arrest at stationary phase. Alternatively, the local molecular environment of Ylr080wp at stationary phase may change such that additional factors would appear that might contribute to the delay in Ylr080wp exit from the ER through establishing additional physical interactions with some unidentified localisation determinants in the structure of Ylr080wp. Thus, according to the latter scenario, it might be that although COP II-mediated transport of Ylr080wp is not saturated, the relationship between the rates of forward and backward transports at stationary phase is such that the point of equilibrium for Ylr080wp shifts from the cis-Golgi to the ER. We cannot say at present, which of the two alternatives will hold true.

It has been a well-documented fact with regard to the structure of ERGIC-53 that C-terminally located di-phenylalanine signal is required for the ER-exit of ERGIC-53. That requirement reflects probably the existence of a direct interaction between the di-phenylalanine signal and the COP II coat complex as is suggested by the peptide binding studies in vitro (Kappeler et al., 1997). Di-aromatic (FF) motif of the mammalian p24 protein family was also shown to bind specifically to COP II component Sec23A (Dominguez et al., 1998). On the same note, an interesting suggestion has been expressed by Hauri et al. (2000) that in yeast Emp47p the di-phenylalanine motif is replaced by two leucine implicating the other hydrophobic amino acids in mediating the efficient ER-exit. Ylr080wp is also possessed of the identically located di-leucine motif. As reported by Schröder et al. (1995), the substitution of the two carboxy-terminal leucine with alanines did not disrupt the Golgi-localisation of Emp47p, suggesting the insignificance of the di-leucine motif for the protein's exit from the ER. There is strong argument, however, for the importance of the C-terminally positioned LV-motif for the ER-to-Golgi anterograde export of the yeast protein Emp24p (Nakamura et al., 1998). As the LV-motif elicits an extreme structural similarity to the LL-sequence, it appears very interesting therefore to fully address the question of whether or not the anterograde transport of Emp47p-like proteins in yeast could also be facilitated by the presence of the two COOH-terminal leucine residues. However, the question of functional relevance of the di-leucine motif to the Ylr080wp export from the ER was left beyond the scope of the present study.

5.2.2.2. Role of COP I in the recycling of Ylr080wp

By analogy with yeast Emp47p and mammalian ERGIC-53, the presence of the di-lysine signal in the carboxy-terminus of Ylr080wp strongly suggested that the protein might undergo the coatomer complex-mediated retention in the Golgi-ER interface by continues recycling between these two early secretory pathway compartments. The first evidence of the specific coatomer binding to the yeast and mammalian ER-retention motifs was obtained by Cosson and Letourneur (1994) in studies in vitro. The yeast Emp47p (Schröder-Köhne et al., 1998) and the mammalian ERGIC-53 (Kappeller et al., 1997) were also shown to bind coatomer *in vitro*. Additionaly, mutations in different COP I subunits abolished the Emp47p Golgi-residency *in vivo* (Schröder et al., 1995). Therefore we assayed the localisation of c-myc-Ylr080wp in the *sec21-1* and *sec27* mutants deficient for γ-COP I and β´-COP I subunits of coatomer respectively. If the Golgi-ER-retention mechanism of di-lysine proteins relies exclusively on the continuous retrieval/recycling of the molecules in the Golgi-ER part of the secretory pathway, then mutations in COP I subunits should abrogate the localisation of the di-lysine proteins in the Golgi-ER interface and lead to their escape to a more distal part of the secretory pathway, which was the vacuole in case of Emp47p (Schröder et al., 1995). Accordingly, under *sec21-1* and *sec27* conditions, we found Ylr080wp localised to the first four sucrose gradient fractions of our subcellular fractionation assay. These fractions contained most cytosolic components as well as the contents of the vacuolar lumen. The presence of the protein in the Golgi was strongly reduced. Remarkably, the distribution of Emp47p in the same COP I mutants was found identical to the one of Ylr080wp. Thus, the subcellular fractionation data on Emp47p behaviour in COP I mutants was fully consistent with the earlier observations of Schröder et al. (1995) showing the vacuolar localisation of Emp47p in different coatomer mutants by indirect immunofluorescence analysis. I assume therefore that, similar to the case with Emp47p, the Golgi-ER localisation of Ylr080wp is also achieved by COP I-dependent retrieval. Retention in the Golgi-ER membranes via the function of the post-ER retrieval machinery is a saturable process as opposed to the non-saturable retention by means of true ER-retention signals like KKAA reported by Andersson et al. (1999). Although we did not analyse the saturability of the Golgi-ER-retention of Ylr080wp under conditions of Ylr080wp overexpression, our data implies that the di-lysine signal of Ylr080wp likely represents functional motif conferring the Golgi-ER localisation exclusively in a COP I coat-dependent manner as we found very little of the protein left in the ER-Golgi membranes in *sec21-1* mutant cells. A good proportion of the signal from c-myc-Ylr080wp was, however, found not only in the vacuolar fractions but also in the last fractions of *sec27*-mutant cells. In our opinion, it probably indicates an indirect block in the ER-to-

Golgi anterograde transport invoked by the lack of recycling of some unknown components (possibly cargo-specific receptors and t-SNAREs) necessary to promote the process of cargo-selection and packaging in the ER, under conditions of compromised Golgi to ER retrieval pathway.

5.2.2.3. Ylr080wp depends on its di-lysine motif for the retention in the Golgi-ER space of the yeast secretory pathway

The structures of Ylr080wp and Emp47p are characterised by the presence of two lysines at positions –3, -5, complying to the consensus of di-lysine signals which is either KKXX or KXKXX (Teasdale and Jackson, 1996). interference with the structure and position of K(X)KXX-motif of Ylr080wp generally lead to the escape of the mutated protein to the vacuole. The Golgi-localisation of Ylr080wp was, however, differentially affected by various mutations introduced into the di-lysine signal. In particular, we found that substitutions of either two or one of the critical lysines with glutamines abolished the Golgi localisation of Ylr080wp in logarithmically growing cells whereas the displacement of the lysines by two serine residues away from the COOH-terminus did not fully disrupt the Golgi-localisation of Ylr080wp. Such masking of the di-lysine signal by two serine residues abrogate Emp47p localisation (Schröder et al., 1995). There is evidence for the mammalian p23 protein that the C-terminal position of the di-lysine signal may not always be strictly required. The reason for such variability in importance of the position is, however, unclear.

5.2.3. Indications of Ylr080wp form a homo-oligomer *in vivo*.

An interesting observation we came across in the study of the c-myc-Ylr080wp “tail”-mutants was the remarkable dependence of the mislocalisation on the absence of endogenous Ylr080wp. The presence of wild-type Ylr080wp was clearly supportive to the Golgi-localisation of c-myc-tagged mutant versions of Ylr080wp. That is suggestive of the existence of intermolecular physical interactions between the different versions of Ylr080wp. We conjecture that Ylr080wp might oligomerise with itself producing homo-oligomers. ERGIC-53 was shown to exist as homodimer and homo-hexamer by forming intermolecular disulphide bridges involving two out of four cysteine residues situated in the luminal domain of the protein (Schweizer et al., 1988; Lahtinen et al., 1992). The dimers of ERGIC-53 were found to represent the minimal requirements for the transport out of the ER to occur. Neither Emp47p nor Ylr080wp appear to be linked into homo-oligomers by disulphide bonds, although they possess cysteines at conserved positions (Stephan Schröder-Köhne, personal communications and my data not shown). However, α-helical coiled coils are capable of

assembling into helix bundles often mediating homo-oligomeric or hetero-oligomeric associations of polypeptides (Lupas, 1996). The coiled coils prediction algorithm (Lupas, 1991) applied to the amino acid sequences of both Ylr080wp and Emp47p uncovered similarly located regions in the luminal part of the respective polypeptide chains with a high potential for coiled coils formation (Fig. 22B). Thus, as an alternative to disulphide-bonding, Ylr080wp and Emp47p may oligomerize via formation of intermolecular α-helical coiled coils.

Preliminary gel-filtration data indicate the presence of two high molecular weight complexes of about 700 kDa and 120-140 kDa each. Furthermore and more importantly, we found no signal from c-myc-Ylr080wp in a molecular range of 50 kDa corresponding to a single monomer. Although the results yielded by analytical gel-filtration analysis apparently corroborate the idea of Ylr080wp forming oligomeric molecular associates they, nevertheless, have to be treated with caution, because molecular weight estimation by gel-filtration is notorious for giving inaccurate results due to the strong dependence of the protein's migration properties on its shape. Further experiments therefore are needed to address the oligomerization status of Ylr080wp and Emp47p.

6. Summary

Retrograde membrane-traffic from the Golgi complex to the endoplasmic reticulum (ER) is driven by COP I coated vesicles. The coat of those vesicles is formed by coatomer, a complex of seven protein subunits, and the small GTPase Arf1/2p. Additional factors required for the retrograde transport between the Golgi complex and the ER in yeast are the SNARE proteins Ufe1p and Sec22p and the ER protein-complex formed by Sec20p and Tip20p. However, most likely the list of factors involved is by far not complete considering the diverse nature of transported cargo and the need to coordinate and regulate their transport. Therefore I initiated a genetic screen in search for new factors participating in the localization of the non-essential Golgi-transmembrane protein Emp47. Emp47p contains a di-lysine signal at its cytosolic carboxy-terminus and undergoes continuous transport between the Golgi and ER dependent on the machinery described above. Mutations in the COP I coated vesicle machinery lead to the mislocalization of Emp47p to the vacuole where it is rapidly degraded by vacuolar proteases. In my work I used chemical mutagenesis to generate a randomly mutagenized yeast cell population in which I was looking for temperature sensitive cells with reduced levels of Emp47p. In informative cases, I expected this phenotype to stem from mutations affecting the sorting capabilities of the early secretory compartments. One mutant that displayed a reduction of Emp47p due to a missorting of the protein to the vacuole proved to be defective in *CYS3*, the gene coding for cystathionine-γ-lyase (Cys3p). Cys3p is the terminal enzyme of the transsulfuration pathway, which is responsible for the de novo synthesis of cysteine. Evidence is presented for the conclusion that it is the inability of *cys3* mutant cells to produce cysteine, the primary source of cytosolic reducing power in yeast, that contributes structurally and functionally to the active centers of dithiol- and monothiol-proteins as well as to short tripeptide GSH, which interferes with the steady state localization of Emp47p. The biosynthetic transport of carboxypeptidase Y to the vacuole or of GPI-anchored protein Gas1p from the ER to the Golgi on the other hand remained unaffected, as was secretion to the periplasmatic space. I furthermore provide evidence for the general importance of glutathione in the protection against heat- and oxidative-stress and I identified a particular phospholipid, CDP-diacylglycerol, as a GSH-dependent target of the temperature adaptation process defective in *cys3-2Δ* mutants.

In the present study I also characterized the intracellular localization and the recycling properties for the hitherto uncharacterized gene-product of *YLR080W*, a non-essential type I transmembrane protein with 45% sequence identity to Emp47p. Ylr080wp and Emp47p share sequence homology with a class of intracellular lectins defined by the mammalian ERGIC-53

and VIP36. Evidence for a role of ERGIC-53 in the intracellular transport of some gylcoproteins has been collected, but the exact function of this class of proteins in general and Emp47p in particular is far from clear. Cell biological investigation of Ylr080wp and elucidation of its deletion phenotypes was therefore important. I could show that the consensus di-lysine-based ER-retrieval signals at the C-terminus of Ylr080wp was functional and restricted the subcellular steady state distribution of the protein to the ER-Golgi interface. At the early logarithmic growth-phase, localization of Ylr080wp was indistinguishable from that of the Golgi-protein Emp47p. Towards stationary phase however, and in marked contrast to the behavior of Emp47p, expression of Ylr080wp was at least 50-fold enhanced. At the same time the protein redistributed from the Golgi to the ER. That drastic accumulation of Ylr080wp suggested the importance of the protein's function at stationary phase. Indeed, I could show that the presence of Ylr080wp, with no contribution from Emp47p, was essential for the recovery of yeast cells from stationary phase at 15°C. Thus, the two homologues apparently have at least partially diverging functions. However, I also found that *YLR080W* and *EMP47* double deletion mutant were fully viable under a variety of growth-conditions and did not display any striking secretory phenotypes.

Similar to Emp47p, the localisation of Ylr080wp was dependent on the di-lysine motif and on coatomer. Mutations of the di-lysine signal and mutations in genes coding for coatomer-subunits both resulted in mistargeting of Ylr080wp to the vacuole. Interestingly, the presence of wild type Ylr080wp restored Golgi-localisation of Ylr080wp with a mutated di-lysine signal. This may be due to homooligomerisation for which I obtained suggestive evidence by analytical gel-filtration.

Blocking protein-exit from the ER by means of a conditional mutation in the gene coding for the COP II component Sec23p and simultaneously blocking protein synthesis lead to the redistribution of Ylr080wp to the ER, providing direct evidence for recycling from the Golgi to the ER. Thus, the Golgi-ER distribution of Ylr080wp is dynamically maintained in a growth phase-dependent manner by retrieval of the protein from post-ER compartments back to the ER in a manner dependent on the di-lysine signal and COP I coat components.

7. References

Andersson H, Kappeler F, Hauri HP. Protein targeting to endoplasmic reticulum by dilysine signals involves direct retention in addition to retrieval. J Biol Chem. 1999 May 21;274(21):15080-4.
Anderson ME, Meister A. Transport and direct utilization of gamma-glutamylcyst(e)ine for glutathione synthesis. Proc Natl Acad Sci U S A. 1983 Feb;80(3):707-11.
Appel RD, Bairoch A, Hochstrasser DF. A new generation of information retrieval tools for biologists: the example of the ExPASy WWW server. Trends Biochem Sci. 1994 Jun;19(6):258-60.
Appenzeller C, Andersson H, Kappeler F, Hauri HP. The lectin ERGIC-53 is a cargo transport receptor for glycoproteins. Nature Cell Biol. 1999. 1:330-334.
Arar C, Carpentier V, Le Caer JP, Monsigny M, Legrand A, Roche AC. ERGIC-53, a membrane protein of the endoplasmic reticulum-Golgi intermediate compartment, is identical to MR60, an intracellular mannose-specific lectin of myelomonocytic cells. J Biol Chem. 1995 Feb 24;270(8):3551-3.
Aridor M, Weissman J, Bannykh S, Nuoffer C, Balch WE. Cargo selection by the COPII budding machinery during export from the ER. J Cell Biol. 1998 Apr 6;141(1):61-70.
Aslund F, Berndt KD, Holmgren A. Redox potentials of glutaredoxins and other thiol-disulphide oxidoreductases of the thioredoxin superfamily determined by direct protein-protein redox equilibria. J Biol Chem. 1997 Dec 5;272(49):30780-6.
Bader M, Winther JR, Bardwell JC. Protein oxidation: prime suspect found 'not guilty'. Nat Cell Biol. 1999 Jul;1(3):E57-8.
Balch WE, McCaffery JM, Plutner H, Farquhar MG. Vesicular stomatitis virus glycoprotein is sorted and concentrated during export from the endoplasmic reticulum. Cell. 1994 Mar 11;76(5):841-52.
Barlowe C. Coupled ER to Golgi transport reconstituted with purified cytosolic proteins. J Cell Biol. 1997 Dec 1;139(5):1097-108.
Barlowe C, Orci L, Yeung T, Hosobuchi M, Hamamoto S, Salama N, Rexach MF, Ravazzola M, Amherdt M, Schekman R. COPII: a membrane coat formed by Sec proteins that drive vesicle budding from the endoplasmic reticulum. Cell. 1994 Jun 17;77(6):895-907.
Barlowe C, Schekman R. SEC12 encodes a guanine-nucleotide-exchange factor essential for transport vesicle budding from the ER. Nature. 1993 Sep 23;365(6444):347-9.
Baroni M, Livian S, Martegani E, Alberghina L. olecular cloning and regulation of the expression of the MET2 gene of Saccharomyces cerevisiae. Gene. 1986;46(1):71-8.
Barton AB, Kaback DB, Clark MW, Keng T, Ouellette BF, Storms RK, Zeng B, Zhong W, Fortin N, Delaney S, et al. Physical localization of yeast CYS3, a gene whose product resembles the rat gamma-cystathionase and Escherichia coli cystathionine gamma-synthase enzymes. Yeast. 1993 Apr;9(4):363-9.
Becker GW, Lester RL. Biosynthesis of phosphoinositol-containing sphingolipids from phosphatidylinositol by a membrane preparation from Saccharomyces cerevisiae. J Bacteriol. 1980 Jun;142(3):747-54.
Belden WJ, Barlowe C. Erv25p, a component of COPII-coated vesicles, forms a complex with Emp24p that is required for efficient endoplasmic reticulum to Golgi transport. J Biol Chem. 1996 Oct 25;271(43):26939-46.
Birnboim HC, Doly J. A rapid alkaline extraction procedure for screening recombinant plasmid DNA. Nucleic Acids Res. 1979 Nov 24;7(6):1513-23.
Boehm J, Letourneur F, Ballensiefen W, Ossipov D, Demolliere C, Schmitt HD. Sec12p requires Rer1p for sorting to coatomer (COPI)-coated vesicles and retrieval to the ER. J Cell Sci. 1997 Apr;110 (Pt 8):991-1003.

Bonfanti L, Mironov AA, Martinez-Menarguez JA, Martella O, Fusella A, Baldassarre M, Buccione R, Geuze HJ, Mironov AA, Luini A. Procollagen traverses the Golgi stack without leaving the lumen of cisternae: evidence for cisternal maturation. Cell. 1998 Dec 23;95(7):993-1003.

Bourbouloux A, Shahi P, Chakladar A, Delrot S, Bachhawat AK. Hgt1p, a high affinity glutathione transporter from the yeast Saccharomyces cerevisiae. J Biol Chem. 2000 May 5;275(18):13259-65.

Bradford MM. A rapid and sensitive method for the quantitation of microgram quantities of protein utilizing the principle of protein-dye binding. Anal Biochem. 1976 May 7;72:248-54.

Bremser M, Nickel W, Schweikert M, Ravazzola M, Amherdt M, Hughes CA, Sollner TH, Rothman JE, Wieland FT. Coupling of coat assembly and vesicle budding to packaging of putative cargo receptors. Cell. 1999 Feb 19;96(4):495-506.

Burnette WN. "Western blotting": electrophoretic transfer of proteins from sodium dodecyl sulphate--polyacrylamide gels to unmodified nitrocellulose and radiographic detection with antibody and radioiodinated protein A. Anal Biochem. 1981 Apr;112(2):195-203.

Cantoni GL. 1977. S-adenosylmethionine: present status and future perspectives, p. 557-577. In F. salvatore, E. Borek, V. Zappa, H.G. Williams-Ashman, and F. Schlenk (ed.), The biochemistry of adenosylmethionine. Columbia University Press, New York, N.Y.

Carman GM, Henry SA. Phospholipid biosynthesis in the yeast Saccharomyces cerevisiae and interrelationship with other metabolic processes. Prog Lipid Res. 1999 Sep-Nov;38(5-6):361-99. Review.

Carmel-Harel O, Storz G. Roles of the glutathione- and thioredoxin-dependent reduction systems in the escherichia coli and saccharomyces cerevisiae responses to oxidative stress. Annu Rev Microbiol. 2000;54:439-61.

Chaudhuri B, Ingavale S, Bachhawat AK. apd1+, a gene required for red pigment formation in ade6 mutants of Schizosaccharomyces pombe, encodes an enzyme required for glutathione biosynthesis: a role for glutathione and a glutathione-conjugate pump. Genetics. 1997 Jan;145(1):75-83.

Cherest H, Eichler F, Robichon-Szulmajster H. Genetic and regulatory aspects of methionine biosynthesis in Saccharomyces cerevisiae. J Bacteriol. 1969 Jan;97(1):328-36.

Cherest H, Nguyen NT, Surdin-Kerjan Y. Transcriptional regulation of the MET3 gene of Saccharomyces cerevisiae. Gene. 1985;34(2-3):269-81.

Cherest H, Surdin-Kerjan Y. Genetic analysis of a new mutation conferring cysteine auxotrophy in Saccharomyces cerevisiae: updating of the sulfur metabolism pathway. Genetics. 1992 Jan;130(1):51-8.

Cherest H, Surdin-Kerjan Y, Antoniewski J, de Robichon-Szulmajster h. Effects of regulatory mutations upon methionine biosynthesis in Saccharomyces cerevisiae: loci eth2-eth3-eth10. J Bacteriol. 1973 Sep;115(3):1084-93.

Cherest H, Thomas D, Surdin-Kerjan Y. Cysteine biosynthesis in Saccharomyces cerevisiae occurs through the transsulfuration pathway which has been built up by enzyme recruitment. J Bacteriol. 1993 Sep;175(17):5366-74.

Coligan JE, Dunn BM, Ploegh HL, Speicher DW, Wingfield PT (ed.) (1995) Current protocols in Protein Science, vol. 2. Wiley&Sons, Inc.

Cosson P, Demolliere C, Hennecke S, Duden R, Letourneur F. Delta- and zeta-COP, two coatomer subunits homologous to clathrin-associated proteins, are involved in ER retrieval. EMBO J. 1996 Apr 15;15(8):1792-8.

Cosson P, Letourneur F. Coatomer (COPI)-coated vesicles: role in intracellular transport and protein sorting. Curr Opin Cell Biol. 1997 Aug;9(4):484-7. Review.

Cosson P, Schroder-Kohne S, Sweet DS, Demolliere C, Hennecke S, Frigerio G, Letourneur F. The Sec20/Tip20p complex is involved in ER retrieval of dilysine-tagged proteins. Eur J Cell Biol. 1997 Jun;73(2):93-7.

Csaikl U, Csaikl F. Molecular cloning and characterization of the MET6 gene of Saccharomyces cerevisiae. Gene. 1986;46(2-3):207-14.
Cukierman E, Huber I, Rotman M, Cassel D. The ARF1 GTPase-activating protein: zinc finger motif and Golgi complex localization. Science. 1995 Dec 22;270(5244):1999-2002.
Cuozzo JW, Kaiser CA. Competition between glutathione and protein thiols for disulphide-bond formation. Nat Cell Biol. 1999 Jul;1(3):130-5.
Dascher C, Ossig R, Gallwitz D, Schmitt HD. Identification and structure of four yeast genes (SLY) that are able to suppress the functional loss of YPT1, a member of the RAS superfamily. Mol Cell Biol. 1991 Feb;11(2):872-85.
Daum G, Lees ND, Bard M, Dickson R. Biochemistry, cell biology and molecular biology of lipids of Saccharomyces cerevisiae. Yeast. 1998 Dec;14(16):1471-510. Review.
DeRisi JL, Iyer VR, Brown PO. Exploring the metabolic and genetic control of gene expression on a genomic scale. Science (1997) 278, 680-686.
Dickso RC. Sphingolipid functions in Saccharomyces cerevisiae: comparison to mammals. Annual Review of Biochemistry (1998) 67:27-48.
Dickson RC, Nagiec EE, Skrzypek M, Tillman P, Wells GB, Lester RL. Sphingolipids are potential heat stress signals in Saccharomyces. J Biol Chem. 1997 Nov 28;272(48):30196-200.
Distel B, Al EJ, Tabak HF, Jones EW. Synthesis and maturation of the yeast vacuolar enzymes carboxypeptidase Y and aminopeptidase I. Biochim Biophys Acta. 1983 Oct 13;741(1):128-35.
Dogic D, de Chassey B, Pick E, Cassel D, Lefkir Y, Hennecke S, Cosson P, Letourneur F. The ADP-ribosylation factor GTPase-activating protein Glo3p is involved in ER retrieval. Eur J Cell Biol. 1999 May;78(5):305-10.
Dominguez A, Ferminan E, Sanchez M, Gonzalez FJ, Perez-Campo FM, Garcia S, Herrero AB, San Vicente A, Cabello J, Prado M, Iglesias FJ, Choupina A, Burguillo FJ, Fernandez-Lago L, Lopez MC. Non-conventional yeasts as hosts for heterologous protein production. Int Microbiol. 1998 Jun;1(2):131-42.
Draculic T, Dawes IW, Grant CM. A single glutaredoxin or thioredoxin gene is essential for viability in the yeast Saccharomyces cerevisiae. Mol Microbiol. 2000 Jun;36(5):1167-74.
Duden R, Griffiths G, Frank R, Argos P, Kreis TE. Beta-COP, a 110 kd protein associated with non-clathrin-coated vesicles and the Golgi complex, shows homology to beta-adaptin. Cell. 1991 Feb 8;64(3):649-65.
Duden R, Hosobuchi M, Hamamoto S, Winey M, Byers B, Schekman R. Yeast beta- and beta'-coat proteins (COP). Two coatomer subunits essential for endoplasmic reticulum-to-Golgi protein traffic. J Biol Chem. 1994 Sep 30;269(39):24486-95.
Duden R, Kajikawa L, Wuestehube L, Schekman R. epsilon-COP is a structural component of coatomer that functions to stabilize alpha-COP. EMBO J. 1998 Feb 16;17(4):985-95.
Dunphy WG, Rothman JE. Compartmental organization of the Golgi stack. Cell. 1985 Aug;42(1):13-21. Review.
Düring-Olsen L, Regenberg B, Gjermansen C, Morten C. Kielland-Brandt, Hansen J. Cysteine uptake by Saccharomyces cerevisiae is accomplished by multiple permeases. Curr Genet 35 (1999) 6, 609-617
Egner R, Thumm M, Straub M, Simeon A, Schuller HJ, Wolf DH. Tracing intracellular proteolytic pathways. Proteolysis of fatty acid synthase and other cytoplasmic proteins in the yeast Saccharomyces cerevisiae. J Biol Chem. 1993 Dec 25;268(36):27269-76.
Elrod-Erickson MJ, Kaiser CA. Genes that control the fidelity of endoplasmic reticulum to Golgi transport identified as suppressors of vesicle budding mutations. Mol Biol Cell. 1996 Jul;7(7):1043-58.
Elskens MT, Jaspers CJ, Penninckx MJ. Glutathione as an endogenous sulphur source in the yeast Saccharomyces cerevisiae. J Gen Microbiol. 1991 Mar;137 (Pt 3):637-44.

Esmon B, Novick P, Schekman R. Compartmentalized assembly of oligosaccharides on exported glycoproteins in yeast. Cell. 1981 Aug;25(2):451-60.
Eugster A, Frigerio G, Dale M, Duden R. COP I domains required for coatomer integrity, and novel interactions with ARF and ARF-GAP. EMBO J. 2000 Aug 1;19(15):3905-17. PMID: 10921873
Farquhar MG. Progress in unraveling pathways of Golgi traffic. Annu Rev Cell Biol. 1985;1:447-88. Review.
Fiedler K, Simons K. A putative novel class of animal lectins in the secretory pathway homologous to leguminous lectins. Cell. 1994 Jun 3;77(5):625-6.
Fiedler K, Simons K. A putative new class of animal lectins in the secretory pathway homologous to leguminose lectins. Cell. 1995. 81:309-312.
Fiedler K, Veit M, Stamnes MA, Rothman JE. Bimodal interaction of coatomer with the p24 family of putative cargo receptors. Science. 1996 Sep 6;273(5280):1396-9.
Fullekrug J, Scheiffele P, Simons K. VIP36 localisation to the early secretory pathway. J Cell Sci. 1999 Sep;112 (Pt 17):2813-21.
Garrett MD, Zahner JE, Cheney CM, Novick PJ. GDI1 encodes a GDP dissociation inhibitor that plays an essential role in the yeast secretory pathway. EMBO J. 1994 Apr 1;13(7):1718-28.
Gaynor EC, Graham TR, Emr SD. COPI in ER/Golgi and intra-Golgi transport: do yeast COPI mutants point the way? Biochim Biophys Acta. 1998 Aug 14;1404(1-2):33-51. Review.
Gimeno RE, Espenshade P, Kaiser CA. SED4 encodes a yeast endoplasmic reticulum protein that binds Sec16p and participates in vesicle formation. J Cell Biol. 1995 Oct;131(2):325-38.
Girod A, Storrie B, Simpson JC, Johannes L, Goud B, Roberts LM, Lord JM, Nilsson T, Pepperkok R. Evidence for a COP-I-independent transport route from the Golgi complex to the endoplasmic reticulum. Nat Cell Biol. 1999 Nov;1(7):423-430.
Glick BS, Elston T, Oster G. A cisternal maturation mechanism can explain the asymmetry of the Golgi stack. FEBS Lett. 1997 Sep 8;414(2):177-81. Review.
Glick BS, Malhotra V. The curious status of the Golgi apparatus. Cell. 1998 Dec 23;95(7):883-9.
Godon C, Lagniel G, Lee J, Buhler JM, Kieffer S, Perrot M, Boucherie H, Toledano MB, Labarre J. The H2O2 stimulon in Saccharomyces cerevisiae. J Biol Chem. 1998 Aug 28;273(35):22480-9.
Goldberg J. Structural and functional analysis of the ARF1-ARFGAP complex reveals a role for coatomer in GTP hydrolysis. Cell. 1999 Mar 19;96(6):893-902.
Golgi C. Arch. Ital. Biol. (1898) 30, 60-71
Grant CM, MacIver FH, Dawes IW. Glutathione is an essential metabolite required for resistance to oxidative stress in the yeast Saccharomyces cerevisiae. Curr Genet 29 (1996) 6, 511-515
Grant CM, MacIver FH, Dawes IW. Glutathione synthetase is dispensable for growth under both normal and oxidative stress conditions in the yeast Saccharomyces cerevisiae due to an accumulation of the dipeptide gamma-glutamylcysteine. Mol Biol Cell 8 (1997), 1699-707.
Greenberg JT, Demple B. Glutathione in Escherichia coli is dispensable for resistance to H2O2 and gamma radiation. J Bacteriol. 1986 Nov;168(2):1026-9.
Grossmann MK, Zimmermann FK. The structural genes of internal invertases in Saccharomyces cerevisiae. Mol Gen Genet. 1979 Sep;175(2):223-9.
Hansen J, Johannesen PF. Cysteine is essential for transcriptional regulation of the sulfur assimilation genes in Saccharomyces cerevisiae. Mol Gen Genet. 2000 Apr;263(3):535-42.
Hansen J, Muldbjerg M, Cherest H, Surdin-Kerjan Y. Siroheme biosynthesis in Saccharomyces cerevisiae requires the products of both the MET1 and MET8 genes. FEBS Lett. 1997 Jan 13;401(1):20-4.

Hansen RJ, Switzer RL, Hinze H, Holzer H. Effects of glucose and nitrogen source on the levels of proteinases, peptidases, and proteinase inhibitors in yeast. Biochim Biophys Acta. 1977 Jan 24;496(1):103-14.
Hara-Kuge S, Ohkura T, Seko A, Yamashita K. Vesicular-integral membrane protein, VIP36, recognizes high-mannose type glycans containing alpha1-->2 mannosyl residues in MDCK cells. Glycobiology. 1999 Aug;9(8):833-9.
Harrison-Lavoie KJ, Lewis VA, Hynes GM, Collison KS, Nutland E, Willison KR. A 102 kDa subunit of a Golgi-associated particle has homology to beta subunits of trimeric G proteins. EMBO J. 1993 Jul;12(7):2847-53.
Harter C, Wieland F. The secretory pathway: mechanisms of protein sorting and transport. Biochim Biophys Acta. 1996 Jun 10;1286(2):75-93. Review.
Hartig A, Ruis H. Nucleotide sequence of the Saccharomyces cerevisiae CTT1 gene and deduced amino-acid sequence of yeast catalase T. Eur J Biochem. 1986 Nov 3;160(3):487-90.
Hauri HP, Kappeler F, Andersson H, Appenzeller C. ERGIC-53 and traffic in the secretory pathway. J Cell Sci. 2000 Feb;113 (Pt 4):587-96. Review.
Henderson RJ, Tocher DR (1992) Thin layer chromatography. In RJ Hamilton, S Hamilton (ed.), Lipid analysis. A practical approach. Oxford University press, Oxford.
Hicke L, Schekman R. Yeast Sec23p acts in the cytoplasm to promote protein transport from the endoplasmic reticulum to the Golgi complex in vivo and in vitro. Embo Journal 8, 1677-84 (1989).
Holmgren A. Hydrogen donor system for Escherichia coli ribonucleoside-diphosphate reductase dependent upon glutathione. Proc Natl Acad Sci U S A. 1976 Jul;73(7):2275-9.
Hosobuchi M, Kreis T, Schekman R. SEC21 is a gene required for ER to Golgi protein transport that encodes a subunit of a yeast coatomer. Nature. 1992 Dec 10;360(6404):603-5.
Hudson RT, Draper RK. Interaction of coatomer with aminoglycoside antibiotics: evidence that coatomer has at least two dilysine binding sites. Mol Biol Cell. 1997 Oct;8(10):1901-10.
Itin C, Roche AC, Monsigny M, Hauri HP. ERGIC-53 Is a Functional Mannose-Selective And Calcium-Dependant Human Homologue of Leguminous Lectins. Mol. Biol. Cell. (1996) 7:483-493.
Itin C, Schindler R, Hauri HP. Targeting of protein ERGIC-53 to the ER/ERGIC/cis-Golgi recycling pathway. J Cell Biol. 1995 Oct;131(1):57-67.
Ito H, Fukuda Y, Murata K, Kimura A. Transformation of intact yeast cells treated with alkali cations. J Bacteriol. 1983 Jan;153(1):163-8.
Izawa S, Inoue Y, Kimura A. Oxidative stress response in yeast: effect of glutathione on adaptation to hydrogen peroxide stress in Saccharomyces cerevisiae. FEBS Lett. 1995 Jul 10;368(1):73-6.
Jamieson DJ. Oxidative stress responses of the yeast Saccharomyces cerevisiae. Yeast. 1998 Dec;14(16):1511-27. Review.
Jones EW. The synthesis and function of proteases in Saccharomyces: genetic approaches. Annu Rev Genet. 1984;18:233-70. Review.
Jones EW, Fink GR. 1982. Regulation of amino acid and nucleotide biosynthesis in yeast, p. 181-299. In J.N. Strathern, E. W. Jones and J.R. Broach (ed.), The molecular biology of the yeast Saccharomyces cerevisiae metabolism and gene expression. Cold Spring Harbor laboratory. Cold Spring Harbor, N.Y.
Jones DT, Taylor WR. Towards structural genomics for transmembrane proteins. Biochem Soc Trans. 1998 Aug;26(3):429-38. Review.
Jones DT, Taylor WR, Thornton JM. A model recognition approach to the prediction of all-helical membrane protein structure and topology. Biochemistry. 1994 Mar 15;33(10):3038-49.
Kaiser CA, Schekman R. Distinct sets of SEC genes govern transport vesicle formation and fusion early in the secretory pathway. Cell. 1990 May 18;61(4):723-33.

Kappeler F, Klopfenstein DR, Foguet M, Paccaud JP, Hauri HP.
The recycling of ERGIC-53 in the early secretory pathway. ERGIC-53 carries a cytosolic endoplasmic reticulum-exit determinant interacting with COPII. J Biol Chem. 1997 Dec 12;272(50):31801-8.
Kerjan P, Cherest H, Surdin-Kerjan Y. Nucleotide sequence of the Saccharomyces cerevisiae MET25 gene. Nucleic Acids Res. 1986 Oct 24;14(20):7861-71.
Kistler M, Maier K, Eckardt-Schupp F. Genetic and biochemical analysis of glutathione-deficient mutants of Saccharomyces cerevisiae. Mutagenesis. 1990 Jan;5(1):39-44.
Klenow H, Henningsen I. Selective elimination of the exonuclease activity of the deoxyribonucleic acid polymerase from Escherichia coli B by limited proteolysis. Proc Natl Acad Sci U S A. 1970 Jan;65(1):168-75.
Klionsky DJ, Herman PK, Emr SD. The fungal vacuole: composition, function, and biogenesis. Microbiol Rev. 1990 Sep;54(3):266-92. Review.
Klumperman J, Schweizer A, Clausen H, Tang BL, Hong W, Oorschot V, Hauri HP. The recycling pathway of protein ERGIC-53 and dynamics of the ER-Golgi intermediate compartment. J Cell Sci. 1998 Nov;111 (Pt 22):3411-25.
Korch C, Mountain HA, Bystrom AS. Cloning, nucleotide sequence, and regulation of MET14, the gene encoding the APS kinase of Saccharomyces cerevisiae. Mol Gen Genet. 1991 Sep;229(1):96-108.
Ktistakis NT, Brown HA, Waters MG, Sternweis PC, Roth MG. Evidence that phospholipase D mediates ADP ribosylation factor-dependent formation of Golgi coated vesicles. J Cell Biol. 1996 Jul;134(2):295-306.
Kuehn MJ, Herrmann JM, Schekman R. COPII-cargo interactions direct protein sorting into ER-derived transport vesicles. Nature. 1998 Jan 8;391(6663):187-90.
Kuehn MJ, Schekman R. COPII and secretory cargo capture into transport vesicles. Curr Opin Cell Biol. 1997 Aug;9(4):477-83. Review.
Kuehn MJ, Schekman R, Ljungdahl PO. Amino acid permeases require COPII components and the ER resident membrane protein Shr3p for packaging into transport vesicles in vitro. J Cell Biol. 1996 Nov;135(3):585-95.
Lahtinen U, Dahllof B, Saraste J. Characterization of a 58 kDa cis-Golgi protein in pancreatic exocrine cells. J Cell Sci. 1992 Oct;103 (Pt 2):321-33.
Lahtinen U, Hellman U, Wernstedt C, Saraste J, Pettersson RF. Molecular cloning and expression of a 58-kDa cis-Golgi and intermediate compartment protein. J Biol Chem. 1996 Feb 23;271(8):4031-7.
Lahtinen U, Svensson K, Pettersson RF. Mapping of structural determinants for the oligomerization of p58, a lectin-like protein of the intermediate compartment and cis-Golgi. Eur J Biochem. 1999 Mar;260(2):392-7.
Langin T, Faugeron G, Goyon C, Nicolas A, Rossignol JL. The MET2 gene of Saccharomyces cerevisiae: molecular cloning and nucleotide sequence. Gene. 1986;49(3):283-93.
Lavoie C, Paiement J, Dominguez M, Roy L, Dahan S, Gushue JN, Bergeron JJ. Roles for alpha(2)p24 and COPI in endoplasmic reticulum cargo exit site formation. J Cell Biol. 1999 Jul 26;146(2):285-99.
Lawrence CW. Classical mutagenesis techniques. Methods Enzymol. 1991;194:273-81.
Lee SM, Park JW. Thermosensitive phenotype of yeast mutant lacking thioredoxin peroxidase. Arch Biochem Biophys. 1998 Nov 1;359(1):99-106.
Lee J, Spector D, Godon C, Labarre J, Toledano MB. A new antioxidant with alkyl hydroperoxide defense properties in yeast. J Biol Chem. 1999 Feb 19;274(8):4537-44.
Letourneur F, Gaynor EC, Hennecke S, Demolliere C, Duden R, Emr SD, Riezman H, Cosson P. Coatomer is essential for retrieval of dilysine-tagged proteins to the endoplasmic reticulum. Cell. 1994 Dec 30;79(7):1199-207.

Lewis MJ, Pelham HR. SNARE-mediated retrograde traffic from the Golgi complex to the endoplasmic reticulum. Cell. 1996 Apr 19;85(2):205-15.
Lewis MJ, Rayner JC, Pelham HR. A novel SNARE complex implicated in vesicle fusion with the endoplasmic reticulum. EMBO J. 1997 Jun 2;16(11):3017-24.
Li ZS, Lu YP, Zhen RG, Szczypka M, Thiele DJ, Rea PA. A new pathway for vacuolar cadmium sequestration in Saccharomyces cerevisiae: YCF1-catalyzed transport of bis(glutathionato)cadmium. Proc Natl Acad Sci U S A. 1997 Jan 7;94(1):42-7.
Li ZS, Szczypka M, Lu YP, Thiele DJ, Rea PA. The yeast cadmium factor protein (YCF1) is a vacuolar glutathione S-conjugate pump. J Biol Chem. 1996 Mar 15;271(11):6509-17.
Ligr M, Madeo F, Frohlich E, Hilt W, Frohlich KU, Wolf DH. Mammalian Bax triggers apoptotic changes in yeast. FEBS Lett. 1998 Oct 30;438(1-2):61-5.
Lowe M, Kreis TE. In vitro assembly and disassembly of coatomer. J Biol Chem. 1995 Dec 29;270(52):31364-71.
Lupas A. Coiled coils: new structures and new functions. Trends Biochem Sci. 1996 Oct;21(10):375-82. Review.
Lupas A, Van Dyke M, Stock J. Predicting coiled coils from protein sequences. Science. 1991 May 24;252(5010):1162-4.
Lyons S, Nelson N. An immunological method for detecting gene expression in yeast colonies. Proc Natl Acad Sci U S A. 1984 Dec;81(23):7426-30.
Madeo F, Frohlich E, Ligr M, Grey M, Sigrist SJ, Wolf DH, Frohlich KU. Oxygen stress: a regulator of apoptosis in yeast. J Cell Biol. 1999 May 17;145(4):757-67.
Madeo F, Schlauer J, Frohlich KU. Identification of the regions of porcine VCP preventing its function in Saccharomyces cerevisiae. Gene. 1997 Dec 19;204(1-2):145-51.
Marchesini N, Santander V, Machado-Domenech E. Diacylglycerol pyrophosphate: a novel metabolite in the Trypanosoma cruzi phosphatidic acid metabolism. FEBS Lett. 1998 Oct 9;436(3):377-81.
Matiach A, Schröder-Köhne S. 1997. Emp47p as a marker to screen for Golgi to ER transport mutants. Meeting-Abstract. Workshop on Membrane Fusion. Istituto Juan March de Estudios e Investigaciones. Band 67.
McNew JA, Sogaard M, Lampen NM, Machida S, Ye RR, Lacomis L, Tempst P, Rothman JE, Sollner TH. Ykt6p, a prenylated SNARE essential for endoplasmic reticulum-Golgi transport. J Biol Chem. 1997 Jul 11;272(28):17776-83.
Meister A. Glutathione metabolism and its selective modification. J. Biol. Chem. 1988 263: 17205-17208.
Meister A, Anderson ME. Glutathione. Annu Rev Biochem. 1983;52:711-60. Review.
Melkonian M, Becker B, Becker D. Scale formation in algae. J Electron Microsc Tech. 1991 Feb;17(2):165-78. Review.
Mellman I, Simons K. The Golgi complex: in vitro veritas? Cell. 1992 Mar 6;68(5):829-40. Review.
Miranda-Vizuete A, Damdimopoulos AE, Gustafsson JÅ, Spyrou G. Cloning, Expression, and Characterization of a Novel Escherichia coli Thioredoxin. J. Biol. Chem. 1997 272: 30841-30847.
Mizuno M, Singer SJ. A soluble secretory protein is first concentrated in the endoplasmic reticulum before transfer to the Golgi apparatus. Proc Natl Acad Sci U S A. 1993 Jun 15;90(12):5732-6.
Moradas-Ferreira P, Costa V, Piper P, Mager W. The molecular defences against reactive oxygen species in yeast. Mol Microbiol. 1996 Feb;19(4):651-8. Review.
Morgan BA, Banks GR, Toone WM, Raitt D, Kuge S, Johnston LH. The Skn7 response regulator controls gene expression in the oxidative stress response of the budding yeast Saccharomyces cerevisiae. EMBO J. 1997 Mar 3;16(5):1035-44.

Mouaheb N, Thomas D, Verdoucq L, Monfort P, Meyer Y. In vivo functional discrimination between plant thioredoxins by heterologous expression in the yeast Saccharomyces cerevisiae. Proc Natl Acad Sci U S A. 1998 Mar 17;95(6):3312-7.
Mountain HA, Bystrom AS, Larsen JT, Korch C. Four major transcriptional responses in the methionine/threonine biosynthetic pathway of Saccharomyces cerevisiae. Yeast. 1991 Nov;7(8):781-803.
Muller EG. Thioredoxin deficiency in yeast prolongs S phase and shortens the G1 interval of the cell cycle. J Biol Chem. 1991 May 15;266(14):9194-202.
Muller EG. A glutathione reductase mutant of yeast accumulates high levels of oxidized glutathione and requires thioredoxin for growth. Mol. Biol. Cell 1996 7: 1805-1813.
Nakamura N, Yamazaki S, Sato K, Nakano A, Sakaguchi M, Mihara K. Identification of potential regulatory elements for the transport of Emp24p. Mol Biol Cell. 1998 Dec;9(12):3493-503.
Netto LES, Chae HZ, Kang SW, Rhee SG, Stadtman ER. Removal of Hydrogen Peroxide by Thiol-specific Antioxidant Enzyme (TSA) Is Involved with Its Antioxidant Properties. TSA possesses thiol peroxidase activity. J. Biol. Chem. 1996 271: 15315-15321.
Newman AP, Shim J, Ferro-Novick S. BET1, BOS1, and SEC22 are members of a group of interacting yeast genes required for transport from the endoplasmic reticulum to the Golgi complex. Mol Cell Biol. 1990 Jul;10(7):3405-14.
Nichols WC, Seligsohn U, Zivelin A, Terry VH, Hertel CE, Wheatley MA, Moussalli MJ, Hauri HP, Ciavarella N, Kaufman RJ, Ginsburg D. Mutations in the ER-Golgi intermediate compartment protein ERGIC-53 cause combined deficiency of coagulation factors V and VIII. Cell. 1998 Apr 3;93(1):61-70.
Nielsen H, Engelbrecht J, Brunak S , Heijne G. Identification of prokaryotic and eukaryotic signal peptides and prediction of their cleavage sites. Protein Engineering, (1997) 10, 1-6.
Nishikawa S, Nakano A. Identification of a gene required for membrane protein retention in the early secretory pathway. Proc Natl Acad Sci U S A. 1993 Sep 1;90(17):8179-83.
Nishimura N, Balch WE. A di-acidic signal required for selective export from the endoplasmic reticulum. Science. 1997 Jul 25;277(5325):556-8.
Nishimura N, Bannykh S, Slabough S, Matteson J, Altschuler Y, Hahn K, Balch WE. A di-acidic (DXE) code directs concentration of cargo during export from the endoplasmic reticulum. J Biol Chem. 1999 May 28;274(22):15937-46.
Nuoffer C, Jeno P, Conzelmann A, Riezman H. Determinants for glycophospholipid anchoring of the Saccharomyces cerevisiae GAS1 protein to the plasma membrane. Mol Cell Biol. 1991 Jan;11(1):27-37.
Ohtake Y, Yabuuchi S. Molecular cloning of the gamma-glutamylcysteine synthetase gene of Saccharomyces cerevisiae. Yeast. 1991 Dec;7(9):953-61.
Oluwatosin YE, Kane PM. Mutations in the CYS4 gene provide evidence for regulation of the yeast vacuolar H+-ATPase by oxidation and reduction in vivo. J Biol Chem. 1997 Oct 31;272(44):28149-57.
Ono BI, Hazu T, Yoshida S, Kawato T, Shinoda S, Brzvwczy J, Paszewski A. Cysteine biosynthesis in Saccharomyces cerevisiae: a new outlook on pathway and regulation. Yeast. 1999 Sep 30;15(13):1365-75.
Ono B, Kijima K, Ishii N, Kawato T, Matsuda A, Paszewski A, Shinoda. Regulation of sulphate assimilation in Saccharomyces cerevisiae. Yeast. 1996 Sep 15;12(11):1153-62.
Ono B, Naito K. 1991. The cysteine transport system of Saccharomyces cerevisiae. Yeast 7:849-855.
Ono B, Naito K, Shirahige Y, Yamamoto M. Regulation of cystathionine gamma-lyase in Saccharomyces cerevisiae. Yeast. 1991 Nov;7(8):843-8.
Ono B, Shirahige Y, Nanjoh A, Andou N, Ohue H, Ishino-Arao Y. Cysteine biosynthesis in Saccharomyces cerevisiae: mutation that confers cystathionine beta-synthase deficiency. J Bacteriol. 1988 Dec;170(12):5883-9.

Ono B, Suruga T, Yamamoto M, Yamamoto S, Murata K, Kimura A, Shinoda S, Ohmori S. Cystathionine accumulation in Saccharomyces cerevisiae. J Bacteriol. 1984 Jun;158(3):860-5.
Ono B, Tanaka K, Naito K, Heike C, Shinoda S, Yamamoto S, Ohmori S, Oshima T, Toh-e A. Cloning and characterization of the CYS3 (CYI1) gene of Saccharomyces cerevisiae. J Bacteriol. 1992 May;174(10):3339-47.
Orci L, Perrelet A, Ravazzola M, Wieland FT, Schekman R, Rothman JE. "BFA bodies": a subcompartment of the endoplasmic reticulum. Proc Natl Acad Sci U S A. 1993 Dec 1;90(23):11089-93.
Orci L, Stamnes M, Ravazzola M, Amherdt M, Perrelet A, Sollner TH, Rothman JE. Bidirectional transport by distinct populations of COPI-coated vesicles. Cell. 1997 Jul 25;90(2):335-49.
Ostermann J, Orci L, Tani K, Amherdt M, Ravazzola M, Elazar Z, Rothman JE. Stepwise assembly of functionally active transport vesicles. Cell. 1993 Dec 3;75(5):1015-25.
Paabo S, Bhat BM, Wold WS, Peterson PA. A short sequence in the COOH-terminus makes an adenovirus membrane glycoprotein a resident of the endoplasmic reticulum. Cell. 1987 Jul 17;50(2):311-7.
Palade G. Intracellular aspects of the process of protein synthesis. Science. 1975 Aug 1;189(4200):347-58. Review.
Pavel J, Harter C, Wieland FT. Reversible dissociation of coatomer: functional characterization of a beta/delta-coat protein subcomplex. Proc Natl Acad Sci U S A. 1998 Mar 3;95(5):2140-5.
Paszewski A, Ono BI. Biosynthesis of sulphur amino acids in Saccharomyces cerevisiae: regulatory roles of methionine and S-adenosylmethionine reassessed. Curr Genet. 1992 Oct;22(4):273-5.
Patton EE, Peyraud C, Rouillon A, Surdin-Kerjan Y, Tyers M, Thomas D. SCF(Met30)-mediated control of the transcriptional activator Met4 is required for the G(1)-S transition. EMBO J. 2000 Apr 3;19(7):1613-24.
Patton EE, Willems AR, Sa D, Kuras L, Thomas D, Craig KL, Tyers M. Cdc53 is a scaffold protein for multiple Cdc34/Skp1/F-box proteincomplexes that regulate cell division and methionine biosynthesis in yeast. Genes Dev. 1998 Mar 1;12(5):692-705.
Pedrajas JR, Kosmidou E, Miranda-Vizuete A, Gustafsson JA, Wright AP, Spyrou G. Identification and functional characterization of a novel mitochondrial thioredoxin system in Saccharomyces cerevisiae. J Biol Chem. 1999 Mar 5;274(10):6366-73.
Pelham HR. Sorting and retrieval between the endoplasmic reticulum and Golgi apparatus. Curr Opin Cell Biol. 1995 Aug;7(4):530-5. Review.
Penninckx MJ, Elskens MT. Metabolism and functions of glutathione in micro-organisms. Adv Microb Physiol. 1993;34:239-301. Review.
Poon PP, Cassel D, Spang A, Rotman M, Pick E, Singer RA, Johnston GC. Retrograde transport from the yeast Golgi is mediated by two ARF GAP proteins with overlapping function. EMBO J. 1999 Feb 1;18(3):555-64.
Prinz WA, Aslund F, Holmgren A, Beckwith J. The role of the thioredoxin and glutaredoxin pathways in reducing protein disulphide bonds in the Escherichia coli cytoplasm. J Biol Chem. 1997 Jun 20;272(25):15661-7.
Pryer NK, Wuestehube LJ, Schekman R. Vesicle-mediated protein sorting. Annu Rev Biochem. 1992;61:471-516. Review.
Rabouille C, Nilsson T. Redrawing compartmental boundaries in the exocytic pathway. FEBS Lett. 1995 Aug 1;369(1):97-100. Review.
Roberts RJ. Restriction and modification enzymes and their recognition sequences. Nucleic Acids Res. 1983 Jan 11;11(1):r135-67
Roberts CJ, Nothwehr SF, Stevens TH. Membrane protein sorting in the yeast secretory pathway: evidence that the vacuole may be the default compartment. J Cell Biol. 1992 Oct;119(1):69-83.

Rodriguez-Manzaneque MT, Ros J, Cabiscol E, Sorribas A, Herrero E. Grx5 glutaredoxin plays a central role in protection against protein oxidative damage in Saccharomyces cerevisiae. Mol Cell Biol. 1999 Dec;19(12):8180-90.
Rojo M, Emery G, Marjomaki V, McDowall AW, Parton RG, Gruenberg J. The transmembrane protein p23 contributes to the organization of the Golgi apparatus. J Cell Sci. 2000 Mar;113 (Pt 6):1043-57.
Rojo M, Pepperkok R, Emery G, Kellner R, Stang E, Parton RG, Gruenberg J. Involvement of the transmembrane protein p23 in biosynthetic protein transport. J Cell Biol. 1997 Dec 1;139(5):1119-35.
Roth J. Topology of glycosylation in the Golgi apparatus. In: E.G. Berger, J. Roth (Eds.), The Golgi apparatus, Birkhäuser, Basel, 1997, p. 131-161.
Roth MG. Lipid regulators of membrane traffic through the Golgi complex. Trends Cell Biol. 1999 May;9(5):174-9. Review.
Rothman JE. Mechanisms of intracellular protein transport. Nature. 1994 Nov 3;372(6501):55-63. Review.
Rothman JE, Orci L. Molecular dissection of the secretory pathway. Nature. 1992 Jan 30;355(6359):409-15. Review.
Rothman JE, Wieland FT. Protein sorting by transport vesicles. Science. 1996 Apr 12;272(5259):227-34. Review.
Rouillon A, Barbey R, Patton EE, Tyers M, Thomas D. Feedback-regulated degradation of the transcriptional activator Met4 is triggered by the SCF(Met30)complex. EMBO J. 2000 Jan 17;19(2):282-94.
Sacher M, Barrowman J, Schieltz D, Yates JR, Ferro-Novick S. Identification and characterization of five new subunits of TRAPP. Eur J Cell Biol. 2000 Feb;79(2):71-80.
Sacher M, Jiang Y, Barrowman J, Scarpa A, Burston J, Zhang L, Schieltz D, Yates JR, Abeliovich H, Ferro-Novick S. TRAPP, a highly conserved novel complex on the cis-Golgi that mediates vesicle docking and fusion. EMBO J. 1998 May 1;17(9):2494-503.
Salama NR, Yeung T, Schekman RW. The Sec13p complex and reconstitution of vesicle budding from the ER with purified cytosolic proteins. EMBO J. 1993 Nov;12(11):4073-82.
Sandbaken MG, Lupisella JA, Di Domenico B, Chakraburtty K. Protein synthesis in yeast. Structural and functional analysis of the gene encoding elongation factor 3. J Biol Chem 265, 15838-44 (1990).
Sangsoda S, Cherest H, Surdin-Kerjan Y. The expression of the MET25 gene of Saccharomyces cerevisiae is regulated transcriptionally. Mol Gen Genet. 1985;200(3):407-14.
Santamaria I, Velasco G, Pendas AM, Fueyo A, Lopez-Otin C. Cathepsin Z, a novel human cysteine proteinase with a short propeptide domain and a unique chromosomal location. J Biol Chem. 1998 Jul 3;273(27):16816-23.
Saraste J, Kuismanen E. Pre- and post-Golgi vacuoles operate in the transport of Semliki Forest virus membrane glycoproteins to the cell surface. Cell. 1984 Sep;38(2):535-49.
Saraste J, Palade GE, Farquhar MG. Antibodies to rat pancreas Golgi subfractions: identification of a 58-kD cis-Golgi protein. J Cell Biol. 1987 Nov;105(5):2021-9.
Sato K, Nishikawa S, Nakano A. Membrane protein retrieval from the Golgi apparatus to the endoplasmic reticulum (ER): characterization of the RER1 gene product as a component involved in ER localization of Sec12p. Mol Biol Cell. 1995 Nov;6(11):1459-77.
Sato M, Sato K, Nakano A. Endoplasmic reticulum localization of Sec12p is achieved by two mechanisms: Rer1p-dependent retrieval that requires the transmembrane domain and Rer1p-independent retention that involves the cytoplasmic domain. J Cell Biol. 1996 Jul;134(2):279-93.
Schauer I, Emr S, Gross C, Schekman R. Invertase signal and mature sequence substitutions that delay intercompartmental transport of active enzyme. J Cell Biol. 1985 May;100(5):1664-75.

Schekman R, Barlowe C, Bednarek S, Campbell J, Doering T, Duden R, Kuehn M, Rexach M, Yeung T, Orci L. Coat proteins and selective protein packaging into transport vesicles. Cold Spring Harb Symp Quant Biol. 1995;60:11-21. Review.
Schekman R, Orci L. Coat proteins and vesicle. Science. 1996 Mar 15;271(5255):1526-33. Review.
Schimmoller F, Singer-Kruger B, Schroder S, Kruger U, Barlowe C, Riezman H. The absence of Emp24p, a component of ER-derived COPII-coated vesicles, causes a defect in transport of selected proteins to the Golgi. EMBO J. 1995 Apr 3;14(7):1329-39.
Schindler R, Itin C, Zerial M, Lottspeich F, Hauri HP. ERGIC-53, a membrane protein of the ER-Golgi intermediate compartment, carries an ER retention motif. Eur J Cell Biol. 1993 Jun;61(1):1-9.
Schröder-Köhne S, Letourneur F, Riezman H. Alpha-COP can discriminate between distinct, functional di-lysine signals in vitro and regulates access into retrograde transport. J Cell Sci. 1998 Dec;111 (Pt 23):3459-70.
Schröder-Köhne S, Schimmöller F, Singer-Kruger B, Riezman H. The Golgi-localization of yeast Emp47p depends on its di-lysine motif but is not affected by the ret1-1 mutation in alpha-COP. J Cell Biol. 1995 Nov;131(4):895-912.
Schweizer A, Fransen JA, Bachi T, Ginsel L, Hauri HP. Identification, by a monoclonal antibody, of a 53-kD protein associated with a tubulo-vesicular compartment at the cis-side of the Golgi apparatus. J Cell Biol. 1988 Nov;107(5):1643-53.
Schweizer A, Fransen JA, Matter K, Kreis TE, Ginsel L, Hauri HP. Identification of an intermediate compartment involved in protein transport from endoplasmic reticulum to Golgi apparatus. Eur J Cell Biol. 1990 Dec;53(2):185-96.
Schweizer A, Kornfeld S, Rohrer J. Cysteine34 of the cytoplasmic tail of the cation-dependent mannose 6-phosphate receptor is reversibly palmitoylated and required for normal trafficking and lysosomal enzyme sorting. J Cell Biol. 1996 Feb;132(4):577-84.
Schworer CM, Mortimore GE. Glucagon-induced autophagy and proteolysis in rat liver: mediation by selective deprivation of intracellular amino acids. Proc Natl Acad Sci U S A. 1979 Jul;76(7):3169-73.
Serafini T, Orci L, Amherdt M, Brunner M, Kahn RA, Rothman JE. ADP-ribosylation factor is a subunit of the coat of Golgi-derived COP-coated vesicles: a novel role for a GTP-binding protein. Cell. 1991 Oct 18;67(2):239-53.
Sharma KG, Sharma V, Bourbouloux A, Delrot S, Bachhawat AK. Glutathione depletion leads to delayed growth stasis in Saccharomyces cerevisiae: evidence of a partially overlapping role for thioredoxin. Curr Genet. 2000 Aug;38(2):71-7.
Shen H, Dowhan W. Regulation of phospholipid biosynthetic enzymes by the level of CDP-diacylglycerol synthase activity. J Biol Chem. 1997 Apr 25;272(17):11215-20.
Shen H, Heacock PN, Clancey CJ, Dowhan W. The CDS1 gene encoding CDP-diacylglycerol synthase in Saccharomyces cerevisiae is essential for cell growth. J Biol Chem. 1996 Jan 12;271(2):789-95.
Shim J, Newman AP, Ferro-Novick S. The BOS1 gene encodes an essential 27-kD putative membrane protein that is required for vesicular transport from the ER to the Golgi complex in yeast. J Cell Biol. 1991 Apr;113(1):55-64.
Siegel IM. 1975. Biochemistry of the sulfur cycle, p. 217-286, In D.M. Greenberg (ed.), Metabolic pathways, vol. VII. Metabolism of sulfur compounds, Academic Press, Inc., New York, N.Y.
Sies H. Strategies of antioxidant defense. Eur J Biochem. 1993 Jul 15;215(2):213-9. Review.
Sikorski RS, Hieter P. A system of shuttle vectors and yeast host strains designed for efficient manipulation of DNA in Saccharomyces cerevisiae. Genetics. 1989 May;122(1):19-27.

Skrzypek MS, Nagiec MM, Lester RL, Dickson RC. Analysis of phosphorylated sphingolipid long-chain bases reveals potential roles in heat stress and growth control in Saccharomyces. J Bacteriol. 1999 Feb;181(4):1134-40.
Spang A, Schekman R. Reconstitution of retrograde transport from the Golgi to the ER in vitro. J Cell Biol. 1998 Nov 2;143(3):589-99.
Spector D, Labarre J, Toledano MB. A genetic investigation of the essential role of glutathione: Mutations in the proline biosynthesis pathway are the only suppressors of glutathione auxotrophy in yeast. J Biol Chem. 2000 Nov 17 [epub ahead of print]
Spector A, Yan GZ, Huang RR, McDermott MJ, Gascoyne PR, Pigiet V. The effect of H2O2 upon thioredoxin-enriched lens epithelial cells. J Biol Chem. 1988 Apr 5;263(10):4984-90.
Springer S, Chen E, Duden R, Marzioch M, Rowley A, Hamamoto S, Merchant S, Schekman R. The p24 proteins are not essential for vesicular transport in Saccharomyces cerevisiae. Proc Natl Acad Sci U S A. 2000 Apr 11;97(8):4034-9.
Stamnes MA, Craighead MW, Hoe MH, Lampen N, Geromanos S, Tempst P, Rothman JE. An integral membrane component of coatomer-coated transport vesicles defines a family of proteins involved in budding. Proc Natl Acad Sci U S A. 1995 Aug 15;92(17):8011-5.
Stenbeck G, Schreiner R, Herrmann D, Auerbach S, Lottspeich F, Rothman JE, Wieland FT. Gamma-COP, a coat subunit of non-clathrin-coated vesicles with homology to Sec21p. FEBS Lett. 1992 Dec 14;314(2):195-8.
Stephen DW, Rivers SL, Jamieson DJ. The role of the YAP1 and YAP2 genes in the regulation of the adaptive oxidative stress responses of Saccharomyces cerevisiae. Mol Microbiol. 1995 May;16(3):415-23.
Storrie B, Pepperkok R, Nilsson T. Breaking the COPI monopoly on Golgi recycling. Trends Cell Biol. 2000 Sep;10(9):385-91. Review.
Sugiyama K, Izawa S, Inoue Y. The Yap1p-dependent induction of glutathione synthesis in heat shock response of Saccharomyces cerevisiae. J Biol Chem. 2000 May 19;275(20):15535-40.
Takeshige K, Baba M, Tsuboi S, Noda T, Ohsumi Y. Autophagy in yeast demonstrated with proteinase-deficient mutants and conditions for its induction. J Cell Biol. 1992 Oct;119(2):301-11.
Teasdale RD, Jackson MR. Signal-mediated sorting of membrane proteins between the endoplasmic reticulum and the golgi apparatus. Annu Rev Cell Dev Biol. 1996;12:27-54. Review.
Thomas D, Barbey R, Surdin-Kerjan Y. Gene-enzyme relationship in the sulphate assimilation pathway of Saccharomyces cerevisiae. Study of the 3'-phosphoadenylylsulphate eductase structural gene. J Biol Chem. 1990 Sep 15;265(26):15518-24.
Thomas D, Surdin-Kerjan Y. The synthesis of the two S-adenosyl-methionine synthetases is differently regulated in Saccharomyces cerevisiae. Mol Gen Genet. 1991 Apr;226(1-2):224-32.
Thomas D, Surdin-Kerjan Y. Metabolism of sulfur amino acids in Saccharomyces cerevisiae. Microbiol Mol Biol Rev. 1997 Dec;61(4):503-32. Review.
VanRheenen SM, Cao X, Lupashin VV, Barlowe C, Waters MG. Sec35p, a novel peripheral membrane protein, is required for ER to Golgi vesicle docking. J Cell Biol. 1998 Jun 1;141(5):1107-19.
Vedel M, Nicolas A. CYS3, a hotspot of meiotic recombination in Saccharomyces cerevisiae. Effects of heterozygosity and mismatch repair functions on gene conversion and recombination intermediates. Genetics. 1999 Apr;151(4):1245-59.
Vido K, Spector D, Lagniel G, Lopez S, Toledano MB, Labarre J. A proteome analysis of the cadmium response in Saccharomyces cerevisiae. J Biol Chem. 2000 Nov 14 [epub ahead of print]

Vollenweider F, Kappeler F, Itin C, Hauri HP. Mistargeting of the lectin ERGIC-53 to the endoplasmic reticulum of HeLa cells impairs the secretion of a lysosomal enzyme. J Cell Biol. 1998 Jul 27;142(2):377-89.
Wach A, Brachat A, Pohlmann R, Philippsen P. 1994. New heterologous modules for classical or PCR-based gene disruptions in Saccharomyces cerevisiae. Yeast 10:1793-1808.
Waters MG, Serafini T, Rothman JE. 'Coatomer': a cytosolic protein complex containing subunits of non-clathrin-coated Golgi transport vesicles. Nature. 1991 Jan 17;349(6306):248-51.
Wells GB, Dickson RC, Lester RL. Heat-induced elevation of ceramide in Saccharomyces cerevisiae via de novo synthesis. J Biol Chem. 1998 Mar 27;273(13):7235-43.
Werner-Washburne M, Stone DE, Craig EA. Complex interactions among members of an essential subfamily of hsp70 genes in Saccharomyces cerevisiae. Mol Cell Biol. 1987 Jul;7(7):2568-77.
Wieser R, Adam G, Wagner A, Schuller C, Marchler G, Ruis H, Krawiec Z, Bilinski T. Heat shock factor-independent heat control of transcription of the CTT1 gene encoding the cytosolic catalase T of Saccharomyces cerevisiae. J Biol Chem. 1991 Jul 5;266(19):12406-11.
Winzeler EA, et al. Functional characterization of the S. cerevisiae genome by gene deletion and parallel analysis. Science (1999) 285:901-906
Wu WI, Liu Y, Riedel B, Wissing JB, Fischl AS, Carman GM. Purification and characterization of diacylglycerol pyrophosphate phosphatase from Saccharomyces cerevisiae. J Biol Chem. 1996 Jan 26;271(4):1868-76.
Wu AL, Moye-Rowley WS. GSH1, which encodes gamma-glutamylcysteine synthetase, is a target gene for yAP-1 transcriptional regulation. Mol Cell Biol. 1994 Sep;14(9):5832-9.
Xu Z, Mayer A, Muller E, Wickner W. A heterodimer of thioredoxin and I(B)2 cooperates with Sec18p (NSF) to promote yeast vacuole inheritance. J Cell Biol. 1997 Jan 27;136(2):299-306.
Xu Z, Wickner W. Thioredoxin is required for vacuole inheritance in Saccharomyces cerevisiae. J Cell Biol. 1996 Mar;132(5):787-94.
Yamagata S, D'Andrea RJ, Fujisaki S, Isaji M, Nakamura K. Cloning and bacterial expression of the CYS3 gene encoding cystathionine gamma-lyase of Saccharomyces cerevisiae and the physicochemical and enzymatic properties of the protein. J Bacteriol. 1993 Aug;175(15):4800-8.
Yamagata S, Takeshima K. O-Acetylserine and O-acetylhomoserine sulfhydrylase of yeast. Further purification and characterization as a pyridoxal enzyme. J Biochem (Tokyo). 1976 Oct;80(4):777-85.
Yang X, Matern HT, Gallwitz D. Specific binding to a novel and essential Golgi membrane protein (Yip1p) functionally links the transport GTPases Ypt1p and Ypt31p. EMBO J. 1998 Sep 1;17(17):4954-63.
Yoshihisa T, Barlowe C, Schekman R. Requirement for a GTPase-activating protein in vesicle budding from the endoplasmic reticulum. Science. 1993 Mar 5;259(5100):1466-8.
Zhao L, Helms JB, Brugger B, Harter C, Martoglio B, Graf R, Brunner J, Wieland FT. Direct and GTP-dependent interaction of ADP ribosylation factor 1 with coatomer subunit beta. Proc Natl Acad Sci U S A. 1997 Apr 29;94(9):4418-23.
Zhao L, Helms JB, Brunner J, Wieland FT. GTP-dependent binding of ADP-ribosylation factor to coatomer in close proximity to the binding site for dilysine retrieval motifs and p23. J Biol Chem. 1999 May 14;274(20):14198-203.

Acknowledgements

I would like to thank cordially Dr. Stephan Schröder-Köhne for the scientific project he initiated me in and also for the invaluable intellectual support, encouragement, attention and care he never ceased to generously provide me with.

My special thanks belong to Dr. Dieter Schmitt, the fruitful scientific discussions with whom have many times positively influenced my research work and contributed very much to any success I ever achieved.

I am very grateful to Prof. Dr. Dieter Gallwitz for his helpful critical remarks, care and assistance in every aspect of my scientific work at the Department.

I would like to thank heartily my scientific supervisor from the University of Kassel - Prof. Dr. Markus Maniak for the support and care he spent on me.

I express my sincere gratitude to PhD student Bernd Sander whose bright humour and also scientific activities in the laboratory we shared contributed a lot to the comfort in my work.

I am deeply thankful to Stephan Albert, Uwe Andag, Christian Votsmeier, Anna De Antoni, Xiaoping Yang, Oliver Spangenberg, Dmitri Ossipov and Viktor Schneider for having created a truly warm, comfortable and supportive atmosphere at the Department.

I thank all the colleagues from the Department of Molecular Genetics for their good-naturedness, tolerance and help they offered me.

A feeling of a deep frank gratitude I experience to my mother and to all my friends who made my life full and happy outside the place of my scientific work.

Curriculum vitae

Name Alexei G. Matiach

Date of Birth 13.11.1972

Place of Birth Wolgograd, Russia

Citizenship Russian

Education and degree

1989 - 1993 St.-Petersburg State University, the Faculty of Biology, Department of Biochemistry; St. Petersburg, Russia. B. Sc. in biology, 5. 08.1993

1993 - 1995 St.-Petersburg State University, the Faculty of Biology, Department of Biochemistry, Laboratory of Protein Chemistry; St. Petersburg, Russia.
M. Sc. in biology, 8.12.1995

1996 St.-Petersburg State University, the Faculty of Biology, Department of Biochemistry, Laboratory of Protein Chemistry; St. Petersburg, Russia. Studies towards Ph.D. degree.

Title of M. Sc. thesis

Sensitivity to the nuclease S1 and nucleosomal array in the promoter region of the rat liver triptophane oxygenase gene.

Professional occupation

1990-1996 Research Assistant at St.-Petersburg State University, Faculty of Biology, Department of Biochemistry, Laboratory of Protein Chemistry headed by Dr Galina Chikhirzhina, St.-Petersburg, Russia.

1997-2001 Graduate student position (Doktorandstelle), Department of Molecular Genetics headed by Prof. Dr. Dieter Gallwitz, Max-Plank-Institute for Biophysical Chemistry, Göttingen, Germany.

Publication

Matiach, A., and S. Schröder-Köhne (1997). Emp47p as a marker to screen for Golgi to ER transport mutants. Meeting-Abstract. Workshop on Membrane Fusion. Istituto Juan March de Estudios e Investigaciones. Band 67.

Versicherung der selbständigen Erarbeitung

Hiermit versichere ich, dass ich die vorliegende Dissertation selbständig und ohne unerlaubte Hilfe angefertigt und andere als die in der Dissertation angegebenen Hilfsmittel nicht benutzt habe. Alle Stellen, die wörtlich oder sinngemäß aus veröffenlichten oder unveröffenlichten Schriften entnommen sind, habe ich als solche kenntlich gemacht. Kein Teil dieser Arbeit ist in einem anderen Promotions- oder Habilitationsverfahren verwendet worden.

Name: Alexei Matiach

Ort / Datum: Göttingen, 21.03.01

Unterschrift:_____